


2006

# Testing financial and real market operations in restructured electricity systems: four theoretical and empirical studies

Junjie Sun  
Iowa State University

Follow this and additional works at: <https://lib.dr.iastate.edu/rtd>

 Part of the [Economics Commons](#), and the [Oil, Gas, and Energy Commons](#)

## Recommended Citation

Sun, Junjie, "Testing financial and real market operations in restructured electricity systems: four theoretical and empirical studies " (2006). *Retrospective Theses and Dissertations*. 3081.  
<https://lib.dr.iastate.edu/rtd/3081>

This Dissertation is brought to you for free and open access by the Iowa State University Capstones, Theses and Dissertations at Iowa State University Digital Repository. It has been accepted for inclusion in Retrospective Theses and Dissertations by an authorized administrator of Iowa State University Digital Repository. For more information, please contact [digirep@iastate.edu](mailto:digirep@iastate.edu).

**Testing financial and real market operations in restructured electricity systems:  
Four theoretical and empirical studies**

by

Junjie Sun

A dissertation submitted to the graduate faculty  
in partial fulfillment of the requirements for the degree of  
**DOCTOR OF PHILOSOPHY**

Major: Economics

Program of Study Committee:  
Leigh Tesfatsion, Major Professor  
Barry Falk  
Sergio Lence  
James McCalley  
Johnny Wong

Iowa State University

Ames, Iowa

2006

Copyright © Junjie Sun, 2006. All rights reserved.

UMI Number: 3243563

UMI<sup>®</sup>

---

UMI Microform 3243563

Copyright 2007 by ProQuest Information and Learning Company.  
All rights reserved. This microform edition is protected against  
unauthorized copying under Title 17, United States Code.

---

ProQuest Information and Learning Company  
300 North Zeeb Road  
P.O. Box 1346  
Ann Arbor, MI 48106-1346

## TABLE OF CONTENTS

<b>LIST OF TABLES</b> . . . . .	vii
<b>LIST OF FIGURES</b> . . . . .	xi
<b>ACKNOWLEDGEMENTS</b> . . . . .	xiii
<b>ABSTRACT</b> . . . . .	xiv
<b>CHAPTER 1. GENERAL INTRODUCTION</b> . . . . .	1
1.1 Introduction . . . . .	1
1.2 Thesis Organization . . . . .	2
<b>CHAPTER 2. U.S. FINANCIAL TRANSMISSION RIGHTS:</b>	
<b>THEORY AND PRACTICE</b> . . . . .	5
2.1 Abstract . . . . .	5
2.2 Introduction . . . . .	6
2.3 FTRs in Theory and Practice . . . . .	9
2.3.1 Theoretical Studies of FTRs . . . . .	9
2.3.2 Empirical Studies of FTRs . . . . .	14
2.3.3 Overview of the Two-stage FTR Model . . . . .	17
2.4 The No-rights Benchmark Model . . . . .	18
2.4.1 Model Specifications and Assumptions . . . . .	19
2.4.2 Model Setup . . . . .	21
2.4.3 The Economic Dispatch (ED) Solution . . . . .	24
2.4.4 Solution Discussion . . . . .	29
2.5 The FTR Model under Network Uncertainty . . . . .	33

2.5.1	Model Specifications and Assumptions . . . . .	34
2.5.2	Model Setup . . . . .	37
2.5.3	FTR Solutions . . . . .	41
2.6	Conclusions and Extensions . . . . .	47
2.7	References . . . . .	49
2.8	Appendix . . . . .	52
2.8.1	Appendix 1 . . . . .	52
2.8.2	Appendix 2 . . . . .	54
2.8.3	Appendix 3 . . . . .	60
2.8.4	Appendix 4 . . . . .	61
2.8.5	Appendix 5 . . . . .	62
<b>CHAPTER 3. EVALUATING THE PERFORMANCE OF FINANCIAL TRANSMISSION RIGHTS AUCTION MARKET: EVIDENCE FROM THE U.S. MIDWEST ENERGY REGION . . . . .</b>		<b>66</b>
3.1	Abstract . . . . .	66
3.2	Introduction . . . . .	67
3.3	MISO Energy and FTR Markets . . . . .	69
3.3.1	LMP Components . . . . .	71
3.3.2	Overview of MISO FTR Acquisition . . . . .	72
3.3.3	MISO Monthly FTR Auctions . . . . .	74
3.4	Theory . . . . .	75
3.4.1	Hedging Role of FTR . . . . .	75
3.4.2	Theoretic Framework . . . . .	83
3.5	Data . . . . .	85
3.6	Empirical Methodologies . . . . .	90
3.6.1	Overview . . . . .	90
3.6.2	Linear Regression Model . . . . .	92
3.6.3	Kernel Regression Model . . . . .	92

3.6.4	Goodness-of-fit Test . . . . .	93
3.7	Results . . . . .	94
3.7.1	Summary Statistics . . . . .	95
3.7.2	Linear Regression Estimation . . . . .	96
3.7.3	Kernel Regression and GOF Test . . . . .	97
3.7.4	Revenue Sufficiency Analysis . . . . .	97
3.8	Conclusions . . . . .	98
3.9	References . . . . .	101
3.10	Appendix . . . . .	103
<b>CHAPTER 4. DYNAMIC TESTING OF WHOLESALE POWER MAR-</b>		
<b>KET DESIGNS: AN OPEN-SOURCE AGENT-BASED FRAMEWORK</b>		<b>116</b>
4.1	Abstract . . . . .	116
4.2	Introduction . . . . .	117
4.3	Overview of the AMES Framework . . . . .	121
4.4	Configuration of the AMES Framework . . . . .	124
4.4.1	Overview . . . . .	124
4.4.2	Structural Configuration of the AMES Transmission Grid . . . . .	125
4.4.3	Structural Configuration of the AMES LSEs . . . . .	127
4.4.4	Structural Configuration of the AMES Generators . . . . .	129
4.4.5	Structural Configuration of the ISO . . . . .	131
4.4.6	Learning Configuration for the AMES Generators . . . . .	134
4.5	Dynamic Five-Node Test Case . . . . .	138
4.5.1	Overview . . . . .	138
4.5.2	Case 1: Generators Report True Supply Data . . . . .	140
4.5.3	Case 2: Generators Report Strategic Supply Offers . . . . .	143
4.6	Concluding Remarks . . . . .	145
4.7	References . . . . .	147
4.8	Appendix: Construction of Generator Action Domains . . . . .	151

4.8.1	A.1 Overview . . . . .	151
4.8.2	A.2 Percentage Representation of Supply Offers . . . . .	153
4.8.3	A.3 Action Domain Construction . . . . .	157
4.8.4	A.4 A Numerical Example . . . . .	160
<b>CHAPTER 5. DC OPTIMAL POWER FLOW FORMULATION AND SO-</b>		
	<b>LUTION USING QUADPROGJ . . . . .</b>	<b>180</b>
5.1	Abstract . . . . .	180
5.2	Introduction . . . . .	181
5.3	Configuration of the Wholesale Power Market . . . . .	183
5.3.1	Overview of the AMES Framework . . . . .	183
5.3.2	Configuration of the AMES Transmission Grid . . . . .	185
5.3.3	Configuration of the AMES LSEs . . . . .	186
5.3.4	Configuration of the AMES Generators . . . . .	186
5.4	DC OPF Problem Formulation . . . . .	188
5.4.1	From AC OPF to DC OPF Per Unit . . . . .	189
5.4.2	Standard DC OPF in Structural PU Form . . . . .	192
5.4.3	Augmentation of the Standard DC OPF Problem . . . . .	195
5.4.4	Augmented DC OPF in Reduced PU Form . . . . .	198
5.5	Augmented DC OPF in SCQP Form . . . . .	199
5.5.1	Objective Function Depiction . . . . .	200
5.5.2	Constraint Depiction . . . . .	203
5.5.3	The Complete SCQP Depiction . . . . .	205
5.6	Illustrative Examples . . . . .	207
5.6.1	A Three-Node Illustration . . . . .	207
5.6.2	A Five-Node Illustration . . . . .	211
5.7	QuadProgJ Input/Output and Logical Progression . . . . .	217
5.8	QP Test Results for QuadProgJ . . . . .	220
5.8.1	Overview . . . . .	220

5.8.2	QP Test Case Results . . . . .	221
5.9	DC OPF Test Case Results . . . . .	225
5.9.1	Overview . . . . .	225
5.9.2	Three-Node Test Results . . . . .	226
5.9.3	Five-Node Test Results . . . . .	229
5.9.4	II Sensitivity Test Results . . . . .	231
5.10	Concluding Remarks . . . . .	232
5.11	References . . . . .	233
5.12	Appendix . . . . .	235
5.12.1	Appendix A: Derivation of Power Flow Branch Equations . . . . .	235
5.12.2	Appendix B: Expressing DC OPF Voltage Angles as a Linear Affine Function of Real Power Injections . . . . .	238
<b>CHAPTER 6. GENERAL CONCLUSIONS . . . . .</b>		<b>257</b>



## LIST OF TABLES

Table 2.1	Overview of Theoretical Studies in FTRs . . . . .	14
Table 2.2	Comparison of FTRs in Major U.S. Wholesale Power Market (Source: Kristiansen 2003, Lyons et al. 2000, NEPOOL FTR manual 2003b, MISO FTR manual 2005) . . . . .	16
Table 3.1	Hourly MCCs of node WPS.PULLIAM3 in May 2005 . . . . .	86
Table 3.2	Reported number of nodes in MISO service region (April 2005 – March 2006) . . . . .	87
Table 3.3	Reported number of distinct FTRs (April 2005 – March 2006) . . . . .	89
Table 3.4	Reported number of non-distinct and distinct FTRs (April 2005 – March 2006) . . . . .	90
Table 3.5	MISO monthly FTR allocation and auction timeline: August 2005 . . . . .	103
Table 3.6	Summary statistics for off-peak and non-distinct (ON) FTRs (Apr05 – Mar06) . . . . .	104
Table 3.7	Summary statistics for off-peak and distinct (OD) FTRs (Apr05 – Mar06)	105
Table 3.8	Summary statistics for peak and non-distinct (PN) FTRs (Apr05 – Mar06) . . . . .	106
Table 3.9	Summary statistics for peak and distinct (PD) FTRs (Apr05 – Mar06)	107
Table 3.10	Linear regression results for off-peak and non-distinct (ON) FTRs (Apr05 – Mar06) . . . . .	108
Table 3.11	Linear regression results for off-peak and distinct (OD) FTRs (Apr05 – Mar06) . . . . .	108

Table 3.12	Linear regression results for peak and non-distinct (PN) FTRs (Apr05 – Mar06) . . . . .	109
Table 3.13	Linear regression results for peak and distinct (PD) FTRs (Apr05 – Mar06) . . . . .	109
Table 3.14	The goodness-of-fit test results for all four types of FTRs (Apr05 – Mar06)	114
Table 3.15	The monthly total net revenue for all four types of FTRs (Apr05 – Mar06)	114
Table 4.1	Admissible Exogenous Variables for the AMES Framework . . . . .	170
Table 4.2	Endogenous Variables for the AMES Framework . . . . .	171
Table 4.3	Dynamic 5-Node Test Case – DC OPF Structural Input Data (SI) . . . . .	172
Table 4.4	Dynamic 5-Node Test Case – Action Domain and Learning Input Data . . . . .	173
Table 4.5	No-Learning Dynamic 5-Node Test Case – Solution Values (SI) for Real Power Branch Flow $P_{km}$ , with Associated Thermal Limit $P_{km}^U$ , for Each Distinct Branch $km$ . . . . .	174
Table 4.6	No-Learning Dynamic 5-Node Test Case – Solution Values (SI) for Real Power Production Levels (in MWs) and Associated Upper Production Limits, together with LMPs (Nodal Balance Constraint Multipliers, \$/MWh) and Minimum Total Variable Cost (\$/h) . . . . .	175
Table 4.7	Learning Dynamic 5-Node Test Case – Means and Standard Deviations for Solution Values (SI) on Day 422 for Real Power Branch Flow $P_{km}$ , with Associated Thermal Limit $P_{km}^U$ , for Each Distinct Branch $km$ . . . . .	176
Table 4.8	Learning Dynamic 5-Node Test Case – Means and Standard Deviations for Solution Values (SI) on Day 422 for Real Power Production Levels (in MWs) . . . . .	177
Table 4.9	Learning Dynamic 5-Node Test Case – Means and Standard Deviations for Solution Values (SI) on Day 422 for LMPs (Nodal Balance Constraint Multipliers, in \$/MWh) . . . . .	178

Table 4.10	Learning Dynamic 5-Node Test Case – Ordinate Values ( $a^R$ ) and Slope Values ( $b^R$ ) for the Linear Marginal Cost Functions Reported to the ISO by the Five Generators on Day 422 in Each of the Twenty Runs, with Summary Statistics . . . . .	179
Table 5.1	DC OPF Admissible Exogenous Variables Per Unit . . . . .	193
Table 5.2	DC OPF Endogenous Variables Per Unit . . . . .	194
Table 5.3	SCQP Test Cases: Structural Attributes and BPMPD Solution Values	223
Table 5.4	QuadProgJ Test Case Results . . . . .	224
Table 5.5	DC OPF Input Data in SI Units for Three-Node Case . . . . .	241
Table 5.6	DC OPF Solution Results in SI Units for Three-Node Case . . . . .	242
Table 5.7	DC OPF Solution Results in SI Units for Three-Node Case - Inequality Constraint Multipliers and Real Power Branch Flows . . . . .	243
Table 5.8	DC OPF Input Data in SI Units for Five-Node Case . . . . .	244
Table 5.9	DC OPF Solution Results in SI Units for Five-Node Case - Optimal Real Power Production Levels and Optimal Voltage Angles (in Radians)	245
Table 5.10	DC OPF Solution Results in SI Units for Five-Node Case - LMP Values (Equality Constraint Multipliers) and Minimized Total Variable Cost .	246
Table 5.11	DC OPF Solution Results in SI Units for Five-Node Case - Thermal Limit Inequality Constraint Multipliers for Each Branch in Each Direction ( $km$ and $mk$ ) . . . . .	247
Table 5.12	DC OPF Solution Results in SI Units for Five-Node Case - Lower and Upper Production Inequality Constraint Multipliers for Each Generator	248
Table 5.13	DC OPF Solution Results in SI Units for Five-Node Case - Optimal Real Power Branch Flow $P_{km}$ and Its Associated Thermal Limit $P_{km}^U$ for Each $km \in \mathbf{BI}$ . . . . .	249
Table 5.14	Sensitivity Test Results for Three-Node Case ( $\pi = 100$ , Angles in Radians)	250
Table 5.15	Sensitivity Test Results for Three-Node Case ( $\pi = 10$ , Angles in Radians)	251
Table 5.16	Sensitivity Test Results for Three-Node Case ( $\pi = 1$ , Angles in Radians)	252

Table 5.17	Sensitivity Test Results for Three-Node Case ( $\pi = 0.1$ , Angles in Radians)	253
Table 5.18	Sensitivity Test Results for Three-Node Case ( $\pi = 0.01$ , Angles in Radians) . . . . .	254
Table 5.19	Sensitivity Test Results for Three-Node Case - Cross Comparison for Sum of Squared Voltage Angle Differences for $\pi = 100, 10, 1, 0.1, 0.01$ , Angles in Radians . . . . .	255
Table 5.20	Sensitivity Test Results for Five-Node Case - Cross Comparison for Sum of Squared Voltage Angle Differences for $\pi = 100, 10, 1, 0.1, 0.01$ , Angles in Radians . . . . .	256

## LIST OF FIGURES

Figure 2.1	Three major U.S. interconnected transmission systems . . . . .	6
Figure 2.2	The two-node electric network benchmark model . . . . .	22
Figure 3.1	The Current Midwest Independent System Operator (MISO) Service Territory . . . . .	70
Figure 3.2	Bilateral contract with no congestion . . . . .	77
Figure 3.3	Bilateral contract with congestion . . . . .	77
Figure 3.4	Transaction via a power pool with congestion . . . . .	79
Figure 3.5	The three-node electric network example . . . . .	80
Figure 3.6	No bilateral transaction with congestion: FTR portfolio . . . . .	81
Figure 3.7	The linear and kernel regression for off-peak and non-distinct (ON) FTRs	110
Figure 3.8	The linear and kernel regression for off-peak and distinct (OD) FTRs .	111
Figure 3.9	The linear and kernel regression for peak and non-distinct (PN) FTRs	112
Figure 3.10	The linear and kernel regression for peak and distinct (PD) FTRs . . .	113
Figure 3.11	The monthly total net revenue for all four types of FTRs (Apr05 – Mar06), Note: all values of monthly total net revenue have been divided by 1000. . . . .	115
Figure 4.1	Existing and Proposed ISO/RTO-Operated U.S. Wholesale Power Markets . . . . .	118
Figure 4.2	Illustrative 5-Node Transmission Grid . . . . .	123
Figure 4.3	AMES Core Features . . . . .	124
Figure 4.4	Activities of the AMES ISO During a Typical Day D . . . . .	125

Figure 4.5	AMES Architecture (Agent Hierarchy) . . . . .	126
Figure 4.6	AMES Dynamic Market Activities: Global View . . . . .	127
Figure 4.7	Core Module Components of the AMES Framework . . . . .	128
Figure 4.8	A Computational Generator (Seller) . . . . .	135
Figure 4.9	A Five-Node Transmission Grid Configuration . . . . .	140
Figure 4.10	24 Hour Load Distribution for the Dynamic 5-Node Test Case . . . . .	141
Figure 4.11	LMP Separation and Spiking in the MISO Energy Region . . . . .	142
Figure 4.12	Dynamic 5-Node Test Case Solution Values for 24-Hour Real Power Production Levels (Day 422) – Generator Learning Compared with No Learning . . . . .	164
Figure 4.13	Dynamic 5-Node Test Case Solution Values for 24-Hour Minimum To- tal Variable Cost (Day 422) – Generator Learning Compared with No Learning . . . . .	165
Figure 4.14	Dynamic 5-Node Test Case Solution Values for 24-Hour LMPs (Day 422) – Generator Learning Compared with No Learning . . . . .	166
Figure 4.15	Dynamic 5-Node Test Case – Mean Reported Marginal Cost Function Versus True Marginal Cost Function for Each Generator (Day 422) . . . . .	167
Figure 4.16	Generator $i$ 's Feasible Supply Offers and True Marginal Cost Function	168
Figure 4.17	AMES Dynamic Flow with Learning Implementations for Generators 1 and 2 . . . . .	169
Figure 5.1	A Three-Node Transmission Grid . . . . .	208
Figure 5.2	A Five-Node Transmission Grid . . . . .	212
Figure 5.3	24 Hour Load Distribution for a 3-Node Case . . . . .	227
Figure 5.4	24 Hour Load Distribution for a 5-Node Case . . . . .	229

## ACKNOWLEDGEMENTS

I would like to take this opportunity to express my thanks to those who helped me with various aspects of conducting research and the writing of this dissertation. First and foremost, I am greatly in debt to my major professor Dr. Leigh Tesfatsion for her guidance and support throughout this research and the writing of this dissertation. Her insights and words of encouragement have inspired and kept me motivated to finish my dissertation. For everything you have done for me, Dr. Tesfatsion, I thank you. I would also like to thank my committee members for their efforts and contributions to this work: Dr. Barry Falk, Dr. Sergio Lence, Dr. James McCalley and Dr. Johnny Wong.

## ABSTRACT

To facilitate the U.S. wholesale electric power restructuring process and promote competitive market outcomes, in April 2003 the U.S. Federal Energy Regulatory Commission (FERC) proposed a complicated market design called the Wholesale Power Market Platform (WPMP) for common adoption by all U.S. wholesale power markets. Despite the fact that versions of the WPMP have been widely implemented in many states, strong opposition to the WPMP persists among some industry stakeholders due largely to a perceived lack of adequate performance testing. In this dissertation, I apply analytical, statistical and agent-based computational simulation tools to analyze and test financial and real power market operations under the current WPMP design. The overall dissertation objective is to better understand how and to what extent the WPMP design facilitates to produce orderly, fair and efficient market outcomes. Four related studies have been undertaken to address four different issues at four different levels. Specifically, my first paper is a theoretical study of financial transmission right (FTR) markets. My second paper is an empirical study on the Midwest FTR market using statistical estimation tools. My third paper is an agent-based computational wholesale power market simulation study for systematic market design tests and market structure analyses. And my fourth paper is an optimization study in which I develop a Java-based DC OPF solver.



## CHAPTER 1. GENERAL INTRODUCTION

### 1.1 Introduction

The electric power industry is one of the largest infrastructure industries in the U.S. Since the 1990s, the U.S. electric power industry has undergone tremendous changes from a heavily regulated and vertically integrated monopoly industry to a more market-oriented environment consisting of smaller specialized firms more open to competition and supervised with lighter regulations. This restructuring process is echoed on a broader level by the deregulation movements in other infrastructure industries such as telecommunications, transportation (e.g., airlines) and other energy industries (e.g., water and gas).

Different from other infrastructure industries, electric power has two distinct features. First, it is extremely expensive, if not impossible, to store power energy. Thus, almost all electric power is delivered through transmission lines for immediate consumption once it is produced. Second, the power flow among transmission paths cannot be controlled and monitored perfectly due to the underlying physical network flow structure. These two features contribute to the fact that there is now a tendency for transmission lines across and within major U.S. electric power markets to become congested. This has a substantial impact on the locational marginal price system and the overall reliability of the wholesale power market.

To help relieve transmission congestion, and to promote reliability and efficiency, in April 2003 the U.S. Federal Energy Regulatory Commission (FERC) proposed a complicated market design called the Wholesale Power Market Platform (WPMP) for common adoption by all U.S. wholesale power markets. One important aspect of the WPMP is the recommended use of financial transmission rights (FTRs) to hedge the risk of volatile energy prices caused by congested transmission lines. Versions of the WPMP have been implemented in New England,

New York, the Mid-Atlantic states, the Midwest, and the Southwest, and have been adopted for implementation in California. In the academic research community as well as among industrial stakeholders, whether FTRs can serve as an effective and efficient hedge instrument as well as whether the overall WPMP design provides a reliable and efficient market environment remain hot issues for debate.

In this dissertation research, I apply analytical, statistical and agent-based computational simulation tools to investigate and test financial and real market operations in the restructured U.S. wholesale power industry. Specifically, four related studies have been undertaken to address four different issues at four different levels.

## 1.2 Thesis Organization

This dissertation consists of four papers and is organized as follows:

My first paper titled “U.S. Financial Transmission Rights: Theory and Practice” addresses an important policy question regarding whether the existence of financial transmission rights (FTRs) as a financial hedge instrument against volatile wholesale electricity prices would increase efficiency and improve social welfare. Using analytical modeling approach, I am able to show that under network uncertainty the acquisition of optimal FTRs by the risk averse market traders will increase the social welfare compared with the case where there are no FTRs available. This result presents a counterexample to the somewhat negative views about FTRs held by some economists in the literature and provides some economic explanations to the fact that FTRs are widely adopted as a financial hedge instrument in the major U.S. wholesale power markets.

Different from the theoretical nature of the first study, my second paper titled “Evaluating the Performance of Financial Transmission Rights Auction Market: Evidence from the U.S. Midwest Energy Region” investigates a specific FTR market, namely the the FTR auction market in the Midwest energy region (MISO), using a set of econometric estimation tools such as linear regression, nonparametric kernel regression and goodness-of-fit tests. As a first attempt to study this newly established market, we are interested in analyzing the performance

of the MISO FTR auction market. The main results show that during the current sample periods the MISO FTR market is systematically losing money (revenue insufficiency), which on the other hand suggests that market participants on average exhibit some degree of risk loving behavior. More data are needed in order to obtain meaningful economic analysis such as estimating the impact of an agent's risk preference on his willingness to pay for the premium of FTR in this complex market. This is a joint work between myself and a fellow Ph.D. student Wenzhuo Shang with me as the lead author. While Wenzhuo collects the initial data from MISO web site and writes the draft of two sections, I conduct all the statistical estimation and tests, finish the rest of sections and make final overall revisions.

Distinct from the first two studies, my third paper titled "Dynamic Testing of Wholesale Power Market Designs: An Open-Source Agent-Based Framework" goes a further micro level to examine the market design issues in the general wholesale power market context. Specifically, we want to test the FERC's WPMP design that has been implemented or adopted in major wholesale power markets in the U.S. Strong opposition to the WPMP persists among some industry stakeholders, due largely to a perceived lack of adequate performance testing. This study reports on the agent-based modeling development and open-source implementation (in Java) of a computational wholesale power market organized in accordance with core WPMP features and operating over a realistically rendered transmission grid. Findings from a dynamic 5-node test case are presented for concrete illustration. With traders being able to submit their offers strategically, it is found that traders (Generators) are able to acquire substantial market power without any explicitly collusions. This suggests that the core WPMP design features, as captured in our current computational framework, do not prevent the considerable exercise of market power by traders. This is a joint work between myself and my major professor Dr. Leigh Tesfatsion with me as the lead author. My responsibilities for completing this paper include designing and implementing the underlying computation test bed using Java, conducting intensive computational experiments, documenting experimental results and reporting them in appropriate tables and figures, writing several sections of the paper. Dr. Tesfatsion provides overall guidance of this project and contributes several sections of the

write-up of the paper.

My last paper titled “DC Optimal Power Flow Formulation and Solution using QuadProgJ” focuses on an critical optimization component of my third paper that the optimal hourly locational marginal prices (LMPs) and commitment/dispatch quantities have to be cleared by a means of DC Optimal Power Flow (OPF) procedure in the wholesale power market. The main contribution of this paper is to present an open-source strictly convex quadratic programming (SCQP) solver QuadProgJ and shows how to use QuadProgJ to solve DC OPF problems. This is another joint work between myself and my major professor Dr. Leigh Tesfatsion. My responsibilities for completing this paper includes designing and implementing the QuadProgJ solver (in Java) using a well-know dual active-set algorithm, conducting intensive accuracy tests using a suite of well-known QP test cases, reporting and documenting DC OPF test results in appropriate tables and figures, and writing several sections of the paper. Dr. Tesfatsion provides overall guidance of this project, involves with me during the development of QuadProgJ and contributes several sections of the write-up of the paper.

## CHAPTER 2. U.S. FINANCIAL TRANSMISSION RIGHTS: THEORY AND PRACTICE

### 2.1 Abstract

Financial Transmission Right (FTR) as a financial hedge instrument against volatile wholesale electricity prices has been widely adopted in the major U.S. wholesale power markets. However, the current literature often shows that FTR decreases efficiency and reduces social welfare. One main problem is that their models do not have a stochastic component. Since FTR is designed to hedge the uncertain profit streams that market participants face, it is no surprise to find that the absence of uncertainty renders the FTR being a source of inefficiency. The contributions of this paper are in two-folds. First, it provides a comprehensive review of both theoretical and empirical studies of FTRs in the current literature. Second, in this paper I present a simple two-node electric network model and show that once stochastic shocks are introduced the acquisition of optimal FTRs by the risk averse market traders will increase and in general will strictly increase the social welfare compared with the case where there are no FTRs available. This result presents a counterexample to the somewhat negative views about FTRs held by other economists in the literature and provides some economic explanations to the fact that FTRs are widely adopted as a financial hedge instrument in the major U.S. wholesale power markets.

**Keywords:** Financial transmission rights, Wholesale electricity market, Locational marginal price, Economic dispatch, Risk hedging, Congestion rent

**JEL Codes:** G1, L9, D4

## 2.2 Introduction

As the largest regulated energy industry in the United States, the U.S. electric power industry has undergone a tremendous change to become more competitive (U.S. Department of Energy 2000). One of the central components in the competitive electricity market is to have open access to the transmission system. In the U.S., the major transmission system can be roughly divided into three regions, the East and West Interconnections and the Electricity Reliability Council of Texas (ERCOT) as shown in Figure 1.

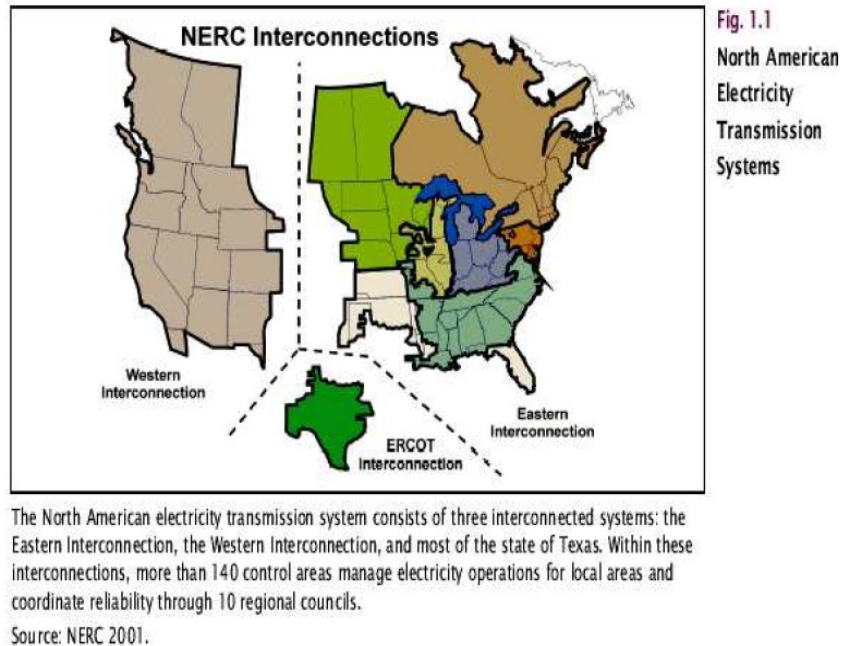


Figure 2.1 Three major U.S. interconnected transmission systems

Electricity as an economic good has its unique features. The most distinct one is that its storage cost is enormously high such that almost all the electric power is delivered through transmission lines for immediate consumption once it is produced. As indicated in a recent National Transmission Grid Study (2002), there is now a tendency for U.S. transmission lines to get congested and thus create substantial impact on the locational pricing system and overall reliability of U.S. wholesale power market (see Stoft 2002 and Wilson 2002). The

U.S. Federal Energy Regulatory Commission (FERC) responds to this issue by calling a new independent institutional entity to manage and handle transmission assets, i.e., *Independent System Operator* (ISO). By the nature of ISO, it is a non-profit organization whose purpose is to monitor the power flow, collect generator's supply offers and load serving entity (LSE)'s demand bids, and calculate the optimal power dispatch taking into account various network constraints such as energy balancing and thermal limit constraint.

To address the above congestion issue, it is a common practice in the U.S. wholesale power market for ISO to issue *financial transmission rights* (FTRs). According to ISO New England Manual (2003a), an FTR is a financial instrument that entitles the holder to receive compensation for transmission congestion costs that arise when the transmission grid is congested in the day-ahead market. The amount of compensation is based on differences in day-ahead *locational marginal prices* (LMPs) result from the dispatch of generators to relieve the congestion. FTR entitles its holders to a share of the *congestion rents* collected in the day-ahead energy market, thus provides the holder a financial hedge in the day-ahead market for the nodal price difference between a node of receipt (source) to a node of delivery (sink).

In the literature four types of FTRs have been proposed <sup>1</sup>, namely, *point-to-point*(PTP) obligation, PTP option, *flowgate* (FG) obligation, and FG option (see Hogan 2002 and 2003). An FTR option entitles its holders to revenue when day-ahead congestion occurs in the desired direction. In contrast,an FTR obligation entitles it holders to a revenue when day-ahead congestion occurs in the desired direction and obligates holders to a payment when day-ahead congestion is in the opposite direction. When using PTP FTRs, market participants can obtain any collection of FTRs corresponding to a feasible power flow in the transmission system. When using FG FTRs, market participants can only obtain FTRs on pre-determined transmission lines (flowgates), which are considered most at risk should the lines get congested.

The definition of a PTP FTR obligation can be more clearly illustrated in the following example. Suppose there are two nodes in the transmission network, node A where power is injected into the transmission network and node B where power is withdrawn from the

<sup>1</sup>As recommended in WPMP by FERC (2003), the U.S. electricity industry have favored PTP FTRs due to its simplicity to implement and its successes in the early restructuring markets such as PJM and New York.

transmission network. Assuming no transmission losses, the PTP FTR entitles the holder to the difference in day-ahead LMP between node A and B. By its obligation nature, the FTR holder receives a positive payment ( $LMP_B - LMP_A$ ) from the ISO if  $LMP_B$  exceeds  $LMP_A$ . On the other hand, the FTR holder is obligated to pay the ISO ( $LMP_A - LMP_B$ ) if  $LMP_A$  exceeds  $LMP_B$ . Thus the wholesale power market participants's risks associated with different LMPs are in principle decreased by purchasing FTRs.

To date, FTRs have been widely used to hedge against the potential loss in the transmission congestion in major U.S. wholesale power markets. For example, FTR was introduced in the PJM (Pennsylvania, New Jersey and Maryland) Interconnection since April 1998, in New York since September 1999, in California since February 2000, and in New England since March 2003. Note that FTRs have been known under different names in different U.S. power markets. For instance, in PJM FTRs are referred to as *Fixed Transmission Rights*, in New York *Transmission Congestion Contracts* (TCCs), in California *Firm Transmission Rights*, in New England *Financial Transmission Rights*, and in Texas *Transmission Congestion Rights* (TCRs).

In spite of the fact that FTR has been widely used in the major U.S. electricity market, it is still a new market instrument that needs theoretical and empirical evaluations. There are issues remaining questionable such as to what extent, if there is any, can FTRs help facilitate the market to generate orderly, fair, and efficient outcomes despite attempts by market participants to gain individual advantage through strategic behaviors? In addition, does the introduction of FTRs create an appropriate incentive for individual firms to invest in the transmission infrastructure?

Although many theoretical models have been proposed and empirical evidences have been discussed in the literature, no attempt has been made to summarize the previous findings about FTRs. The contribution of this paper is to first provide a comprehensive review of various FTR findings from both theoretical and empirical perspectives, and then to better illustrate economic efficiency improvement of introducing FTR in the presence of uncertainty, a simple economic network model is presented and results are discussed. Therefore, this paper



is organized as follows. The second section conducts a literature review on both theoretical and empirical studies of FTRs in the U.S. wholesale power market. Section 3 presents the no-rights benchmark model, which is essentially the competitive equilibrium framework applied to the economic dispatch model in a simple two-node electric network. Section 4 then uses the economic dispatch solution from the benchmark model as the building block to construct a two-node FTR model where uncertainty is introduced as stochastic shocks to both demand and supply sides. Section 5 discusses the conclusions and potential extensions of future work.

## 2.3 FTRs in Theory and Practice

### 2.3.1 Theoretical Studies of FTRs

#### *FTRs and market power*

Although FTR advocates argue that tradable FTRs should facilitate electricity trade in the short run through the alleviation of transmission bottlenecks caused by congestion (see Hogan(2003)), in the current economic literature, people hold more negative views toward FTRs.

For example, in a well-known study, Joskow and Tirole (2000) reach a negative conclusion about FTRs. In their two-node network model with cheap cost generators in the north node, expensive cost generators in the south node, and a transmission line linking the North and the South that has a fixed thermal capacity, they argue that the acquisition of financial rights may enhance the market power in the South if the generators in the South are owned by a monopoly firm. In addition, they carry out a welfare comparison and show that the social welfare derived from the absence of transmission rights is at least as high as and in general higher than the social welfare derived from the system with the financial transmission rights. This striking result clearly indicates the negative views about FTRs held by the authors.

Responding to Joskow and Tirole's result, Hogan (2000) provides an example which shows that introducing financial rights enhances monopoly profits but it increases efficiency as well. This is in contrast to Joskow and Tirole's result which implies that the no-rights solution

is always the most efficient one. Hogan's paper differs from Joskow and Tirole in that the monopolist controls generation at more than one location and some of its generation is at low cost. The detailed derivation is in Cardel, Hitt and Hogan (1997). This example shows the complex nature of the deregulated U.S. electricity market structure such as having significant different results and policy implications due to different network configurations.

By using a Cournot model of competition in a congested transmission network, Oren (1997) illustrates that even in the absence of market concentration, the expectation of congestion and passive transmission rights can lead to implicit collusion among generators and departure from marginal cost pricing. This invalidates the key premise underlying the indirect implementation of transmission rights trading through optimal dispatch by the ISO. The author concludes that passive transmission rights (in the form of transmission congestion contracts (TCCs)) will be preempted by the active traders who will adjust their prices so as to capture the congestion rents. Price distortions due to congestion and passive transmission ownership can result in short and long term inefficiency.

By re-investigating the issues in Oren (1997), Stoft (1999) demonstrates that financial transmission rights such as TCCs allow their owners to capture at least a portion, and sometimes all, of the congestion rents, and thus is shown to be effective in reducing market power. Moreover, the extent to which TCCs can reduce the market power depends on the extent to which total generation capacity exceeds the capacity of the largest generator. This result is in contrast with Oren's. The author states the reasons why his conclusions differ from Oren's in two perspectives. First, he points out that in Oren's second example, which is intended to be a Cournot model, is mistakenly constructed as a Bertrand model and then mis-analyzed. When the model is re-built along Cournot lines, Oren's conclusion is refuted. Second, in Oren's model, it is assumed that generators could not purchase financial transmission rights while in Stoft's model, this assumption is relaxed.

In another paper, Bushnell (1999) expresses his concern that transmission rights can be manipulated by its owners to reduce transmission capacity made available to the competitive market during hours in which there would otherwise be no congestion. In the short run, such

withholding behavior could prove profitable for firms in several ways such as increasing the value of local generators and the value of the transmission rights themselves. The author illustrates his point by using a simple two-node network case with one fixed marginal cost generator at one node and a downward-sloping demand at the other node. Lastly the author argues that due to the concerns about transmission capacity withholding and the inherent network uncertainties, the initial offering of transmission rights in California was to be limited to a level below the full transmission capacity available to the California ISO.

Using human-subject experiment, Kench (2004) conducts an interesting study to test the theoretical results in Joskow and Tirole (2000). Specifically, the author carries out a double-oral auction (DOA) experiment to test the predictions of Joskow and Tirole's theoretical results for a radial electricity market without transmission rights, with financial transmission rights, and with physical rights. The author found that physical rights lead to more "right" market signals, decrease some market power, and remove an uncertainty about electricity transmission congestion better than financial rights or the absence of rights. However, the author also pointed out that one should be very cautious in trying to interpret his experimental results into policy implications because the stylized market setting in his paper does not capture many intricacies (such as the "loop flow effect") in the real world electricity markets.

#### *FTRs and auction design issue*

Bautista and Quintana (2005) develop a methodology to screen and discriminate FTRs that may exacerbate the market power for some monopoly market participants. The proposed methodology is based upon the use of relative hedging position ratios. These ratios comprise the network configuration, market outcomes, and the participants position in the market, and quantify the relationship between the positions of an FTR bidder in the energy market and in the transmission rights allocation. The authors also point out that since an FTR scheme has a reduced liquidity, which may be worsened if a discrimination such as in this study is introduced. Due to the potential complexity for carrying out any regulatory intervention on FTRs ownership, the authors suggest to build the FTRs framework upon their allocation to

other entities, such as LSEs or traders, rather than generators.

Mendez and Rudnick (2004) propose a new congestion management system under nodal and zonal dispatches with implementation of fixed transmission rights (FTR) and flowgate rights (FGR), respectively. Using a static simulation model, which implements marginal theory where congestion components are introduced in the pricing model, they show that the FTR model is suitable for congestion management in deregulated centralized market structures with nodal dispatch, while the FGR is suitable for decentralized markets. Their application indicates that FGR presents advantages over FTR regarding signals on grid use, but its application is too complicated to make its implementation attractive.

In a related study trying to accommodate both point-to-point and flowgate transmission rights, O'Neill et al (2002) propose a “joint energy and transmission rights auction” (JETRA) to allow transmission users to specify which type of transmission rights, point-to-point or flowgate, they prefer to use and reconfigure them over time. JETRA is able to simultaneously accommodate flowgate and point-to-point options and obligations, along with energy production and consumption futures. Under certain conditions, the authors prove that the auction is revenue adequate for the market operator in the sense that payments to rights holders cannot exceed congestion revenues.

#### *FTRs and transmission investment and expansion*

In another set of papers several authors address the issues of transmission investment or expansion in the hope to find the best way to attract investment for the long-term expansion of an electricity transmission network.

Joskow and Tirole (2003) examine the performance of a “merchant transmission” model in which investment in electric transmission capacity rely upon competition and free entry to exploit profitable transmission investment opportunities rather than on regulated monopoly transmission companies. Under strict assumptions, the authors show that the merchant investment model is able to solve the natural monopoly problem traditionally associated with electricity transmission networks. However, when the authors extend their model by introduc-

ing assumptions that more accurately reflect the physical and economic attributes of transmission networks, many attractive properties of the merchant model disappear and inefficient transmission investment decisions are made.

In a related study, Kristiansen and Rosellon (2004) propose a merchant mechanism to expand electricity transmission based on long-term FTRs. As the authors argue, the system operator needs a protocol for awarding incremental FTRs that maximize investor's preferences, and preserves certain unallocated FTRs (or proxy awards) so as to maintain revenue adequacy. They define a proxy award as the best use of the current network along the same direction as the incremental awards, and develop a bi-level computational model for allocating long-term FTRs according to this rule and apply it to different network topologies. They find that simultaneous feasibility for a transmission expansion project crucially depends on the investor-preference and the proxy-preference parameters.

In another interesting study, Rudkevich (2004) investigates the investment and bidding strategies for firm transmission rights. The study first addresses the applicability of the Markowitz portfolio theory to investing in firm transmission rights (FTRs) or transmission congestion contracts (TCCs) typical for Northeastern U.S. electricity market. Specifically, the author uses the principal component analysis to select subsets of statistically independent FTRs/TCCs and obtain the necessary and sufficient conditions for arbitrage opportunities. In the second part of paper, the author analyzes the profit-maximizing bidding strategies for large players with significant Auction Revenue Rights (ARRs).

In a survey study on the topic of transmission expansion, Rosellon (2003) studies the three existing approaches to electricity transmission expansion, i.e., transmission expansion through long-term FTRs, through regulatory mechanisms and through strategic behavior of generators (market power). The first approach relies on the auction of long-term FTRs by an independent system operator (also known as the merchant approach). The second approach is to provide a Transco with the incentive to expand transmission by making it confront the social cost of transmission congestion. The last approach defines optimal expansion of the transmission network according to the strategic behavior of generators. After comparing each

Table 2.1 Overview of Theoretical Studies in FTRs

FTRs and Market Power	FTR Auction Design	Transmission Investment
Joskow and Tirole (2000)	Bautista and Quintana (2005)	Joskow and Tirole (2003)
Hogan (2000)	Mendez and Rudnick (2004)	Kristiansen and Rosellon (2004)
Oren (1997)	O'Neill et al (2002)	Rudkevich (2004)
Stoft (1999)		Rosellon (2003)
Bushnell (1999)		
Kench (2004)		

approach's advantage and disadvantage, the author concludes that there is no single mechanism that guarantees the optimal expansion of the electricity transmission network, and suggest that there may exists the second-best approach which is to combine the merchant and the regulated transmission model.

The current literature of theoretical FTRs studies is summarized in Table 1.

### 2.3.2 Empirical Studies of FTRs

Siddiqui et al. (2003) analyze the public data from 2000 and 2001, and find out that New York transmission congestion contracts (TCCs) provides market participants with a potentially effective hedge against volatile congestion rents. However, the prices paid for TCCs systematically deviated from the associated congestion rents for distant locations and at high prices. Based on their analyses, the authors suggest that there exists an inefficient market for TCCs due to the fact that the price paid for the hedge not being in line with the congestion rents, i.e., unreasonably high risk premiums are being paid. The authors then offer two possible explanations to their empirical finding. One is the low liquidity of TCC markets and the other is the deviation of TCC feasibility requirements from actual energy flows.

In response to Siddiqui et al. (2003) regarding the inefficient pricing of TCCs in New York market, Deng et al. (2004) try to investigate further on the question that whether the price deviations are due to price discovery errors which will eventually vanish or due to inherent inefficiencies in the auction structure. They show that even with perfect foresight of average

congestion rents the clearing prices for the FTRs depends on the bid quantity and therefore may not be priced correctly in the FTR auction. The authors conclude that price discovery alone would not remedy the discrepancy between the auction prices and the realized values of the FTRs, and secondary markets or frequent reconfiguration auctions are necessary in order to achieve such convergence.

In a practical study, Lyons et al. (2000) use simple numerical examples to show how the FTRs work in a two-node network model and give a gentle introduction of various aspects of FTRs such as property rights and transmission expansion, price hedging, and allocation of FTRs. Also the authors conduct a market-wise study and show how various FTRs are handled in PJM, New York and California markets. Their results are summarized and extended in Table 2. Finally, the authors stress that although there is no universally superior model for FTRs, they are still very useful tools in electricity markets with locational pricing.

In another survey study, Kristiansen (2003) investigates how FTRs are acquired and implemented in a range of markets such as PJM, New York, New England, California, Texas, and New Zealand. In each market, the author describes in detail the features of FTRs, some design issues, strength and weakness, and the market performances in different FTR markets. His result along with Lynos et al.(2000) is summarized in Table 2.

Denton and Waterworth (2002) conduct a comprehensive practical study about how FTRs could be introduced in Australian National Electricity Market (NEM)<sup>2</sup>. The Settlements Residue Auction (SRA) was established shortly after NEM to help market participants manage risks. The authors start their report by stating the rationale for changing the SRA process to create a better environment for implementing FTRs. They compare the FTRs in the U.S. markets such as PJM and New England. Then they introduce a workable FTR solution in line with the modified SRA and discuss how the proposed FTR solution addresses the critical issues in the Australian electricity market.

<sup>2</sup>Although their report mainly focuses on the application in Australian national electricity market, there are indeed many similarities between Australian market and major U.S. markets such as PJM, New York and New England.

Table 2.2 Comparison of FTRs in Major U.S. Wholesale Power Market  
(Source: Kristiansen 2003, Lyons et al. 2000, NEPOOL FTR manual 2003b, MISO FTR manual 2005)

	PJM	New York	New England
Name	Fixed Transmission Rights	Trans. Congestion Contracts	Financial Trans. Rights
Contract	Obligations & options , no hedge against losses	Obligations, no hedge against losses	Obligations, no hedge against losses
Duration	Monthly auction, annual network integration service FTRs	6 months and 1, 2 and 5 year auction, monthly reconfiguration	Monthly auction
Acquisition	Network integration service, firm point-to-point service, auction, secondary market	Centralized TCC auction, direct sales, and secondary market	Auction, secondary market, transmission updates, entities paying congestion charges
Auction design	Monthly, single-round, uniform-price auction	Seasonal (multi-round), monthly reconfiguration uniform-price auction	Monthly, single-round, uniform-price auction
Congestion rents	Excess rents distributed to deficiencies in other periods, deficient rents reduce payments proportionally	Excess rents offset trans. system cost, deficit rents covered by trans. owners	Excess rents distributed to FTR holders, deficit rents reduce payments proportionally
Distribution of revenues	FTR auction revenues are allocated among the regional transmission owners in proportion to their transmission revenue requirements	All revenues received by trans. owners from the sale of TCCs are credited against the trans. owner's cost of service	FTR auction revenues are distributed to sellers of FTRs and auction revenue rights recipients
Website	<a href="http://www.pjm.com/">http://www.pjm.com/</a>	<a href="http://www.nyiso.com/">http://www.nyiso.com/</a>	<a href="http://www.iso-ne.com/">http://www.iso-ne.com/</a>
	California	Texas	Midwest
Name	Firm Transmission Rights	Trans. Congestion Rights	Financial Trans. Rights
Contract	Option-like, no hedge against losses	Inter-zonal option	Obligation, phase in option in the future
Duration	Annual auction	Monthly and annual auction	3 months or 1 year auction
Acquisition	Auction, secondary market, hour-ahead market	Auction, secondary market	Auction, secondary market, allocated based on existing transmission rights
Auction design	Annual, multi-round uniform-price auction	Annual, monthly, single-round, 24 simult. auction	Annual, seasonal(3 months), monthly auction
Congestion rents	Excess rents partly cover the fixed costs of the grid deficient rents reduce payments proportionally	Any rent shortfall is uplifted to load and any surplus is credited against other uplift to load	Excess rents redistributed to FTR holders
Distribution of revenues	Credited to trans. owners	Credited to load entities in proportion to their load ratio share	To be determined
Website	<a href="http://www.caiso.com/">http://www.caiso.com/</a>	<a href="http://www.ercot.com/">http://www.ercot.com/</a>	<a href="http://www.midwestiso.org/">http://www.midwestiso.org/</a>



### 2.3.3 Overview of the Two-stage FTR Model

Although the current literature expresses mixed opinions about FTRs, it is not unfair to say more negative views are held toward FTRs (Joskow and Tirole 2000, Oren 1997, Bushnell 1999, Siddiqui et al. 2003, Deng et al. 2004, etc). While FTRs are widely adopted as a financial hedging instrument to help market participants to reduce their risks in the major U.S. wholesale power market, it seems not working very well. Why? Is it because of the complicated wholesale power market structure, or because the market participants are still learning how to place the bids and offers more efficiently, or because there is something fundamentally wrong about it?

Some close examination of previous work might give us some clues. For example, in a well-known paper by Joskow and Tirole (2000), we found that although the authors demonstrated that introducing FTRs can decrease the overall efficiency, enhance the market power and reduce the welfare, their model seems to be too restrictive in the sense that *there is no uncertainty involved*. Since FTR, by construction, is used as a financial instrument to hedge against *uncertain* profit, if there is no uncertainty, the only conclusion that can be drawn is that FTR at most will not do any good and may in general do worse than the case where there are no FTRs available. In fact, Joskow and Tirole's welfare comparison shows that the social welfare in the absence of FTRs is as high as and in general strictly higher than that with FTRs in the case of no uncertainty.

One contribution of this paper is to illustrate how a simple two-stage FTR model can work to improve social welfare should there be any uncertainty. Specifically, we would like to address the following fundamental question: when a source of uncertainty is introduced in the model, does FTR matter? In addition we want to conduct a welfare comparison in the uncertainty case to see whether introducing FTRs is able to improve the social welfare. We start in Section 3 (Stage 1) by constructing a benchmark model, which focuses on a two-node electric network where there are one generator and one LSE at each node with parameterized marginal cost and demand functions, supervised by an independent system operator (ISO). This is essentially the competitive equilibrium (CE) case. By solving this benchmark model as the usual CE case, we obtain a economic dispatch solution. Section 4 (Stage 2) presents the FTR model with

stochastic shocks. Using the results from the benchmark model as building blocks, we then solve for the optimal FTR hedge solutions, and show that once uncertainty (even in a very simple form) is introduced, the acquisitions of optimal FTRs by the risk averse generators and LSEs will increase and in general will strictly increase the social welfare compared with the case where there are no FTRs available. This result thus serves as a counterexample to the somewhat negative views of FTRs by other economists in the literature, and provides some economic explanations to the fact that FTRs are widely adopted as a financial hedge instrument in the major U.S. wholesale power markets.

## 2.4 The No-rights Benchmark Model

The benchmark model consists of a simple two-node electric network connected by a transmission line with a thermal limit. There is only one good in this model: electric power, which is supplied by a group of unregulated generating companies (or simply generators), and is demanded by a group of Load Serving Entities (LSEs). LSEs can be thought of as the distribution companies that can buy the “bundled” electric power in the wholesale market and resell it to downstream retail consumers. There is also an Independent System Operator (ISO) that operates the transmission network and manages the energy market. One of the main functions of ISO is to serve as the central clearing house in the wholesale electric power market. In summary, there are three types of agents in this model: generators, LSEs and ISO.

Furthermore, each LSE has a price-sensitive and downward sloping demand curve. Each generator supplies electric power with a non-decreasing marginal cost. To obtain a dispatched quantity of power, all generators submit their supply offers and all LSEs submit their demand bids to ISO in the wholesale power market. ISO by its nature is a not-for-profit organization and act as a “social planner” to maximize the total net benefit of generators and LSEs based on their submitted offers and bids by solving the optimal quantities of power supply and demand for each generator and LSE subject to the physical network constraints <sup>3</sup>.

<sup>3</sup>This modelling framework is a simplified version of Standard Market Design(SMD) implemented by ISO New England since March 2003. See ISO New England (2003a) for detailed descriptions.

### 2.4.1 Model Specifications and Assumptions

To simplify the benchmark model, I make the following specifications and assumptions:

- There are only two nodes, namely node 1 and node 2, in this benchmark model. This implies that power may either flow from node 1 to node 2 or node 2 to node 1 through the transmission line with the maximum power flow equal to the thermal limit capacity  $T$  ( $T > 0$ ). Also assume there is no loss during power transmission.
- For simplicity, suppose there is only one generator at each node, i.e.,  $G_1$  at node 1 and  $G_2$  at node 2. Let  $Q_{G1}$  and  $Q_{G2}$  be the power supply quantities (injections) at node 1 and 2, respectively. The total cost function  $TC_i(Q_{Gi})$ , variable cost function  $VC_i(Q_{Gi})$ , and marginal cost function  $MC_i(Q_{Gi})$  for generator  $G_i$  ( $i = 1, 2$ ) are specified as follows:

$$TC_1(Q_{G1}) = f_1 + b_1^S Q_{G1} + \frac{1}{2} a_1^S Q_{G1}^2 \quad (2.1)$$

$$TC_2(Q_{G2}) = f_2 + b_2^S Q_{G2} + \frac{1}{2} a_2^S Q_{G2}^2 \quad (2.2)$$

$$VC_1(Q_{G1}) = b_1^S Q_{G1} + \frac{1}{2} a_1^S Q_{G1}^2 \quad (2.3)$$

$$VC_2(Q_{G2}) = b_2^S Q_{G2} + \frac{1}{2} a_2^S Q_{G2}^2 \quad (2.4)$$

$$MC_1(Q_{G1}) = b_1^S + a_1^S Q_{G1} \quad (2.5)$$

$$MC_2(Q_{G2}) = b_2^S + a_2^S Q_{G2} \quad (2.6)$$

where parameters  $(a_i^S, b_i^S, f_i)$  are all positive for  $i = 1, 2$ .

- For simplicity, suppose there is only one LSE at each node, i.e.,  $LSE_1$  at node 1 and  $LSE_2$  at node 2. Let  $Q_{L1}$  and  $Q_{L2}$  be the power demand quantities (withdrawals) at node 1 and 2, respectively. The demand function  $D_j(Q_{Lj})$  and gross consumer surplus  $GCS_j(Q_{Lj})$  for  $LSE_j$  ( $j = 1, 2$ ) are specified as follows:

$$D_1(Q_{L1}) = b_1^D - a_1^D Q_{L1} \quad (2.7)$$

$$D_2(Q_{L2}) = b_2^D - a_2^D Q_{L2} \quad (2.8)$$

$$GCS_1(Q_{L1}) = b_1^D Q_{L1} - \frac{1}{2} a_1^D Q_{L1}^2 \quad (2.9)$$

$$GCS_2(Q_{L2}) = b_2^D Q_{L2} - \frac{1}{2} a_2^D Q_{L2}^2 \quad (2.10)$$

where parameters  $(a_j^D, b_j^D)$  are all positive for  $j = 1, 2$ . After purchasing  $Q_{Lj}$  amount of power in the wholesale market, each  $LSE_j$  can then sell the  $Q_{Lj}$  amount of power to its local downstream consumers and receive resale revenue equal to  $R_j$ <sup>4</sup>

- There are no learning or strategic behaviors for both generators and LSEs. Each generator offers its true marginal cost function and each LSE bids its true demand function into the electric power market. The information set consists of each generator's  $TC, VC, MC$  functions as well as each LSE's  $GCS$  and demand functions, which can be characterized by the structure parameter vector  $(a_j^D, b_j^D; a_i^S, b_i^S, f_i; T) > 0$  for  $i, j = 1, 2$ . This information set is publicly known by all agents. In short there is no uncertainty or no private information in this benchmark model.
- After receiving generator supply offers and LSE demand bids, ISO then solves a *Economic Dispatch* (ED)<sup>5</sup> problem by maximizing the total net benefit subject to a set of physical power network constraints in the day-ahead power market<sup>6</sup> to solve for the optimal dispatch quantities for all generators and LSEs and derive the associated *locational marginal prices*<sup>7</sup>(LMPs) for each node. Consequently, each generator produces  $Q_{Gi}$  amount of power at the ISO's dispatch and is paid by ISO the  $LMP_k$  per unit of its produced power for  $i, k = 1, 2$ , while each LSE purchases  $Q_{Lj}$  amount of power at the ISO's dispatch and pays ISO the  $LMP_k$  per unit of purchased power for  $j, k = 1, 2$ . Recall that since there is one transmission line connecting the two nodes, the total power

<sup>4</sup>The downstream resale revenue for  $LSE_j$  could be specified as  $R_j(Q_{Lj}) = (\beta_j - \alpha_j Q_{Lj})Q_{Lj}$  for  $j = 1, 2$ , where  $\beta_j$  and  $\alpha_j$  are the parameters of aggregate demand function in the resale market at node 1 ( $j = 1$ ) and node 2 ( $j = 2$ ).

<sup>5</sup>See the following section for a discussion of this ED problem formulation.

<sup>6</sup>According to ISO New England Standard Market Design (SMD), the U.S. wholesale power market is operated through a two-settlement system which consists of several submarkets including Day-Ahead, Real-Time, Supply Re-offers, FTR, and bilateral markets to reduce uncertainty for market participants and ensure orderly, fair, and efficient market outcomes. For simplicity, assume the scheduled quantities of powers in the Day-Ahead market are exactly carried out into the Real-Time market, all generators submit their true marginal cost (so no Supply Re-offer market is needed), and assume bilateral trades are prohibited. Thus in this paper only the Day-Ahead (in this section) and FTR (in the next section) (sub)markets are considered.

<sup>7</sup>*Roughly stated, locational price at any given node is the minimum incremental cost of providing one additional unit of power at that node.*

produced at a local node does not have to be the same with its local demand. For example, some low-cost generator may produce more than its local demand and transfer the “overproduced” power through the transmission line to fulfill the residual demand at a high-cost generation node. However the power flow through the transmission line has an upper limit equal to the line thermal capacity  $T$ . When the power flow reaches that upper limit  $T$ , we call the line is congested. One important consequence of congestion is that the LMPs will no longer be the same across all nodes. Assuming no loss during power transmission, the separation of LMPs creates the *congestion rent* (CR) (difference between  $LMP_1$  and  $LMP_2$  multiplied by  $T$ ), which is accrued to ISO.

- To further simplify the model, assume the minimum production capacities for  $G_1$  and  $G_2$  are both zero implying that it is feasible for generators to stop producing power while bearing the fixed cost. Also assume the maximum production capacities for  $G_1$  and  $G_2$  are both infinitely large so that the generators can meet arbitrarily high demands in the power market. Therefore the *locational marginal prices* for node 1 and 2,  $LMP_1$  and  $LMP_2$ , are the last unit marginal cost for Generator 1 and 2 or the marginal unit of willingness to pay for LSE 1 and LSE 2 when the thermal constraint  $T$  is binding;  $LMP_1$  and  $LMP_2$  become the same and are equal to the market clearing price of the aggregate demand and supply functions when the thermal constraint is not binding, i.e., no line congestions.
- The benchmark model can best summarized in Figure 2.

### 2.4.2 Model Setup

Based on the above assumptions and specifications, this benchmark model can be formulated as the *Economic Dispatch* (ED) problem<sup>8</sup>. As detailed in Stoft (2002), *dispatch* is the process of determining generator output level for servicing the load demand by LSEs. *Economic Dispatch* means that the dispatch process is efficient.

Specifically, the objective of the ED problem is to maximize the “total net benefit” (TNB) subject to the balancing, non-negativity, and thermal limit constraints. The balancing con-

<sup>8</sup>The ED problem is essentially a constrained optimization problem.

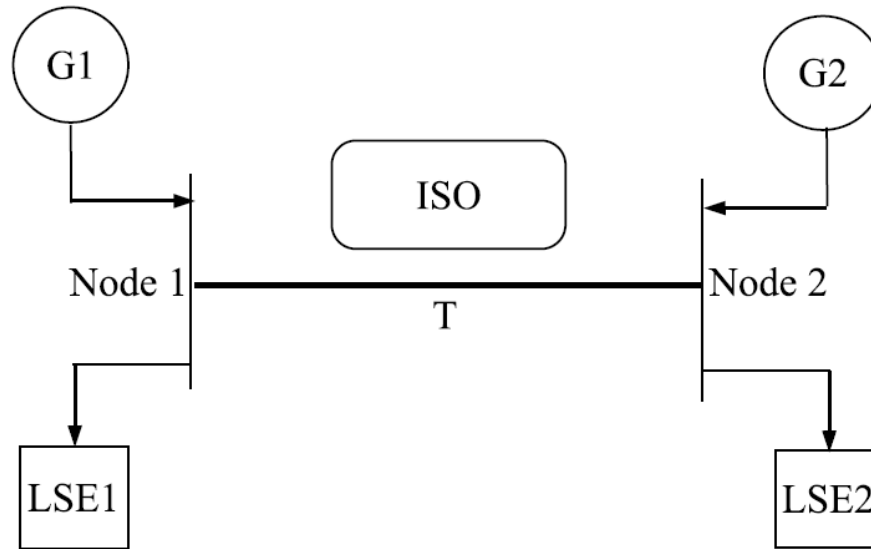


Figure 2.2 The two-node electric network benchmark model

straint should be respected because it represents the physical aspect of the electric network, i.e., total power injections should be equal to total power withdrawals at any time and at any node in the electric network. In our benchmark model, this requires that the power supplies by  $G_1$  and  $G_2$  should be equal to power demands by  $LSE_1$  and  $LSE_2$ . The non-negativity constraint holds naturally since we only allow the real power production and purchasing in this model, and exclude the speculative behaviors such as taking short positions in the wholesale power market. Lastly the thermal limit constraints have to be observed because the power flow between two nodes cannot exceed the thermal capacity limit of the transmission line.

When the thermal constraint becomes binding, it might be necessary to supply the next unit of power by dispatching the relatively expensive local generation *out of merit order*, i.e., in place of the other generation with lower marginal cost. *Locational marginal prices* (LMPs) reflect the cost of this out-of-merit-order dispatch. Separate LMPs are calculated for each pricing location (node). Technically,  $LMP_k$  at any node  $k$  is defined to be the change in total

system variable costs that would result if one more unit of power were to be serviced at node  $k$ . In our simple benchmark model,  $LMP_k$  then reduces to the marginal cost of the last unit of power for generator at node  $k$ ,  $k = 1, 2$ . In the absence of binding thermal limit constraint, and assuming no transmission losses, each node has the same LMP. Otherwise, however, *price separation* can occur, meaning that different nodes can have different LMPs.

Next, TNB is defined as the sum of all LSE surpluses and all generator surpluses. In the benchmark model, TNB is just the sum of surpluses from  $LSE_1, LSE_2, G_1, G_2$ . Geometrically, TNB represents the summed area under the demand curve less the area under the supply curve (marginal cost curve) over two nodes. Formally the model is set up as follows:

Maximize

$$TNB = \int_0^Q [D_1(Q_{L1}) - MC_1(Q_{G1})]dQ + \int_0^Q [D_2(Q_{L2}) - MC_2(Q_{G2})]dQ \quad (2.11)$$

$$= [GCS_1(Q_{L1}) - VC_1(Q_{G1})] + [GCS_2(Q_{L2}) - VC_2(Q_{G2})] \quad (2.12)$$

where

$$GCS_1(Q_{L1}) - VC_1(Q_{G1}) = (b_1^D Q_{L1} - \frac{1}{2}a_1^D Q_{L1}^2) - (b_1^S Q_{G1} + \frac{1}{2}a_1^S Q_{G1}^2) \quad (2.13)$$

$$GCS_2(Q_{L2}) - VC_2(Q_{G2}) = (b_2^D Q_{L2} - \frac{1}{2}a_2^D Q_{L2}^2) - (b_2^S Q_{G2} + \frac{1}{2}a_2^S Q_{G2}^2) \quad (2.14)$$

with respect to  $Q_{G1}, Q_{G2}, Q_{L1}, Q_{L2}$

subject to:

$$Q_{G1} + Q_{G2} = Q_{L1} + Q_{L2} \text{ (balancing constraint)} \quad (2.15)$$

$$Q_{G1} \geq 0, Q_{G2} \geq 0, Q_{L1} \geq 0, Q_{L2} \geq 0 \text{ (non-negativity constraint)} \quad (2.16)$$

$$-T \leq Q_{G1} - Q_{L1} \leq T \text{ (thermal constraint for node 1)} \quad (2.17)$$

$$-T \leq Q_{G2} - Q_{L2} \leq T \text{ (thermal constraint for node 2)} \quad (2.18)$$

In this ED problem, we want to solve for the vector

$$s^* = (Q_{G1}^*, Q_{G2}^*, Q_{L1}^*, Q_{L2}^*)$$

which maximizes (11) or (12) subject to (15) - (18). Based on this solution we can then derive  $LMP_1$  and  $LMP_2$ <sup>9</sup>. Note that the ED solution vector  $s^*$  is ISO's dispatch quantities in the day-ahead market, and  $LMP_1$  and  $LMP_2$  are the locational marginal price applied to node 1 and node 2, respectively.

### 2.4.3 The Economic Dispatch (ED) Solution

To present the solution to this ED problem in a more orderly fashion, it is proposed in this paper to solve the ED problem in two steps. In the first step, assume the thermal limit  $T$  is so large that the thermal constraints will never get binding (thus the two thermal constraints are ignored), which simplifies the problem at hand to be a standard maximization problem. Then use the solved optimal solutions to check if the thermal limit constraints are indeed binding or not. If not binding, then problem is solved; if binding, then proceed to step 2. In step 2, resolve the ED problem by adding one of the thermal limit constraint as the equality constraint. The formal procedure of solving this model is presented as follows:

#### 2.4.3.1 Step 1: Thermal constraint $T$ is NOT binding

In this step, suppose the thermal limit  $T$  is so large that the thermal constraint will never get binding. According to the model setup section, this is a standard optimization problem with one equality constraint (the balancing constraint) and four inequality constraints (the non-negativity constraints for  $Q_{G1}$ ,  $Q_{G2}$ ,  $Q_{L1}$  and  $Q_{L2}$ ). Use  $\mu$  as the multiplier for equality constraint and  $\lambda$ 's as the multipliers for inequality constraints, and formulate the Lagrangian equation:

$$L = (b_1^D Q_{L1} - \frac{1}{2} a_1^D Q_{L1}^2) - (b_1^S Q_{G1} + \frac{1}{2} a_1^S Q_{G1}^2) + (b_2^D Q_{L2} - \frac{1}{2} a_2^D Q_{L2}^2) - (b_2^S Q_{G2} + \frac{1}{2} a_2^S Q_{G2}^2) \\ + \mu(Q_{G1} + Q_{G2} - Q_{L1} - Q_{L2}) + \lambda_{G1} Q_{G1} + \lambda_{G2} Q_{G2} + \lambda_{L1} Q_{L1} + \lambda_{L2} Q_{L2} \quad (2.19)$$

<sup>9</sup>By definition, the locational marginal price (LMP) at node  $k$  is the minimum incremental cost of producing one additional unit of power at node  $k$ . Recall in this benchmark model, we assume the zero minimum production and infinitely large maximum production capacity, the minimum incremental cost of producing one more unit of power is just the marginal cost at that node. Furthermore, as we will show in the Appendix 1 and 2, LMP is indeed captured by the Lagrangian multiplier associated with the balancing constraint.



For simplicity, only consider the case where all dispatched quantities are positive, i.e., all non-negativity constraints are not binding<sup>10</sup>, we obtain the following non-thermal-constraint solution (denoted with a hat). (The detailed derivation is provided in Appendix 1):

$$\hat{Q}_{G1} = (\mathbb{G}_1 + \mathbb{B}_1)/\mathbb{A} \quad (2.20)$$

$$\hat{Q}_{G2} = (\mathbb{G}_2 + \mathbb{B}_2)/\mathbb{A} \quad (2.21)$$

$$\hat{Q}_{L1} = (\mathbb{L}_1 + \mathbb{C}_1)/\mathbb{A} \quad (2.22)$$

$$\hat{Q}_{L2} = (\mathbb{L}_2 + \mathbb{C}_2)/\mathbb{A} \quad (2.23)$$

where

$$\begin{aligned} \mathbb{G}_1 &= D_2 B_1 + a_1^D a_2^S B_2, \quad \mathbb{B}_1 = a_1^D A_2 C_1, \quad \mathbb{L}_1 = (D_2 + a_1^S A_2) B_1 - a_1^S a_2^S B_2, \quad \mathbb{C}_1 = a_1^S A_2 C_2; \\ \mathbb{G}_2 &= D_1 B_2 + a_1^S a_2^D B_1, \quad \mathbb{B}_2 = a_2^D A_1 C_2, \quad \mathbb{L}_2 = (D_1 + a_2^S A_1) B_2 - a_1^S a_2^S B_1, \quad \mathbb{C}_2 = a_2^S A_1 C_1; \\ \mathbb{A} &= D_1 A_2 + D_2 A_1; \end{aligned}$$

$$\begin{aligned} A_1 &= a_1^D + a_1^S, \quad B_1 = b_1^D - b_1^S, \quad C_1 = b_2^S - b_1^S, \quad D_1 = a_1^D a_1^S; \\ A_2 &= a_2^D + a_2^S, \quad B_2 = b_2^D - b_2^S, \quad C_2 = b_1^S - b_2^S, \quad D_2 = a_2^D a_2^S. \end{aligned}$$

Now that we solve the non-thermal-constraint ED problem and need to examine closely the solution  $(\hat{Q}_{G1}, \hat{Q}_{G2}, \hat{Q}_{L1}, \hat{Q}_{L2})$  to determine whether the thermal limit constraints are actually binding or not. Before proceeding further, we formally define the term *thermal constraint is not binding*, *thermal constraint is binding from 1 to 2*, and *thermal constraint is binding from 2 to 1* as follows:

**Definition 1** *In this two-node electric network model, after solving the non-thermal-constraint ED problem and obtaining the solution vector  $(\hat{Q}_{G1}, \hat{Q}_{G2}, \hat{Q}_{L1}, \hat{Q}_{L2})$ , regarding the thermal limit  $T$ , we say,*

- *$T$  is binding from 1 to 2 if  $\hat{Q}_{G1} - \hat{Q}_{L1} > T$  or  $\hat{Q}_{G2} - \hat{Q}_{L2} < -T$ ;*
- *$T$  is binding from 2 to 1 if  $\hat{Q}_{G2} - \hat{Q}_{L2} > T$  or  $\hat{Q}_{G1} - \hat{Q}_{L1} < -T$ .*

<sup>10</sup>To be exhaustive, we find 9 other possible solution cases, i.e., (1)  $Q_{G1} = 0$ ; (2)  $Q_{G2} = 0$ ; (3)  $Q_{L1} = 0$ ; (4)  $Q_{L2} = 0$ ; (5)  $Q_{G1} = Q_{L1} = 0$ ; (6)  $Q_{G1} = Q_{L2} = 0$ ; (7)  $Q_{G2} = Q_{L1} = 0$ ; (8)  $Q_{G2} = Q_{L2} = 0$ ; (9)  $Q_{G1} = Q_{G2} = Q_{L1} = Q_{L2} = 0$ .

- $T$  is not binding if  $|\hat{Q}_{G1} - \hat{Q}_{L1}| \leq T$  or  $|\hat{Q}_{G2} - \hat{Q}_{L2}| \leq T$ ;

**Remarks:** this definition elaborates the relationship between the optimal ED solution and network physical conditions. Recall in this step we assume the thermal constraint will not be binding and proceed to solve the ED problem, and the solution is the actual dispatched quantity that each generator will produce and each LSE will purchase. If the ED solution requires at node 1 what  $G_1$  produces ( $\hat{Q}_{G1}$ ) be greater than what  $LSE_1$  purchases ( $\hat{Q}_{L1}$ ), then  $\hat{Q}_{G1} - \hat{Q}_{L1}$  amount of power will be transported from node 1 to node 2 through the transmission line to meet the residual demand  $\hat{Q}_{L2} - \hat{Q}_{G2}$ <sup>11</sup> at node 2. Nevertheless, the power flow is not allowed to exceed the upper limit of thermal capacity ( $T$ ) for the transmission line. So if that does happen, i.e.,  $\hat{Q}_{G1} - \hat{Q}_{L1} > T$  or equivalently,  $\hat{Q}_{L2} - \hat{Q}_{G2} > T$ , we call the thermal constraint is binding with power flowing from node 1 to node 2, or use the definition,  $T$  is binding from 1 to 2. In this case, the non-thermal-constraint ED solution is not appropriate any more, and we will need to continue on to solve the ED problem in Step 2.

If, on the other hand, the ED solution requires that at node 2 what  $G_2$  produces ( $\hat{Q}_{G2}$ ) be greater than what  $LSE_2$  purchases ( $\hat{Q}_{L2}$ ), then  $\hat{Q}_{G2} - \hat{Q}_{L2}$  amount of power will be transported from node 2 to node 1 through the transmission line to meet the residual demand, which is equal to  $\hat{Q}_{L1} - \hat{Q}_{G1}$  at node 1. By the similar argument, the thermal constraint is binding with power flowing from node 2 to node 1, or use the definition,  $T$  is binding from 2 to 1. In this case, again we will need to continue on to solve the ED problem in Step 2 since the non-thermal-constraint ED solution is no longer valid.

If the power flow in the above two cases indeed does not exceed thermal limit  $T$ , i.e.,  $|\hat{Q}_{G1} - \hat{Q}_{L1}| \leq T$  or  $|\hat{Q}_{G2} - \hat{Q}_{L2}| \leq T$ , we call  $T$  is not binding<sup>12</sup>. In this case, the non-thermal-constraint ED solution is the right solution we seek, i.e., the solution vector is

$$s^* = (Q_{G1}^*, Q_{G2}^*, Q_{L1}^*, Q_{L2}^*)$$

<sup>11</sup>Note that the balancing constraint is observed here, i.e., extra production meets residual demand implying  $\hat{Q}_{G1} - \hat{Q}_{L1} = \hat{Q}_{L2} - \hat{Q}_{G2}$ , which is equivalent to the balancing constraint  $\hat{Q}_{G1} + \hat{Q}_{G2} = \hat{Q}_{L1} + \hat{Q}_{L2}$

<sup>12</sup>In this two-node benchmark model, there is small likelihood that the ED solution requires what Generator 1 produces happen to be the same as what LSE 1 purchases. Then by the balancing constraint, this implies that what Generator 2 produces has to be the same as what LSE 2 purchases. So there is zero power flow between node 1 and node 2. This case certainly falls into the category of “ $T$  is not binding”.

where

$$Q_{G1}^* = \hat{Q}_{G1}$$

$$Q_{G2}^* = \hat{Q}_{G2}$$

$$Q_{L1}^* = \hat{Q}_{L1}$$

$$Q_{L2}^* = \hat{Q}_{L2}$$

$$LMP_1 = LMP_2 = (D_2 E_1 + D_1 E_2) / \mathbb{A}$$

where  $\mathbb{A}$ ,  $D_1$ ,  $D_2$  are as previously specified and  $E_1 = a_1^D b_1^S + a_1^S b_1^D$ ,  $E_2 = a_2^D b_2^S + a_2^S b_2^D$ .

By the nature of this problem, the thermal constraint is not binding, each generator offers its true marginal cost function, each LSE bid its true demand functions, and ISO acts as a “social planner” trying to maximize the total net benefit taking into account of all generator’s production cost and all LSE’s willingness to pay, and there is no strategic behaviors or any other system distortions. From the standard microeconomics point of view, this is both the competitive equilibrium and Pareto optimal outcome. LMPs are the same across two nodes as a result of aggregate market (node) clearing process <sup>13</sup>.

#### 2.4.3.2 Step 2: Thermal constraint $T$ is binding

Based on Step 1, if we know  $T$  is binding from 1 to 2, i.e.,  $\hat{Q}_{G1} - \hat{Q}_{L1} > T$ , we can set  $Q_{G1} - Q_{L1} = T$ , the ED problem does not change from Step 1 other than adding one more constraint  $Q_{G1} - Q_{L1} = T$ . Denoting  $\mu$ ’s as the multipliers for equality constraints and  $\lambda$ ’s as the multipliers for inequality constraints, and form the Lagrangian equation as follows:

$$\begin{aligned} L = & (b_1^D Q_{L1} - \frac{1}{2} a_1^D Q_{L1}^2) - (b_1^S Q_{G1} + \frac{1}{2} a_1^S Q_{G1}^2) + (b_2^D Q_{L2} - \frac{1}{2} a_2^D Q_{L2}^2) - (b_2^S Q_{G2} + \frac{1}{2} a_2^S Q_{G2}^2) \\ & + \mu_B (Q_{G1} + Q_{G2} - Q_{L1} - Q_{L2}) + \mu_T (T - Q_{G1} + Q_{L1}) + \lambda_{G1} Q_{G1} + \lambda_{G2} Q_{G2} + \lambda_{L1} Q_{L1} + \lambda_{L2} Q_{L2} \end{aligned} \quad (2.24)$$

<sup>13</sup>It is worth mentioning that when thermal constraint is not binding, the ED solution can also be obtained through the market clearing point of the aggregate supply (marginal cost) and aggregate demand curves, i.e., finding the aggregate market clearing price (the common LMP) and referring it back to the individual demand and supply curves to obtain the ED solution.

For simplicity, only consider the case where all dispatched quantities are positive, i.e., all non-negativity constraints are not binding <sup>14</sup>, we obtain the following thermal-constraint-binding solution  $(Q_{G1}^*, Q_{G2}^*, Q_{L1}^*, Q_{L2}^*)$  (The detailed derivation is provided in Appendix 2):

$$Q_{G1}^* = (B_1 + a_1^D T)/A_1 \quad (2.25)$$

$$Q_{G2}^* = (B_2 - a_2^D T)/A_2 \quad (2.26)$$

$$Q_{L1}^* = (B_1 - a_1^S T)/A_1 \quad (2.27)$$

$$Q_{L2}^* = (B_2 + a_2^S T)/A_2 \quad (2.28)$$

$$LMP_1 = (E_1 + D_1 T)/A_1 \quad (2.29)$$

$$LMP_2 = (E_2 - D_2 T)/A_2 \quad (2.30)$$

where

$$\begin{aligned} A_1 &= a_1^D + a_1^S, & B_1 &= b_1^D - b_1^S, & D_1 &= a_1^D a_1^S, & E_1 &= a_1^D b_1^S + a_1^S b_1^D; \\ A_2 &= a_2^D + a_2^S, & B_2 &= b_2^D - b_2^S, & D_2 &= a_2^D a_2^S, & E_2 &= a_2^D b_2^S + a_2^S b_2^D. \end{aligned}$$

Similarly, if, from Step 1, we know  $T$  is binding from 2 to 1, i.e.,  $\hat{Q}_{G2} - \hat{Q}_{L2} > T$ , we can set  $Q_{G2} - Q_{L2} = T$ , and obtain the following thermal-constraint-binding solution  $(Q_{G1}^*, Q_{G2}^*, Q_{L1}^*, Q_{L2}^*)$ :

$$Q_{G1}^* = (B_1 - a_1^D T)/A_1 \quad (2.31)$$

$$Q_{G2}^* = (B_2 + a_2^D T)/A_2 \quad (2.32)$$

$$Q_{L1}^* = (B_1 + a_1^S T)/A_1 \quad (2.33)$$

$$Q_{L2}^* = (B_2 - a_2^S T)/A_2 \quad (2.34)$$

$$LMP_1 = (E_1 - D_1 T)/A_1 \quad (2.35)$$

$$LMP_2 = (E_2 + D_2 T)/A_2 \quad (2.36)$$

<sup>14</sup>To see the complete solutions, refer to Appendix 2.

#### 2.4.4 Solution Discussion

Based on the two-step ED solution and the associated locational marginal prices  $LMP_1$  and  $LMP_2$ , we can obtain the following propositions:

**Proposition 1** *In the two-node electric network model, when thermal constraint  $T$  is binding, power flows from node 1 to node 2 (or node 2 to node 1) if and only if  $LMP_2 > LMP_1$  (or  $LMP_1 > LMP_2$ )(assuming the dispatched quantities are all positive in the ED solution). Furthermore,*

$$(*1) \ T \text{ is binding from 1 to 2} \Leftrightarrow LMP_2 > LMP_1 \Leftrightarrow \Omega > T \quad (2.37)$$

$$(*2) \ T \text{ is binding from 2 to 1} \Leftrightarrow LMP_2 < LMP_1 \Leftrightarrow \Omega < -T \quad (2.38)$$

$$(*3) \ T \text{ is NOT binding} \Leftrightarrow LMP_2 = LMP_1 \Leftrightarrow -T \leq \Omega \leq T \quad (2.39)$$

where

$$\Omega = (A_1E_2 - A_2E_1)/(D_1A_2 + D_2A_1);$$

$$A_1 = a_1^D + a_1^S, \quad D_1 = a_1^D a_1^S, \quad E_1 = a_1^D b_1^S + a_1^S b_1^D;$$

$$A_2 = a_2^D + a_2^S, \quad D_2 = a_2^D a_2^S, \quad E_2 = a_2^D b_2^S + a_2^S b_2^D.$$

Proposition 1 has shown the relationship between the power flow direction and magnitude of LMPs under the condition that the thermal constraint is binding in the two-node electric network model<sup>15</sup>. Recall that if the thermal constraint is not binding, even if there is power flow, the LMPs will be the same across two nodes (see the Step 1 ED solution). So this proposition basically asserts that whenever the thermal constraint  $T$  is binding, the power (which is equal to  $T$ ) always flows from low LMP node to high LMP node in a two-node network model. This result can be derived mathematically from the ED solution and thermal constraint binding conditions in this benchmark model. The detailed proof of Proposition 1 is provided in Appendix 3.

The economic intuition behind this proposition is that the generator at the high LMP node has a high marginal cost and the generator at the low LMP node has a low marginal cost<sup>16</sup>.

<sup>15</sup>However, as the counter example in Kirschen and Strbac (2004) shows, the result in this proposition does not generalize to the case where the number of nodes is greater than or equal to three due to the externality brought by the “loop flow” effect.

<sup>16</sup>Recall LMP is defined as the last unit marginal cost of the generator at the local node

So when ISO, acting as a TNB maximizer, dispatches the high cost generator to produce less than its local demand and the low cost generator to produce more than its local demand and transfer the excess supply (which is equal to  $T$ ) over the transmission line to meet the excess demand (which is equal to  $T$ ) in the high LMP node, the power is indeed flowing from low LMP node to high LMP node. As we will see in the later section, this proposition serves as the crucial foundation to derive FTR values,

**Proposition 2** *In the two-node electric network model, the ED solution guarantees each generator's profit has a function form as:*

$$\pi_{Gk} = \frac{1}{2}a_k^S Q_{Gk}^2 - f_k, \quad \forall k = 1, 2 \quad (2.40)$$

and each LSE's profit has a function form as:

$$\pi_{Lk} = R_k(Q_{Lk}) - LMP_k Q_{Gk} \quad \forall k = 1, 2 \quad (2.41)$$

**Proof:** As the ED solution suggests, in the benchmark model, regardless whether thermal constraint is binding or not, each generator submitting its true marginal cost function produces the dispatched quantity  $Q_{Gk}$  and receives revenue equal to  $LMP_k Q_{Gk}$  while incurring a total cost equal to  $f_k + b_k^S Q_{Gk} + \frac{1}{2}a_k^S Q_{Gk}^2$ . Also recall that  $LMP_k$  is equal to the last unit marginal cost of generator  $k$  for  $k = 1, 2$ . The profit function of generator  $k$  is:

$$\begin{aligned} \pi_{Gk} &= LMP_k Q_{Gk} - TC_k(Q_{Gk}) \\ &= (b_k^S + a_k^S Q_{Gk})Q_{Gk} - (f_k + b_k^S Q_{Gk} + \frac{1}{2}a_k^S Q_{Gk}^2) \\ &= \frac{1}{2}a_k^S Q_{Gk}^2 - f_k, \quad \forall k = 1, 2 \end{aligned}$$

Similarly, each LSE submitting its true demand function gets the dispatched quantity  $Q_{Lk}$  and receives revenue equal to  $R_k(Q_{Lk})$  from downstream consumers while paying a total amount of  $LMP_k Q_{Lk}$  for purchasing the power energy. The profit function of LSE  $k$  is:

$$\pi_{Lk} = R_k(Q_{Lk}) - LMP_k Q_{Gk} \quad \forall k = 1, 2$$

This proposition shows that in the benchmark model, if generator  $G_k$  gets dispatched it will produce  $Q_{Gk}$  to cover its fixed cost  $f_k$ . Note that if a generator does not get any dispatch,

then  $G_k$  must bear the negative profit equal to its fixed cost  $-f_k$ . Similarly, if  $LSE_k$  gets demand dispatch it will purchase  $Q_{Lk}$  to meet its downstream consumer demand and acquires profit equal to its resale revenue less its payment.

**Proposition 3** *In this two-node electric network model, the social welfare can be measured by total net benefit (TNB), and TNB increases as the thermal limit  $T$  increases, provided that the thermal constraint is still binding. The comparative statics are shown as follows:*

$$\frac{\partial TNB}{\partial T} = \begin{cases} \frac{E_2}{A_2} - \frac{E_1}{A_1} - \left( \frac{D_1}{A_1} + \frac{D_2}{A_2} \right) T > 0 & \text{iff } T \text{ is binding from 1 to 2;} \\ \frac{E_1}{A_1} - \frac{E_2}{A_2} - \left( \frac{D_1}{A_1} + \frac{D_2}{A_2} \right) T > 0 & \text{iff } T \text{ is binding from 2 to 1.} \end{cases} \quad (2.42)$$

where

$$\begin{aligned} A_1 &= a_1^D + a_1^S, & D_1 &= a_1^D a_1^S, & E_1 &= a_1^D b_1^S + a_1^S b_1^D; \\ A_2 &= a_2^D + a_2^S, & D_2 &= a_2^D a_2^S, & E_2 &= a_2^D b_2^S + a_2^S b_2^D. \end{aligned}$$

The proof is provided in Appendix 4. This proposition has a rich economic meaning and important policy implications. It states that if the thermal limit of transmission line  $T$  can be increased it will increase TNB<sup>17</sup> and thus lead to a more efficient production and a higher social welfare, provided that  $T$  is still binding. (Once the thermal constraint  $T$  becomes non-binding, according to the ED solution, we have already obtained the first-best outcome in the sense that it's both competitive and Pareto optimal solution. Further investment in the transmission line will thus be a waste of resources, provided that there is no uncertainty.) However, expanding the capacity of transmission line (so as to increase the thermal limit  $T$ ) involves issues such as “free ride” due to its public good feature. So how to create incentives for market participants to make transmission investment remains an important and yet challenging concern to ISO.

To finish the benchmark model and proceed to the next section, we define the definition of congestion rent.

<sup>17</sup>Recall that total net benefit (TNB) consists of two components, consumer surplus (CS) and producer surplus (PS). This proposition only shows that TNB increases when thermal limit  $T$  increases. It does not indicate the individual effect of CS and PS. As a matter of fact, in one of their examples, Kirschen and Strbac (2004) shows that when the thermal limit  $T$  increases, in some circumstances, CS will decrease and then increase while PS is monotonically increasing. So the policy implication is that to promote the idea of transmission investment may improve the payoffs of generators at the cost of worsening the payoff of LSEs (for some range of thermal capacity  $T$ ) although the total net effect is Pareto improvement.

**Definition 2** *In the two-node electric network model, when thermal constraint is binding, i.e., the transmission line is congested, ISO acquires the congestion rent (CR) as its revenue, which is equal to the difference in LMPs multiplied by  $T$ , that is,*

$$CR = |LMP_2 - LMP_1|T \quad (2.43)$$

**Remarks:** (a) When the thermal constraint  $T$  is binding from 1 to 2, i.e.,  $T$  amount of power flowing from node 1 to node 2. At node 1,  $G_1$  receives revenue  $LMP_1 * Q_{G1}$  from ISO and  $LSE_1$  makes payment  $LMP_1 * Q_{L1}$  to ISO. Since  $T$  is binding from 1 to 2,  $Q_{G1} - Q_{L1} = T$ . Therefore ISO has a revenue deficit equal to  $-LMP_1 * T$ . Conversely, at node 2,  $G_2$  receives revenue  $LMP_2 * Q_{G2}$  from ISO and  $LSE_2$  makes payment  $LMP_2 * Q_{L2}$  to ISO. Since  $T$  is binding from 1 to 2,  $Q_{L2} - Q_{G2} = T$ . Therefore ISO has a revenue surplus equal to  $LMP_2 * T$ . The ISO's clearing process can be expressed as:

$$\begin{aligned} \text{ISO's revenue} &= -LMP_1 Q_{G1} + LMP_1 Q_{L1} - LMP_2 Q_{G2} + LMP_2 Q_{L2} \\ &= -LMP_1 T + LMP_2 T \\ &= (LMP_2 - LMP_1)T \end{aligned}$$

Hence the ISO's revenue (congestion rent) is equal to  $(LMP_2 - LMP_1)T$ . This congestion rent is positive since  $LMP_2 > LMP_1$  when  $T$  is binding from 1 to 2 by Proposition 1.

(b) On the other hand, when the thermal constraint  $T$  is binding from 2 to 1, i.e.,  $T$  amounts of power flowing from node 2 to node 1, by the similar argument, the congestion rent accrued to ISO is equal to  $(LMP_1 - LMP_2)T$ . This congestion rent is positive since  $LMP_1 > LMP_2$  when  $T$  is binding from 2 to 1 by Proposition 1.

Hence by (a) and (b) we conclude that when thermal constraint is binding the congestion rent accrued to ISO is equal to  $|LMP_2 - LMP_1|T$ . This is a natural consequence of having a binding thermal constraint. In other words, the fact that thermal constraint is binding implies that the more expensive generation has been dispatched locally which could otherwise be serviced by the less expensive generation had the thermal constraint were not binding.

Note that the congestion rent can be related to the tariff issue in the international trade literature with the difference that tariff is imposed by government to purposely protect domestic



producers while congestion rent is the natural outcome of having a congested transmission line. Just like in international trade, decreasing the tariff would increase total social welfare, decreasing the congestion rent, thus increasing thermal limit  $T$ , would also enhance total net benefit (TNB) in this two-node electric network model(see Proposition 3).

## 2.5 The FTR Model under Network Uncertainty

Since the benchmark model depends exclusively on the structure parameters  $(a_j^D, b_j^D; a_i^S, b_i^S, f_i; T \forall i, j = 1, 2)$  that are fixed and known to public, there is no uncertainty and no private information, which implies that the ED solution derived from the benchmark model is already the competitive equilibrium (first-best) outcome. Therefore there is no incentive for agents to purchase FTRs, and introducing FTRs can at best do no good to the model economy. Indeed as Joskow and Tirole (2000) indicate in their model, the existence of FTRs in the absence of uncertainty will only decrease social welfare compared with the case there is no FTRs available. However, the benchmark model is very important because the ED solution and corresponding propositions serve as the building blocks to solve for the FTR model in this section.

Since the absence of uncertainty dooms the fate of FTRs, we are now interested to see whether introducing uncertainty into this model would create an incentive for agents to purchase FTRs, and if yes, to what extent could FTRs possibly help enhance the social welfare.

Based on the benchmark case, we will introduce a simple source of uncertainty into the model: the parameter values that characterize the cost attributes of generators and demand attributes of LSEs are now under stochastic shocks so that the direction of power flow and the magnitude of LMPs are no longer known in advance. This should create an incentive for both generators and LSEs to hedge against their uncertain profit streams through purchasing FTRs. We will develop a formal model to investigate this hypothesis and analyze the associated welfare effects.

Recall that a *financial transmission right* (FTR) is a financial hedging instrument that entitles the holder to receive compensation for transmission congestion costs that arise when a transmission line is congested. The *Wholesale Power Market Platform* (WPMP) proposed by

FERC (2003) recommends that transmission congestion be managed by the ISO through the issuance of *point-to-point* (PTP) FTRs obligation in the day-ahead power market. Holders of PTP FTR obligations would be charged or credited based on the congestion components in day-ahead market LMPs.

Two issues here need to be clarified before we proceed further. First, recall that there are four types of FTRs (PTP obligation, PTP option, FG<sup>18</sup> obligation, and FG option) currently available in the U.S. wholesale power markets. For simplicity, this model investigates only the first one, namely, the PTP FTR obligation. Hereafter if not stated explicitly, FTR means PTP FTR obligation. The second issue is concerned with the time horizon of the model. Recall that in this model, generators and LSEs can purchase FTRs to hedge against their future profit in the day-ahead power market. So the FTR market works as a forward market (denoted with time  $t = 0$ ), and day-ahead power market works as a spot market (denoted with time  $t = 1$ ). Hence terms such as FTR forward market or day-ahead spot market should not cause any confusions.

### 2.5.1 Model Specifications and Assumptions

- This model consists of two markets, one is FTR forward market and the other is day-ahead power market. The basic day-ahead power market structure is the same as the benchmark model in the last section, i.e., the two-node electric network model with one generator and one LSE at each node and an ISO in the middle to manage the transmission network and collect the congestion rent if the line is congested. All the cost and demand function forms remain the same as those in the benchmark model. Also for simplicity, assume the dispatched quantities are all positive from the ED problem in the benchmark model.
- To make the case of FTR interesting, assume the thermal limit constraint  $T$  is so small that it is always binding. The justification is that if the thermal constraint is not binding, there will be no price separation, i.e.,  $LMP_1 = LMP_2$ , which directly implies that the

<sup>18</sup>FG stands for *flowgate*, which is mainly implemented by ERCOT in Texas and partly implemented by CAISO in California.

value of FTR based on the difference of LMPs becomes zero for sure regardless whether there is uncertainty or not. Therefore to preclude this trivial case,  $T$  is assumed to be binding all the time.

- Introduce a stochastic shock to the two-node electric network model with a binding thermal limit constraint  $T$ : in the FTR forward market ( $t=0$ ) all agents know they will be in one of the two states, *state 1* or *state 2*, in the day-ahead power spot market ( $t=1$ ). If agents are in *state 1*,  $T$  will be binding from node 1 to node 2 with probability *prob*; if in *state 2*,  $T$  will be binding from node 2 to node 1 with probability  $1 - \text{prob}$ . Then according to Proposition 1, we have:

$$\begin{cases} \text{state 1: } T \text{ is binding from 1 to 2} \Leftrightarrow LMP_2 > LMP_1 \Leftrightarrow \Omega > T & \text{with } \text{prob}; \\ \text{state 2: } T \text{ is binding from 2 to 1} \Leftrightarrow LMP_2 < LMP_1 \Leftrightarrow \Omega < -T & \text{with } 1 - \text{prob}. \end{cases}$$

To differentiate the notations in two states, denote the realized values of parameters in state 1 with  $'$  and state 2 with  $''$ . All the structure parameters except thermal limit  $T$  are random variables denoted by  $\tilde{\cdot}$  such that

$$\begin{aligned} \tilde{a}_k^Z &= \begin{cases} a_k^{Z'} & \text{with } \text{prob}; \\ a_k^{Z''} & \text{with } 1 - \text{prob}, \quad \forall k = 1, 2; Z = D, S. \end{cases} \\ \tilde{b}_k^Z &= \begin{cases} b_k^{Z'} & \text{with } \text{prob}; \\ b_k^{Z''} & \text{with } 1 - \text{prob}, \quad \forall k = 1, 2; Z = D, S. \end{cases} \\ \tilde{f}_k &= \begin{cases} f_k' & \text{with } \text{prob}; \\ f_k'' & \text{with } 1 - \text{prob}, \quad \forall k = 1, 2. \end{cases} \end{aligned}$$

$$\begin{cases} \text{state 1: } T \text{ is binding from 1 to 2} \Leftrightarrow LMP_2' > LMP_1' \Leftrightarrow \Omega' > T & \text{with } \text{prob}; \\ \text{state 2: } T \text{ is binding from 2 to 1} \Leftrightarrow LMP_2'' < LMP_1'' \Leftrightarrow \Omega'' < -T & \text{with } 1 - \text{prob}. \end{cases}$$

In reality, the stochastic shocks may come from various sources. For example, weather change may suddenly increase or decrease LES's demand attributes. Or the price volatility of raw material for producing electricity such as coal or natural gas may suddenly increase or decrease generator's cost attributes. Since these kinds of changes are out of

control of any market participants, it seems to be reasonable to introduce these random shocks into the model to create a source of uncertainty.

- Introduce two types of FTRs in this model,  $FTR_{12}$  and  $FTR_{21}$ . (a) Define  $FTR_{12}$  as the PTP FTR obligation that obligates the owner to get paid if thermal constraint  $T$  is binding from 1 to 2 or get charged if thermal constraint  $T$  is binding from 2 to 1. The total amount of payments or charges are equal to the number of FTR contracts times  $LMP_2 - LMP_1$ . (b) Similarly, define  $FTR_{21}$  as the PTP FTR obligation that obligates the owner to get paid if thermal constraint  $T$  is binding from 2 to 1 or get charged if thermal constraint  $T$  is binding from 1 to 2. The total amount of payments or charges are equal to the number of FTR contracts times  $LMP_1 - LMP_2$ .
- In this model, it is ISO who has the authority to issue these two types of FTRs at pre-announced prices. Generators and LSEs can choose to buy these FTR contracts from ISO by paying the corresponding FTR prices and benefit from its payoffs. On the other hand, ISO receives the FTR sales revenue while paying for its associated payoffs to generators or LSEs. Recall that ISO still receive certain amount of congestion rent (CR) (what differs from the benchmark model is that now ISO does not know exactly how much CR it will obtain at time  $t = 0$ , but it can use the expected CR as an approximation). So the ISO's revenue adequacy condition is respected in expectation. Lastly, ISO also sets the maximum amounts of FTRs for sale.
- Relying on the literature of corporate risk management, which argues that firms could benefit from hedging market risks (Stulz (1990), Froot et al. (1993)), it is assumed in this study that firms (generators and LSEs) in the electric power market are risk averse and are likely to benefit from reducing the risk of their profits. Therefore, we assume generators and LSEs are risk averse with a *constant relative risk aversion* (CRRA) utility function. Furthermore, to make the calculation simple, assume all generators and LSEs possess a logarithmic utility function.
- Finally in this model, assume generators and LSEs can only buy FTRs (can take long

positions) but they cannot sell them (cannot take short positions), i.e., the FTR secondary market is not available in this model. Furthermore, note  $G_1$  and  $LSE_2$  will only buy  $FTR_{12}$  and  $G_2$  and  $LSE_1$  will only buy  $FTR_{21}$ . The reason is that since the agents are all assumed to be risk averse, they will not be willing to purchase a financial instrument that will make the risk of their profits even higher. For example, if  $G_1$  can buy  $FTR_{21}$ , it will only make its profit stream more volatile. That is, when  $G_1$  buys  $FTR_{21}$ , if  $LMP_1 > LMP_2$ ,  $FTR_{12}$  can bring  $LMP_1 - LMP_2$  amount of per contract profit to  $G_1$ , but  $G_1$  is already paid by the high  $LMP_1$ ; similarly, if  $LMP_1 < LMP_2$ ,  $G_1$  will incur  $LMP_1 - LMP_2$  amount of per contract loss for buying  $FTR_{21}$ , but  $G_1$  is already paid by the low  $LMP_1$ . So purchasing the  $FTR_{12}$  will only make the  $G_1$ 's profit stream even riskier. Similar arguments apply to  $G_2$ ,  $L_1$  and  $L_2$  too.

### 2.5.2 Model Setup

Generator and LSE total profits come from two sources: profit from power transactions (supply or demand) and profit from holding FTRs.

Denote  $G_k$ 's profit from power production as the random variable  $\tilde{\pi}_{Gk}$ . Then by Proposition 2, we have:

$$\tilde{\pi}_{Gk} = \begin{cases} \pi'_{Gk} = LMP'_k Q'_{Gk} - TC_k(Q'_{Gk}) = \frac{1}{2} a_k^{S'} Q'^2_{Gk} - f'_k & \text{with } prob; \\ \pi''_{Gk} = LMP''_k Q''_{Gk} - TC_k(Q''_{Gk}) = \frac{1}{2} a_k^{S''} Q''^2_{Gk} - f''_k & \text{with } 1 - prob, \quad \forall k = 1, 2. \end{cases} \quad (2.44)$$

Denote  $LSE_k$ 's profit from bulk power purchasing at the wholesale market and reselling it to downstream consumers as the random variable  $\tilde{\pi}_{Lk}$ . Then by Proposition 2, we have:

$$\tilde{\pi}_{Lk} = \begin{cases} \pi'_{Lk} = R_k(Q'_{Lk}) - LMP'_k Q'_{Lk} & \text{with } prob; \\ \pi''_{Lk} = R_k(Q''_{Lk}) - LMP''_k Q''_{Lk} & \text{with } 1 - prob, \quad \forall k = 1, 2. \end{cases} \quad (2.45)$$

where  $Q'_{Gk}$  and  $Q'_{Lk}$  are the Step 2 thermal-constraint-binding ED solution (binding from 1 to 2) in the benchmark model, and  $Q''_{Gk}$  and  $Q''_{Lk}$  are the Step 2 thermal-constraint-binding ED solution (binding from 2 to 1) in the benchmark model. Furthermore, to make the case interesting, it is reasonable to assume  $\frac{1}{2} a_k^{S'} Q'^2_{Gk} > f'_k$  and  $\frac{1}{2} a_k^{S''} Q''^2_{Gk} > f''_k$  so that  $\tilde{\pi}_{Gk} > 0$ .

This means in either state, the generator has a positive production profit thus does not go bankrupt. For the similar reason, assume  $R_k(Q'_{Lk}) > LMP'_k Q'_{Lk}$  and  $R_k(Q''_{Lk}) > LMP''_k Q''_{Lk}$  so that  $\tilde{\pi}_{Lk} > 0$ .

Denote  $FTR_{12}$ 's per contract payoff function as the random variable  $\tilde{H}_{12}$ . By the definition of an FTR and LMP solutions from Step 2 benchmark model, we have:

$$\tilde{H}_{12} = \begin{cases} H'_{12} = LMP'_2 - LMP'_1 = \frac{(A'_1 E'_2 - A'_2 E'_1) - (D'_2 A'_1 + D'_1 A'_2)T}{A'_1 A'_2} > 0 & \text{with prob;} \\ H''_{12} = LMP''_2 - LMP''_1 = \frac{(A''_1 E''_2 - A''_2 E''_1) + (D''_2 A''_1 + D''_1 A''_2)T}{A''_1 A''_2} < 0 & \text{with } 1 - \text{prob.} \end{cases} \quad (2.46)$$

Denote  $FTR_{21}$ 's per contract payoff function as the random variable  $\tilde{H}_{21}$ . By the definition of an FTR, we have  $\tilde{H}_{21} = -\tilde{H}_{12}$ .

At this point, it may be of some interest to know the relationship between the FTR payoff spread and the thermal limit  $T$ . Define the FTR payoff spread ( $FTR^{SP}$ ) as the net difference in the realized FTR payoffs in two states ( $|H' - H''|$ ). The following proposition will show that the increasing thermal limit  $T$  will always decrease the FTR payoff spread  $FTR^{SP}$ .

**Proposition 4** Define the FTR payoff spread as the net difference in the realized FTR payoffs in two states, that is,  $FTR_{12}^{SP} = H'_{12} - H''_{12}$  and  $FTR_{21}^{SP} = H''_{21} - H'_{21}$ . Then we have the following:

$$\frac{\partial FTR_{12}^{SP}}{\partial T} < 0, \quad \frac{\partial FTR_{21}^{SP}}{\partial T} < 0 \quad (2.47)$$

**Proof:** From the definition of FTR payoff function and FTR payoff spread, we have:

$$\begin{aligned} \frac{\partial FTR_{12}^{SP}}{\partial T} &= \frac{\partial H'_{12}}{\partial T} - \frac{\partial H''_{12}}{\partial T} \\ &= -\frac{D'_2 A'_1 + D'_1 A'_2}{A'_1 A'_2} - \frac{D''_2 A''_1 + D''_1 A''_2}{A''_1 A''_2} \\ &< 0 \quad (\text{since all parameters are positive}) \end{aligned}$$

$$\begin{aligned} \frac{\partial FTR_{21}^{SP}}{\partial T} &= \frac{\partial H''_{21}}{\partial T} - \frac{\partial H'_{21}}{\partial T} \\ &= -\frac{D''_2 A''_1 + D''_1 A''_2}{A''_1 A''_2} - \frac{D'_2 A'_1 + D'_1 A'_2}{A'_1 A'_2} \\ &< 0 \quad (\text{since all parameters are positive}) \end{aligned}$$

Q.E.D.

Now let's look at ISO's revenue components. Similar to generators and LSEs, ISO's total revenue comes from two parts as well: one from collecting the congestion rent and the other from selling FTRs.

Denote the congestion rent that accrues to ISO as the random variable  $\widetilde{CR}$ . Then by Definition 2, we have:

$$\widetilde{CR} = \begin{cases} CR' = (LMP'_2 - LMP'_1)T & \text{with } prob; \\ CR'' = (LMP''_1 - LMP''_2)T & \text{with } 1 - prob. \end{cases} \quad (2.48)$$

So the total profits for  $G_1$ ,  $G_2$ ,  $LSE_1$ , and  $LSE_2$  and the total revenue for ISO can be expressed as random variables  $\tilde{\Pi}_{G_1}$ ,  $\tilde{\Pi}_{G_2}$ ,  $\tilde{\Pi}_{L_1}$ ,  $\tilde{\Pi}_{L_2}$  and  $\tilde{\Pi}_{ISO}$ , respectively, that is,

$$\tilde{\Pi}_{G_1} = \tilde{\pi}_{G_1} + (\tilde{H}_{12} - \eta_{12})FTR_{12(G_1)} \quad (2.49)$$

$$\tilde{\Pi}_{G_2} = \tilde{\pi}_{G_2} + (\tilde{H}_{21} - \eta_{21})FTR_{21(G_2)} \quad (2.50)$$

$$\tilde{\Pi}_{L_1} = \tilde{\pi}_{L_1} + (\tilde{H}_{21} - \eta_{21})FTR_{21(L_1)} \quad (2.51)$$

$$\tilde{\Pi}_{L_2} = \tilde{\pi}_{L_2} + (\tilde{H}_{12} - \eta_{12})FTR_{12(L_2)} \quad (2.52)$$

$$\tilde{\Pi}_{ISO} = \tilde{CR} + (\eta_{12} - \tilde{H}_{12})\overline{FTR}_{12} + (\eta_{21} - \tilde{H}_{21})\overline{FTR}_{21} \quad (2.53)$$

where  $\eta_{12}$  and  $\eta_{21}$  are the ISO pre-announced prices of  $FTR_{12}$  and  $FTR_{21}$  at beginning of FTR market, i.e, at time  $t = 0$ . To make the case interesting, assume  $H'_{12} > \eta_{12}$  and  $H''_{21} > \eta_{21}$ , that is, ISO sets the FTR price below its positive payoff so that generators and LSEs know that if they buy FTRs they are not losing money for sure. To see this, suppose  $H'_{12} < \eta_{12}$  and take  $G_1$  for example. If  $G_1$  is in *state 1*, FTR's total payoff is  $(\tilde{H}_{12} - \eta_{12})FTR_{12(G_1)} = (H'_{12} - \eta_{12})FTR_{12(G_1)} < 0$ ; if  $G_1$  is in *state 2*, FTR's total payoff is  $(\tilde{H}_{12} - \eta_{12})FTR_{12(G_1)} = (H''_{12} - \eta_{12})FTR_{12(G_1)} = [(LMP''_2 - LMP''_1) - \eta_{12}]FTR_{12(G_1)} < 0$ . Since there is no private information,  $G_1$  knows for sure that he will lose money if he purchases  $FTR_{12(G_1)}$ . Similar argument applies to  $H''_{21} > \eta_{21}$ .  $\overline{FTR}_{12}$  and  $\overline{FTR}_{21}$  are the maximum amounts of  $FTR_{12}$  and  $FTR_{21}$  that are available to sell.

Recall in the benchmark model, the main problem is for ISO to maximize the TNB subject to a set of constraints in the day-ahead spot market where generators and LSEs have no control

at all. In this model, however, the main problem is for generators and LSEs in the FTR forward market to choose their optimal numbers of FTR contracts to hedge against the profit risks in the day-ahead spot market in order to maximize their expected utility of profit<sup>19</sup>. The total number of FTRs must satisfy ISO's revenue adequacy constraint (RAC), which in turn will ensure ISO passes the simultaneous feasibility test (SFT) (see Hogan (2002)).

Finally, to illustrate the point that FTRs really serve as hedging instruments in the sense that FTRs can shrink the total profit spread of agents in two states and thus risk averse agents are willing to pay some amount of premium to buy FTRs, let's look at the case for  $G_1$ .

With probability  $prob$ ,  $G_1$ 's total profit becomes  $\Pi'_{G_1}$  such that

$$\begin{aligned}\Pi'_{G_1} &= \pi'_{G_1} + (H'_{12} - \eta_{12})FTR_{12(G_1)} \\ &= LMP'_1 Q'_{G_1} - TC_{G_1}(Q'_{G_1}) + (LMP'_2 - LMP'_1 - \eta_{12})FTR_{12(G_1)}\end{aligned}$$

We see that with probability  $prob$ ,  $G_1$  is in *state 1* where  $LMP'_1$  is less than  $LMP'_2$  which makes  $FTR_{12}$  bring positive profit to  $G_1$ , but  $G_1$  was receiving the low  $LMP'_1$  (relative to  $LMP'_2$ ), which directly decreases its production profit  $\pi'_{G_1}$ . Thus in this case, the FTR compensates  $G_1$  for being in the unfavorable state by paying  $G_1$  a positive amount of profit.

On the other hand, with probability  $1 - prob$ ,  $G_1$ 's total profit becomes  $\Pi''_{G_1}$  such that

$$\begin{aligned}\Pi''_{G_1} &= \pi''_{G_1} + (H''_{12} - \eta_{12})FTR_{12(G_1)} \\ &= LMP''_1 Q''_{G_1} - TC_{G_1}(Q''_{G_1}) + (LMP''_2 - LMP''_1 - \eta_{12})FTR_{12(G_1)}\end{aligned}$$

We see that with probability  $1 - prob$ ,  $G_1$  is in *state 2* where  $LMP''_2$  is less than  $LMP''_1$  which makes  $FTR_{12}$  bring negative profit to  $G_1$ , but  $G_1$  was receiving the high  $LMP''_1$  (relative to  $LMP''_2$ ), which directly increases its production profit  $\pi''_{G_1}$ . Thus in this case, the FTR penalizes  $G_1$  for being in its favorable state by taking away part of  $G_1$ 's production profit.

So whether in *state 1* or *state 2*,  $FTR_{12}$ 's profit stream will always be in the opposite direction of  $G_1$ 's production profit to fulfill its hedging purpose. Similar argument applies to

<sup>19</sup>After generators and LSEs make their FTR purchasing decision in the forward market, they wait until the states get revealed. At that time they will be in the day-ahead spot market and everything follows the results derived from benchmark model.



$G_2$ ,  $LSE_1$  and  $LSE_2$ . Therefore, FTRs are indeed hedging instruments for generators and LSEs to reduce their systematic profit risks.

### 2.5.3 FTR Solutions

Assume all generators and LSEs possess logarithmic utilities (i.e.,  $u(\pi) = \log(\pi)$ ) and maximize their expected utility of total profit <sup>20</sup> by choosing the optimal FTR contracts, i.e., optimal hedge positions subject to the ISO's revenue adequacy constraint (RAC). Then  $G_1$ ,  $G_2$ ,  $LSE_1$  and  $LSE_2$ 's problem can be expressed as follows:

$$G_1 : \quad \text{Max } E[U(\tilde{\Pi}_{G1})] = \text{prob} \log(\Pi'_{G1}) + (1 - \text{prob}) \log(\Pi''_{G1}) \quad \text{w.r.t. } FTR_{12(G1)} \quad (2.54)$$

$$G_2 : \quad \text{Max } E[U(\tilde{\Pi}_{G2})] = \text{prob} \log(\Pi'_{G2}) + (1 - \text{prob}) \log(\Pi''_{G2}) \quad \text{w.r.t. } FTR_{21(G2)} \quad (2.55)$$

$$LSE_1 : \quad \text{Max } E[U(\tilde{\Pi}_{L1})] = \text{prob} \log(\Pi'_{L1}) + (1 - \text{prob}) \log(\Pi''_{L1}) \quad \text{w.r.t. } FTR_{21(L1)} \quad (2.56)$$

$$LSE_2 : \quad \text{Max } E[U(\tilde{\Pi}_{L2})] = \text{prob} \log(\Pi'_{L2}) + (1 - \text{prob}) \log(\Pi''_{L2}) \quad \text{w.r.t. } FTR_{12(L2)} \quad (2.57)$$

subject to:

$$FTR_{12(G1)} + FTR_{12(L2)} \leq \overline{FTR}_{12}$$

$$FTR_{21(G2)} + FTR_{21(L1)} \leq \overline{FTR}_{21}$$

$$E(\tilde{\Pi}_{ISO}) = E(\tilde{C}R) + (\eta_{12} - E(\tilde{H}_{12}))\overline{FTR}_{12} + (\eta_{21} - E(\tilde{H}_{21}))\overline{FTR}_{21} \geq 0 \quad (\text{RAC})$$

Solving the first order conditions (FOCs), we obtain the following FTR optimal hedge solutions (OHSs):

$$(\text{OHS1}) \quad FTR_{12(G1)}^* = \frac{\text{prob}(H'_{12} - \eta_{12})\pi''_{G1} + (1 - \text{prob})(H''_{12} - \eta_{12})\pi'_{G1}}{(H'_{12} - \eta_{12})(\eta_{12} - H''_{12})} \quad (2.58)$$

$$(\text{OHS2}) \quad FTR_{21(G2)}^* = \frac{\text{prob}(H'_{21} - \eta_{21})\pi''_{G2} + (1 - \text{prob})(H''_{21} - \eta_{21})\pi'_{G2}}{(H'_{21} - \eta_{21})(\eta_{21} - H''_{21})} \quad (2.59)$$

$$(\text{OHS3}) \quad FTR_{21(L1)}^* = \frac{\text{prob}(H'_{21} - \eta_{21})\pi''_{L1} + (1 - \text{prob})(H''_{21} - \eta_{21})\pi'_{L1}}{(H'_{21} - \eta_{21})(\eta_{21} - H''_{21})} \quad (2.60)$$

$$(\text{OHS4}) \quad FTR_{12(L2)}^* = \frac{\text{prob}(H'_{12} - \eta_{12})\pi''_{L2} + (1 - \text{prob})(H''_{12} - \eta_{12})\pi'_{L2}}{(H'_{12} - \eta_{12})(\eta_{12} - H''_{12})} \quad (2.61)$$

First we derive the following important proposition:

<sup>20</sup>Since the underlying parameters are not normally distributed, the expected utility is not linear in expected profit and the variance of profit. Thus the usual mean-variance analysis does not work well here.

**Proposition 5** *In a two-node electric network model facing uncertain parameter shocks, all risk averse agents, i.e., generators and LSEs (assuming log utilities), will hold a positive amount of FTRs if and only if the shock probability satisfies the following regularity condition (RC):*

$$\max\{\overline{prob}_{G1}, \overline{prob}_{L2}\} < prob < \min\{\overline{prob}_{G2}, \overline{prob}_{L1}\} \quad (RC) \quad (2.62)$$

where

$$\begin{aligned} \overline{prob}_{G1} &= \frac{(\eta_{12} - H''_{12})\pi'_{G1}}{(H'_{12} - \eta_{12})\pi''_{G1} + (\eta_{12} - H''_{12})\pi'_{G1}} \\ \overline{prob}_{G2} &= \frac{(\eta_{21} - H''_{21})\pi'_{G2}}{(H'_{21} - \eta_{21})\pi''_{G2} + (\eta_{21} - H''_{21})\pi'_{G2}} \\ \overline{prob}_{L1} &= \frac{(\eta_{21} - H''_{21})\pi'_{L1}}{(H'_{21} - \eta_{21})\pi''_{L1} + (\eta_{21} - H''_{21})\pi'_{L1}} \\ \overline{prob}_{L2} &= \frac{(\eta_{12} - H''_{12})\pi'_{L2}}{(H'_{12} - \eta_{12})\pi''_{L2} + (\eta_{12} - H''_{12})\pi'_{L2}} \end{aligned}$$

**Proof:**

Recall that  $\tilde{\pi}_{Gk} > 0$  and  $\tilde{\pi}_{Lk} > 0$  implies  $\pi'_{Gk} > 0$ ,  $\pi''_{Gk} > 0$ ,  $\pi'_{Lk} > 0$  and  $\pi''_{Lk} > 0$ , for  $k = 1, 2$ .

Then from (OHS1)—(OHS4) we have the following:

$$\begin{aligned} FTR^*_{12(G1)} &= \frac{prob(H'_{12} - \eta_{12})\pi''_{G1} + (1 - prob)(H''_{12} - \eta_{12})\pi'_{G1}}{(H'_{12} - \eta_{12})(\eta_{12} - H''_{12})} > 0 \\ \iff prob(H'_{12} - \eta_{12})\pi''_{G1} + (1 - prob)(H''_{12} - \eta_{12})\pi'_{G1} &> 0 \quad (\because H'_{12} - \eta_{12} > 0, H''_{12} - \eta_{12} < 0) \\ \iff prob > \frac{(\eta_{12} - H''_{12})\pi'_{G1}}{(H'_{12} - \eta_{12})\pi''_{G1} + (\eta_{12} - H''_{12})\pi'_{G1}} \in (0, 1) & \quad (\because \pi'_{G1} > 0, \pi''_{G1} > 0) \\ &= \overline{prob}_{G1} \\ \\ FTR^*_{21(G2)} &= \frac{prob(H'_{21} - \eta_{21})\pi''_{G2} + (1 - prob)(H''_{21} - \eta_{21})\pi'_{G2}}{(H''_{21} - \eta_{21})(\eta_{21} - H'_{21})} > 0 \\ \iff prob(H'_{21} - \eta_{21})\pi''_{G2} + (1 - prob)(H''_{21} - \eta_{21})\pi'_{G2} &> 0 \quad (\because H'_{21} - \eta_{21} < 0, H''_{21} - \eta_{21} > 0) \\ \iff prob < \frac{(\eta_{21} - H''_{21})\pi'_{G2}}{(H'_{21} - \eta_{21})\pi''_{G2} + (\eta_{21} - H''_{21})\pi'_{G2}} \in (0, 1) & \quad (\because \pi'_{G2} > 0, \pi''_{G2} > 0) \\ &= \overline{prob}_{G2} \end{aligned}$$

$$\begin{aligned}
FTR_{21(L1)}^* &= \frac{prob(H'_{21} - \eta_{21})\pi''_{L1} + (1 - prob)(H''_{21} - \eta_{21})\pi'_{L1}}{(H''_{21} - \eta_{21})(\eta_{21} - H'_{21})} > 0 \\
\iff prob(H'_{21} - \eta_{21})\pi''_{L1} + (1 - prob)(H''_{21} - \eta_{21})\pi'_{L1} &> 0 \quad (\because H'_{21} - \eta_{21} < 0, H''_{21} - \eta_{21} > 0) \\
\iff prob < \frac{(\eta_{21} - H''_{21})\pi'_{L1}}{(H'_{21} - \eta_{21})\pi''_{L1} + (\eta_{21} - H''_{21})\pi'_{L1}} &\in (0, 1) \quad (\because \pi'_{L1} > 0, \pi''_{L1} > 0) \\
&= \overline{prob}_{L1}
\end{aligned}$$

$$\begin{aligned}
FTR_{12(L2)}^* &= \frac{prob(H'_{12} - \eta_{12})\pi''_{L2} + (1 - prob)(H''_{12} - \eta_{12})\pi'_{L2}}{(H'_{12} - \eta_{12})(\eta_{12} - H''_{12})} > 0 \\
\iff prob(H'_{12} - \eta_{12})\pi''_{L2} + (1 - prob)(H''_{12} - \eta_{12})\pi'_{L2} &> 0 \quad (\because H'_{12} - \eta_{12} > 0, H''_{12} - \eta_{12} < 0) \\
\iff prob > \frac{(\eta_{12} - H''_{12})\pi'_{L2}}{(H'_{12} - \eta_{12})\pi''_{L2} + (\eta_{12} - H''_{12})\pi'_{L2}} &\in (0, 1) \quad (\because \pi'_{L2} > 0, \pi''_{L2} > 0) \\
&= \overline{prob}_{L2}
\end{aligned}$$

Therefore, to ensure that  $FTR_{12(G1)}^* > 0$ ,  $FTR_{21(G2)}^* > 0$ ,  $FTR_{21(L1)}^* > 0$ , and  $FTR_{12(L2)}^* > 0$ , we need to have  $prob > \overline{prob}_{G1}$ ,  $prob > \overline{prob}_{L2}$ ,  $prob < \overline{prob}_{G2}$ , and  $prob < \overline{prob}_{L1}$ , which is equivalent to  $\max\{\overline{prob}_{G1}, \overline{prob}_{L2}\} < prob < \min\{\overline{prob}_{G2}, \overline{prob}_{L1}\}$ . Q.E.D.

Furthermore, when we investigate how the optimal FTR hedge positions change with the change of shock probability  $prob$ , we have the following proposition:

**Proposition 6** *In a two-node electric network model facing uncertain parameter shocks, the optimal  $FTR_{12}$  increases with increasing  $prob$  while the optimal  $FTR_{21}$  decreases with increasing  $prob$ , provided that  $prob$  satisfies the regularity condition. The comparative statics are shown as follows:*

$$\frac{\partial FTR_{12(G1)}}{\partial prob} > 0, \quad \frac{\partial FTR_{12(L2)}}{\partial prob} > 0, \quad \frac{\partial FTR_{21(G2)}}{\partial prob} < 0, \quad \text{and} \quad \frac{\partial FTR_{21(L1)}}{\partial prob} < 0. \quad (2.63)$$

The economic intuition behind this proposition is straightforward. Recall that  $prob$  is the probability that the transmission line is congested from node 1 to node 2. Increasing  $prob$  thus implies that the transmission line is more likely to get congested from node 1 to node 2. Since congestion from node 1 to node 2 makes  $FTR_{12}$  bring positive profit to its owner but makes  $FTR_{21}$  bring negative profit to its owner, the risk-averse agents who own  $FTR_{12}$  ( $G_1$  and  $L_2$ ) will tend to buy more of  $FTR_{12}$  while the agents who own  $FTR_{21}$  ( $G_2$  and  $L_1$ ) will tend to buy less of  $FTR_{21}$ . The formal proof is provided below.

**Proof:**

Recall that  $H'_{12} - \eta_{12} > 0$ ,  $H''_{12} - \eta_{12} < 0$  and  $H'_{21} - \eta_{21} < 0$ ,  $H''_{21} - \eta_{21} > 0$ .

$$\begin{aligned} \frac{\partial FTR_{12(G1)}}{\partial prob} &= [(H'_{12} - \eta_{12})\pi''_{G1} + (\eta_{12} - H''_{12})\pi'_{G1}] / [(H'_{12} - \eta_{12})(\eta_{12} - H''_{12})] > 0; \\ \frac{\partial FTR_{12(L2)}}{\partial prob} &= [(H'_{12} - \eta_{12})\pi''_{L2} + (\eta_{12} - H''_{12})\pi'_{L2}] / [(H'_{12} - \eta_{12})(\eta_{12} - H''_{12})] > 0; \\ \frac{\partial FTR_{21(G2)}}{\partial prob} &= [(H'_{21} - \eta_{21})\pi''_{G2} + (\eta_{21} - H''_{21})\pi'_{G2}] / [(H'_{21} - \eta_{21})(\eta_{21} - H''_{21})] < 0; \\ \frac{\partial FTR_{21(L1)}}{\partial prob} &= [(H'_{21} - \eta_{21})\pi''_{L1} + (\eta_{21} - H''_{21})\pi'_{L1}] / [(H'_{21} - \eta_{21})(\eta_{21} - H''_{21})] < 0; \quad \text{Q.E.D.} \end{aligned}$$

Now we are ready establish the most important proposition in this paper, that is, to show the existence of FTRs actually increases the social welfare in this two-node electric network model under stochastic parameter shocks.

**Proposition 7** *In a two-node electric network model facing uncertain parameter shocks, the acquisition of optimal FTRs by the risk averse generators and LSEs increases and in general strictly increases the social welfare compared with the case where there is no FTRs. Social welfare function  $W$  can be measured by generators and LSEs' total expected utilities. Denote the welfare under optimal FTRs as  $W_F$  and the welfare without FTRs as  $W_0$ . Then,*

$$W_F \geq W_0 \quad (2.64)$$

The economic intuition behind this proposition is that since there is uncertainty in this model, generators and LSEs are not sure about their future profits: they may happen to obtain the high profits in one state or end up receiving the low profits in the other state. However they know ISO issues a financial instrument, FTR, which can be used to hedge against their risky profit by reducing the profit spread between the two states. The risk averse generators and LSEs are thus willing to pay some premium to buy FTRs in order to maximize their expected utilities of future profits. If all generators and LSEs maximize their expected utilities by purchasing FTRs, then we can say FTRs increase the social welfare which is measured by total expected utilities. The formal proof of the proposition is provided in Appendix 5.

This proposition has important economic implications. First, it shows that in this simple two-node electric network model, once we introduce uncertainty (even in a very simple form),

the acquisition of FTRs by risk averse agents can increase total social welfare. Moreover, as the proof shows, this result is strong and robust in the sense that regardless whether agents take long or short positions, the social welfare with FTRs is higher and in general is strictly higher than that without FTRs. This result thus refutes the far more negative views of FTRs by other economists such as Joskow and Tirole (2000), and provides an economic explanation to the fact that FTRs are widely used in the major U.S. wholesale power markets.

Finally, in an attempt to endogenize the prices of FTRs,  $\eta_{12}$  and  $\eta_{21}$ , consider an ISO's problem. Since all information is public, that is, ISO knows that generators and LSEs will purchase FTRs to hedge against their risky profit in the energy spot market. Then ISO can solve generators and LSEs' problems to get the optimal FTR hedge solutions and substitute them into ISO's revenue adequacy constraint (RAC):

$$E(\tilde{\Pi}_{ISO}) = E(\tilde{C}R) + (\eta_{12} - E(\tilde{H}_{12}))\overline{FTR}_{12} + (\eta_{21} - E(\tilde{H}_{21}))\overline{FTR}_{21} \geq 0$$

where

$$\overline{FTR}_{12} = FTR_{12(G1)}^* + FTR_{12(L2)}^*$$

$$\overline{FTR}_{21} = FTR_{21(G2)}^* + FTR_{21(L1)}^*$$

$$E(\tilde{C}R) = \text{prob} CR' + (1 - \text{prob})CR'' = \text{prob}(LMP_2' - LMP_1')T + (1 - \text{prob})(LMP_1'' - LMP_2'')$$

$$E(\tilde{H}_{12}) = \text{prob} H_{12}' + (1 - \text{prob})H_{12}'' = \text{prob}(LMP_2' - LMP_1') + (1 - \text{prob})(LMP_2'' - LMP_1'')$$

$$E(\tilde{H}_{21}) = \text{prob} H_{21}' + (1 - \text{prob})H_{21}'' = \text{prob}(LMP_1' - LMP_2') + (1 - \text{prob})(LMP_1'' - LMP_2'')$$

Now ISO has several options to proceed. (a) The simplest option is to adjust  $\eta_{12}$  and  $\eta_{21}$  so that the RAC becomes binding. Then the relationship between  $\eta_{12}$  and  $\eta_{21}$  can be obtained as an implicit function denoted as  $g_1()$  such that  $g_1(\eta_{12}, \eta_{21}) = 0$ . (b) The more complicated option ISO can adopt is to adjust  $\eta_{12}$  and  $\eta_{21}$  so that it can extract a maximum amount of residual congestion rent (RCR). Then ISO invests this RCR to expand the transmission line, i.e., increase thermal limit  $T$ , which will reduce the uncertain profit spread, enhance efficiency, and increase social welfare. With this option, ISO can get another set of relationship between  $\eta_{12}$  and  $\eta_{21}$  in an implicit function denoted as  $g_1()$  such that  $g_1(\eta_{12}, \eta_{21}) = 0$ .

To possibly obtain a unique solution for  $\eta_{12}$  and  $\eta_{21}$ , we need to turn around and look at the problem from generator and LSE points of view. Since all generators and LSEs are assumed to be risk averse, they must be willing to pay certain amount of premiums to reduce the profit risks. Then in equilibrium the risk premiums are equivalent to the price of FTRs multiplied by the corresponding FTR contracts, that is, we have,

$$U[E(\tilde{\pi}_{G1} + \tilde{H}_{12}FTR_{12(G1)}) - \eta_{12}FTR_{12(G1)}] = E[U(\tilde{\pi}_{G1} + \tilde{H}_{12}FTR_{12(G1)})] \quad (2.65)$$

$$U[E(\tilde{\pi}_{G2} + \tilde{H}_{21}FTR_{21(G2)}) - \eta_{21}FTR_{21(G2)}] = E[U(\tilde{\pi}_{G2} + \tilde{H}_{21}FTR_{21(G2)})] \quad (2.66)$$

$$U[E(\tilde{\pi}_{L1} + \tilde{H}_{21}FTR_{21(L1)}) - \eta_{21}FTR_{21(L1)}] = E[U(\tilde{\pi}_{L1} + \tilde{H}_{21}FTR_{21(L1)})] \quad (2.67)$$

$$U[E(\tilde{\pi}_{L2} + \tilde{H}_{12}FTR_{12(L2)}) - \eta_{12}FTR_{12(L2)}] = E[U(\tilde{\pi}_{L2} + \tilde{H}_{12}FTR_{12(L2)})] \quad (2.68)$$

With the logarithmic utilities, in principle we can solve for  $FTR_{12(G1)}^{**}$ ,  $FTR_{21(G2)}^{**}$ ,  $FTR_{21(L1)}^{**}$ , and  $FTR_{12(L2)}^{**}$  such that:

$$E(\tilde{\pi}_{G1}) + (E(\tilde{H}_{12}) - \eta_{12})FTR_{12(G1)}^{**} = (\pi'_{G1} + H'_{12}FTR_{12(G1)}^{**})^{prob}(\pi''_{G1} + H''_{12}FTR_{12(G1)}^{**})^{1-prob}$$

$$E(\tilde{\pi}_{G2}) + (E(\tilde{H}_{21}) - \eta_{21})FTR_{21(G2)}^{**} = (\pi'_{G2} + H'_{21}FTR_{21(G2)}^{**})^{prob}(\pi''_{G2} + H''_{21}FTR_{21(G2)}^{**})^{1-prob}$$

$$E(\tilde{\pi}_{L1}) + (E(\tilde{H}_{21}) - \eta_{21})FTR_{21(L1)}^{**} = (\pi'_{L1} + H'_{21}FTR_{21(L1)}^{**})^{prob}(\pi''_{L1} + H''_{21}FTR_{21(L1)}^{**})^{1-prob}$$

$$E(\tilde{\pi}_{L2}) + (E(\tilde{H}_{12}) - \eta_{12})FTR_{12(L2)}^{**} = (\pi'_{L2} + H'_{12}FTR_{12(L2)}^{**})^{prob}(\pi''_{L2} + H''_{12}FTR_{12(L2)}^{**})^{1-prob}$$

where  $E(\tilde{H}_{12})$  and  $E(\tilde{H}_{21})$  are as defined as above and  $E(\tilde{\pi})$ 's are defined as follows:

$$E(\tilde{\pi}_{G1}) = prob \pi'_{G1} + (1 - prob)\pi''_{G1};$$

$$E(\tilde{\pi}_{G2}) = prob \pi'_{G2} + (1 - prob)\pi''_{G2};$$

$$E(\tilde{\pi}_{L1}) = prob \pi'_{L1} + (1 - prob)\pi''_{L1};$$

$$E(\tilde{\pi}_{L2}) = prob \pi'_{L2} + (1 - prob)\pi''_{L2}.$$

After substituting the  $FTR^{**}$  solutions into the ISO's RAC and let ISO adjust  $\eta_{12}$  and  $\eta_{21}$ . Regardless whether ISO chooses option(a) or option(b), we can, in principle, derive another relationship between  $\eta_{12}$  and  $\eta_{21}$  in an implicit function denoted as  $g_2()$  such that  $g_2(\eta_{12}, \eta_{21}) = 0$ .

Hence by solving the system of equation for  $\eta_{12}$  and  $\eta_{21}$ ,

$$\begin{cases} g_1(\eta_{12}, \eta_{21}) = 0; \\ g_2(\eta_{12}, \eta_{21}) = 0. \end{cases}$$

in principle we can solve for the equilibrium FTR price vector  $\eta^* = (\eta_{12}^*, \eta_{21}^*)$  such that

$$\begin{cases} g_1(\eta_{12}^*, \eta_{21}^*) = 0; \\ g_2(\eta_{12}^*, \eta_{21}^*) = 0. \end{cases}$$

## 2.6 Conclusions and Extensions

In this paper, we've studied the competitive behaviors of electricity generators and LSEs, and analyzed welfare effects of financial transmission rights (FTRs) in a restructured U.S. wholesale power market model. The analysis focuses on a two-node electric network model where there is one generator and one LSE at each node with parameterized marginal cost and demand functions, supervised by an independent system operator (ISO). In the first part of the paper, a no-rights benchmark model is developed to solve for the optimal quantity of power production and consumption (the ED solutions) and derive the locational marginal prices for each node, which serve as the building blocks to solve for the optimal FTR hedge positions in the second model. Then in the second model, we introduce a stochastic parameter shock into the two-node electric network model, and show that in the absence of market power the acquisition of optimal FTRs by the risk averse generators and LSEs increases and in general strictly increases the social welfare compared with the case where there is no FTRs available. This result refutes the somehow negative views of FTRs by other economists in the literature and provides the economic explanations to the fact that FTRs are widely adopted as a financial hedge instrument in the major U.S. wholesale power markets.

This study can be extended in several ways. First, we can extend the model to have an arbitrary number of generators and LSEs at each node. Admittedly, this extension adds the burden of calculations, but it does not change the essence of the solution. Mainly what we should be concerned about is to obtain an aggregate marginal cost (supply) function  $AS_k(G_k)$  and an aggregate demand function  $AD_k(L_k)$  for each node  $k = 1, 2$ . Then proceed to solve

the model as if there were one “representative” generator and one “representative” LSE. After the aggregate solution is acquired, the solution quantities can be referred back through LMPs to get the individual dispatched quantities. Although the process of solving the problem is more tedious, the essence of the solution algorithm in this paper remains the same. We expect that including multiple generators and LSEs at each node will not have dramatic effects on the solution outcomes.

Second, we can extend our two-node electric network model to three nodes or more. Then we will be introducing an important feature of real world electric network, i.e., the “loop flow effect”, which considerably increases the modeling complications. Basically, the “loop flow effect” is associated with the fact that electrons follow the path of least resistance. In an electric network with a transmission grid consisting of multiple connection lines, the patterns of electric flows follow the Kirchhoff’s laws in physics. For example, in a three-node network, if there is a power injection  $Q$  at one node, say node 1 and an equal amount of withdrawal at another node, say node 2, then depending on the reactance of line 1-2, line 1-3 and line 2-3, a proportion amount of power, say  $\alpha Q$  flows from node 1 to node 2 while the rest  $(1 - \alpha)Q$  flows from node 1 to node 3 then flows from node 3 to node 2. For instance, if the line reactance is the same for all three lines, then  $\alpha = 2/3$ . In this case, we need to add one more variable, the phase angle ( $\phi$ ), in order to control the power flows between transmission lines<sup>21</sup>. Although there is significant amount of work involved when we model the three-node case, the result is expected to be closer to reality than the two-node case.

Third, in our two-node model, we assume generators and LSEs always submit their true marginal cost functions and true demand functions to ISO. So we always obtain the competitive solution which is also Pareto optimal<sup>22</sup>. But if we relax this assumption such that generators and LSEs can strategically submit their marginal cost and demand functions in the attempt to gain individual advantages through strategic behaviors, we will generally not be able to obtain the competitive solutions.

<sup>21</sup>Technically, we need to model the 3-node case using a Direct Current (DC) power flow formulation.

<sup>22</sup>In the 3-node case, it becomes unclear that the outcome will still be Pareto optimal because of externality brought by “loop flow” effect.



Fourth, we could extend the static two-node model into a dynamic model with multiple periods, where in each period, generators and LSEs submit their strategic bids and offers in a double auction framework in both FTR and day-ahead power markets. Generators and LSEs could be endowed with an initial wealth. If they don't make enough profits within a certain period of time, then they will be out of market. Moreover, these generators and LSEs can "learn" what is the best strategies for them over time. The learning methods may include reinforcement learning and anticipatory learning, etc.

With these complicated extensions, it seems almost impossible to proceed with the analytical tools used in this paper. A natural candidate that may fit very well for this purpose is the agent-based computational approach. For a comprehensive introduction of Agent-based Computational Economics (ACE), see the ACE survey by Tesfatsion (2003).

## 2.7 References

- Bautista, G., and V. Quintana. (2005). "Screening and Mitigation of Exacerbated Market Power Due to Financial Transmission Rights," *IEEE Transactions on Power Systems*, 20(1): 213-222.
- Bushnell, J. (1999), "Transmission Rights and Market Power," *The Electricity Journal*, 12(8):77-85.
- Cardell, J., Hitt, C., and Hogan, W. (1997). "Market Power and Strategic Interaction in Electricity Networks," *Resource and Energy Economics* 18(4): 107-141.
- Deng, S., S. Oren, and S. Meliopoulos (2004). "The Inherent Inefficiency of Simultaneously Feasible Financial Transmission Rights Auctions," *IEEE Proceedings of the 37th Hawaii International Conference on System Sciences*.
- FERC (2003), Notice of White Paper (U.S. Federal Energy Regulatory Commission, Issued April 28).
- Froot, K., D. Scharfstein, and J. Stein (1993), "Risk Management: Coordinating corporate Investment and Financing Policies," *Journal of Finance* 48: 1629-1658.

- Hogan, W. (2000). "Market Power in Theory and Practice, Comments on Joskow and Tirole (2000) and Johnsen, Verma and Wolfram (1999)," POWER Conference, University of California, Berkeley, Berkeley, CA, March 17.
- Hogan, W. (2002). "Financial Transmission Right Formulations," Working Paper, Center for Business and Government, John F. Kennedy School of Government, Harvard University, Cambridge, MA, March 15.
- Hogan, W. (2003). "Transmission Market Design," Paper prepared for the conference "Electricity Deregulation: Where From Here?" at the Bush Presidential Conference Center, Texas A & M University, April 4.
- ISO New England (2003a). Market Rule 1 - NEPOOL Standard Market Design, Revision 2, September 9. Available at <http://www.iso-ne.com/smd/>
- ISO New England (2003b). NEPOOL Manual for Financial Transmission Rights, Manual M-06, Revision 2, April 4. Available at <http://www.iso-ne.com/smd/>
- ISO New England (2004). NEPOOL Manual for Market Operations, Manual M-11, Revision 8, May 10. Available at <http://www.iso-ne.com/smd/>
- Joskow, P., and J. Tirole, (2000). "Transmission Rights and Market Power on Electric Power Networks," *RAND Journal of Economics* 31(3): 450-487.
- Joskow, P., and J. Tirole, (2003). "Merchant Transmission Investment," NBER working paper, No. 9534.
- Kamat, R., and S. Oren, (2004). "Two-settlement Systems for Electricity Markets under Network Uncertainty and Market Power," *Journal of Regulatory Economics* 25(1): 5-37.
- Kench, B., (2004). "Let's Get Physical! Or Financial? A Study of Electricity Transmission Rights," *Journal of Regulatory Economics* 25(2): 187-214.
- Kirschen, D., and G. Strbac, (2004). *Fundamentals of Power System Economics* (John Wiley & Sons, Ltd., Hoboken, NJ).

- Kristiansen, T. (2003). "Markets for Financial Transmission Rights," Working Paper, Norwegian University of Science and Technology, Department of Electrical Power Engineering.
- Lyons, K, H. Fraser, and H. Parmesano, (2000). "An Introduction to Financial Transmission Rights," *The Electricity Journal* 13(10): 31-37.
- Mendez, R., and H. Rudnick, (2004). "Congestion Management and Transmission Rights in Centralized Electric Markets," *IEEE Transactions on Power Systems*, 19(2): 889-896.
- Midwest ISO, 2005, MISO Financial Transmission Rights Market Participant User's Manual. Available at <http://www.midwestiso.com/>
- O'Neill, R, U. Helman, and B. Hobbs, (2002). "A Joint Energy and Transmission Rights Auction: Proposal and Properties," *IEEE Transactions on Power Systems*, 17(4): 1058-1067.
- Oren, S., (1997). "Economic Inefficiency of Passive Transmission Rights in Congested Electricity Systems with Competitive Generation," *The Energy Journal*, 18(1): 63-83.
- Rosellon, J. (2003). "Different Approaches Towards Electricity Transmission Expansion," *Review of Network Economics*, 2(3): 238-269.
- Rudkevich, A. (2004). "Investment and Bidding Strategies in Markets for Firm Transmission Rights," IEEE Proceedings of the 37th Hawaii International Conference on System Sciences.
- Siddiqui, A., Bartholomew, E., Marnay, C., and Oren, S. (2003). "On the Efficiency of the New York Independent System Operator Market for Transmission Congestion Contracts," Working Paper, Environmental Energy Technologies Division, Ernest Orlando Lawrence Berkeley National Laboratory, Berkeley, CA, April 30.
- Stoft, S. (1999). "Financial Transmission Rights Meet Cournot: How TCCs Curb Market Power," *The Energy Journal*, 20(1): 1-4.

- Stoft, S. (2002). *Power System Economics: Designing Markets for Electricity*, IEEE Press, Wiley-Interscience, New York, NY.
- Stulz, R. (1990), “Managerial Discretion and Optimal Financing Policies,” *Journal of Financial Economics* 26: 3-28.
- Tesfatsion, L, (2003). “Agent-Based Computational Economics,” Department of Economics, Iowa State University, Ames, Iowa 50011-1070, ISU Economics Working Paper No. 1, Revised August 24.
- U.S. Department of Energy (2000) “The Changing Structure of the Electric Power Industry 2000: An Update,” Energy Information Administration, Washington DC.
- U.S. Department of Energy (2002) “National Transmission Grid Study,” May.
- Wilson, R. (2002). “Architecture of Power Markets,” *Econometrica*, 70(4): 1299-1340.

## 2.8 Appendix

### 2.8.1 Appendix 1

The non-thermal-constraint ED solution in Step 1 is derived as follows:

In step 1, when the thermal limit  $T$  never binds, the ED problem is to maximize the “total net benefit” (TNB) subject to the balancing and non-negativity constraints. This is just a standard optimization problem with one equality constraint (the balancing constraint) and four inequality constraints (the non-negativity constraints for  $Q_{G1}$ ,  $Q_{G2}$ ,  $Q_{L1}$  and  $Q_{L2}$ ). Using  $\mu$  as the multiplier for the equality constraint and  $\lambda$ 's as the multipliers for inequality constraints, and formulate the Lagrangian equation:

$$L = (b_1^D Q_{L1} - \frac{1}{2} a_1^D Q_{L1}^2) - (b_1^S Q_{G1} + \frac{1}{2} a_1^S Q_{G1}^2) + (b_2^D Q_{L2} - \frac{1}{2} a_2^D Q_{L2}^2) - (b_2^S Q_{G2} + \frac{1}{2} a_2^S Q_{G2}^2) \\ + \mu(Q_{G1} + Q_{G2} - Q_{L1} - Q_{L2}) + \lambda_{G1} Q_{G1} + \lambda_{G2} Q_{G2} + \lambda_{L1} Q_{L1} + \lambda_{L2} Q_{L2}$$

Derive the first order conditions (FOCs):

$$\frac{\partial L}{\partial Q_{L1}} = b_1^D - a_1^D Q_{L1} - \mu + \lambda_{L1} = 0$$

$$\frac{\partial L}{\partial Q_{G1}} = -b_1^S - a_1^S Q_{G1} + \mu + \lambda_{G1} = 0$$

$$\frac{\partial L}{\partial Q_{L2}} = b_2^D - a_2^D Q_{L2} - \mu + \lambda_{L2} = 0$$

$$\frac{\partial L}{\partial Q_{G2}} = -b_2^S - a_2^S Q_{G2} + \mu + \lambda_{G2} = 0$$

$$\frac{\partial L}{\partial \mu} = Q_{G1} + Q_{G2} - Q_{L1} - Q_{L2} = 0$$

$$Q_{G1} \geq 0, \lambda_{G1} \geq 0, \lambda_{G1} Q_{G1} = 0$$

$$Q_{G2} \geq 0, \lambda_{G2} \geq 0, \lambda_{G2} Q_{G2} = 0$$

$$Q_{L1} \geq 0, \lambda_{L1} \geq 0, \lambda_{L1} Q_{L1} = 0$$

$$Q_{L2} \geq 0, \lambda_{L2} \geq 0, \lambda_{L2} Q_{L2} = 0$$

For simplicity, only consider the case where all dispatched quantities are positive, i.e., all non-negativity constraints are not binding ( $\lambda_{G1} = \lambda_{G2} = \lambda_{L1} = \lambda_{L2} = 0$ )<sup>23</sup>. Thus from FOCs we have:

$$\begin{cases} a_1^S Q_{G1} + a_1^D Q_{L1} = b_1^D - b_1^S; \\ a_1^S Q_{G1} + a_2^D Q_{L2} = b_2^D - b_1^S; \\ a_2^S Q_{G2} + a_2^D Q_{L2} = b_2^D - b_2^S; \\ Q_{G1} + Q_{G2} = Q_{L1} + Q_{L2}; \\ \mu = b_1^S + a_1^S Q_{G1}. \end{cases}$$

Notice the last equation shows that the Lagrangian multiplier associated with balancing constraint is equal to the marginal cost, which by the nature of this ED problem is also the LMP. Solving five unknown variables with five equations, we obtain the Step 1 non-thermal-constraint ED solution:

<sup>23</sup>We find a total of nine other possible solution cases, i.e., (1)  $Q_{G1} = 0$ ; (2)  $Q_{G2} = 0$ ; (3)  $Q_{L1} = 0$ ; (4)  $Q_{L2} = 0$ ; (5)  $Q_{G1} = Q_{L1} = 0$ ; (6)  $Q_{G1} = Q_{L2} = 0$ ; (7)  $Q_{G2} = Q_{L1} = 0$ ; (8)  $Q_{G2} = Q_{L2} = 0$ ; (9)  $Q_{G1} = Q_{G2} = Q_{L1} = Q_{L2} = 0$ .

$$\begin{aligned}
\hat{Q}_{G1} &= \frac{a_2^D a_2^S (b_1^D - b_1^S) + a_1^D a_2^S (b_2^D - b_2^S) + a_1^D (a_2^D + a_2^S) (b_2^S - b_1^S)}{a_1^D a_1^S (a_2^D + a_2^S) + a_2^D a_2^S (a_1^D + a_1^S)} \\
\hat{Q}_{G2} &= \frac{a_1^D a_1^S (b_2^D - b_2^S) + a_1^S a_2^D (b_1^D - b_1^S) - a_2^D (a_1^D + a_1^S) (b_2^S - b_1^S)}{a_1^D a_1^S (a_2^D + a_2^S) + a_2^D a_2^S (a_1^D + a_1^S)} \\
\hat{Q}_{L1} &= \frac{(a_2^D a_2^S + a_1^S a_2^D + a_1^S a_2^S) (b_1^D - b_1^S) - a_1^S a_2^S (b_2^D - b_2^S) - a_1^S (a_2^D + a_2^S) (b_2^S - b_1^S)}{a_1^D a_1^S (a_2^D + a_2^S) + a_2^D a_2^S (a_1^D + a_1^S)} \\
\hat{Q}_{L2} &= \frac{(a_1^D a_1^S + a_1^D a_2^S + a_1^S a_2^S) (b_2^D - b_2^S) - a_1^S a_2^S (b_1^D - b_1^S) + a_2^S (a_1^D + a_1^S) (b_2^S - b_1^S)}{a_1^D a_1^S (a_2^D + a_2^S) + a_2^D a_2^S (a_1^D + a_1^S)} \\
LMP_1 = LMP_2 = \hat{\mu} &= b_1^S + a_1^S \hat{Q}_{G1} = \frac{a_2^D a_2^S (a_1^D b_1^S + a_1^S b_1^D) + a_1^D a_1^S (a_2^D b_2^S + a_2^S b_2^D)}{a_1^D a_1^S (a_2^D + a_2^S) + a_2^D a_2^S (a_1^D + a_1^S)}
\end{aligned}$$

which can be expressed as:

$$\hat{Q}_{G1} = (\mathbb{G}_1 + \mathbb{B}_1) / \mathbb{A}$$

$$\hat{Q}_{G2} = (\mathbb{G}_2 + \mathbb{B}_2) / \mathbb{A}$$

$$\hat{Q}_{L1} = (\mathbb{L}_1 + \mathbb{C}_1) / \mathbb{A}$$

$$\hat{Q}_{L2} = (\mathbb{L}_2 + \mathbb{C}_2) / \mathbb{A}$$

$$LMP_1 = LMP_2 = \hat{\mu} = b_1^S + a_1^S \hat{Q}_{G1}$$

where

$$\begin{aligned}
\mathbb{G}_1 &= D_2 B_1 + a_1^D a_2^S B_2, & \mathbb{B}_1 &= a_1^D A_2 C_1, & \mathbb{L}_1 &= (D_2 + a_1^S A_2) B_1 - a_1^S a_2^S B_2, & \mathbb{C}_1 &= a_1^S A_2 C_2; \\
\mathbb{G}_2 &= D_1 B_2 + a_1^S a_2^D B_1, & \mathbb{B}_2 &= a_2^D A_1 C_2, & \mathbb{L}_2 &= (D_1 + a_2^S A_1) B_2 - a_1^S a_2^S B_1, & \mathbb{C}_2 &= a_2^S A_1 C_1; \\
\mathbb{A} &= D_1 A_2 + D_2 A_1;
\end{aligned}$$

$$\begin{aligned}
A_1 &= a_1^D + a_1^S, & B_1 &= b_1^D - b_1^S, & C_1 &= b_2^S - b_1^S, & D_1 &= a_1^D a_1^S; \\
A_2 &= a_2^D + a_2^S, & B_2 &= b_2^D - b_2^S, & C_2 &= b_1^S - b_2^S, & D_2 &= a_2^D a_2^S.
\end{aligned}$$

## 2.8.2 Appendix 2

The binding-thermal-constraint ED solution in Step 2 is derived as follows:

(a) Based on Step 1 non-thermal-constraint ED solution, if we know  $T$  is binding from 1 to 2, i.e.,  $\hat{Q}_{G1} - \hat{Q}_{L1} > T$  or  $\hat{Q}_{L2} - \hat{Q}_{G2} > T$ . We can set either  $Q_{G1} - Q_{L1} = T$  or  $Q_{L2} - Q_{G2} = T$ . But one of them is redundant due to the fact that the balancing constraint

$(Q_{G1} + Q_{G2} = Q_{L1} + Q_{L2})$  always holds in this two-node electric network model. So without loss of generality, let  $Q_{G1} - Q_{L1} = T$ .

This is a standard optimization problem subject to two equality constraints (balancing and thermal constraint) and four inequality constraints (the non-negativity constraints for  $Q_{G1}$ ,  $Q_{G2}$ ,  $Q_{L1}$  and  $Q_{L2}$ ). Using  $\mu$ 's as the multipliers for equality constraints and  $\lambda$ 's as the multipliers for inequality constraints, and formulate the Lagrangian equation:

$$L = (b_1^D Q_{L1} - \frac{1}{2} a_1^D Q_{L1}^2) - (b_1^S Q_{G1} + \frac{1}{2} a_1^S Q_{G1}^2) + (b_2^D Q_{L2} - \frac{1}{2} a_2^D Q_{L2}^2) - (b_2^S Q_{G2} + \frac{1}{2} a_2^S Q_{G2}^2) \\ + \mu_B (Q_{G1} + Q_{G2} - Q_{L1} - Q_{L2}) + \mu_T (T - Q_{G1} + Q_{L1}) + \lambda_{G1} Q_{G1} + \lambda_{G2} Q_{G2} + \lambda_{L1} Q_{L1} + \lambda_{L2} Q_{L2}$$

Recall all the parameters are positive, i.e.,  $T > 0$ ,  $a_j^D > 0$ ,  $b_j^D > 0$ , and  $a_i^S > 0$ ,  $b_i^S > 0$  for  $i, j = 1, 2$ . Derive the FOCs:

$$\frac{\partial L}{\partial Q_{L1}} = b_1^D - a_1^D Q_{L1} - \mu_B + \mu_T + \lambda_{L1} = 0$$

$$\frac{\partial L}{\partial Q_{G1}} = -b_1^S - a_1^S Q_{G1} + \mu_B - \mu_T + \lambda_{G1} = 0$$

$$\frac{\partial L}{\partial Q_{L2}} = b_2^D - a_2^D Q_{L2} - \mu_B + \lambda_{L2} = 0$$

$$\frac{\partial L}{\partial Q_{G2}} = -b_2^S - a_2^S Q_{G2} + \mu_B + \lambda_{G2} = 0$$

$$\frac{\partial L}{\partial \mu_B} = Q_{G1} + Q_{G2} - Q_{L1} - Q_{L2} = 0$$

$$\frac{\partial L}{\partial \mu_T} = T - Q_{G1} + Q_{L1} = 0$$

$$Q_{G1} \geq 0, \lambda_{G1} \geq 0, \lambda_{G1} Q_{G1} = 0$$

$$Q_{G2} \geq 0, \lambda_{G2} \geq 0, \lambda_{G2} Q_{G2} = 0$$

$$Q_{L1} \geq 0, \lambda_{L1} \geq 0, \lambda_{L1} Q_{L1} = 0$$

$$Q_{L2} \geq 0, \lambda_{L2} \geq 0, \lambda_{L2} Q_{L2} = 0$$

Rearranging the FOCs w.r.t  $Q_{L1}$  and  $Q_{G1}$ , the FOCs w.r.t  $Q_{L2}$  and  $Q_{G2}$ , and the FOCs w.r.t  $\mu_B$  and  $\mu_T$ , we have:

$$\begin{cases} a_1^S Q_{G1} + a_1^D Q_{L1} = b_1^D - b_1^S + \lambda_{L1} + \lambda_{G1}; \\ a_2^S Q_{G2} + a_2^D Q_{L2} = b_2^D - b_2^S + \lambda_{L2} + \lambda_{G2}; \\ Q_{G1} - Q_{L1} = T; \\ Q_{L2} - Q_{G2} = T. \end{cases}$$

Solving four unknown variables with four equations, we have:

$$Q_{G1} = \frac{b_1^D - b_1^S + a_1^D T + \lambda_{L1} + \lambda_{G1}}{a_1^D + a_1^S}$$

$$Q_{G2} = \frac{b_2^D - b_2^S - a_2^D T + \lambda_{L2} + \lambda_{G2}}{a_2^D + a_2^S}$$

$$Q_{L1} = \frac{b_1^D - b_1^S - a_1^S T + \lambda_{L1} + \lambda_{G1}}{a_1^D + a_1^S}$$

$$Q_{L2} = \frac{b_2^D - b_2^S + a_2^S T + \lambda_{L2} + \lambda_{G2}}{a_2^D + a_2^S}$$

Now to tackle the corner solutions, first let the solutions be all positive, i.e.,  $Q_{G1} > 0, Q_{G2} > 0, Q_{L1} > 0, Q_{L2} > 0$ , so  $\lambda_{G1} = \lambda_{G2} = \lambda_{L1} = \lambda_{L2} = 0$ . We then can get the following:

$$Q_{G1} = \frac{b_1^D - b_1^S + a_1^D T}{a_1^D + a_1^S}$$

$$Q_{G2} = \frac{b_2^D - b_2^S - a_2^D T}{a_2^D + a_2^S}$$

$$Q_{L1} = \frac{b_1^D - b_1^S - a_1^S T}{a_1^D + a_1^S}$$

$$Q_{L2} = \frac{b_2^D - b_2^S + a_2^S T}{a_2^D + a_2^S}$$

For the solutions indeed to be all positive, the parameters  $(b_j^D, a_j^D, b_i^S, a_i^S, T, \text{ for } i, j = 1, 2)$  must satisfy the following conditions (in other words, any violations to the following conditions will lead to corner solutions):

$$(*1) \quad b_1^D - b_1^S + a_1^D T > 0 \quad \text{or} \quad Q_{G1} > 0$$

$$(*2) \quad b_2^D - b_2^S - a_2^D T > 0 \quad \text{or} \quad Q_{G2} > 0$$

$$(*3) \quad b_1^D - b_1^S - a_1^S T > 0 \quad \text{or} \quad Q_{L1} > 0$$



$$(*4) \quad b_2^D - b_2^S + a_2^S T > 0 \quad \text{or} \quad Q_{L2} > 0$$

Close examination on the above conditions indicates that Condition (\*1) and (\*4) will not be violated because in this case the thermal constraint is binding from node 1 to node 2, i.e., node 1 as the net export node (NEN) and node 2 as the net import node (NIN). Recall in the simplifying assumptions we assume that there is only one generator and one LSE at each node. So node 1 as the NEN and node 2 as the NIN would imply that  $G_1$  has to supply a positive amount of power over the transmission line and  $LSE_2$  has to demand a positive amount of power from  $G_1$  in this two-node electric network model. Hence the total power supply by  $G_1$ ,  $Q_{G1}$ , and the total power demand by  $LSE_2$ ,  $Q_{L2}$ , must be greater than zero, which proves that (\*1) and (\*4) will always hold in this case. Then the Complementary Slackness Conditions (CSCs) for  $Q_{G1}$  and  $Q_{L2}$  will ensure  $\lambda_{G1} = 0$  and  $\lambda_{L2} = 0$ .

In summary, the general solution (GS) is:

$$(GS1) \quad Q_{G1} = \frac{b_1^D - b_1^S + a_1^D T + \lambda_{L1}}{a_1^D + a_1^S}$$

$$(GS2) \quad Q_{G2} = \frac{b_2^D - b_2^S - a_2^D T + \lambda_{G2}}{a_2^D + a_2^S}$$

$$(GS3) \quad Q_{L1} = \frac{b_1^D - b_1^S - a_1^S T + \lambda_{L1}}{a_1^D + a_1^S}$$

$$(GS4) \quad Q_{L2} = \frac{b_2^D - b_2^S + a_2^S T + \lambda_{G2}}{a_2^D + a_2^S}$$

Since Condition (\*1) and (\*4) will always hold, we only need to examine Condition (\*2) and (\*3) to get the ED solutions. There are four cases to consider, i.e., [i] both (\*2) and (\*3) hold; [ii] (\*2) holds while (\*3) is violated; [iii] (\*3) holds while (\*2) is violated; [iv] both (\*2) and (\*3) are violated.

### Case I: Both (\*2) and (\*3) hold (interior solution)

When (\*2) and (\*3) hold, i.e.,  $Q_{G2} > 0$  and  $Q_{L1} > 0$ , the CSCs for  $Q_{G2}$  and  $Q_{L1}$  will give us:  $\lambda_{G2} = 0$  and  $\lambda_{L1} = 0$ .

Then the Step 2 ED solution vector is simply  $s^* = (Q_{G1}^*, Q_{G2}^*, Q_{L1}^*, Q_{L2}^*)$ , where

$$Q_{G1}^* = \frac{b_1^D - b_1^S + a_1^D T}{a_1^D + a_1^S}$$

$$\begin{aligned}
Q_{G2}^* &= \frac{b_2^D - b_2^S - a_2^D T}{a_2^D + a_2^S} \\
Q_{L1}^* &= \frac{b_1^D - b_1^S - a_1^S T}{a_1^D + a_1^S} \\
Q_{L2}^* &= \frac{b_2^D - b_2^S + a_2^S T}{a_2^D + a_2^S} \\
LMP_1 &= b_1^S + a_1^S Q_{G1}^* = \frac{a_1^D b_1^S + a_1^S b_1^D + a_1^D a_1^S T}{a_1^D + a_1^S} \\
LMP_2 &= b_2^S + a_2^S Q_{G2}^* = \frac{a_2^D b_2^S + a_2^S b_2^D - a_2^D a_2^S T}{a_2^D + a_2^S}
\end{aligned}$$

### Case II: (\*2) holds while (\*3) is violated

When (\*2) holds, i.e.,  $Q_{G2} > 0$ , then the CSC for  $Q_{G2}$  will give us  $\lambda_{G2} = 0$ . Then from the general solution (GS2) and (GS4), we know that  $Q_{G2}^*$  and  $Q_{L2}^*$  are the same as in Case I.

When (\*3) is violated, i.e.,  $Q_{L1} < 0$ , then by the non-negativity constraint for  $Q_{L1}$  we have  $Q_{L1}^* = 0$ . From (GS3) we have  $Q_{L1}^* = \frac{b_1^D - b_1^S - a_1^S T + \lambda_{L1}^*}{a_1^D + a_1^S} = 0$ . Solving for  $\lambda_{L1}^* = b_1^S - b_1^D + a_1^S T$  and substituting it into (GS1), we have  $Q_{G1}^* = T$

So the Step 2 ED solution vector is  $s^* = (Q_{G1}^*, Q_{G2}^*, Q_{L1}^*, Q_{L2}^*)$ , where

$$\begin{aligned}
Q_{G1}^* &= T \\
Q_{G2}^* &= \frac{b_2^D - b_2^S - a_2^D T}{a_2^D + a_2^S} \\
Q_{L1}^* &= 0 \\
Q_{L2}^* &= \frac{b_2^D - b_2^S + a_2^S T}{a_2^D + a_2^S} \\
LMP_1 &= b_1^S + a_1^S Q_{G1}^* = b_1^S + a_1^S T \\
LMP_2 &= b_2^S + a_2^S Q_{G2}^* = \frac{a_2^D b_2^S + a_2^S b_2^D - a_2^D a_2^S T}{a_2^D + a_2^S}
\end{aligned}$$

### Case III: (\*3) holds while (\*2) is violated

When (\*3) holds, i.e.,  $Q_{L1} > 0$ , then the CSC for  $Q_{L1}$  will give us  $\lambda_{L1} = 0$ . Then from the general solution (GS1) and (GS3), we know that  $Q_{G1}^*$  and  $Q_{L1}^*$  are the same as in Case I.

When (\*2) is violated, i.e.,  $Q_{G2} < 0$ , then by the non-negativity constraint for  $Q_{G2}$  we have  $Q_{G2}^* = 0$ . From (GS2) we have  $Q_{G2}^* = \frac{b_2^D - b_2^S - a_2^D T + \lambda_{G2}^*}{a_2^D + a_2^S} = 0$ . Solving for  $\lambda_{G2}^* = b_2^S - b_2^D + a_2^D T$  and substituting it into (GS4), we have  $Q_{L2}^* = T$ .

So the Step 2 ED solution vector is  $s^* = (Q_{G1}^*, Q_{G2}^*, Q_{L1}^*, Q_{L2}^*)$ , where

$$\begin{aligned} Q_{G1}^* &= \frac{b_1^D - b_1^S + a_1^D T}{a_1^D + a_1^S} \\ Q_{G2}^* &= 0 \\ Q_{L1}^* &= \frac{b_1^D - b_1^S - a_1^S T}{a_1^D + a_1^S} \\ Q_{L2}^* &= T \\ LMP_1 &= b_1^S + a_1^S Q_{G1}^* = \frac{a_1^D b_1^S + a_1^S b_1^D + a_1^D a_1^S T}{a_1^D + a_1^S} \\ LMP_2 &= b_2^D - a_2^D Q_{L2}^* = b_2^D - a_2^D T \end{aligned}$$

#### Case IV: Both (\*2) and (\*3) are violated

When (\*2) is violated, i.e.,  $Q_{G2} < 0$ , then by the non-negativity constraint for  $Q_{G2}$  we have  $Q_{G2}^* = 0$ .  $Q_{L2}$  is the same as in Case III, i.e.,  $Q_{L2}^* = T$ . When (\*3) is violated, i.e.,  $Q_{L1} < 0$ , then by the non-negativity constraint for  $Q_{L1}$  we have  $Q_{L1}^* = 0$ .  $Q_{G1}$  is the same as in Case II, i.e.,  $Q_{G1}^* = T$

So the Step 2 ED solution vector is  $s^* = (Q_{G1}^*, Q_{G2}^*, Q_{L1}^*, Q_{L2}^*)$ , where

$$\begin{aligned} Q_{G1}^* &= T \\ Q_{G2}^* &= 0 \\ Q_{L1}^* &= 0 \\ Q_{L2}^* &= T \\ LMP_1 &= b_1^S + a_1^S Q_{G1}^* = b_1^S + a_1^S T \\ LMP_2 &= b_2^D - a_2^D Q_{L2}^* = b_2^D - a_2^D T \end{aligned}$$

So the Step 2 ED solutions can be summarized as follows:

#### Step 2 ED Solution (T is binding from 1 to 2)

Case I	Case II	Case III	Case IV
$Q_{G1}^* = \frac{B_1 + a_1^D T}{A_1}$	$Q_{G1}^* = T$	$Q_{G1}^* = \frac{B_1 + a_1^D T}{A_1}$	$Q_{G1}^* = T$
$Q_{G2}^* = \frac{B_2 - a_2^D T}{A_2}$	$Q_{G2}^* = \frac{B_2 - a_2^D T}{A_2}$	$Q_{G2}^* = 0$	$Q_{G2}^* = 0$
$Q_{L1}^* = \frac{B_1 - a_1^S T}{A_1}$	$Q_{L1}^* = 0$	$Q_{L1}^* = \frac{B_1 - a_1^S T}{A_1}$	$Q_{L1}^* = 0$
$Q_{L2}^* = \frac{B_2 + a_2^S T}{A_2}$	$Q_{L2}^* = \frac{B_2 + a_2^S T}{A_2}$	$Q_{L2}^* = T$	$Q_{L2}^* = T$
$LMP_1 = \frac{E_1 + D_1 T}{A_1}$	$LMP_1 = b_1^S + a_1^S T$	$LMP_1 = \frac{E_1 + D_1 T}{A_1}$	$LMP_1 = b_1^S + a_1^S T$
$LMP_2 = \frac{E_2 - D_2 T}{A_2}$	$LMP_2 = \frac{E_2 - D_2 T}{A_2}$	$LMP_2 = b_2^D - a_2^D T$	$LMP_2 = b_2^D - a_2^D T$

where

$$\begin{aligned} A_1 &= a_1^D + a_1^S, & B_1 &= b_1^D - b_1^S, & D_1 &= a_1^D a_1^S, & E_1 &= a_1^D b_1^S + a_1^S b_1^D; \\ A_2 &= a_2^D + a_2^S, & B_2 &= b_2^D - b_2^S, & D_2 &= a_2^D a_2^S, & E_2 &= a_2^D b_2^S + a_2^S b_2^D. \end{aligned}$$

(b) If, on the other hand, we know  $T$  is binding from 2 to 1 based on Step 1 non-thermal-constraint ED solution, i.e.,  $\hat{Q}_{G2} - \hat{Q}_{L2} > T$  or  $\hat{Q}_{L1} - \hat{Q}_{G1} > T$ . We can set either  $Q_{G2} - Q_{L2} = T$  or  $Q_{L1} - Q_{G1} = T$ . But one of them is redundant due to the fact that the balancing constraint ( $Q_{G1} + Q_{G2} = Q_{L1} + Q_{L2}$ ) always holds in this two-node electric network model. So without loss of generality, let  $Q_{G2} - Q_{L2} = T$ .

Using the same procedure as in (a), we can derive another set of Step 2 ED solutions:

### Step 2 ED Solution (T is binding from 2 to 1)

Case I	Case II	Case III	Case IV
$Q_{G1}^* = \frac{B_1 - a_1^D T}{A_1}$	$Q_{G1}^* = \frac{B_1 - a_1^D T}{A_1}$	$Q_{G1}^* = 0$	$Q_{G1}^* = 0$
$Q_{G2}^* = \frac{B_2 + a_2^D T}{A_2}$	$Q_{G2}^* = T$	$Q_{G2}^* = \frac{B_2 + a_2^D T}{A_2}$	$Q_{G2}^* = T$
$Q_{L1}^* = \frac{B_1 + a_1^S T}{A_1}$	$Q_{L1}^* = \frac{B_1 + a_1^S T}{A_1}$	$Q_{L1}^* = T$	$Q_{L1}^* = T$
$Q_{L2}^* = \frac{B_2 - a_2^S T}{A_2}$	$Q_{L2}^* = 0$	$Q_{L2}^* = \frac{B_2 - a_2^S T}{A_2}$	$Q_{L2}^* = 0$
$LMP_1 = \frac{E_1 - D_1 T}{A_1}$	$LMP_1 = \frac{E_1 - D_1 T}{A_1}$	$LMP_1 = b_1^D - a_1^D T$	$LMP_1 = b_1^D - a_1^D T$
$LMP_2 = \frac{E_2 + D_2 T}{A_2}$	$LMP_2 = b_2^S + a_2^S T$	$LMP_2 = \frac{E_2 + D_2 T}{A_2}$	$LMP_2 = b_2^S + a_2^S T$

### 2.8.3 Appendix 3

Proof of Proposition 1:

First we want to show  $LMP_2 > LMP_1 \Leftrightarrow \Omega = (A_1 E_2 - A_2 E_1) / (D_1 A_2 + D_2 A_1) > T$ .

Recall in Step 2 ED solution, we know  $LMP_1 = \frac{E_1 + D_1 T}{A_1}$  and  $LMP_2 = \frac{E_2 - D_2 T}{A_2}$ . Then

$$\begin{aligned} LMP_2 > LMP_1 &\Leftrightarrow \frac{E_2 - D_2 T}{A_2} - \frac{E_1 + D_1 T}{A_1} > 0 \\ &\Leftrightarrow \frac{A_1 E_2 - A_2 E_1 - (D_1 A_2 + D_2 A_1) T}{A_1 A_2} > 0 \\ &\Leftrightarrow \frac{A_1 E_2 - A_2 E_1}{D_1 A_2 + D_2 A_1} > T \quad (\text{since } A_1, A_2, D_1, D_2 > 0) \end{aligned}$$

Next, let  $B_1 = b_1^D - b_1^S$ ,  $B_2 = b_2^D - b_2^S$  and  $C = b_2^S - b_1^S$  and we want to show  $T$  is binding from 1 to 2  $\Leftrightarrow \frac{A_1 E_2 - A_2 E_1}{D_1 A_2 + D_2 A_1} > T$ . Recall in the Step 1 ED solution and Definition 1,

$T$  is binding from 1 to 2  $\Leftrightarrow \hat{Q}_{G1} - \hat{Q}_{L1} > T$ , where

$$\hat{Q}_{G1} = \frac{D_2 B_1 + a_1^D a_2^S B_2 + a_1^D A_2 C}{D_1 A_2 + D_2 A_1}$$

$$\hat{Q}_{L1} = \frac{(D_2 + a_1^S a_2^D + a_1^S a_2^S) B_1 - a_1^S a_2^S B_2 - a_1^S A_2 C}{D_1 A_2 + D_2 A_1}$$

$$\begin{aligned} \hat{Q}_{G1} - \hat{Q}_{L1} > T &\Leftrightarrow \frac{a_2^S B_2 A_1 - a_1^S B_1 A_2 + A_1 A_2 C_1}{D_1 A_2 + D_2 A_1} > T \\ &\Leftrightarrow \frac{a_2^S (b_2^D - b_2^S) A_1 - a_1^S (b_1^D - b_1^S) A_2 + A_1 A_2 (b_2^S - b_1^S)}{D_1 A_2 + D_2 A_1} > T \\ &\Leftrightarrow \frac{A_1 (a_2^S (b_2^D - b_2^S) + b_2^S (a_2^D + a_2^S)) - A_2 (a_1^S (b_1^D - b_1^S) + b_1^S (a_1^D + a_1^S))}{D_1 A_2 + D_2 A_1} > T \\ &\Leftrightarrow \frac{A_1 (a_2^S b_2^D + a_2^D b_2^S) - A_2 (a_1^S b_1^D + a_1^D b_1^S)}{D_1 A_2 + D_2 A_1} > T \\ &\Leftrightarrow \frac{A_1 E_2 - A_2 E_1}{D_1 A_2 + D_2 A_1} > T \\ &\Leftrightarrow \Omega > T \end{aligned}$$

Since we showed  $T$  is binding from 1 to 2  $\Leftrightarrow \Omega > T$  and  $LMP_2 > LMP_1 \Leftrightarrow \Omega > T$ , we've proved (\*1) in Proposition 1. Similar procedures can easily be applied to prove (\*2) and (\*3). Q.E.D.

#### 2.8.4 Appendix 4

Proof of Proposition 3:

(i)  $T$  is binding from node 1 to node 2

Recall in the benchmark model total net benefit (TNB) is defined as the total net surplus for all generators and LSEs, that is,

$$TNB = (b_1^D Q_{L1} - \frac{1}{2} a_1^D Q_{L1}^2) - (b_1^S Q_{G1} + \frac{1}{2} a_1^S Q_{G1}^2) + (b_2^D Q_{L2} - \frac{1}{2} a_2^D Q_{L2}^2) - (b_2^S Q_{G2} + \frac{1}{2} a_2^S Q_{G2}^2)$$

$$\begin{aligned}
\frac{\partial TNB}{\partial T} &= (b_1^D \frac{\partial Q_{L1}}{\partial T} - a_1^D Q_{L1} \frac{\partial Q_{L1}}{\partial T}) - (b_1^S \frac{\partial Q_{G1}}{\partial T} + a_1^S Q_{G1} \frac{\partial Q_{G1}}{\partial T}) \\
&+ (b_2^D \frac{\partial Q_{L2}}{\partial T} - a_2^D Q_{L2} \frac{\partial Q_{L2}}{\partial T}) - (b_2^S \frac{\partial Q_{G2}}{\partial T} + a_2^S Q_{G2} \frac{\partial Q_{G2}}{\partial T}) \\
&= -\frac{a_1^S b_1^D}{A_1} + \frac{a_1^D a_1^S Q_{L1}}{A_1} - \frac{a_1^D b_1^S}{A_1} - \frac{a_1^D a_1^S Q_{G1}}{A_1} + \frac{a_2^S b_2^D}{A_2} - \frac{a_2^D a_2^S Q_{L2}}{A_2} - \frac{a_2^D b_2^S}{A_2} - \frac{a_2^D a_2^S Q_{G2}}{A_2} \\
&= \frac{a_2^S b_2^D + a_2^D b_2^S}{A_2} - \frac{a_1^S b_1^D + a_1^D b_1^S}{A_1} - \frac{a_1^D a_1^S (Q_{G1} - Q_{L1})}{A_1} - \frac{a_2^D a_2^S (Q_{L2} - Q_{G2})}{A_2} \\
&= \frac{E_2}{A_2} - \frac{E_1}{A_1} - (\frac{D_1}{A_1} + \frac{D_2}{A_2})T \\
\implies \frac{\partial TNB}{\partial T} > 0 &\Leftrightarrow \frac{E_2}{A_2} - \frac{E_1}{A_1} - (\frac{D_1}{A_1} + \frac{D_2}{A_2})T > 0 \\
&\Leftrightarrow \frac{A_1 E_2 - A_2 E_1}{A_1 A_2} > \frac{(D_1 A_2 + D_2 A_1)T}{A_1 A_2} \\
&\Leftrightarrow \frac{A_1 E_2 - A_2 E_1}{D_1 A_2 + D_2 A_1} > T \quad (\text{since } A_1, A_2, D_1, D_2 > 0)
\end{aligned}$$

From Proposition 1 we know that

$$T \text{ is binding from 1 to 2} \Leftrightarrow \frac{A_1 E_2 - A_2 E_1}{D_1 A_2 + D_2 A_1} > T$$

Therefore

$$\frac{\partial TNB}{\partial T} = \frac{E_2}{A_2} - \frac{E_1}{A_1} - \left(\frac{D_1}{A_1} + \frac{D_2}{A_2}\right)T > 0 \Leftrightarrow T \text{ is binding from 1 to 2;}$$

(ii)  $T$  is binding from node 2 to node 1

Very similar, we can show

$$\frac{\partial TNB}{\partial T} = \frac{E_1}{A_1} - \frac{E_2}{A_2} - \left(\frac{D_1}{A_1} + \frac{D_2}{A_2}\right)T > 0 \Leftrightarrow T \text{ is binding from 2 to 1.}$$

Q.E.D.

## 2.8.5 Appendix 5

### Proof of Proposition 7:

By a definition of social welfare, we have  $W_F = E[U(\tilde{\Pi}_{G1})] + E[U(\tilde{\Pi}_{G2})] + E[U(\tilde{\Pi}_{L1})] + E[U(\tilde{\Pi}_{L2})]$  and  $W_0 = E[U(\tilde{\pi}_{G1})] + E[U(\tilde{\pi}_{G2})] + E[U(\tilde{\pi}_{L1})] + E[U(\tilde{\pi}_{L2})]$ .

We can prove  $W_F - W_0 = \Delta_{G1} + \Delta_{G2} + \Delta_{L1} + \Delta_{L2} \geq 0$  if we can show (i)–(iv) are satisfied.

- (i)  $\Delta_{G1} \geq 0$ ;
- (ii)  $\Delta_{G2} \geq 0$ ;
- (iii)  $\Delta_{L1} \geq 0$ ;
- (iv)  $\Delta_{L2} \geq 0$ .

where

$$\begin{aligned}\Delta_{G1} &= E[U(\tilde{\Pi}_{G1})] - E[U(\tilde{\pi}_{G1})]; \\ \Delta_{G2} &= E[U(\tilde{\Pi}_{G2})] - E[U(\tilde{\pi}_{G2})]; \\ \Delta_{L1} &= E[U(\tilde{\Pi}_{L1})] - E[U(\tilde{\pi}_{L1})]; \\ \Delta_{L2} &= E[U(\tilde{\Pi}_{L2})] - E[U(\tilde{\pi}_{L2})].\end{aligned}$$

We'll prove (i)–(iv) one by one as follows:

Part (i), denote  $p \equiv prob$ , then,

$$\begin{aligned}\Delta_{G1} &= E[U(\tilde{\Pi}_{G1})] - E[U(\tilde{\pi}_{G1})] \\ &= pU(\pi'_{G1} + (H'_{12} - \eta_{12})FTR_{12(G1)}) + (1-p)U(\pi''_{G1} + (H''_{12} - \eta_{12})FTR_{12(G1)}) \\ &\quad - pU(\pi'_{G1}) - (1-p)U(\pi''_{G1}) \\ &= p \log \left( 1 + \frac{(H'_{12} - \eta_{12})FTR_{12(G1)}}{\pi'_{G1}} \right) + (1-p) \log \left( 1 + \frac{(H''_{12} - \eta_{12})FTR_{12(G1)}}{\pi''_{G1}} \right) \\ &= p \log \left( 1 + \frac{p(H'_{12} - \eta_{12})\pi''_{G1} + (1-p)(H''_{12} - \eta_{12})\pi'_{G1}}{(\eta_{12} - H''_{12})\pi'_{G1}} \right) \\ &\quad + (1-p) \log \left( 1 + \frac{p(H'_{12} - \eta_{12})\pi''_{G1} + (1-p)(H''_{12} - \eta_{12})\pi'_{G1}}{(\eta_{12} - H'_{12})\pi''_{G1}} \right) \\ &= \log \left( p^p(1-p)^{1-p} \left[ 1 + \frac{(H'_{12} - \eta_{12})\pi''_{G1}}{(\eta_{12} - H''_{12})\pi'_{G1}} \right]^p \left[ 1 + \frac{(\eta_{12} - H''_{12})\pi'_{G1}}{(H'_{12} - \eta_{12})\pi''_{G1}} \right]^{1-p} \right) \\ &= \log \left( p^p(1-p)^{1-p} [1 + X_{G1}]^p \left[ 1 + \frac{1}{X_{G1}} \right]^{1-p} \right)\end{aligned}$$

where

$$X_{G1} \equiv \frac{(H'_{12} - \eta_{12})\pi''_{G1}}{(\eta_{12} - H''_{12})\pi'_{G1}} > 0$$

Then in order to show  $\Delta_{G_1} \geq 0$ , we need to show

$$p^p(1-p)^{1-p} [1 + X_{G_1}]^p \left[ 1 + \frac{1}{X_{G_1}} \right]^{1-p} \geq 1$$

For notation simplicity, let  $x \equiv X_{G_1} > 0$ , and  $A \equiv p^p(1-p)^{1-p} > 0$ , and define a function  $f(\cdot)$  such that

$$f(x) = A(1+x)^p \left(1 + \frac{1}{x}\right)^{1-p}$$

Notice that when  $x = \frac{1}{p} - 1$ ,  $f(\frac{1}{p} - 1) = 1$ . So to prove  $f(x) \geq 1$  is equivalent to prove the function  $f(x)$  is monotonically decreasing over the domain  $(0, \frac{1}{p} - 1)$  and monotonically increasing over the domain  $(\frac{1}{p} - 1, +\infty)$ . Rewrite  $f(x)$  as follows:

$$f(x) = A(1+x)x^{p-1}$$

$$\begin{aligned} f'(x) &= Ax^{p-1} + A(1+x)(p-1)x^{p-2} \\ &= Ax^{p-2}[p(1+x) - 1] \\ &= Ax^{p-2}p[x - (\frac{1}{p} - 1)] \end{aligned}$$

$$\Rightarrow f'(x) \begin{cases} < 0 & \text{if } x < \frac{1}{p} - 1; \\ > 0 & \text{if } x > \frac{1}{p} - 1; \\ = 0 & \text{if } x = \frac{1}{p} - 1. \end{cases}$$

That is,  $f(x)$  has a global minimum at  $x = \frac{1}{p} - 1$ . The minimum is:

$$f\left(\frac{1}{p} - 1\right) = 1$$

Hence,  $f(x) \geq 1$ ,  $\forall x \in (0, \infty)$ , or  $f(p) \geq 1$ ,  $\forall p \in (0, 1)$ . Notice if the regularity condition is satisfied we have

$$\begin{aligned} 1 > prob > \overline{prob}_{G_1} &= \frac{(\eta_{12} - H''_{12})\pi'_{G_1}}{(H'_{12} - \eta_{12})\pi''_{G_1} + (\eta_{12} - H''_{12})\pi'_{G_1}} = \frac{1}{\frac{(H'_{12} - \eta_{12})\pi''_{G_1}}{(\eta_{12} - H''_{12})\pi'_{G_1}} + 1} = \frac{1}{X_{G_1} + 1} \\ \Leftrightarrow p \in \left(\frac{1}{1+x}, 1\right) &\subseteq (0, 1) \quad (\text{Recall } p \equiv prob, x \equiv X_{G_1}) \end{aligned}$$

So when the regularity condition is satisfied, i.e.,  $G_1$  takes long positions in the FTR market, we certainly have  $f(p) > 1$ , which directly implies  $\Delta_{G_1} > 0$ . If, on the other hand, the



regularity condition is not satisfied, it can be easily shown that it corresponds to the case where  $p \in (0, \frac{1}{1+x})$  and  $G_1$  takes short positions (although it is not allowed in this model) in the FTR market, which also implies  $\Delta_{G_1} > 0$ . Finally, in the degenerate case where  $p$  happens to be  $\frac{1}{1+x}$ , then  $G_1$  takes zero position in the FTR market and  $\Delta_{G_1} = 0$ . Therefore regardless whether  $G_1$  takes long, short or zero position in the FTR market,  $\Delta_{G_1} \geq 0$ .

It is straightforward to verify that (ii), (iii) and (iv) are true using the exactly same procedures as in (i). Since we have showed that (i)–(iv) are all satisfied, we've proved the proposition result,  $W_F \geq W_0$ . Q.E.D.

## CHAPTER 3. EVALUATING THE PERFORMANCE OF FINANCIAL TRANSMISSION RIGHTS AUCTION MARKET: EVIDENCE FROM THE U.S. MIDWEST ENERGY REGION

### 3.1 Abstract

This paper applies empirical methods to analyze performance of *financial transmission rights* (FTRs) auction markets in the Midwest energy region (MISO). The data we used are monthly FTR auction clearing prices and associated congestion revenues for the period April 2005 - March 2006. Based on the preliminary statistical analysis, we summarize and present the stylized facts about the MISO FTR auction market. Moreover, we fit the data with linear regressions and nonparametric kernel regressions, and carry out a bootstrap-based goodness-of-fit test on the linear versus kernel fits. Regression results suggest that the MISO FTR market participants are neither risk neutral or risk averse during the current sample periods. The revenue sufficiency results show that the MISO FTR market is systematically losing money, which suggests that market participants on average exhibit some degree of risk loving behavior. More data are needed in order to obtain meaningful economic analysis such as estimating the impact of an agent's risk preference on his willingness to pay for the premium of FTR in this complex market. It would be especially helpful to acquire the actual bidding and asking prices of market participants in the MISO FTR auctions over time.

**Keywords:** Financial transmission rights (FTRs), FTR auctions, Congestion revenues, Risk hedging, Nonparametric estimation, Kernel regression, Goodness-of-fit test

**JEL Codes:** G1, L9, C14

### 3.2 Introduction

In March 2005, the Midwest Independent System Operator (MISO) officially adopted the Wholesale Power Market Platform (WPMP) proposed by U.S. Federal Energy Regulatory Commission (FERC) in April 2003. An important feature of FERC's WPMP design is to help alleviate the transmission congestion problems by issuing *financial transmission rights (FTRs)*. By construction, an FTR is a financial contract that entitles the holder to a stream of revenues (or charges) based on the difference between the hourly day-ahead locational marginal price (LMP) at the sink and source nodes. Due to congestion on transmission lines, day-ahead LMPs can be very volatile, and FTRs make a hedging instrument against the price risks. In principle, market participants could reduce the price uncertainty by purchasing FTRs for a specified amount of MWs on the paths<sup>1</sup> of the transmission grid that they anticipate to be congested during a given period of time.

But in real practice, to what extent FTRs have performed in helping market participants hedge transmission congestion exposure in the new Midwest wholesale power market is still unclear. It is also interesting to empirically test and assess the risk preferences for the FTR market participants. For example, do they exhibit the "usual" risk averse behavior as commonly assumed in theoretical models? Moreover, does the current FTR market satisfy the revenue sufficiency condition resulted from a good market design? In this study, we will address these questions and issues using econometric estimation tools with publicly available MISO FTR auction data and historical LMP data.

As far as we know, no empirical work up to date has been done to analyze the MISO FTR market. Even for a broader geographic range, only a handful few studies have been conducted to investigate the empirical aspects of FTR market in other regions such as in the state of New York. Adamson and Englander (2005) examined the efficiency of the New York transmission congestion contract (TCC)<sup>2</sup> market. They used monthly TCC auction prices and congestion revenues between November 1999 and April 2003. A two-stage modeling approach

<sup>1</sup>FTRs are available not only for physical paths. They can be defined between any two nodes in the grid.

<sup>2</sup>TCC: Transmission Congestion Contract, which is one implemented form of FTR.

was adopted to analyze the data. In the first stage, they used the time series ARCH-ARMA model to forecast the mean and variance of spot prices (congestion rents). Then in the second stage, a simple linear model was proposed to regress TCC auction prices on the predicted mean and variance of spot prices from the first stage of modeling. From the results, they concluded that the New York TCC auctions were highly inefficient, even after allowing for risk aversion among bidders in the auctions.

Siddiqui et al. (2005) carried out another empirical study for the New York TCC market based on annual TCC auctions in years 2000 and 2001. They found that although TCCs appeared to provide a potentially effective hedge against volatile congestion rents, the prices paid for TCCs were systematically different from the resulting congestion rents. Their conclusion was that the unreasonably high risk premiums paid for the TCCs suggested an inefficient market and that the possible explanations were the lack of liquidity in TCC markets and the difference between TCC feasibility requirements and actual energy flows. However, these results held only under the assumption that market participants are all risk-neutral. Risk-averse agents, instead, may pay for TCCs the amount more than the expected congestion charges. Therefore, the deviation of TCC payments from resulting congestion revenues did not necessarily indicate market inefficiency.

In their follow-up work (Siddiqui et al. 2006), they re-analyzed the New York TCC data, taking into account possible risk aversion of market participants. Instead of using a linear model, they employed three different concave “utility functions” and fitted nonlinear regressions to the TCC payments and revenues data. Their results showed that market participants were only slightly risk averse (or even risk seeking, depending on the utility function employed). Thus, risk aversion by itself could not fully explain the systematic divergence between the TCC prices and congestion rents. The authors concluded that it was the very design of these markets, rather than the behavior of market participants that led to the observed discrepancy between prices and revenues.

In our study, we focus on the FTR market in the Midwest energy region (MISO), which has never been investigated empirically in the literature. Compared with the other FTR markets

such as New York's, the MISO FTR market has a much shorter history. The scarcity of available data with MISO poses a great challenge to reaching any complete conclusion about this emerging market. Unavoidably, we need to make assumptions in order to analyze, to the best extent, the data we could obtain. Although some of the assumptions cannot be tested due to insufficient data, we will be able to check for validity of these assumptions once more data become available. Through our analysis, we find a number of stylized facts as well as evidence of the performance of the MISO FTR market. The main results show that based on the current sample periods, the MISO FTR market is systematically losing money, which in turn suggest that on average the market participants exhibit some degree of risk loving.

The rest of the paper is organized as follows. Section 2 provides some background information about the MISO energy and FTR auction markets. In section 3, we review the underlying theory of hedging and risk preferences on which our analysis is based. Section 4 provides a detailed description of the data. The empirical methods and assumptions are discussed in section 5. In section 6, we present and interpret our results. Finally, the concluding remarks are given in section 7.

### 3.3 MISO Energy and FTR Markets

Founded on February 12, 1996, MISO is an independent and non-profit organization whose primary roles are to provide equal access to the transmission system and ensure reliable and efficient electric system in a competitive wholesale power market in the Midwest region. Currently MISO is managing transmission operations for all or parts of 15 U.S. states plus Manitoba province in Canada.

Figure 3.1 shows the current MISO operation territory. Since April 2005, MISO has been operating a day-ahead energy market, a real-time energy market and an FTR market. The day-ahead market is a forward market in which hourly LMPs are calculated for each hour of the next operating day. According to MISO's Market Concepts Study Guide (MISO 2005c), the day-ahead market is cleared using the security-constrained unit commitment (SCUC) and security-constrained economic dispatch (SCED) algorithms to satisfy energy demand bid and



Figure 3.1 The Current Midwest Independent System Operator (MISO) Service Territory

supply offer requirements. To be specific, the objective in clearing the day-ahead market is to minimize the costs of day-ahead energy procurement over the 24-hour dispatch horizon based on the offers and bids, subject to network constraints and resource operating constraints. The results of the day-ahead market clearing include hourly LMP values and hourly demand and supply quantities, which are posted on MISO's market portal on 1700 hours EST. The real-time energy market, in contrast, is an instant balancing market in which the LMPs are calculated every five minutes, based on MISO dispatch instructions and actual system operations. These two markets operate in a coordinated sequence and are settled separately. In the settlement of the day-ahead market each hourly MW injection is paid the day-ahead LMP at its node and withdrawals are charged the day-ahead LMP at their respective nodes. The day-ahead LMPs are also used to establish the settlement value of FTRs and bilateral transactions. The real-time settlement is based on actual hourly quantity deviations from the day-ahead scheduled quantities and on real-time prices integrated over the hour. Any deviation in the quantity from

the day-ahead schedule (including bilateral transactions) is charged or paid real-time LMPs.

### 3.3.1 LMP Components

Since FTRs crucially depend on locational marginal prices (LMPs), it is important to take a close examination on LMP and its components. By definition, LMP at any given pricing location is the minimum incremental cost of servicing one additional unit of demand at that location under the constraints of production, congestion and transmission losses. LMPs vary by time and location. Variability of LMPs is due to the physical constraints, congestion and losses. For each node, MISO determines three separate components of its LMP, namely the marginal energy component (MEC), marginal congestion component (MCC) and marginal loss component (MLC). MEC is the LMP of the reference node, so is the same for all the nodes. MCC and MLC of a certain node represent the marginal cost of congestion and marginal cost of losses, respectively at that node relative to the reference node. Formally,

$$\begin{aligned} LMP_n &= MEC_r + MCC_n + MLC_n \\ LMP_r &= MEC_r \end{aligned}$$

where  $r$  is the reference node and  $n$  is any node other than the reference one.

Of the three LMP components,  $MEC_r$  is calculated as the marginal cost of energy at the reference node  $r$ , so is determined by the cost functions of the generators at that node. The congestion component,  $MCC_n$  is calculated as follows:

$$MCC_n = - \left( \sum_{k=1}^K GSF_{nk} \times FSP_k \right)$$

where  $K$  is the number of thermal or interface transmission constraints (also called *flowgates*),  $GSF_{nk}$  is the shift factor (or distribution factor) for the generation at node  $n$  on flowgate  $k$  and  $FSP_k$  is the shadow price of the thermal limit on flowgate  $k$ . Intuitively,  $GSF_{nk}$  is the proportion of each MW injected at node  $n$  and withdrawn at the reference node  $r$  and  $FSP_k$  is the cost saved from one MW increase in the capacity of flowgate  $k$ <sup>3</sup>. In the Midwest market,

<sup>3</sup>According to the industry convention, the effect of losses is ignored in determining  $GSFs$ .

congestion is handled financially through the MCC of the LMP, and the congestion revenue from holding the FTR is determined by the difference in MCCs.

$MLC_n$  is calculated using the equation

$$MLC_n = (DF_n - 1) \times MEC_r$$

where  $DF_n$  is the delivery factor for node  $n$  to the reference node.  $DF_n$  is equal to  $1 - \frac{\partial L}{\partial G_n}$ , where  $L$  is system losses and  $G_n$  is the amount of power injected at node  $n$ . Therefore,  $\frac{\partial L}{\partial G_n}$  is the change in system losses due to an incremental change in the power injection at node  $n$  holding everything else constant.

### 3.3.2 Overview of MISO FTR Acquisition

FTRs are tradable financial instruments that allow market participants to hedge against the cost and uncertainty that may arise from congestion in the transmission grid. The FTR holders are entitled to a stream of revenues or charges based on the congestion over the FTR path. FTRs are used in the day-ahead market only and do not apply to the real-time market. They do not protect market participants from congestion charges related to scheduling power in the real-time market or deviation from the day-ahead schedule. Nor do they hedge against transmission loss charges. Besides, FTRs are independent of the physical power dispatch. The FTR holder has the financial right to the congestion between two specified nodes regardless of the actual energy deliveries.

An FTR is specified by its source and sink location, the MW amount, the term for which the FTR is in effect, the time period (peak or off-peak hours), and whether the FTR is an obligation or option. FTR options are currently not available in the MISO market. An FTR obligation grants the holder the right to collect, for each MW of FTR, the congestion rent accumulated from the source to the sink for every hour during the effective period. The congestion rent is determined by the difference between the congestion components in the day-head LMPs at the sink and source. Therefore, an FTR obligation can have a positive or negative economic value, depending on the actual congestion pattern between the source and sink on which the FTR is defined. During the hours when the congestion component at the sink is greater than



the congestion component at the source, the FTR yields a positive revenue to the holder. If, instead, the congestion occurs from the sink to the source, the holder of the FTR will have to pay MISO an amount equal to the congestion rent in the congested direction, or equivalently receive a negative revenue.

In the Midwest, market participants can acquire FTRs through allocations (annual and monthly), auctions (annual and monthly) and the secondary market. FTRs are first allocated in the annual allocation based on existing entitlements from transmission service reservations and grandfathered agreements. The annual FTR auction is held right after the annual allocation and prior to the beginning of each year for the subsequent four seasons<sup>4</sup>. In this auction, market participants can submit offers to sell or bids to buy FTRs and MISO determines the winning (i.e., market-cleared) sellers and buyers. In order to be eligible for the annual auction, the FTR must be valid for the entire period of the seasons in the auction. A monthly allocation is performed for each operating month to come. Those FTRs eligible in the initial allocation that did not receive their full entitlement in FTR awards can be re-considered in this monthly allocation process. Then after the monthly allocation takes place, the monthly auction is conducted. Any FTR eligible for the monthly auction must be valid for the entire month in the auction. The exact timeline for the MISO monthly FTR allocations and auctions are given in Appendix for a sample month (August 2005). There is also a secondary market for buying and selling FTRs. The FTR allocations are irrelevant to our research purpose in this paper, as there is no market or price for the allocation. Therefore, we do not consider the allocations in evaluating the market performance. In both the annual and monthly auctions, FTRs are sold and bought at the market clearing prices. The determination of the market clearing prices will be explained later. However, the data for the annual allocations are not sufficient since MISO has only adopted FERC's WPMP design since March 2005. In addition, a time interval of three months may be too long for discerning any change or trend in this market during the one-year period. Therefore, a monthly basis is proper for our research purpose. Although the secondary market is also relevant to our study, we have to ignore it, because little information

<sup>4</sup>The four seasons are: (i) Winter: December, January, February; (ii) Spring: March, April, May; (iii) Summer: June, July, August; (iv) Fall: September, October, November.

is available about it. In all, considering relevance and availability, we finally choose to focus on the monthly FTR auctions and ignore the possible effects of other means to obtain FTRs.

### 3.3.3 MISO Monthly FTR Auctions

MISO conducts monthly FTR auctions for two purposes: (1) to allow MISO to sell FTRs for the adjusted monthly FTR capability of the market footprint, and (2) to facilitate the buying and selling of existing FTRs between market participants. Market participants buy from or sell to the available “pool” of system FTR capacity. All FTRs at the monthly auction have a term of one month beginning on the first day of the month following the auction. Market participants must submit their offers or bids to MISO during the monthly bidding period and MISO posts the auction results no later than 5 business days before the start of the subject month (see Appendix for a more detailed MISO FTR allocation and auction timeline for a sample month - August 2005). Each monthly auction consists of two separate auctions: one for the peak period and the other for the off-peak period. Peak is the period of time from 0600 hours Eastern Standard Time (EST) to 2200 hours EST on weekdays excluding holidays<sup>5</sup>. Off-peak is all periods not classified as peak. The buyer of a peak (off-peak) FTR from the monthly auction is entitled to the aggregate congestion rents of the peak (off-peak) hours during the whole month.

FTR buyers are responsible for submitting a bid that indicates the following:

1. Type of FTR (obligation or option)
2. FTR source and sink
3. Maximum MW quantity desired
4. Maximum acceptable price, in \$/MW
5. Period (peak or off-peak)

---

<sup>5</sup>These holidays are specified by North American Electric Reliability Council (NERC)

Similarly, FTR sellers should submit an offer including the above items 1 through 5 except that item 3 now becomes the maximum MW quantity offered instead of desired. Given the offers and bids for each monthly auction, MISO determines the winners (traders that get cleared, i.e., the infra-marginal traders) as well as FTR clearing quantities and clearing prices by solving a linear programming problem. Specifically, it maximizes the value of FTRs bought minus FTRs sold by auction participants subject to simultaneous feasibility constraints with “n-1” security constraints. All comparable FTRs are sold at the same market clearing price expressed in \$/MW, which is calculated as the difference in the shadow price of the power flow balance constraint at the FTR source and sink in the FTR auction linear programming problem above. It can be interpreted as the negative of the marginal change in the objective function value due to an infinitesimal change in the flow from the FTR source to the sink. It is worth noting that the FTR clearing price can be negative, which means that the market participants who buy the FTR will receive money from MISO whereas those who sell the FTR will pay money to MISO. This usually happens when the particular line associated with this FTR is anticipated to be congested in the direction opposite to that specified by the FTR.

### 3.4 Theory

In this section, we first illustrate, through several examples, the role of FTRs in hedging against risks caused by the volatile location marginal prices (LMPs). In doing so, we consider two cases: electricity transaction scheduled on bilateral agreements and electricity transaction purely via the market-based power pool. Then we demonstrate the relationship between the expected revenue from holding FTRs and the agent’s willingness to pay.

#### 3.4.1 Hedging Role of FTR

LMPs in the wholesale electricity market not only provide the right incentives for generation and consumption, but also create a need to hedge the price changes. This leads to the interest in FTRs. Power transactions are usually settled through bilateral schedules or via the market-based power pool. In either case, FTR provides a hedge against the congestion charge by

reimbursing the holders part or all of the charge. How FTR works as an hedging instrument is illustrated through the following examples<sup>6</sup>.

Let us first consider the case of bilateral agreements. If there were no transmission congestion, we can treat all production and consumption as if they took place in the same location since both buyer and seller are settled with the same price, which is the single equilibrium price in the market. Then the natural arrangement is to contract for differences against the equilibrium price. As depicted in Figure 3.2, a GENCO (G) and an LSE (L) are located at node 1 and node 2, respectively. The two nodes do not have to be directly connected by a transmission line, so we use the dashed line between them. The nodes and lines may only be part of a larger network, which is not drawn in the figure. Suppose G and L agree on a (bilaterally agreed) price of  $p_B$  (\$/MWh) for trading a fixed quantity of electricity  $q$  MWs at a specific hour. If there is no congestion in the network during this hour, the prices (or more precisely the LMPs) at all nodes would turn out to be the same, hence denoted by a common price  $LMP$ . G will then sell electricity to the market at  $LMP$  and L will buy electricity from the market at  $LMP$ . Note that the  $q$  MWs that L purchases do not have to be produced by G, and the electricity that G generates may be bought by other LSEs. So the arrows indicate the direction of the contract path. If  $LMP > p_B$ , under the contract, G owes L  $LMP - p_B$  for each of the  $q$  MWs over this hour. On the opposite, if  $p_B > LMP$ , L owes G  $p_B - LMP$  for each of the  $q$  MWs over this hour. This is the so-called “contract for difference” (CFD), which locks the actual transaction price at the predetermined price  $p_B$  for both G and L, and thus provides a perfect hedge against the price risk. Therefore, in the absence of congestion, a bilateral arrangement between the GENCO and the LSE can capture the effect of aggregate movements in the market, as the single market price gets up or down over time.

Most of the time, however, there is congestion somewhere in the transmission network. In that case, nodal prices will differ depending on the locations, and G and L may no longer face the same price. This situation is illustrated in Figure 3.3. Let  $LMP_1$  and  $LMP_2$  be the locational marginal prices at node 1 and 2, respectively, and  $LMP_1 \neq LMP_2$  due to the

<sup>6</sup>For simplicity, we do not consider transmission losses in our examples.

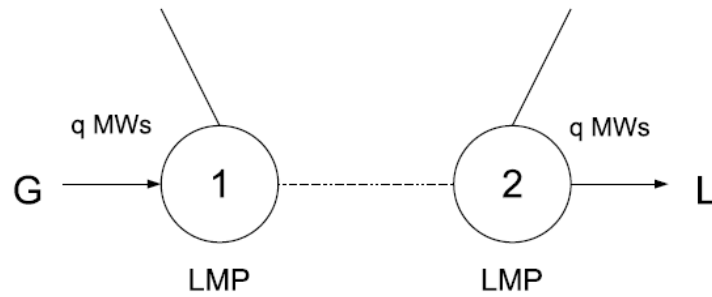


Figure 3.2 Bilateral contract with no congestion

congestion. Also let  $p_B$  be the bilaterally agreed contract price between G and L. Then at the settlement G will sell electricity to the market for  $LMP_1$  and L will buy electricity from the market for  $LMP_2$ . If  $LMP_1 < p_B < LMP_2$ , then L pays  $LMP_2 - p_B$  more than the contracted price and needs to be compensated for the excessive payment. On the other hand, G receives  $p_B - LMP_1$  less than the contracted price, which also needs to be compensated. Obviously, it is impossible to satisfy both parties only through the CFD and something else is needed to completely hedge the price risk.

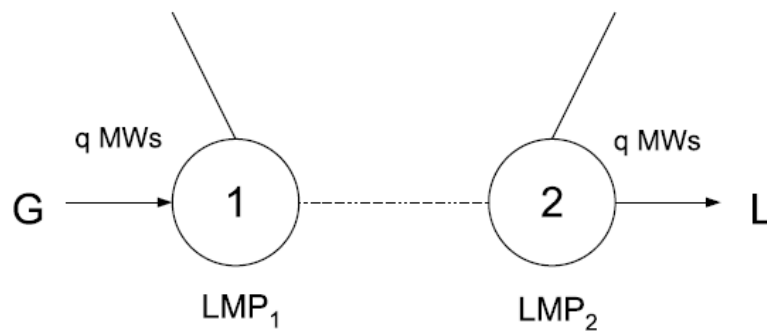


Figure 3.3 Bilateral contract with congestion

Still consider the situation in Figure 3.3. Now suppose that apart from the CFD, G may

obtain an FTR for  $q$  MWs defined from node 1 to node 2. The FTR entitles G to the difference in the LMP between the two nodes, i.e.  $LMP_2 - LMP_1$  for that hour. L pays  $LMP_2$  for the power. The settlement system in turn pays G  $LMP_1$  for the power supplied. As the holder of the FTR, G would receive  $LMP_2 - LMP_1$  for each of the  $q$  MWs covered under the FTR. Therefore G ends up receiving  $LMP_2$  for each MWs sold and L ends up paying  $LMP_2$  for each MW bought. In this sense, we come back to the previous situation when the price is the same at all nodes and the CFD will work out now. If  $LMP_2 > p_B$ , G will compensate L for its excessive payment  $LMP_2 - p_B$  according to the CFD. If  $LMP_2 < p_B$ , G will be compensated for the loss  $p_B - LMP_2$  of L. As a result, no matter how the LMPs change, the transaction would be effectively settled at the deterministically and bilaterally agreed price  $p_B$ . On the other hand, L can also buy the same FTR for  $q$  MWs but in the opposite direction, i.e. from node 2 to node 1, and receive the difference  $LMP_1 - LMP_2$  for each MW. Together with  $LMP_2$  it pays for buying power from the market, L actually pays  $LMP_1$ , exactly the price at which G sells power. Again, G and L face the same price with the aid of the FTR. Then by the CFD, the final price for each party will be the predetermined contracted price  $p_B$ . Therefore, in the presence of transmission congestion, FTR together with CFD can provide full hedge against the risk associated with the LMPs. The function of FTRs in the scenario of bilateral contract actually lies in equalizing the price that the seller and buyer face, which provides the condition for the CFD to be workable. The FTR provides hedge against locational price risks, while the CFD, against temporal price risks. In this example, the FTR together with CFD provides a perfect hedge for both parties, because the quantity of FTRs obtained exactly matches the contracted quantity of electricity. If G or L buys the FTR for an amount less than the contracted quantity of electricity, they will only have partial coverage.

In summary, a seller and a buyer entering into a bilateral transaction of electricity between two nodes can always hedge against the price risk by using the FTR and CFD jointly. The FTR that the seller or buyer purchases should always be in the direction from its own node to the other's.

Now let us come to the case with no bilateral schedules. That is, each GENCO simply

injects electricity to the power pool and gets the LMP at its own node for each MW injected. Each LSE withdraws electricity from the same power pool and pays the LMP at its own node for each MW withdrawn. Hence a GENCO does not know or care about where its power is withdrawn and who actually buys the power it has produced. Similarly, an LSE does not know where the power it buys comes from and who generates it. This is different from the transaction under a bilateral contract in which the seller and the buyer as well as the injection and ejection nodes are designated and the transaction price is predetermined<sup>7</sup>. In the bilateral contract case, a combination of the FTR and CFD can provide a perfect hedge and make the payment and revenue nonrandom. Without a bilateral contract, however, it is not obvious to a market participant that between which two nodes he pays the congestion charge. Hence he does not know for sure between which two nodes he should obtain the FTR to hedge the potential congestion. We can see this from the following example as depicted in Figure 3.4.

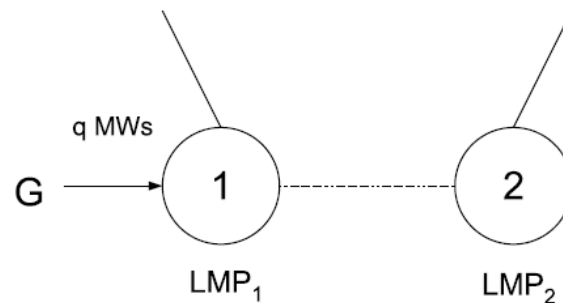


Figure 3.4 Transaction via a power pool with congestion

This figure looks similar to Figure 3.3, but notice that only the  $q$  MWs injection of  $G$  is given.  $G$  does not know where these  $q$  MWs would be withdrawn or through what paths they would be transited.  $G$  only knows that it would get  $LMP_1$  for each MW it produces.  $LMP_1$  is volatile and fluctuates with the generation, loads and congestion patterns.  $G$  is exposed to the price risk and might want to hedge against it. Suppose that  $LMP_2$ , for some reason, is

<sup>7</sup>Though in the case of bilateral transaction, the  $q$  MWs purchased by the LSE may not be the same  $q$  MWs that GENCO produces, either.

relatively stable and does not change much<sup>8</sup>. If G purchases an FTR of  $q$  MWs from node 1 to node 2, it would get  $LMP_1 + (LMP_2 - LMP_1) = LMP_2$  for each MW generated. In this sense, holding the FTR reduces G's price uncertainty by making its revenue less volatile. If  $LMP_2$  is virtually nonrandom, then the FTR provides a perfect hedge for G. If  $LMP_2$  is also random, but is much more stable than  $LMP_1$ , then the FTR provides a non-perfect partial hedge. To reduce its revenue uncertainty, G could effectively associate its revenue with  $LMP_2$  by holding the FTR from node 1 to node 2.

This is not the only choice for the hedging. In fact, G can choose a set of FTRs (portfolio of FTRs) to achieve the same result. Let us take another example with a three-node network in Figure 3.5.

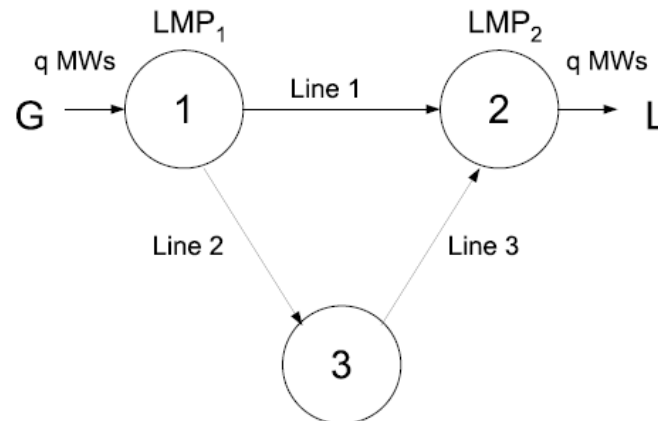


Figure 3.5 The three-node electric network example

In this example, the only generator G is located at node 1 and the only LSE L is located at node 2. For computational simplicity, assume that each line has the same impedance. Then of each MW injected at node 1,  $\frac{2}{3}$ ,  $\frac{1}{3}$  and  $\frac{1}{3}$  will move along line 1, line 2 and line 3, respectively. Clearly, G will have a revenue of  $q \times LMP_1$  from injecting  $q$  MWs of electricity at node 1. To

<sup>8</sup>This might occur at a hub which consists of a set of nodes and whose LMP is derived from the average of the LMPs of those nodes.



hedge against the congestion charge, G may obtain  $q$  MWs of FTR defined from node 1 to node 2. Then G's total revenue will be  $q \times LMP_1 + q \times (LMP_2 - LMP_1) = qLMP_2$ . As mentioned earlier, if  $LMP_2$  is nonrandom, then the FTR provides G with a perfect hedge. This is not the only way to achieve the deterministic revenue  $qLMP_2$ . An alternative could be that G obtains a portfolio of FTRs with  $\frac{2}{3}q$  MWs of FTR from node 1 to node 2,  $\frac{1}{3}q$  MWs of FTRs from node 1 to node 3 and  $\frac{1}{3}q$  MWs of FTRs from node 3 to node 2. G will again end up with  $q \times LMP_1 + \frac{2}{3}q \times (LMP_2 - LMP_1) + \frac{1}{3}q(LMP_3 - LMP_1) + \frac{1}{3}q(LMP_2 - LMP_3) = qLMP_2$ . This FTR portfolio also links G's revenue to  $LMP_2$ , which is less volatile than  $LMP_1$ . As will be seen later, market participants in practice sometimes purchase more than one single FTR and indeed construct FTR portfolios.

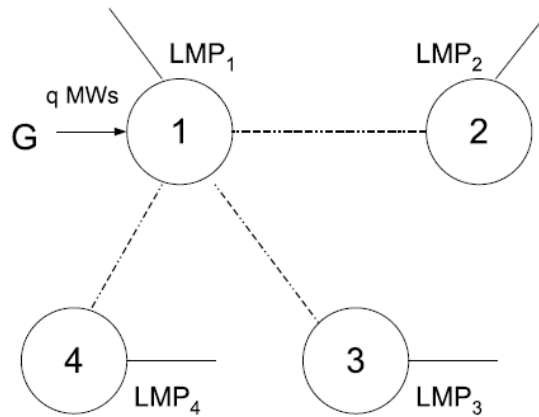


Figure 3.6 No bilateral transaction with congestion: FTR portfolio

Figure 3.6 gives another example of hedging using an FTR portfolio. Similar to the previous examples, G injects  $q$  MWs to the power pool and receive payments at its own nodal price  $LMP_1$  for each MW injected. Since  $LMP_1$  is varriate, G may want to hedge against the uncertainty using FTRs. Suppose that the LMPs at nodes 2, 3 and 4 change almost independently, such that the pairwise correlations between the LMPs at the nodes 2, 3 and 4 are very small. Let  $\sigma_n^2$  be the variance of the LMP at node  $n$ , for  $n = 1, 2, 3, 4$ . Then G can reduce the

price risk by holding a portfolio of FTRs associated with the nodes 2, 3 and 4. Let  $q_{12}$ ,  $q_{13}$ , and  $q_{14} \geq 0$  be the quantity of MWs that G obtains for the FTR from 1 to 2, from 1 to 3 and from 1 to 4, respectively and assume that  $q_{12} + q_{13} + q_{14} = q$ . Consequently, G will get

$$\begin{aligned} & LMP_1 q + (LMP_2 - LMP_1) q_{12} + (LMP_3 - LMP_1) q_{13} + (LMP_4 - LMP_1) q_{14} \\ = & q_{12} LMP_2 + q_{13} LMP_3 + q_{14} LMP_4 \end{aligned}$$

which is a weighted average of the LMPs of the three nodes. This revenue is still random and its variance can be calculated as

$$\begin{aligned} & var(q_{12} LMP_2 + q_{13} LMP_3 + q_{14} LMP_4) \\ = & q_{12}^2 \sigma_2^2 + q_{13}^2 \sigma_3^2 + q_{14}^2 \sigma_4^2 + 2q_{12} q_{13} \sigma_{23} + 2q_{12} q_{14} \sigma_{24} + 2q_{13} q_{14} \sigma_{34} \\ = & q_{12}^2 \sigma_2^2 + q_{13}^2 \sigma_3^2 + q_{14}^2 \sigma_4^2 \end{aligned}$$

where  $\sigma_{23}$ ,  $\sigma_{24}$  and  $\sigma_{34}$  are the pairwise covariances of the LMPs at nodes 2, 3 and 4. The second equality holds when the three LMPs are pairwise uncorrelated. The variance of G's revenue in the absence of the FTR portfolio is

$$var(q LMP_1) = (q_{12} + q_{13} + q_{14})^2 \sigma_1^2$$

If  $LMP_2$ ,  $LMP_3$  and  $LMP_4$  are almost constant, that is,  $\sigma_2^2$ ,  $\sigma_3^2$  and  $\sigma_4^2$  are nearly zero, then  $var(q_{12} LMP_2 + q_{13} LMP_3 + q_{14} LMP_4) \approx 0$  and holding the FTRs completely eliminates the risk associated with  $LMP_1$ . If  $LMP_2$ ,  $LMP_3$  and  $LMP_4$  are no more volatile than  $LMP_1$ , that is, if  $\sigma_2^2 \leq \sigma_1^2$ ,  $\sigma_3^2 \leq \sigma_1^2$  and  $\sigma_4^2 \leq \sigma_1^2$ , then

$$var(q_{12} LMP_2 + q_{13} LMP_3 + q_{14} LMP_4) \leq var(q LMP_1)$$

This relationship may also hold if  $LMP_2$ ,  $LMP_3$  or  $LMP_4$  are negatively correlated. Hence, holding this FTR portfolio lowers G's risk exposure, although the portfolio may not completely eliminate the risk. In all, the FTRs provide G with a hedge, but not necessarily a perfect one.

From the above examples, we find that under a bilateral agreement, FTRs together with CFDs can always provide a perfect hedge against the price risk and a GENCO ends up with

a fixed revenue. In comparison, in the absence of bilateral agreements, the resulting revenue that a GENCO receives from selling electricity and holding FTRs is usually a function of the LMPs. So the revenue may not be fixed and its variability depends on the variations of LMPs at different nodes and their covariances. Under some conditions, this variability of G's revenue is less than the one if G does not have FTRs, and FTRs provide a hedge against the risk. The hedging functionality of FTRs is similar for LSEs who purchase, rather than sell power. In analogy, holding FTRs can also provide a hedge against the volatile revenue of an LSE.

A complete analysis of FTR hedging requires knowledge of the power transactions in which market participants are primarily engaged – whether it is through bilateral contract or via the power pool. The literature, however, often ignores the type of power transactions which motivates the market participants to obtain FTRs and only focuses on the random congestion charges. Knowing that the volatility in congestion charges comes from the volatility in LMPs, most papers conclude that market participants simply have to purchase enough FTRs to hedge their transmission congestion exposure perfectly. They regard the congestion charges as the only random variables and make their reasoning this way: since market participants can have these charges reimbursed by holding FTRs, FTRs will provide a perfect hedge. This, as can be seen from our previous examples, generally does not hold. An agent chooses FTRs to hedge against the risk with the LMP exposure, not simply the congestion charges. The FTRs may provide a full coverage for the congestion payment but not for the market participant's total income from power transactions via the pool.

### 3.4.2 Theoretic Framework

Although from the previous subsection, we know that in some cases holding FTRs may not completely eliminate the uncertainty that an agent faces in the market, we make a simplifying assumption that FTRs will always provide a perfect hedge for our theoretical analysis. That is, an agent can make his profit deterministic or free of price risk by holding an FTR. Let  $w$  denote the non-stochastic total profit of an agent resulting from obtaining an FTR. Then without the FTR, the agent's profit is  $w - R$ , where  $R$  is the congestion charge (or revenue)

the agent has to pay, and  $R$  is a random variable. Hence,  $w - R$  is also a random variable and the agent's profit is uncertain. An FTR reimburses the congestion charge  $R$  for the agent no matter how much  $R$  is. So the expected revenue from holding the FTR is  $E(R)$ . As a result, holding the FTR locks the agent's profit at  $w$  and provides a perfect hedge against the risk. Of course the agent has to pay in order to acquire the FTR. We will use  $F$  to denote the maximum \$ amount he is willing to pay for the FTR.

Consider a risk-neutral agent, his utility function can be expressed as

$$u(\pi) = a + b\pi$$

where  $a$  and  $b$  are constants and  $b > 0$ ;  $\pi$  is the agent's profit or payoff. Suppose that the congestion charge  $R$  is distributed according to a probability density function (PDF)  $f(R)$ . Then in the absence of FTR, the agent's profit  $\pi = w - R$  is a random variable and his expected utility is given by

$$\begin{aligned} Eu(w - R) &= \int u(w - R) f(R) dR \\ &= a + b(w - E(R)) \end{aligned}$$

If he purchases FTR for  $\$F$ , his utility will be

$$u(w - F) = a + b(w - F)$$

By certainty equivalence theory, the agent's willingness to pay ( $F$ ) for the FTR satisfies

$$Eu(w - R) = u(w - F)$$

Hence,

$$F = E(R) \tag{3.1}$$

which means that a risk-neutral agent is willing to pay up to exactly the expected charge or revenue from holding the FTR. Note that the relationship still holds if we divide both sides of equation (3.1) by any positive constant. Choosing the MWs of the FTR as the divisor, we then have that the expected congestion revenue of one MW FTR or the expected unit revenue (which is equal to the sink LMP less the source LMP) should be equal to the unit willingness to

pay under risk neutrality. This justifies our use of congestion revenue per MW of FTR and the unit price in later analysis, instead of multiplying them by the purchase quantity. Therefore, if the expected unit revenue is plotted against the unit willingness to pay, it should be a 45 degree line if all agents are risk neutral.

Now consider a risk-averse agent, he would be willing to pay extra premium to stabilize his profit to a deterministic amount. By certainty equivalence theory, we have the following equation

$$Eu(w - R) = u(w - F) \quad (3.2)$$

By Jensen's inequality, it follows that

$$u(w - F) = Eu(w - R) < u(E(w - R)) = u(w - ER)$$

Since utility function  $u(\cdot)$  is monotonically increasing, it is straightforward that the willingness-to-pay for FTR ( $F$ ) is always greater than the expected value for congestion charge ( $R$ ), that is,

$$F > ER \quad (3.3)$$

This means a risk-averse agent is willing to pay more than the expected charge or revenue from holding the FTR. However, the further relationship between  $F$  and  $ER$  depends not only on the entire distribution of random variable  $R$  but also on the specific functional form of utility function  $u(\cdot)$ . It is beyond the scope of this paper to explore such relationship in full detail.

### 3.5 Data

Our study focuses on the one-month FTRs that were purchased in the monthly FTR auctions in MISO from April 2005 to March 2006. The data we use are obtained from the FTR auction results of the twelve months and the historical day-ahead LMP files, which are all

publicly available on MISO's website<sup>9</sup>. Specifically, the results of each FTR monthly auction include, the buyer, the source and sink, the MW amount awarded, the class (peak or offpeak), whether it is an obligation or option and the market clearing price measured in \$/MW<sup>10</sup>. For each MW of FTR awarded, the buyer must pay the clearing price of that FTR, which is determined in the auction for each month  $t$ . So the clearing price is actually the *unit cost* of obtaining an FTR. Let  $F_t^{m,n}$  denote the market clearing price of the FTR defined from node  $m$  to node  $n$  for month  $t$ ,  $t = 1, \dots, T$ .

The auction results do not directly report the unit revenue from holding an FTR, that is, the congestion rent per MW accumulated from the source to the sink for the effective month. Hence in the data pre-processing stage, we calculate the unit revenue using the congestion component (MCC) of the day-ahead LMPs, which can be found in the historical day-ahead LMP files. For each of the twelve sample months, the historical day-ahead LMP data set includes the MCC of each node for each of the 24 hours in each day of that month. For example, in May 2005, there are 31 days, each having 24 hours. So, for a node such as WPS.PULLIAM3, we have  $24 \times 31 = 744$  hourly MCCs. The frame of the hourly MCCs for node WPS.PULLIAM3 in May 2005 is given in Table 3.1 as follows.

Table 3.1 Hourly MCCs of node WPS.PULLIAM3 in May 2005

MCC	$d = 1$	$d = 2$	$d = 3$	...	$d = 31$
$h = 1$	0.04	0.46	2.89	...	0.62
$h = 2$	0.02	0.88	2.99	...	1.69
$h = 3$	0.04	0.60	2.92	...	1.67
...	...	...	...	...	...
$h = 24$	0.04	0.29	1.34	...	3.79

The value in each cell in the figure is the MCC of node WPS.PULLIAM3 for the corresponding hour  $h$  of the corresponding day  $d$  in May 2005. For example, the cell corresponding to  $h = 1$  and  $d = 1$  is the MCC of node WPS.PULLIAM3 in the first hour on May 1, 2005. This table structure applies to all the other nodes in each month of the sample period. During

<sup>9</sup><http://www.midwestiso.org/>

<sup>10</sup>So far, all the FTRs auctioned in MISO are obligations.

the twelve months in our study, the nodes and number of nodes for each month stay the same within that month, but may not be so across months. As time goes on, new nodes are added to MISO's transmission network or some existing nodes are removed from it. The number of nodes for each month as well as the change in the number from the previous to the current month are given in Table 3.2.

Table 3.2 Reported number of nodes in MISO service region (April 2005 – March 2006)

Month	Number of nodes	Change	Percentage
Apr-05	1471		
May-05	1471	0	0.00%
Jun-05	1496	25	1.70%
Jul-05	1496	0	0.00%
Aug-05	1496	0	0.00%
Sep-05	1508	12	0.80%
Oct-05	1508	0	0.00%
Nov-05	1508	0	0.00%
Dec-05	1535	27	1.79%
Jan-06	1536	1	0.07%
Feb-06	1536	0	0.00%
Mar-06	1520	-16	-1.04%

Given the MCC data described above, the revenue that the FTR owner gets for each MW of FTR held can be derived as the sum of the difference between the hourly sink and source MCCs in the day-ahead market over all hours in the effective month. Let  $h = 1, \dots, 24$  index the hour, and  $d = 1, \dots, D_t$  index the day, where  $D_t$  is the number of days in month  $t$ . Let  $p_{hdt}^n$  be the MCC of node  $n$  at hour  $h$  on day  $d$  in month  $t$ . Then  $R_t^{m,n}$ , the revenue from holding one MW of the FTR from node  $m$  to node  $n$  during month  $t$  can be computed as

$$R_t^{m,n} = \sum_d \sum_h (p_{hdt}^n - p_{hdt}^m) \quad (3.4)$$

We can also call  $R_t^{m,n}$  the unit revenue of the FTR from  $m$  to  $n$ . Note that for peak FTRs, the revenues are calculated by aggregating MCC differences for the peak hours; for off-peak FTRs, the MCC differences used in calculating the revenues are all those for the off-peak hours. So,

in equation (3.4), the range of  $d$  and  $h$  over which the MCC difference is aggregated depends on whether the FTR is peak or off-peak.

We notice that in some months, some sources or sinks on which the FTRs are defined cannot be found in the list of the day-ahead LMP file of the corresponding months. In that case, we are unable to calculate the revenue from holding those FTRs. For example, in June 2005, the market participant EMMT bought 5.8 MWs of the FTR from node NSP.CHARA6 to node GRE.WILM, but the source node is not found in the LMP file for the same month. Such discrepancies occur because the commercial model changed after the FTR auction results were finalized. For example, the June 2005 auction was conducted in May 2005. The June commercial model was propagated into the FTR system after the June 2005 auction was completed. Sources and sinks on the awarded FTRs were corrected to match the updated model, but the reported auction result was not updated since it reflected the actual outcome from the auction as it was conducted. A snapshot of the most current active FTRs in the system is available on the portal, but not currently posted on MISO public website. In our analysis, we shall ignore any FTR defined on the “missing” nodes.

Similar to the number of nodes, the number of FTRs purchased in the monthly auctions is not the same across all months either. More FTRs were bought in some months than others, as is shown in Table 3.3. Several factors contribute to the fluctuating number of the FTRs purchased. As the number of nodes on which FTRs are defined varies across month, the change in the FTR purchase number is natural and understandable. For example, if new nodes are added to the network, more FTRs will be available, since they can be defined on more combinations of nodes. Besides, seasonality may also cause more FTRs to be purchased in some months than others. With only one year’s data, we cannot tell much about the effect of seasonality on the FTRs purchased. A longer sample period for a relatively stable transmission network is needed for analyzing the seasonality effect. This will be possible for MISO as time goes on.

Before proceeding, let us introduce some notations for FTR types that is applied systematically throughout the rest of this paper. Since all auctioned FTR can be classified as either



Table 3.3 Reported number of distinct FTRs (April 2005 – March 2006)

Month	Number of distinct FTRs	Month	Number of distinct FTRs
Apr-05	164	Oct-05	932
May-05	255	Nov-05	1448
Jun-05	349	Dec-05	1446
Jul-05	863	Jan-06	1278
Aug-05	989	Feb-06	2105
Sep-05	870	Mar-06	1761

peak or off-peak<sup>11</sup>, and people's purchasing decisions regarding peak and off-peak FTRs are expected to be different, we classify our data into two parts: peak and off-peak accordingly. In addition, since there are certain FTRs (defined by point of source and point of sink) that are purchased by more than one buyers, and since all of them will receive the same prices and congestion rents, we will also distinguish our data between non-distinct and distinct. The non-distinct data are simply the original data while the distinct data are the data where duplicated FTR purchase on the same FTRs are removed.

By this POND (Peak, Off-peak, Non-distinct, Distinct) classification, we will have four different classes of FTRs over the period April 2005 - March 2006. These four classes of FTRs are: ON (Off-peak and Non-distinct), OD (Off-peak and Distinct), PN (Peak and Non-distinct) and PD (Peak and Distinct). All the statistical computations are implemented using R<sup>12</sup>.

A quick overview of the data gives us some stylized facts of the MISO's FTR market. First of all, for all four types of FTRs, the average clearing prices and congestion revenues collected are highly volatile across all months. For example, the average clearing price of PD FTRs in April 2005 is highly negative (-6313.36), while the value in January 2006 is highly positive (960.31). This might be a sign of an immature and unstable new market. The second observation is that for most of the FTRs awarded, there was only one buyer for each FTR. In other words, the difference between distinct and non-distinct FTRs is not large, which may

<sup>11</sup>Peak and off-peak periods are as defined on Section 3.3.3 in this paper.

<sup>12</sup>R is an open-source software environment for statistical computing and graphics. More information about R can be found at <http://www.r-project.org>.

imply that the MISO monthly FTR auction market is quite thin. See Table 3.4 for reported number of non-distinct and distinct FTRs and their difference for the sample period.

Table 3.4 Reported number of non-distinct and distinct FTRs (April 2005 – March 2006)

Month	NumN <sup>a</sup>	NumD <sup>b</sup>	NumN-NumD
Apr-05	167	164	3
May-05	311	255	56
Jun-05	353	349	4
Jul-05	890	863	27
Aug-05	1062	989	73
Sep-05	911	870	41
Oct-05	1011	932	79
Nov-05	1569	1448	121
Dec-05	1707	1446	261
Jan-06	1510	1278	232
Feb-06	2218	2105	113
Mar-06	1988	1761	227

<sup>a</sup>Number of non-distinct FTRs

<sup>b</sup>Number of distinct FTRs

The result from Table 3.4 indicates that the liquidity of the monthly MISO FTR market increases during the one-year period. In April 2005, the market was so illiquid that there were only 3 more non-distinct FTRs than distinct FTRs. The overall tendency in the difference was increasing as time went on, although the difference in June, September 2005 and March 2006 decreased from the previous month. These fluctuations may be explained by seasonality factors, but we need more information to provide a definite answer.

## 3.6 Empirical Methodologies

### 3.6.1 Overview

In this study, the goal is to empirically analyze the performance of MISO FTR market based on 12 month data. In addition, we want to explore the possible risk preference exhibited by the market participants. As shown earlier, a risk-neutral agent is willing to pay FTR up

to his expected congestion revenue accumulated from the source to the sink specified by the FTR.

An interesting hypothesis we would like to test is as follows:

$$H_0 : ER_t^{m,n} = F_t^{m,n}, \quad \forall m, n \in \Omega, t = 1, \dots, T \quad (3.5)$$

where  $R_t^{m,n}$  is the revenue from holding one MW of the FTR from node  $m$  to node  $n$  for month  $t$ ,  $F_t^{m,n}$  is the market clearing price of the FTR defined from node  $m$  to node  $n$  for month  $t$ , and  $\Omega$  is the set of all possible pairs of injection and withdrawal node. This hypothesis is to test if the expectation of the unit congestion revenue of an FTR (\$/MWh) is equal to the clearing price of that FTR during month  $t$ .

Or equivalently, we can test this hypothesis via the following regression specification:

$$ER_t^{m,n} = \alpha_0 + \alpha_1 F_t^{m,n} + \eta_t \quad (3.6)$$

where  $\eta_t$  is a mean zero iid error term. Since we do not have data for the expected value of unit congestion revenue  $ER_t^{m,n}$ , we have to make a transformation on the above regression specification.

$$R_t^{m,n} = \beta_0 + \beta_1 F_t^{m,n} + \epsilon_t \quad (3.7)$$

where  $\epsilon_t = (R_t^{m,n} - ER_t^{m,n}) + \eta_t$  and  $E[\epsilon_t] = 0$ <sup>13</sup>.

The estimated  $\beta_0$  and  $\beta_1$  should be close to 0 and 1, respectively, if the MISO FTR market is populated with market participants with risk neutral risk preference.

In the following subsection, we first discuss briefly the linear regression model to estimate Equation (3.7); then move on to introduce the nonparametric kernel regression model to estimate general relationship between  $R_t^{m,n}$  and  $F_t^{m,n}$ . Finally, we carry out a goodness-of-fit test

<sup>13</sup>Note that the transformation step from (3.6) to (3.7) is justified because (a) the transformed error term  $\epsilon_t$  is still mean zero, and (b) the independent variable  $F_t^{m,n}$  is truly predetermined, i.e., market participants purchase FTRs at the clearing price before the associated congestion revenue accrues to them one month later. The cost of doing so is the potential loss of statistical power. But since as the estimation result shows later, we actually reject all the significance tests for the parameters, the loss of power is then not of a concern in this study.

to see if the simple linear relationship between expected congestion revenue of FTR and its clearing price could be refuted.

### 3.6.2 Linear Regression Model

For simple notation, let  $x$  denote the monthly FTR auction clearing price ( $F_t^{m,n}$ ) and  $y$  denote its associated congestion revenue ( $R_t^{m,n}$ ). The simple linear model can be specified as:

$$y_i = \beta_0 + \beta_1 x_i + \epsilon_i \quad (3.8)$$

Under ordinary least squares (OLS) estimation, the estimated coefficients  $\hat{\beta}$  is:

$$\hat{\beta} = (\mathbf{x}^T \mathbf{x})^{-1} \mathbf{x}^T \mathbf{y} \quad (3.9)$$

where  $\beta = (\beta_0 \ \beta_1)^T$  and  $\mathbf{x} = (\mathbf{1} \ x)$ . Then the estimated linear fit function is

$$\hat{y} = \hat{m}_{\hat{\beta}}(x) = \mathbf{x} \hat{\beta} = \mathbf{x} (\mathbf{x}^T \mathbf{x})^{-1} \mathbf{x}^T \mathbf{y} \quad (3.10)$$

### 3.6.3 Kernel Regression Model

Under the weaker assumption of IID observations  $(x_1, y_1) \dots (x_n, y_n) \in \mathbb{R}^2$ , the general non-parametric regression model can be written as:

$$y_i = m(x) + \epsilon_i \quad (3.11)$$

where  $m(x) = E(Y|X = x)$  is the conditional mean function (regression function)

This conditional mean function  $m(\cdot)$  tells us how  $y$  and  $x$  are related “on average”, which can be estimated using modern nonparametric technique such as kernel regression method. The most commonly used kernel smoothing estimator for estimating  $m(\cdot)$  is called the *Nadaraya-Watson* (NW) estimator, which is given by

$$\hat{m}_h(x) = \frac{\sum_{i=1}^n K\left(\frac{x-x_i}{h}\right) y_i}{\sum_{i=1}^n K\left(\frac{x-x_i}{h}\right)} \quad (3.12)$$

where  $K(\cdot)$  is the kernel function, which is usually a probability density function (PDF)<sup>14</sup>, and  $h$  is the smoothing parameter or bandwidth, which controls the amount of smoothness in the fitted density estimate. The nice structural form of the NW estimator can be derived from the definition of the conditional expectation. See Sun (2006) for a detailed treatment.

### 3.6.4 Goodness-of-fit Test

To formally test whether the linear model is adequate enough to explain the relationship between expected congestion revenue of FTRs and its clearing price, we use the kernel-based nonparametric goodness-of-fit test. The null hypothesis is that the true underlying relationship between variable  $x$  and  $y$  can be represented by function  $m$  which is characterized by parameter  $\beta$ , that is,

$$H_0 : m = m_\beta \quad \text{v.s.} \quad H_1 : m \neq m_\beta$$

where  $m_\beta(x)$  is some  $\beta$ -parameterized function of  $x$ . Let  $\hat{m}_h(x)$  denote the NW estimator of  $m(x)$ , and let

$$\tilde{m}_\beta(x) = \frac{\sum_{i=1}^n K\left(\frac{x-x_i}{h}\right) m_\beta(x_i)}{\sum_{i=1}^n K\left(\frac{x-x_i}{h}\right)},$$

denote an NW smoothing of  $m_\beta(x)$ . Note that  $m_\beta(x)$  is just the parametric estimate of function  $m_\beta(x)$ . Hardle and Mammen (1993) propose the following test statistic:

$$T_n = nh^{d/2} \int_{-\infty}^{\infty} \{\hat{m}_h(x) - \tilde{m}_\beta(x)\}^2 w(x) dx \quad (3.13)$$

For simplicity, let  $w(x) = f(x)$  where  $f(x)$  is a PDF, and  $d = 1$  as usually done in the literature, then we can approximate  $T_n$  by:

$$T_n \approx nh^{1/2} \sum_{i=1}^n \{\hat{m}_h(x) - \tilde{m}_\beta(x)\}^2 \quad (3.14)$$

<sup>14</sup>Technically, a kernel function  $K(\cdot)$  should satisfy the following four conditions: (i)  $\int K(u)du = 1$  (pdf), (ii)  $\int uK(u)du = 0$  (symmetry), (iii)  $\int u^2K(u)du = \sigma_K^2 > 0$  (finite variace), (iv)  $K(u) \geq 0$  for all  $u$  in the domain of  $K$  (non-negativity).

In addition to calculate the test statistic, we need to find its critical value to carry out the test. Since the distribution of this test statistic does not fall into any easily-identifiable parametric distributions, there are basically two approaches to obtain its critical value – either through asymptotic normality approximation or through bootstrap simulation. Since in this case the asymptotic approximation yields a rather inefficient speed of convergence (at the rate of  $n^{-1/10}$ , see Hardle and Mammen (1993) for details procedures in this approach), we opt for using the bootstrap approach to obtain the critical value. Furthermore, since naive bootstrap (i.e., resampling of  $\{(x_i^*, y_i^*)\}_{i=1}^n$  from  $\{(x_i, y_i)\}_{i=1}^n$ ) fails in regression context, we may use the *wild bootstrap* originally introduced by Wu (1986).

Denote  $\hat{t}_\alpha^*$  as the critical value, then the bootstrap assisted GOF test for  $H_0 : m = m_\beta$  is rejected if  $T_n > \hat{t}_\alpha^*$ . Detailed procedures about this approach can be found in Sun (2006).

### 3.7 Results

In this section, we discuss the results of the MISO monthly FTR auctions using the data from April 2005 through March 2006. Recall that we classify the FTR data into four categories, i.e., Off-peak and non-distinct (ON), Off-peak and distinct (OD), peak and non-distinct (PN), and peak and distinct (PD). The following results are reported for all these four FTR types. First, we present summary statistics and stylized facts about MISO FTR auction market, and calculate the degree to which market participants predicted congestion patterns correctly. Second, we apply a set of econometric tools including linear regression, nonparametric kernel regression and goodness-of-fit test to provide a descriptive analysis of the relationship between the FTR clearing price and the associated congestion revenue in the MISO FTR market. Finally, we investigate another issue of this complicated market - whether the revenue sufficiency condition holds, i.e., whether MISO as a central clearinghouse is systematically losing money or earning money from the FTR auction market.

### 3.7.1 Summary Statistics

For each FTR purchase in each monthly auction between April 2005 and March 2006, we determine the unit cost of purchasing that FTR and unit revenue from holding it. Based on the data, we calculate a set of summary statistics for all the four types of FTRs over the entire sample months<sup>15</sup>, and report them in Table 3.6–3.9.

The upper half of Table 3.6–3.9 reports the total number of observations and the average price and congestion revenues as well as their standard deviations. From the summary result, it appears that both the FTR price and congestion revenue are highly volatile, which suggests that MISO FTR market is still in its immature stage. It is worth noting that the FTR price can be negative. This can be explained as follows. Let node A and node B be the source and sink nodes, on which an FTR is defined. Then the agents anticipating congestion from node A to node B (hence with positive congestion revenue) would be willing to pay a positive amount for this FTR, while those that expect congestion in the opposite direction (hence with negative congestion revenue) would be willing to pay a negative amount for this FTR, i.e., expecting to get paid for purchasing this FTR.

As we examine the bottom half of Table 3.6–3.9, this relationship between the FTR price and congestion revenue is also confirmed by the data. For example, the positive Pearson correlation coefficient for each month indicates that  $F$  and  $R$  move together to some degree. Specifically, the average correlation is medium high at 0.54 during the sample period. We also calculate and report the number of correct prediction, which is defined as the data point where the FTR price  $F$  and the congestion revenue  $R$  have the same sign. The result shows that most market participants predict the congestion directions correctly, as the proportion of the correct predictions in the total number of awarded FTRs is always greater than 50% and for some months it is nearly 80%. Furthermore, we examine the number and the percentage of the awarded FTRs for which the price paid is lower than the congestion revenue collected. We call these FTRs “winners” in the sense that market participants can make positive profit from purchasing these FTRs. For all four types of FTRs, the percentage of “winners” is relatively

<sup>15</sup>We do notice that the summary result for the first month (April 2005) are considerably different from those in the later months.

high (the mean value for all these winner percentage is 59%).

### 3.7.2 Linear Regression Estimation

We fit the linear regression in (3.7) for all four types of FTR data for each month. The results are summarized in Table 3.10-3.13 and also depicted in Figure 3.7-3.10.

The description of the figures is as follows: the brown dotted lines are the zero-zero lines; the red dashed line is the 45 degree line; the green line is the linear regression fit; and the blue curved line is the nonparametric kernel fit.

As in the figures, the results show that every quadrant has some points, although some have more points than others. For each month, there are some “wild” points far from the origin, and the observations are widely spread. In spite of that, most of the points lie close to the zero-price or zero-revenue axis, meaning that the prices and congestion revenues of most FTRs are not extremely positive or extremely negative. This is consistent with the reality of line physical condition that most of the time the congestion levels are moderate.

There is clear evidence that the slope of the regression line is different from one<sup>16</sup>, but is always positive, which confirms the positive correlation between the revenue and price. For some months, the slope is greater than one, while for other months, it is lower than one. This means that sometimes market participants systematically lose money and sometimes systematically earn money when they try to hedge congestion risk exposures. For most of the months, the intercept is far away from zero.

These graphic observations can also be confirmed by the estimated results reported in Table 3.10-3.13. Clearly the estimated regression coefficients  $\beta_0$  and  $\beta_1$  are very different from 0 and 1, and most of their associated p-values are far less than 0.01. Therefore we can reject the null hypothesis that market participants are all risk neutral in the MISO FTR market. Due to the complicated nature of this market, it may not be sophisticated enough to only fit a linear regression. To explore other possible relationship between FTR clearing price and the associated congestion revenue, we apply a nonparametric kernel regression to estimate the

<sup>16</sup>There are some cases where the slope is very close to one such as ON FTRs in Oct-05 and Mar-06.



relationship between FTR price and the congestion revenue.

### 3.7.3 Kernel Regression and GOF Test

As briefly introduced in Section 3.6.3, we applied NW kernel regression to all four types of FTR data over 12 months. The fitted kernel curves appear to be highly non-linear as they shown in Figure 3.7-3.10. Although, due to the noise data, the kernel fit does not suggest any plausible non-linear relationship between the FTR price and the congestion revenue, we still can use it to construct a goodness-of-fit (GOF) test against the linear model. The bootstrap sample size is chosen to be 1000. The GOF test result is reported in Table 3.14. The result shows that all the tests are rejected at significance level 0.004 or better, which implies that the underlying relationship between  $F$  and  $R$  is significantly different from the linear fit.

The linear regression results in the preceding subsection indicate that the market participants in the MISO FTR market are not risk neutral. The goodness of fit test shows that the linear fit may not be proper for the data observed. Naturally, we are motivated to ask if the market participants exhibit other risk preferences such as risk aversion. As shown earlier, by Jensen's inequality we know that agent's willingness to pay ( $F$ ) should be larger than the expected congestion revenue from holding the FTR ( $ER$ ) under risk-aversion assumption,  $F > ER$ . However, from the estimated kernel regression functions, we observe that many fitted kernel curves are above the 45 degree line, which means that the risk "premium" is negative. Therefore, using the kernel fits as exploratory methods to examine the validity of the risk-aversion assumption, we may conclude that the market participants may not be risk averse either.

### 3.7.4 Revenue Sufficiency Analysis

Another interesting aspect of MISO FTR market is to examine to what degree this market observes revenue sufficiency. In other words, we would like to calculate the monthly total net revenue for each type of FTRs, where net revenue for each individual FTR contract is defined as the difference between the FTR clearing price and the associated revenue multiplied by the

number of contracts, and the monthly total net revenue is the sum of all net revenue for each individual FTR contracts at each month. If the monthly total net revenue is positive or close to zero, then we can say the MISO FTR market exhibits revenue sufficiency. If on the other hand, the monthly total net revenue is negative, then the MISO FTR market does not have revenue sufficiency.

Denote the monthly total net revenue for the ON FTR as  $\text{NetRev.ON}_t$  and denote the number of contracts for FTR at month  $t$  and effective between node  $m$  and  $n$  as  $Q_t^{m,n}$ , then we have the following expression for  $\text{NetRev.ON}_t$ .

$$\text{NetRev.ON}_t = \sum_{m,n \in \Omega} (F_t^{m,n} - R_t^{m,n}) Q_t^{m,n} \quad (3.15)$$

Similar calculations apply to other three types of FTRs for all month of data. The results are reported in Table 3.15 and Figure 3.11. The results show that for all four types of FTRs and for all months except two the total net revenue is largely negative, indicating that the MISO is systematically losing money in the FTR market. The monthly pattern for two offpeak (ON and OD) FTRs are very similar with each other. There is a large negative dip in the month of August 2006 and a small negative dip in the month of December 2006. Likewise the monthly pattern for two peak (PN and PD) FTRs are very similar with each other too. There is a small negative dip in the month of September 2006 and a large negative dip in the month of December 2006.

This result on the other hand suggests that the market participants on average might exhibit some degree of risk affection by paying less than the expected congestion revenue to purchase FTRs. However since the calculated total net revenue is an aggregated result, more data are needed to reach a more definite conclusion about market participant's risk preferences in the FTR market.

### 3.8 Conclusions

Some empirical work has been conducted with the existing FTR markets, such as the NYISO TCC market, but none has been done to empirically investigate the newly established

MISO FTR market. In this paper, we examine the performance of this market, using publicly available data on the FTR clearing prices and the associated congestion revenues in the monthly auctions between April 2005 and March 2006. Our study provides some empirical evidence of how this young market has been performing so far. We find that the new market has something in common with the mature ones and also possesses some unique features. The features that the MISO FTR market and NYISO TCC market share are listed as follows:

1. The correlation between FTR clearing prices and congestion revenues is positive for each month.
2. For each month, most of the FTR holders make correct predictions about the direction of congestions, that is, the price and revenue have the same sign.
3. A considerable portion of FTR holders make money by purchasing the FTRs, that is, the clearing price is lower than the revenue collected.

At the same time, the MISO FTR market has some stylized facts that are not seen in the more mature markets:

1. The number of distinct and non-distinct awards is different for different months, but increases over the 12 months on the whole.
2. The FTR market is quite thin, in the sense that there is only one buyer for most FTRs; But the difference between the number of non-distinct FTR awards and the number of distinct ones increases, meaning that this market gets thicker over time.
3. The average FTR auction clearing prices and revenues are very volatile across all months.
4. The correlation between FTR clearing prices and congestion revenues has a slightly increasing trend over the 12 months.
5. The results for the first month (April 2005) are very different from later months.

Compared with the first three common features, these five unique characteristics are indicators of this new market, but they could also imply that this market is getting more mature

as time goes on. If we had a longer sample period, we might be able to see more clearly the progressing of this market and differentiate between the trend and the seasonal component. This is a task to be accomplished in the future.

As to the performance of the MISO FTR market, we find that the market works well in terms of some measures such as the proportion of correct predictions. The results from the simple linear regression suggest that the market participants in this market are not risk neutral. To further explore the relationship between the FTR clearing price the congestion revenue, we apply the nonparametric kernel regression method. The kernel fit results suggest that the MISO FTR market might not be risk averse either. Moreover we carried out a goodness-of-fit test against the linear fit. The test results indicate that comparing with the kernel fit, the linear fit is not adequate enough to capture the underlying structure of the relationship between the FTR clearing price and the congestion revenue in this market. Last but not the least, we calculate the monthly total net revenue of all four types of FTRs to evaluate the revenue sufficiency condition in the FTR market. The results show that the MISO is systematically losing money in the FTR market, which on the other hand suggests that the market participants might to some degree exhibit risk affection behavior.

Due to lack of more detailed data, such as the bids and offers data submitted by the market participants, we cannot make strong conclusion about the risk preference exhibited in this market and other more detailed performance analyses in the market. This may be accomplished in the future when more data become available.

The contributions of this paper are in two-folds. First, this paper explores the newly formed MISO FTR market using empirical methods. With the available data, we summarize the stylized facts about MISO FTR market and apply various econometric methods to characterize the performance of the FTR market. Second, in this paper we conduct theoretic analysis of the hedging role of FTRs and provide reference for further empirical analysis once we have access to more data. For example, we point out the need to know if a power transaction is bilateral or via a pool when examining the risk coverage provided by FTRs. Since the available data do not provide such information, we do not differentiate between these two types of power

transactions in our study. We also mention that one should consider the FTR purchase in the context of the more fundamental wholesale electric power market, but we are not able to do this in the paper due again to the data availability. To fully understand the underlying data generating process for the MISO FTR market, both FTRs and power transactions need to be considered simultaneously.

There can be several extensions to our work. One is to compare the MISO FTR market with the more mature markets such as New England and New York FTR markets to see exactly what the difference is and why. With data of a longer sample period, we can carry out time series analysis to further investigate the development of the young market and to see if it will be similar to those well established markets. Another extension might be to analyze FTR auctions together with the electricity transactions and individual behaviors, so as to get an integrated view of how FTRs are used to reduce the risk associated with the agent's profit. This is quite challenging and requires data not only from the FTR and energy market, but also from individual market participants. This may be accomplished by either human-subject experiments or agent-based computational simulations. For the agent-based computational approach, see Sun and Tesfatsion (2006) for an agent-based simulation study of wholesale power market design tests.

### 3.9 References

- Adamson, Seabron and Scott L. Englander (2005), "Efficiency of New York Transmission Congestion Contract Auctions," Tabors Caramanis & Associates, Proceedings of the 38th Hawaii International Conference on System Sciences, IEEE.
- Hardle, W. and E. Mammen (1993), "Comparing Nonparametric versus Parametric Regression Fits," *The Annals of Statistics*, Vol. 21, No. 4, 1926-1947.
- MISO (2005a), Business Practices Manual for Financial Transmission Rights, Midwest Market Initiative, Manual No. 004, Version 6, Last updated: December 6, 2005.
- MISO (2005b), Midwest Market Tutorial Session 3 - Financial Transmission Rights (FTRs),

November.

Siddiqui, Afzal S., Emily S. Bartholomew, Chris Marnary, and Shmuel S. Oren (2005), "Efficiency of the New York Independent System Operator Market for Transmission Congestion Contracts," *Managerial Finance*, 31(6): 1-45.

Siddiqui, Afzal S., Emily S. Bartholomew, Chris Marnary, and Shmuel S. Oren (2006), "Risk Aversion and the Efficiency of the New York Independent System Operator Market for Transmission Congestion Contracts," Working paper.

Sun, Junjie (2006), "Kernel Smoothing Estimation of GDP Growth and Inflation Rate in Finland: A Nonparametric Approach," Working Paper, Department of Economics, Iowa State University.

Sun, Junjie and Leigh Tesfatsion (2006), "Dynamic Testing of Wholesale Power Market Designs: An Open-Source Agent-Based Framework," Economics Working Paper No. 06025, Department of Economics, Iowa State University.

Wu, C.(1986), "Jackknife, Bootstrap and Other Resampling Methods in Regression Analysis" *Annals of Statistics* 14: 1261-1350.

### 3.10 Appendix

Table 3.5 MISO monthly FTR allocation and auction timeline: August 2005

Start Date <sup>a</sup>	Stop Date	Activities <sup>b</sup>
	Aug. 12	MISO – Post auction model
	Aug. 15	MP <sup>c</sup> – Credit deadline for Sept. auction
Aug. 15	Aug. 16	MP – Allocation nominations may be submitted for Sept. monthly FTR allocation
	Aug. 19	MISO – Post Sept. monthly FTR allocation results
Aug. 22	Aug. 23	MP – Bid/offers may be submitted to buy and sell FTRs for Sept. monthly FTR auction
	Aug. 26	MISO – Post Sept. monthly FTR auction results

<sup>a</sup>We only list the timeline for August since all other months are very similar to August except the exact start and stop dates are slightly different across each month.

<sup>b</sup>Source: MISO public website <http://www.midwestiso.org>

<sup>c</sup>MP: Market participants

Table 3.6 Summary statistics for off-peak and non-distinct (ON) FTRs  
(Apr05 – Mar06)

Month	Num Obs	Avg Price	Std Price	Avg Rev	Std Rev
Apr-05	88	-903.05	6310.04	53.04	172.15
May-05	174	-361.41	644.51	-32.57	1193.91
Jun-05	140	173.88	646.18	1080.48	1773.36
Jul-05	379	332.05	854.44	237.68	1110.77
Aug-05	547	134.15	748.91	1521.22	3187.88
Sep-05	336	235.65	868.86	2086.30	3328.20
Oct-05	461	26.08	467.24	467.96	1434.43
Nov-05	637	242.57	1518.96	769.04	2029.69
Dec-05	622	487.53	950.72	2030.69	3286.07
Jan-06	607	451.59	1233.12	256.18	853.17
Feb-06	857	463.42	1148.30	396.64	724.79
Mar-06	855	-14.18	948.73	-48.93	1411.83

Month	Correlation	CorrectPred	%CorrectPred	Winners	%Winners
Apr-05	0.30	48	0.55	35	0.40
May-05	0.79	151	0.87	137	0.79
Jun-05	0.67	99	0.71	93	0.66
Jul-05	0.54	250	0.66	164	0.43
Aug-05	0.64	318	0.58	418	0.76
Sep-05	0.87	230	0.68	276	0.82
Oct-05	0.31	271	0.59	310	0.67
Nov-05	0.25	395	0.62	413	0.65
Dec-05	0.44	477	0.77	463	0.74
Jan-06	0.80	489	0.81	224	0.37
Feb-06	0.59	649	0.76	408	0.48
Mar-06	0.74	639	0.75	390	0.46



Table 3.7 Summary statistics for off-peak and distinct (OD) FTRs (Apr05 – Mar06)

Month	Num Obs	Avg Price	Std Price	Avg Rev	Std Rev
Apr-05	86	-929.43	6381.41	54.34	173.57
May-05	121	-103.08	607.90	301.77	1295.94
Jun-05	139	173.84	648.52	1078.53	1779.62
Jul-05	365	342.02	868.58	213.56	1108.39
Aug-05	502	136.59	768.43	1513.29	3171.41
Sep-05	310	251.33	902.16	2115.19	3438.81
Oct-05	428	20.88	482.21	451.04	1421.70
Nov-05	587	268.47	1575.06	799.56	2055.52
Dec-05	523	480.56	948.87	1799.63	2936.88
Jan-06	505	413.39	1302.46	219.86	897.12
Feb-06	746	515.70	1198.22	407.07	718.46
Mar-06	767	-48.20	972.58	-75.59	1470.36

Month	Correlation	CorrectPred	%CorrectPred	Winners	%Winners
Apr-05	0.30	45	0.52	36	0.42
May-05	0.75	98	0.81	85	0.70
Jun-05	0.67	98	0.71	92	0.66
Jul-05	0.55	241	0.66	151	0.41
Aug-05	0.64	294	0.59	379	0.75
Sep-05	0.88	214	0.69	254	0.82
Oct-05	0.32	249	0.58	285	0.67
Nov-05	0.24	356	0.61	373	0.64
Dec-05	0.32	395	0.76	386	0.74
Jan-06	0.81	401	0.79	178	0.35
Feb-06	0.60	573	0.77	329	0.44
Mar-06	0.76	592	0.77	373	0.49

Table 3.8 Summary statistics for peak and non-distinct (PN) FTRs (Apr05 – Mar06)

Month	Num Obs	Avg Price	Std Price	Avg Rev	Std Rev
Apr-05	79	-6461.63	15306.82	-45.95	523.53
May-05	137	-173.27	1596.70	135.89	1147.91
Jun-05	213	1.400	962.10	889.56	1579.37
Jul-05	511	79.65	673.75	-73.46	1165.19
Aug-05	515	78.50	659.53	599.39	1495.04
Sep-05	575	-200.42	1356.63	-2390.49	10241.13
Oct-05	550	78.56	804.33	1104.68	3769.84
Nov-05	932	-22.37	1814.00	585.87	3397.96
Dec-05	1085	533.19	1424.65	2173.83	4200.80
Jan-06	903	909.33	2018.14	474.55	985.61
Feb-06	1361	602.43	1111.91	253.83	1355.96
Mar-06	1133	19.79	1128.67	90.65	1367.92

Month	Correlation	CorrectPred	%CorrectPred	Winners	%Winners
Apr-05	0.08	46	0.58	53	0.67
May-05	0.84	101	0.74	82	0.60
Jun-05	0.55	130	0.61	159	0.75
Jul-05	0.39	383	0.75	242	0.47
Aug-05	0.32	344	0.67	349	0.68
Sep-05	0.86	444	0.77	285	0.50
Oct-05	0.45	369	0.67	373	0.68
Nov-05	0.37	633	0.68	569	0.61
Dec-05	0.41	766	0.71	821	0.76
Jan-06	0.65	703	0.78	312	0.35
Feb-06	0.43	892	0.66	662	0.49
Mar-06	0.61	795	0.70	610	0.54

Table 3.9 Summary statistics for peak and distinct (PD) FTRs (Apr05 – Mar06)

Month	Num Obs	Avg Price	Std Price	Avg Rev	Std Rev
Apr-05	78	-6313.36	15348.69	-36.13	519.53
May-05	134	-179.69	1612.36	126.22	1152.99
Jun-05	210	-0.93	968.46	900.61	1587.58
Jul-05	498	78.48	679.72	-85.65	1174.92
Aug-05	487	77.51	673.89	592.34	1481.90
Sep-05	560	-210.86	1368.89	-2511.67	10345.57
Oct-05	504	77.37	836.07	1086.22	3836.27
Nov-05	861	-38.31	1881.22	567.92	3403.62
Dec-05	923	538.81	1432.51	2016.86	4121.66
Jan-06	773	960.31	2128.17	486.67	1023.50
Feb-06	1359	602.29	1112.50	251.64	1355.52
Mar-06	994	-12.86	1170.65	63.21	1410.34

Month	Correlation	CorrectPred	%CorrectPred	Winners	%Winners
Apr-05	0.06	45	0.58	52	0.67
May-05	0.84	97	0.72	79	0.59
Jun-05	0.55	128	0.61	158	0.75
Jul-05	0.39	373	0.75	232	0.47
Aug-05	0.33	327	0.67	331	0.68
Sep-05	0.87	434	0.78	274	0.49
Oct-05	0.45	335	0.66	343	0.68
Nov-05	0.37	581	0.67	530	0.62
Dec-05	0.37	679	0.74	673	0.73
Jan-06	0.65	597	0.77	268	0.35
Feb-06	0.43	890	0.65	660	0.49
Mar-06	0.63	708	0.71	541	0.54

Table 3.10 Linear regression results for off-peak and non-distinct (ON) FTRs (Apr05 – Mar06)

Month	Intercept	p.value	Price	p.value	resid.se	d.f.	r.sq	adj.r.sq	f.stat
Apr-05	60.32	0.00	0.01	0.01	165.40	86	0.09	0.08	8.24
May-05	498.75	0.00	1.47	0.00	728.50	172	0.63	0.63	292.65
Jun-05	760.35	0.00	1.84	0.00	1319.80	138	0.45	0.45	112.95
Jul-05	5.90	0.91	0.70	0.00	938.32	377	0.29	0.29	152.71
Aug-05	1158.01	0.00	2.71	0.00	2462.17	545	0.40	0.40	370.29
Sep-05	1302.03	0.00	3.33	0.00	1650.33	334	0.75	0.75	1028.44
Oct-05	443.01	0.00	0.96	0.00	1364.45	459	0.10	0.10	49.39
Nov-05	688.22	0.00	0.33	0.00	1967.13	635	0.06	0.06	42.10
Dec-05	1286.80	0.00	1.53	0.00	2950.91	620	0.19	0.19	150.07
Jan-06	5.13	0.82	0.56	0.00	508.31	605	0.65	0.65	1102.22
Feb-06	224.92	0.00	0.37	0.00	587.08	855	0.34	0.34	449.65
Mar-06	-33.33	0.31	1.10	0.00	951.01	853	0.55	0.55	1029.13

Table 3.11 Linear regression results for off-peak and distinct (OD) FTRs (Apr05 – Mar06)

Month	Intercept	p.value	Price	p.value	resid.se	d.f.	r.sq	adj.r.sq	f.stat
Apr-05	61.88	0.00	0.01	0.01	166.67	84	0.09	0.08	8.19
May-05	465.74	0.00	1.59	0.00	866.36	119	0.56	0.55	149.50
Jun-05	758.46	0.00	1.84	0.00	1324.41	137	0.45	0.45	112.17
Jul-05	-27.19	0.60	0.70	0.00	925.79	363	0.30	0.30	158.75
Aug-05	1152.87	0.00	2.64	0.00	2441.04	500	0.41	0.41	345.65
Sep-05	1276.36	0.00	3.34	0.00	1663.83	308	0.77	0.77	1011.94
Oct-05	431.29	0.00	0.95	0.00	1348.16	426	0.10	0.10	48.86
Nov-05	714.96	0.00	0.32	0.00	1996.40	585	0.06	0.06	36.22
Dec-05	1320.80	0.00	1.00	0.00	2783.20	521	0.10	0.10	60.24
Jan-06	-10.64	0.67	0.56	0.00	527.26	503	0.66	0.65	956.11
Feb-06	222.08	0.00	0.36	0.00	576.08	744	0.36	0.36	414.74
Mar-06	-20.39	0.56	1.15	0.00	960.54	765	0.57	0.57	1029.91

Table 3.12 Linear regression results for peak and non-distinct (PN) FTRs  
(Apr05 – Mar06)

Month	Intercept	p.value	Price	p.value	resid.se	d.f.	r.sq	adj.r.sq	f.stat
Apr-05	-28.92	0.65	0.00	0.50	525.35	77	0.01	-0.01	0.46
May-05	240.35	0.00	0.60	0.00	627.62	135	0.70	0.70	319.94
Jun-05	888.31	0.00	0.90	0.00	1326.05	211	0.30	0.30	89.74
Jul-05	-127.19	0.01	0.67	0.00	1073.96	509	0.15	0.15	91.33
Aug-05	543.26	0.00	0.72	0.00	1420.11	513	0.10	0.10	56.67
Sep-05	-1084.22	0.00	6.52	0.00	5172.01	573	0.75	0.75	1677.55
Oct-05	939.23	0.00	2.11	0.00	3370.97	548	0.20	0.20	138.61
Nov-05	601.31	0.00	0.69	0.00	3160.57	930	0.14	0.13	146.11
Dec-05	1521.93	0.00	1.22	0.00	3824.44	1083	0.17	0.17	224.85
Jan-06	185.85	0.00	0.32	0.00	749.34	901	0.42	0.42	659.49
Feb-06	-60.64	0.11	0.52	0.00	1225.91	1359	0.18	0.18	304.87
Mar-06	75.95	0.02	0.74	0.00	1081.63	1131	0.38	0.37	679.57

Table 3.13 Linear regression results for peak and distinct (PD) FTRs  
(Apr05 – Mar06)

Month	Intercept	p.value	Price	p.value	resid.se	d.f.	r.sq	adj.r.sq	f.stat
Apr-05	-22.48	0.73	0.00	0.58	521.87	76	0.00	-0.01	0.31
May-05	234.26	0.00	0.60	0.00	626.52	132	0.71	0.70	318.43
Jun-05	901.45	0.00	0.90	0.00	1330.22	208	0.30	0.30	89.69
Jul-05	-138.34	0.00	0.67	0.00	1083.74	496	0.15	0.15	88.16
Aug-05	536.58	0.00	0.72	0.00	1401.80	485	0.11	0.11	58.13
Sep-05	-1130.09	0.00	6.55	0.00	5161.07	558	0.75	0.75	1688.16
Oct-05	926.62	0.00	2.06	0.00	3430.12	502	0.20	0.20	127.17
Nov-05	593.33	0.00	0.66	0.00	3168.56	859	0.13	0.13	133.33
Dec-05	1444.37	0.00	1.06	0.00	3832.41	921	0.14	0.14	145.43
Jan-06	187.79	0.00	0.31	0.00	780.76	771	0.42	0.42	555.63
Feb-06	-62.51	0.10	0.52	0.00	1225.49	1357	0.18	0.18	304.47
Mar-06	72.96	0.04	0.76	0.00	1096.48	992	0.40	0.40	650.84

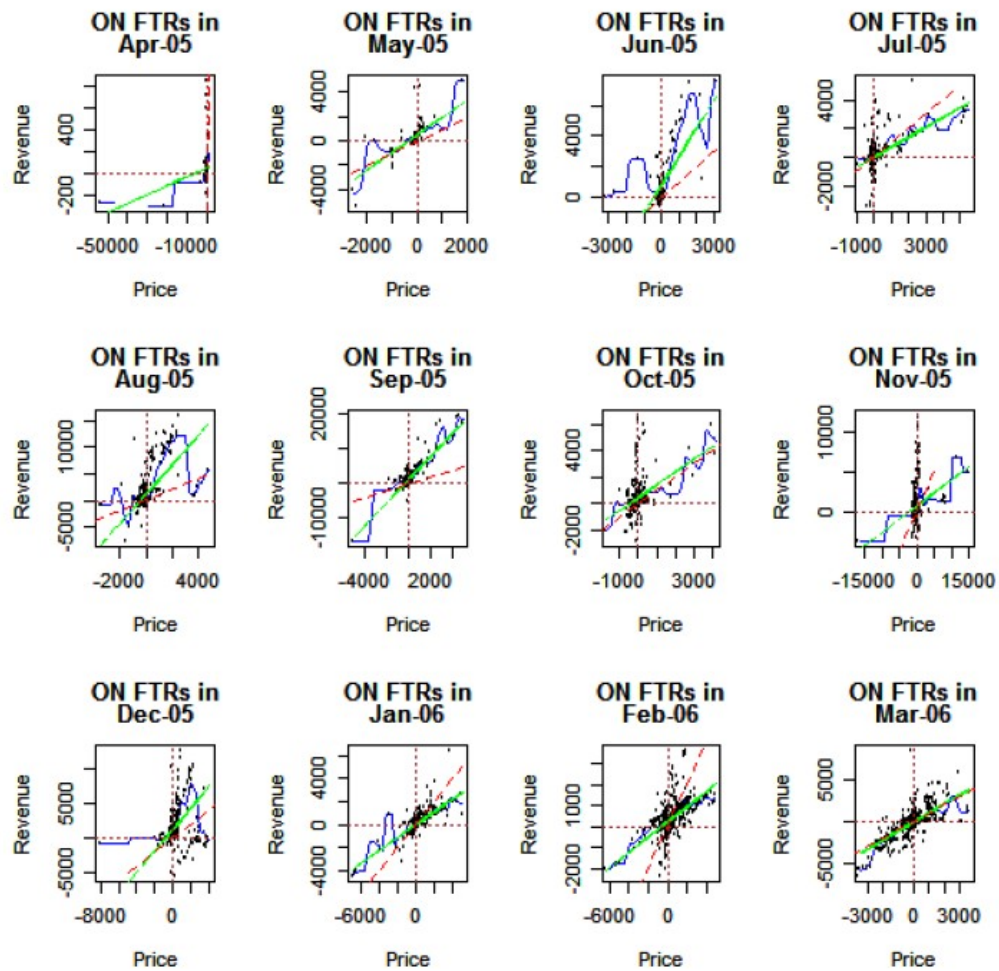


Figure 3.7 The linear and kernel regression for off-peak and non-distinct (ON) FTRs

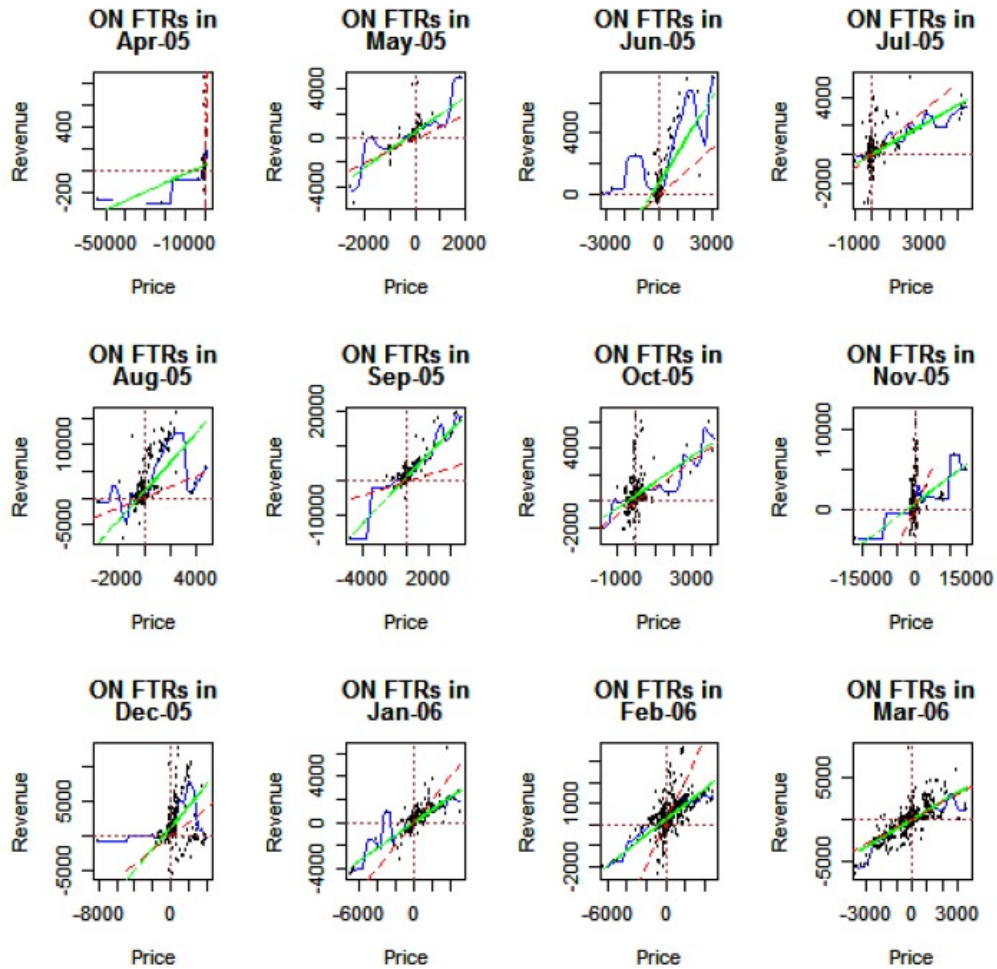


Figure 3.8 The linear and kernel regression for off-peak and distinct (OD) FTRs

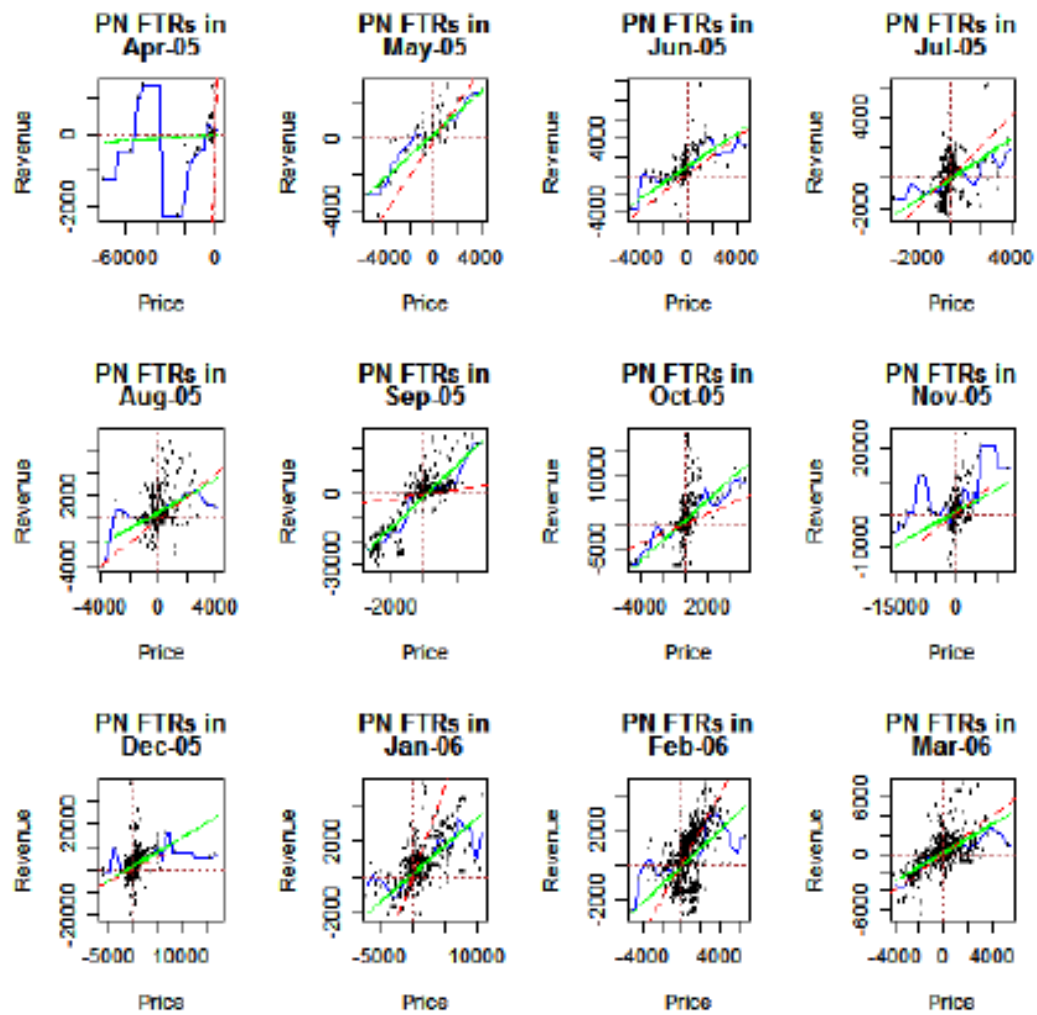


Figure 3.9 The linear and kernel regression for peak and non-distinct (PN) FTRs



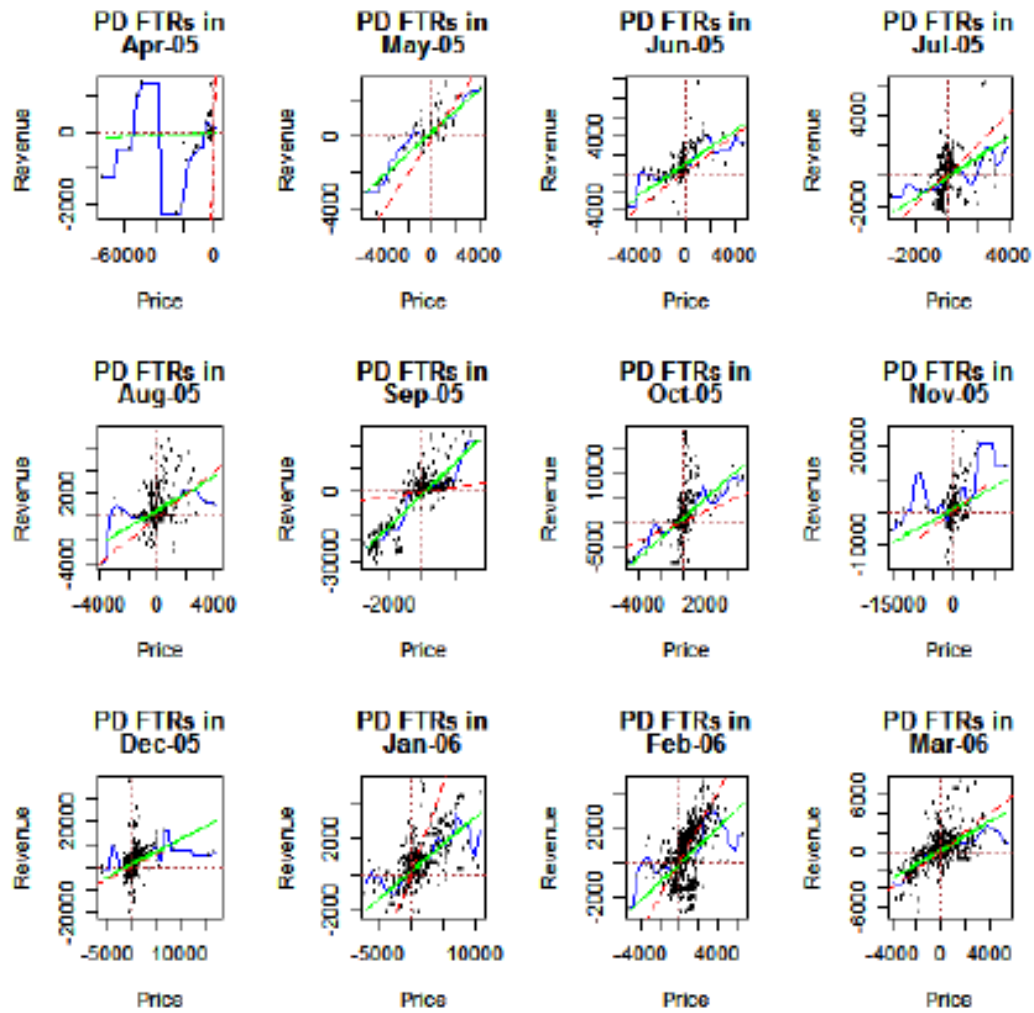


Figure 3.10 The linear and kernel regression for peak and distinct (PD) FTRs

Table 3.14 The goodness-of-fit test results for all four types of FTRs (Apr05 – Mar06)

Month	p-value.ON	p-value.OD	p-value.PN	p-value.PD
Apr-05	0.000	0.000	0.000	0.000
May-05	0.000	0.000	0.001	0.000
Jun-05	0.000	0.000	0.000	0.000
Jul-05	0.004	0.004	0.000	0.000
Aug-05	0.000	0.000	0.001	0.001
Sep-05	0.000	0.000	0.000	0.000
Oct-05	0.000	0.000	0.000	0.000
Nov-05	0.000	0.000	0.000	0.000
Dec-05	0.000	0.000	0.000	0.000
Jan-06	0.000	0.000	0.000	0.001
Feb-06	0.000	0.000	0.000	0.000
Mar-06	0.000	0.000	0.000	0.000

Table 3.15 The monthly total net revenue for all four types of FTRs (Apr05 – Mar06)

Month	NetRev.ON <sup>a</sup>	NetRev.OD	NetRev.PN	NetRev.PD
Apr-05	97.607	91.594	1136.644	1136.644
May-05	-608.242	-608.354	-173.966	-164.165
Jun-05	-2196.301	-2196.301	-2518.669	-2518.669
Jul-05	-690.774	-709.981	-1106.602	-1104.469
Aug-05	-16146.065	-16146.065	-2733.898	-2717.289
Sep-05	-4825.486	-4825.486	-7294.692	-7304.574
Oct-05	-2385.498	-2385.498	-5819.088	-5775.968
Nov-05	-5165.214	-5165.214	-6397.217	-6398.028
Dec-05	-8194.178	-8203.520	-12282.049	-12282.049
Jan-06	457.857	457.857	530.545	518.906
Feb-06	-1318.938	-1320.908	-1131.792	-1131.792
Mar-06	-1596.208	-1598.376	-1649.562	-1652.240

<sup>a</sup>All values of monthly total net revenue have been divided by 1000.

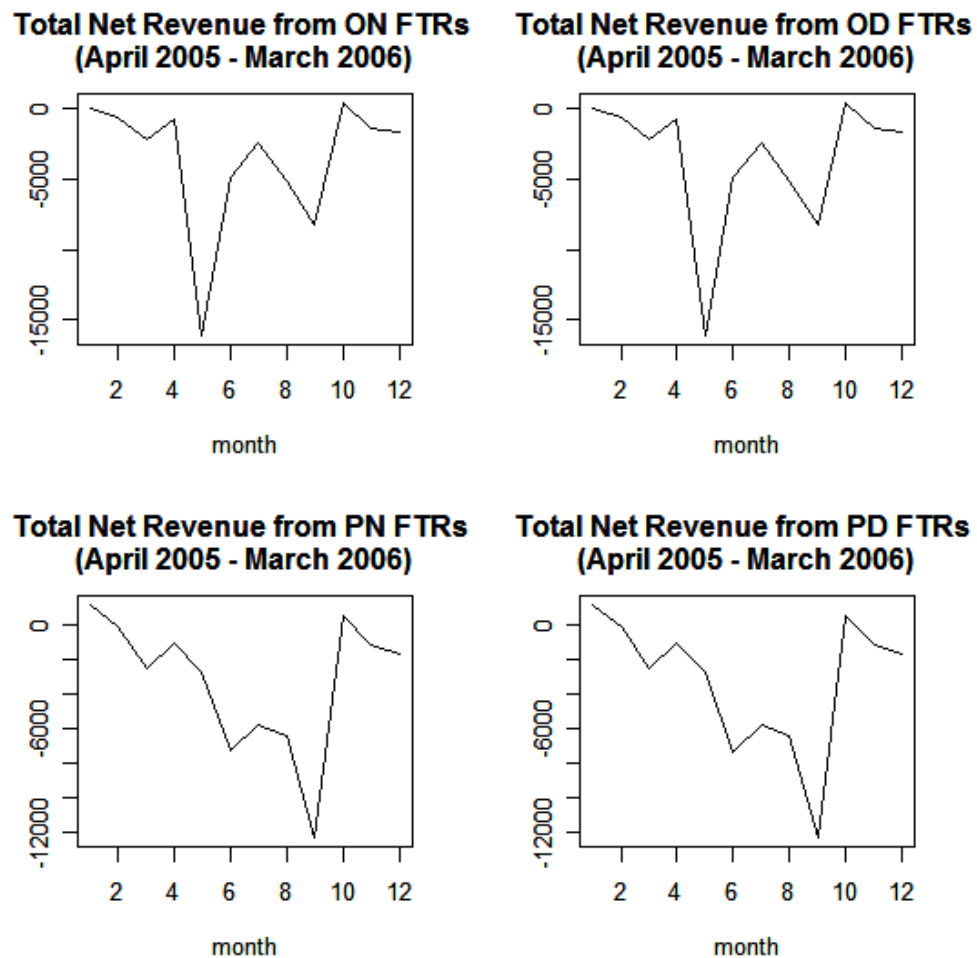


Figure 3.11 The monthly total net revenue for all four types of FTRs (Apr05 – Mar06), Note: all values of monthly total net revenue have been divided by 1000.

## CHAPTER 4. DYNAMIC TESTING OF WHOLESALE POWER MARKET DESIGNS: AN OPEN-SOURCE AGENT-BASED FRAMEWORK

### 4.1 Abstract

In April 2003 the U.S. Federal Energy Regulatory Commission proposed a complicated market design – the *Wholesale Power Market Platform (WPMP)* – for common adoption by all U.S. wholesale power markets. Versions of the WPMP have been implemented in New England, New York, the mid-Atlantic states, the Midwest, and the Southwest, and adopted for implementation in California. Strong opposition to the WPMP persists among some industry stakeholders, however, due largely to a perceived lack of adequate performance testing. This study reports on the model development and open-source implementation (in Java) of a computational wholesale power market organized in accordance with core WPMP features and operating over a realistically rendered transmission grid. The traders within this market model are strategic profit-seeking agents whose learning behaviors are based on data from human-subject experiments. Our key experimental focus is the complex interplay among structural conditions, market protocols, and learning behaviors in relation to short-term and longer-term market performance. Findings for a dynamic 5-node transmission grid test case are presented for concrete illustration.

**Keywords:** Wholesale power market restructuring, Empirical input validation, Market design, Behavioral economics, Learning, Market power, Agent-based modeling, AMES wholesale power market framework, Java, RepastJ

**JEL Codes:** L1, D8, L9, C6

## 4.2 Introduction

The meltdown in the restructured California wholesale power market in the summer of 2000 has shown what can happen when a poorly designed market mechanism is implemented without proper testing. The California crisis is believed to have resulted in part from strategic behaviors encouraged by inappropriate market design features (Borenstein, 2002). Following the California crisis, many energy researchers have eloquently argued the need to combine structural understanding with economic analysis of incentives in order to develop wholesale power market designs with good real-world performance characteristics; see, for example, Amin (2004).

In April 2003 the U.S. Federal Energy Regulatory Commission proposed the *Wholesale Power Market Platform (WPMP)* as a template for all U.S. wholesale power markets (FERC, 2003). This design recommends the operation of wholesale power markets by Independent System Operators (ISOs) or Regional Transmission Organizations (RTOs) using locational marginal pricing to price energy by the location of its injection into or withdrawal from the transmission grid. Versions of this design have been implemented in New England (ISO-NE), New York (NYISO), the mid-Atlantic states (PJM), the Midwest (MISO), and the Southwest (SPP), and adopted for implementation in California (CAISO). Joskow (2006, p. 6) reports that ISO/RTO operated energy regions now include over 50% of the generating capacity in the U.S.; see Figure 4.1.

The complexity of the WPMP market design has made it extremely difficult to undertake economic and physical reliability studies of the design using standard statistical and analytical tools. Strong opposition to the market design thus persists among some industry stakeholders due in part to a perceived lack of sufficient performance testing.

In recent years, however, powerful new agent-based computational tools have been developed to analyze this degree of complexity. A variety of commercial agent-based frameworks are now available for the study of restructured electricity markets; see, for example, the EMCAS framework developed by researchers at the Argonne National Laboratory (Conzelmann et al., 2004). In addition, researchers such as Bower and Bunn (2001), Nicolaisen et al. (2001), Veit et al. (2006), and Widergren et al. (2004) have used agent-based models to study important

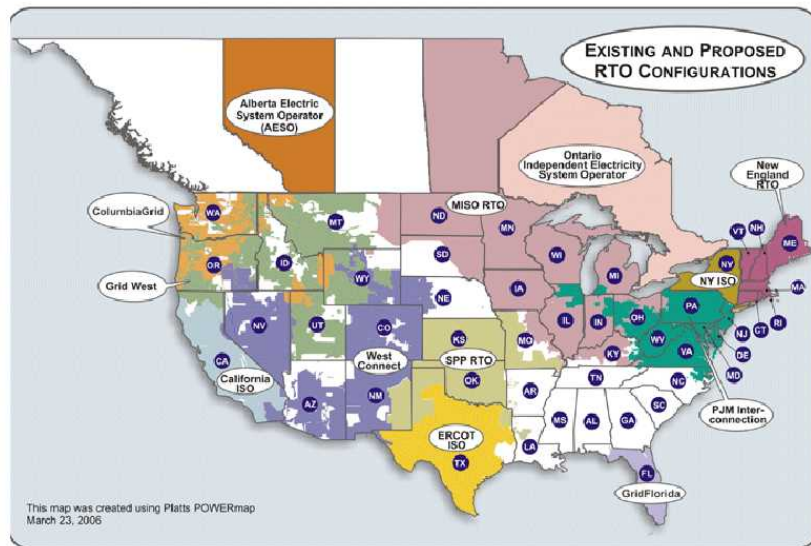


Figure 4.1 Existing and Proposed ISO/RTO-Operated U.S. Wholesale Power Markets

aspects of restructured electricity markets.<sup>1</sup>

In a preliminary study (Koesrindartoto et al., 2005), we examined the feasibility and potential fruitfulness of *Agent-based Computational Economics (ACE)* specifically for the study of the WPMP market design. ACE is the computational study of economic processes modeled as dynamic systems of interacting agents.<sup>2</sup>

Building on this prior work, the present study reports on the development and implementation of an ACE framework for testing the dynamic efficiency and reliability of the WPMP market design. This framework – referred to as *AMES (Agent-based Modeling of Electricity Systems)* – models strategic traders interacting over time in a wholesale power market that is organized in accordance with core WPMP features and that operates over a realistically rendered transmission grid. To our knowledge, AMES is the first non-commercial open-source

<sup>1</sup>See Tesfatsion (2006a) for extensive annotated pointers to agent-based electricity research.

<sup>2</sup>See Axelrod and Tesfatsion (2006), Tesfatsion (2006b), and Tesfatsion and Judd (2006) for extensive introductory materials on ACE.

framework permitting the computational study of the WPMP design.

To help ensure empirical input validity, the AMES framework has been developed by means of an iterative participatory modeling approach.<sup>3</sup> Specifically, we are engaging with industry participants and policy makers in an ongoing collaborative learning process involving four repeated stages of analysis: fieldwork and data collection; scenario discussion and role-playing games; agent-based model development; and intensive computational experiments. We are relying heavily on business practices from two adopters of the WPMP design (New England and the Midwest) for our implementation of market structure, market architecture, and dispatch and pricing solutions. We have also incorporated reinforcement learning representations for the electricity traders that are based on findings from human-subject multi-agent game experiments conducted by Roth and Erev (1995).<sup>4</sup>

We are currently using the AMES framework to investigate the intermediate-term performance of wholesale power markets operating under the WPMP market design. In particular, we are exploring the extent to which this design is capable of supporting the efficient, profitable, and sustainable operation over time of existing generation and transmission facilities, despite possible attempts by some market participants to gain individual advantage through strategic pricing, capacity withholding, and induced transmission congestion.

To illustrate concretely the potential usefulness of the AMES framework for this purpose, experimental findings are reported below for a dynamic extension of a static five-node transmission grid test case used extensively for training purposes by the ISO-NE and PJM. In the static training case, the generators are assumed to report their true cost and production capacity attributes to the ISO; the possibility that generators might engage in strategic reporting behavior is not considered. In contrast, the AMES generators use reinforcement learning to decide the exact nature of the supply offers (marginal cost functions and production intervals) that they daily report to the AMES ISO for use in the WPMP day-ahead market. We

<sup>3</sup>See Barreteau (2003) for a fuller discussion of iterative participatory modeling, also called *companion modeling*. For more general materials on empirical validation methods for agent-based computational models, see Fagiolo et al. (2006) and Tesfatsion (2006c).

<sup>4</sup>Real-world market traders are understandably reluctant to discuss with us the precise manner in which they determine their supply offers and demand bids, so indirect identification methods must be used.

show that all of the AMES generators learn over time to implicitly collude on the reporting of higher-than-true marginal costs, thus considerably raising total variable costs of operation at the ISO-determined “optimal” solutions.

Our longer-run goal for AMES is a framework that rings true to industry participants and policy makers and that can be used as a research and training tool. Specifically targeted framework features include:

- Operational validity (structure, architecture, and behavioral dispositions);
- Permits dynamic testing with learning traders;
- Permits intensive sensitivity experiments;
- Open source (full access to implementation);
- Easy modification (extensible/modular architecture).

We envision academic researchers and teachers using this framework to increase their qualitative understanding of the dynamic operation of restructured wholesale power markets. Industry participants should be able to use the framework to familiarize themselves with market rules and to test business strategies. And policy makers should find the framework useful for conducting intensive experiments to explore the performance of actual or proposed market designs from a social welfare viewpoint. In particular, does a design encourage the efficient and reliable operation of existing generation and transmission capacity in the short term, and does it provide appropriate incentives for investment in new generation and new transmission capacity in the longer term?

An overview of the AMES wholesale power market framework is presented in Section 4.3, and detailed configuration settings for the AMES transmission grid, energy traders, and ISO are presented in Section 4.4. Experimental findings for a dynamic five-node transmission grid test case are presented in Section 4.5 making use of the configuration settings from Section 4.4. Concluding remarks are given in Section 5.10. Notes on the construction of “action domains” (supply offer choice sets) for the AMES generators are provided in an appendix.



### 4.3 Overview of the AMES Framework

The AMES wholesale power market framework is programmed in Java using RepastJ, a Java-based toolkit designed specifically for agent-based modeling in the social sciences.<sup>5</sup> The framework is modular, extensible, and open source in order to provide a useful foundation for further electricity research.<sup>6</sup>

The AMES framework currently incorporates in stylized form several core elements of the WPMP market design as implemented by the New England Independent System Operator (ISO-NE) and the Midwest Independent System Operator (MISO), respectively. By adhering closely to the architecture of these regional energy markets, we have been able to take advantage of the business practice manuals, training guides, and reports publicly released by the ISO-NE (2006) and the MISO (2006) for use by their market participants. These publications provide a wealth of specific implementation details missing from the more abstract WPMP template.

As depicted in Figures 4.2 through 4.4, the core elements of the WPMP market design that have been incorporated into the AMES framework to date are as follows:

- The AMES wholesale power market operates over an AC transmission grid for DMax successive days, with each day D consisting of 24 successive hours  $H = 00, 01, \dots, 23$ .
- The AMES wholesale power market includes an Independent System Operator (ISO) and a collection of energy traders consisting of Load-Serving Entities (LSEs) and Generators distributed across the nodes of the transmission grid.<sup>7</sup>

<sup>5</sup>See Tesfatsion (2006d) for resources related to the agent-based toolkit RepastJ. Agent-based researchers are increasingly making use of powerful object-oriented programming (OOP) languages such as Java, C++, or C# either directly or through some form of agent-based toolkit. Weisfeld (2003) provides an excellent introduction to OOP. For a general annotated listing of OOP software and toolkits suitable for agent-based modeling, see Tesfatsion (2006e).

<sup>6</sup>In particular, the goal of the larger NSF project encompassing the development of the AMES framework (McCalley et al., 2005) is to explore ways of achieving a more effectively integrated U.S. energy transportation network encompassing electricity, gas, coal, and water subsectors. The longer-term plan is to incrementally extend the AMES framework to include consideration of these related energy subsectors.

<sup>7</sup>An *Independent System Operator (ISO)* is an organization charged with the primary responsibility of maintaining the security of a power system and often with system operation responsibilities as well. The ISO is independent to the extent that it does not have a conflict of interest in carrying out these responsibilities, such as an ownership stake in generation or transmission facilities within the power system. A *Load Serving Entity (LSE)* is an electric utility, transmitting utility, or Federal power marketing agency that has an obligation under Federal, State, or local law, or under long-term contracts, to provide electrical power to end-use (residential or commercial) consumers or to other LSEs with end-use consumers. An LSE aggregates individual end-use

- The AMES ISO undertakes the daily operation of the transmission grid within a two-settlement system consisting of a Real-Time Market and a Day-Ahead Market, each separately settled by means of *locational marginal pricing*.<sup>8</sup>
- During the afternoon of each day D the AMES ISO determines power commitments and *locational marginal prices (LMPs)*<sup>9</sup> for the Day-Ahead Market for day D+1 based on Generator supply offers and LSE demand bids (forward financial contracting) submitted during hours 00 – 11 of day D.
- At the end of each day D the AMES ISO produces and posts a day D+1 commitment schedule for Generators and LSEs and settles these financially binding contracts on the basis of day D+1 LMPs.
- Any differences that arise during day D+1 between real-time conditions and the day-ahead financial contracts settled at the end of day D must be settled in the Real-Time Market for day D+1 at real-time LMPs for day D+1 .
- Transmission grid congestion in the Day-Ahead Market is managed via the inclusion of congestion components in LMPs.

Five additional elements that will subsequently be incorporated into AMES to reflect more fully the dynamic operational capabilities of the WPMP market design are: (a) *market power mitigation measures*; (b) *bilateral trading*, which permits longer-term contracting; (c) a market for *financial transmission rights*<sup>10</sup> to permit AMES traders to hedge against transmission congestion costs arising in the Day-Ahead Market; (d) *security constraints* incorporated into the DC OPF problems solved by the AMES ISO for the Real-Time Market and Day-Ahead

consumer demand into “load blocks” for bulk buying at the wholesale level. A *Generator* is a unit that produces and sells electrical power in bulk at the wholesale level. A *node* is a point on the transmission grid where power is injected or withdrawn.

<sup>8</sup>*Locational marginal pricing* is the pricing of electrical power according to the location of its withdrawal from, or injection into, a transmission grid.

<sup>9</sup>A *locational marginal price (LMP)* at any particular node is the least cost of meeting demand at that node for one additional unit of power, i.e. for one additional megawatt (MW).

<sup>10</sup>A *financial transmission right (FTR)* purchased on a transmission line *from* node A *to* node B entitles the holder to a compensation if the LMP at node B exceeds the LMP at node A, and obligates the holder to make a payment if the LMP at node A exceeds the LMP at node B. See Sun (2005).

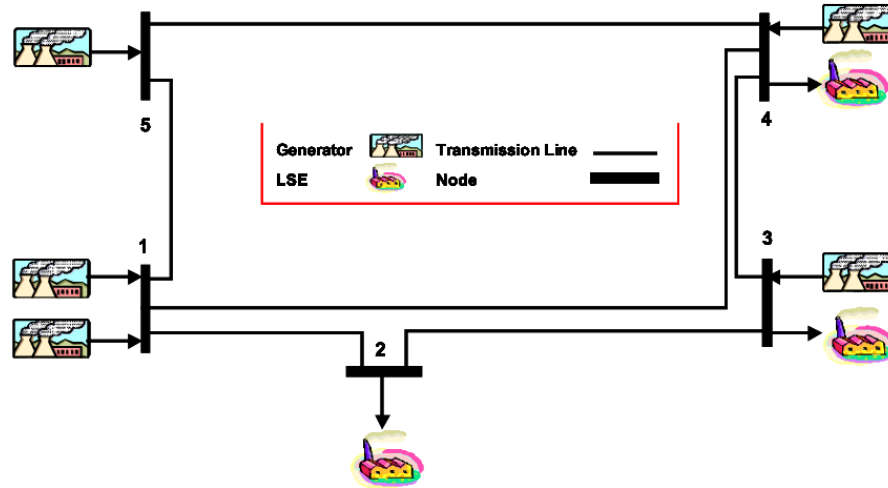


Figure 4.2 Illustrative 5-Node Transmission Grid

Market as a hedge against system disturbances; and (e) a *(Resource Offer) Re-Bid Period*<sup>11</sup> during each day D as part of a resource adequacy assessment undertaken by the AMES ISO to help ensure that forecasted loads and reserve requirements are always met. Figures 4.5 and 4.6 schematically depict the architecture and dynamic flow of this extended AMES framework.

As explained more carefully in Section 4.4.5 below, the AMES ISO determines hourly power commitments/dispatch levels and LMPs for the Day-Ahead Market and Real-Time Market by solving *DC Optimal Power Flow (OPF)* problems that approximate underlying AC OPF problems. To handle these aspects, we have developed an accurate and efficient strictly convex quadratic programming (SCQP) solver module, *QuadProgJ*, wrapped in an outer DC OPF data conversion shell, *DCOPFJ* (Sun and Tesfatsion, 2006). The AMES ISO solves its DC OPF problems by invoking *QuadProgJ* through *DCOPFJ*.

As detailed in Section 4.4.6 below, trader learning is implemented in the AMES framework

<sup>11</sup>Here we follow the MISO market architecture and terminology. The ISO-NE implements a similar design feature during each day D called the “(Real-Time Energy Market) Supply Re-Offer Period.”

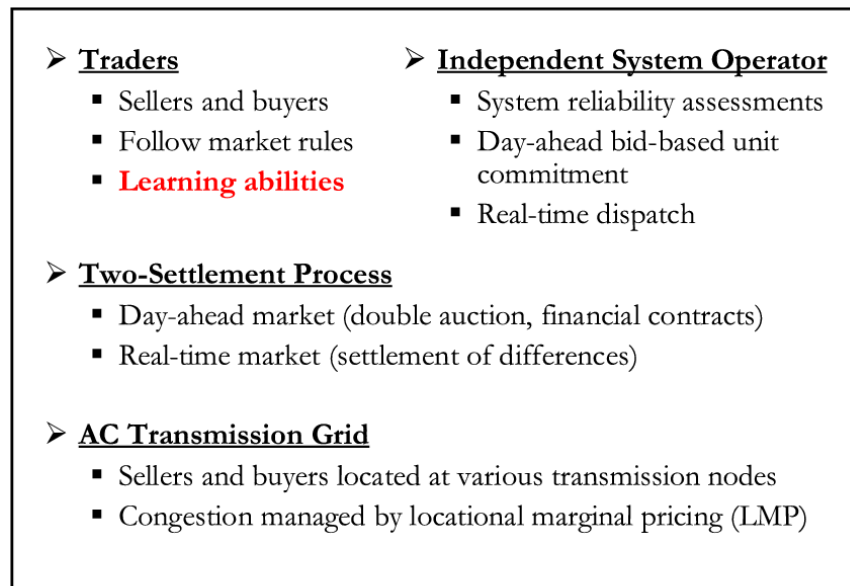


Figure 4.3 AMES Core Features

by a reinforcement learning module, *JReLM*, developed by Gieseler (2005). *JReLM* can implement a variety of different reinforcement learning methods, permitting flexible representation of trader learning within this family of methods. In later extensions of AMES, other possible trader learning methods (e.g. social mimicry and belief learning) will also be considered.

The QuadProgJ/DCOPFJ and *JReLM* modules for ISO grid operation and trader learning constitute the core components supporting the implementation of the AMES wholesale power market framework. This implementation is schematically depicted in Figure 4.7.

## 4.4 Configuration of the AMES Framework

### 4.4.1 Overview

This section provides detailed configuration information for the AMES wholesale power market framework as currently implemented. All subsequently reported experiments make use of these configurations.

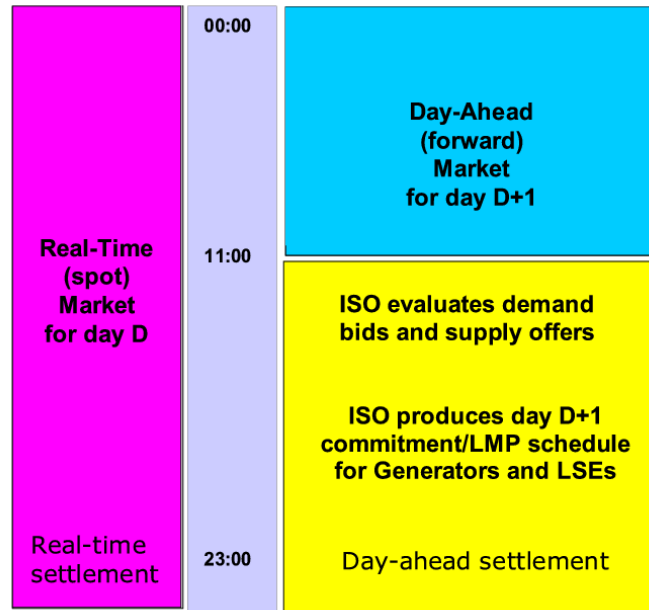


Figure 4.4 Activities of the AMES ISO During a Typical Day D

For later ease of reference, the admissible exogenous variables for the AMES framework are depicted and defined in Table 5.1 and the endogenous variables are depicted and defined in Table 5.2.<sup>12</sup> These variable depictions and definitions will be used throughout the remainder of this study.

#### 4.4.2 Structural Configuration of the AMES Transmission Grid

The AMES transmission grid is an alternating current (AC) grid modeled as a balanced three-phase network with  $N \geq 1$  branches and  $K \geq 2$  nodes. The reactance on each branch is assumed to be a total branch reactance (rather than a per mile reactance), meaning that the branch length is already taken into account. All transformer phase angle shifts are assumed to be zero, all transformer tap ratios are assumed to be 1, all line-charging capacitances are assumed to be 0, and the temperature is assumed to remain constant over time.

<sup>12</sup>Only persistent variables appear in these tables. Locally scoped variables temporarily introduced to carry out method implementations are not included.

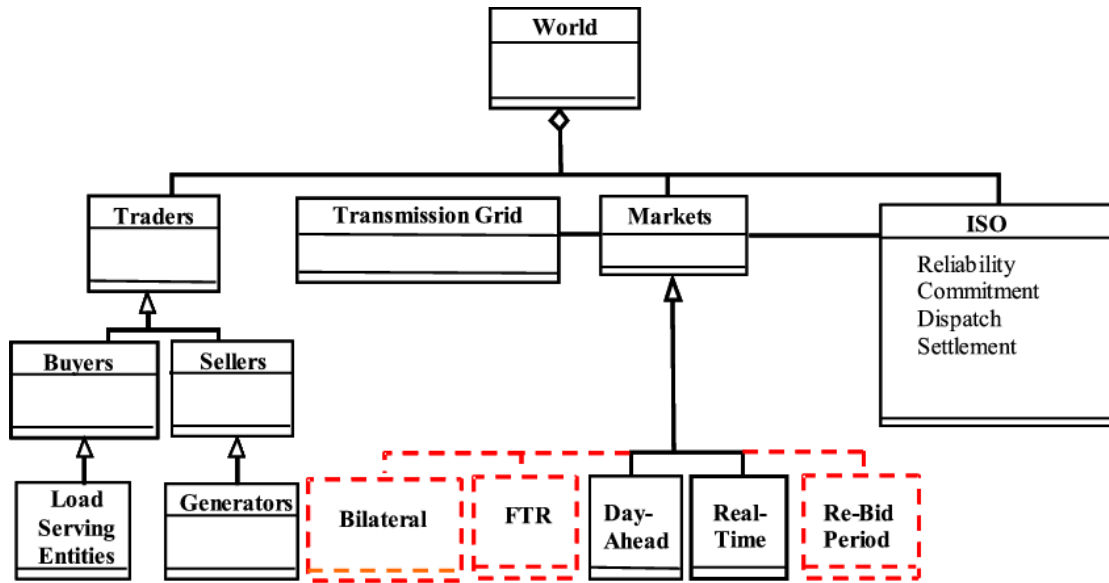


Figure 4.5 AMES Architecture (Agent Hierarchy)

The AMES transmission grid is assumed to be *connected* in the sense that it has no isolated components; each pair of nodes  $k$  and  $m$  is connected by a linked branch path consisting of one or more branches. If two nodes are in direct connection with each other, it is assumed to be through at most one branch, i.e., branch groups are not explicitly considered. However, complete connectivity is *not* assumed. That is, node pairs are *not* necessarily in *direct* connection with each other through a single branch.

For per unit normalization in DC OPF implementations, it is conventional to specify base value settings for apparent power (in megavoltamperes MVA) and voltage (in kilovolts kV). For the AMES transmission grid, the base apparent power, denoted by  $S_o$ , is assumed to be measured in three-phase MVAs, and the base voltage, denoted by  $V_o$ , is assumed to be measured in line-to-line kVs.

It is also assumed that *Kirchoff's Current Law (KCL)* governing current flows in electrical networks holds for the AMES transmission grid for each hour of operation. As detailed in

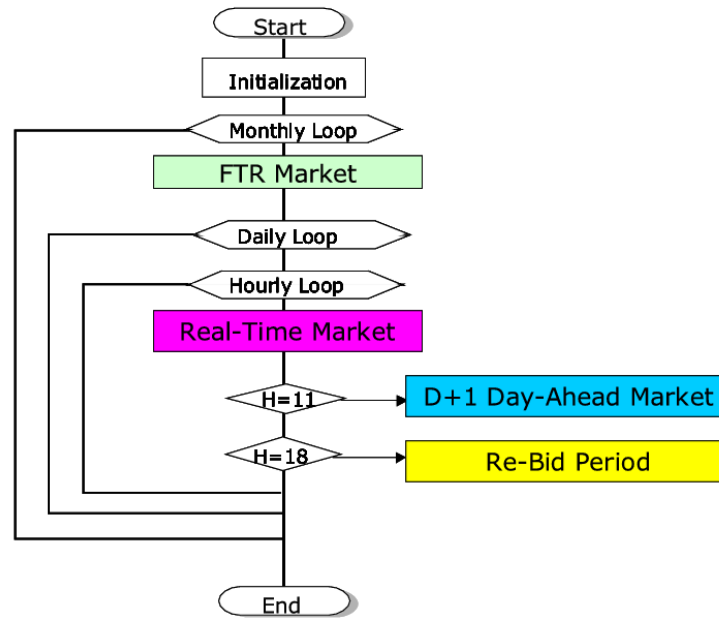


Figure 4.6 AMES Dynamic Market Activities: Global View

Kirschen and Strbac (2004, Sec. 6.2.2.1), KCL implies that real and reactive power must each be in balance at each node. Thus, real power must also be in balance across the entire grid, in the sense that aggregate real power withdrawal plus aggregate transmission losses must equal aggregate real power injection.

In wholesale power markets restructured in accordance with the WPMP market design, the transmission grid is overlaid with a commercial network consisting of “pricing locations” for the purchase and sale of electric power. A *pricing location* is a location at which market transactions are settled using publicly available LMPs. For simplicity, it is assumed that the set of pricing locations for AMES coincides with the set of transmission grid nodes.

#### 4.4.3 Structural Configuration of the AMES LSEs

The AMES LSEs purchase bulk power in the AMES wholesale power market each day in order to service customer demand (load) in a downstream retail market. The user specifies the

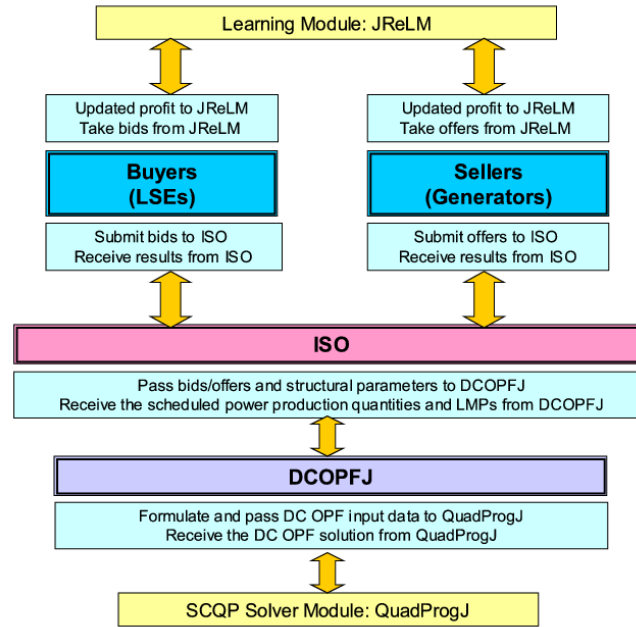


Figure 4.7 Core Module Components of the AMES Framework

number  $J$  of LSEs as well as the location of these LSEs at various nodes of the transmission grid. LSEs do not engage in production or sale activities in the wholesale power market. Hence, LSEs purchase power only from Generators, not from each other.

For initial simplicity, the current study makes the usual empirically-based assumption that the downstream retail demands serviced by the AMES LSEs exhibit negligible price sensitivity and hence reduce to daily load profiles. In addition, the LSEs are modeled as passive entities who submit these daily load profiles into the Day-Ahead Market as their demand bids without strategic consideration. Specifically, at the beginning of each day  $D$  each LSE  $j$  submits a daily load profile into the day-ahead market for day  $D+1$ . This daily load profile indicates the real power demand  $p_{L_j}(H)$  (in MWs) that must be serviced by LSE  $j$  in its downstream retail market for each of 24 successive hours  $H$ .



#### 4.4.4 Structural Configuration of the AMES Generators

The AMES Generators are electric power generating units. The user specifies the number  $I$  of Generators as well as the location of these Generators at various nodes of the transmission grid. Generators sell power only to LSEs, not to each other. Each AMES Generator  $i$  is user-configured with a production technology, learning capabilities, and an initial level  $\text{Money}_i^o$  of money holdings. Here we elaborate on Generator production technologies; learning capabilities are separately taken up in Subsection 4.4.6 below.

With regard to production technology, it is assumed that each Generator has variable and fixed costs of production. However, Generators do not incur no-load, startup, or shutdown costs, and they do not face ramping constraints.<sup>13</sup>

More precisely, the technology attributes assumed for each Generator  $i$  take the following form. Generator  $i$  has lower and upper production limits (in MWs), denoted by  $\text{Cap}_i^L$  and  $\text{Cap}_i^U$ , that define the *feasible production interval* for its hourly real-power production level  $p_{Gi}$  (in MWs).<sup>14</sup> That is, for each  $i$ ,

$$\text{Cap}_i^L \leq p_{Gi} \leq \text{Cap}_i^U \quad (4.1)$$

In addition, Generator  $i$  has a *total cost function* giving its total costs of production per hour for each  $p_{Gi}$ . This total cost function takes the form

$$\text{TC}_i(p_{Gi}) = a_i \cdot p_{Gi} + b_i \cdot p_{Gi}^2 + \text{FCost}_i \quad (4.2)$$

where  $a_i$  (\$/MWh),  $b_i$  (\$/MW<sup>2</sup>h), and  $\text{FCost}_i$  (\$/h) are exogenously given constants. Note that  $\text{TC}_i(p_{Gi})$  is measured in dollars per hour (\$/h). Generator  $i$ 's *total variable cost function*

<sup>13</sup>As is standard in economics, *variable costs* are costs that vary with the level of production, and *fixed costs* are costs such as debt and equity obligations associated with plant investments that are not dependent on the level of production and that are incurred even if production ceases. As detailed by Kirschen and Strbac (2004, Sec. 4.3), the concept of *no-load costs* in power engineering refers to *quasi-fixed* costs that would be incurred by Generators if they could be kept running at zero output but that would vanish once shut-down occurs. *Startup costs* are costs specifically incurred when a Generator starts up, and *shutdown costs* are costs specifically incurred when a Generator shuts down. Finally, *ramping constraints* refer to physical restrictions on the rates at which Generators can increase or decrease their outputs.

<sup>14</sup>In the current AMES modeling, the lower production limit  $\text{Cap}_i^L$  for each Generator  $i$  is a firm "must run" minimum real-power production level. That is, if  $\text{Cap}_i^L$  is positive, then shutting down Generator  $i$  is not an option for the AMES ISO. Consequently, for most applications of AMES, these lower production limits should be set to zero.

and (*hourly prorated*) *fixed costs* for any  $p_{Gi}$  are then given by

$$\text{TVC}_i(p_{Gi}) = \text{TC}_i(p_{Gi}) - \text{TC}_i(0) = a_i \cdot p_{Gi} + b_i \cdot p_{Gi}^2 \quad (4.3)$$

and

$$\text{FCost}_i = \text{TC}_i(0) \quad (4.4)$$

respectively. Finally, the *marginal cost function* for Generator  $i$  takes the form

$$\text{MC}_i(p_{Gi}) = a_i + 2 \cdot b_i \cdot p_{Gi} \quad (4.5)$$

At the beginning of each day  $D$ , each Generator  $i$  reports a *supply offer*  $s_i^R(D)$  to the AMES ISO for use in each hour  $H$  of the Day-Ahead Market for day  $D+1$ . This supply offer consists of a reported marginal cost function

$$\text{MC}_i^R(p_{Gi}) = a_i^R + 2 \cdot b_i^R \cdot p_{Gi} \quad (4.6)$$

defined over a reported feasible production interval<sup>15</sup>

$$\text{Cap}_i^{RL} \leq p_{Gi} \leq \text{Cap}_i^{RU} \quad (4.7)$$

This supply offer can be *strategic* in the sense that the reported cost coefficients  $a_i^R$  and  $b_i^R$  in (4.6) can deviate from Generator  $i$ 's true cost coefficients  $a_i$  and  $b_i$  in (5.9) and the reported feasible production interval  $[\text{Cap}_i^{RL}, \text{Cap}_i^{RU}]$  in (4.7) can deviate from Generator  $i$ 's true feasible production interval  $[\text{Cap}_i^L, \text{Cap}_i^U]$  in (4.1).

Suppose Generator  $i$  is located at node  $k$ , and suppose Generator  $i$  in some day  $D$  reports a supply offer  $s_i^R(D)$  to the AMES ISO for the day  $D+1$  Day-Ahead Market (along with all other Generators). Let  $LMP_k$  denote the node- $k$  locational marginal price (LMP) that is then subsequently determined by the AMES ISO in day  $D$  for some hour  $H$  of day  $D+1$ , and let  $p_{Gi}^*$  denote the real power that Generator  $i$  has been cleared to inject at node  $k$  in hour  $H$  of day

<sup>15</sup>Here we follow closely the timing and basic form of the supply offers required by generators in the MISO (2006) and ISO-NE (2006). One difference, however, is that the latter supply offers are in the form of step-functions whereas we assume linearity to ease the representation of learning for the AMES Generators; see Section 4.4.6 below. Interestingly, in the ISO-NE the generators can check a "UseOfferSlope" box permitting the ISO to approximate their step-function offers by smooth curves.

D+1 . Then the (possibly negative) profit accruing to Generator  $i$  in day D from the day- $D$  settlement of this financially binding contract for hour H of day D+1 is

$$\text{Profit}_i^{\text{new}}(p_{Gi}^*) = \text{LMP}_k \cdot p_{Gi}^* - \text{TC}_i(p_{Gi}^*) \quad (4.8)$$

Moreover, as a result of this settlement, the updated cumulated money holdings for Generator  $i$  are given by

$$\text{Money}_i^{\text{new}} = \text{Money}_i^{\text{prev}} + \text{Profit}_i^{\text{new}}(p_{Gi}^*) \quad (4.9)$$

Since Generator  $i$ 's profits (4.8) can be negative, it is clear from (4.9) that Generator  $i$  faces a risk of *insolvency*, i.e., a risk that its money holdings will run out. It is assumed in the AMES framework that any Generator who becomes insolvent must immediately exit the market.

#### 4.4.5 Structural Configuration of the ISO

As in actual ISO-managed wholesale power markets operating under the WPMP market design, the AMES ISO during each day D is charged with determining a schedule of optimal power commitments and LMPs for each hour of the Day-Ahead Market in day D+1 . This schedule is conditional on reported LSE demand bids, reported Generator supply offers (marginal cost functions plus production limits), thermal limits on branch flows, and nodal balance constraints ensuring supply equals demand (load) at each transmission grid node.

As usual, “optimal” is interpreted to mean that total net surplus is maximized. The resulting optimization problem is known as a *bid-based AC optimal power flow (OPF)* problem. As typically done in actual markets, the AMES ISO approximates this difficult bid-based AC OPF problem by means of a simpler bid-based DC OPF problem in which real power constraints are linearized and reactive power constraints are ignored.<sup>16</sup>

Recall from Section 4.4.3 that the AMES LSEs are currently modeled as non-strategic entities servicing price-insensitive loads whose reported demand bids in each day D take the form of their true daily load profiles. In this case the maximization of total net surplus reduces

<sup>16</sup>See Sun and Tesfatsion (2006) for a detailed discussion of this approximation.

to the minimization of total variable cost. Consequently, using the variable definitions in Tables 5.1 and 5.2, the bid-based DC OPF problem solved by the AMES ISO in day D for each hour of the Day-Ahead Market in day D+1 takes the following specific form:

**Minimize Generator-reported total variable cost**

$$\sum_{i=1}^I [a_i^R p_{Gi} + b_i^R p_{Gi}^2] \quad (4.10)$$

**with respect to real-power production levels and voltage angles**

$$p_{Gi}, i = 1, \dots, I; \quad \delta_k, k = 1, \dots, K$$

**subject to:**

**Real power balance constraint for each node  $k = 1, \dots, K$ :**

$$0 = PLoad_k - PGen_k + PNetInject_k \quad (4.11)$$

where

$$PLoad_k = \sum_{j \in J_k} p_{Lj} \quad (4.12)$$

$$PGen_k = \sum_{i \in I_k} p_{Gi} \quad (4.13)$$

$$PNetInject_k = \sum_{km \text{ or } mk \in BR} P_{km} \quad (4.14)$$

$$P_{km} = B_{km} [V_o]^2 [\delta_k - \delta_m] \quad (4.15)$$

**Real power thermal constraints for each branch  $km \in BR$ :**

$$|P_{km}| \leq P_{km}^U \quad (4.16)$$

**Reported real-power production constraints for each Generator  $i = 1, \dots, I$ :**

$$\text{Cap}_i^{RL} \leq p_{Gi} \leq \text{Cap}_i^{RU} \quad (4.17)$$

**Voltage angle setting at reference node 1:**

$$\delta_1 = 0 \quad (4.18)$$

As shown in Sun and Tesfatsion (2006), this DC OPF problem can equivalently be represented in the numerically desirable form of a strictly convex quadratic programming (SCQP) problem if the balance constraints (5.26) are used to eliminate the voltage angles  $\delta_k$  by substitution. However, this elimination prevents direct generation of solution values for LMPs since, by definition, the LMP for node  $k$  is the solution value for the multiplier (shadow price) for the  $k$ th nodal balance constraint.

For this reason, we replace the standard DC OPF objective function (4.10) with the following augmented form:

$$\sum_{i=1}^I [a_i^R p_{Gi} + b_i^R p_{Gi}^2] + \pi \left[ \sum_{km \in BR} [\delta_k - \delta_m]^2 \right], \quad (4.19)$$

where  $\pi$  is a positive soft penalty weight on the sum of squared voltage angle differences. As carefully demonstrated in Sun and Tesfatsion (2006), the augmented DC OPF objective function (4.19) provides a number of benefits based on both physical and mathematical considerations.

First, the resulting augmented DC OPF problem now has a numerically desirable SCQP form permitting the direct generation of solution values for LMPs as well as for real power production levels, branch flows, and voltage angles. Second, the validity of the DC OPF as an approximation for the underlying AC OPF relies on an assumption of small voltage angle differences, and the augmented DC OPF problem permits this assumption to be subjected to systematic sensitivity tests through variations in the penalty weight  $\pi$ . Third, solution differences between the non-augmented and augmented forms of the DC OPF problem can be reduced to arbitrarily small levels by selecting an appropriately small value for  $\pi$ .

To solve this augmented DC OPF problem, the AMES ISO invokes the SCQP solver QuadProgJ through an outer shell DCOPFJ. More precisely, as illustrated below in Section 4.5, the AMES ISO passes to DCOPFJ current DC OPF input data in standard (SI) units together with base apparent power and voltage values  $S_o$  and  $V_o$ . DCOPFJ converts this SI input data into per unit (pu) form and performs all needed matrix and vector representations. DCOPFJ then invokes QuadProgJ to solve for LMPs, voltage angles, real power production levels, real power branch flows, and various other useful quantities with all internal calculation carried out in pu terms. QuadProgJ then passes these pu solution values back to DCOPFJ, which outputs them in SI units.

In future studies, the AMES ISO will also have to solve DC OPF problems for the Real-Time Market to settle any differences that arise between day-ahead commitments and real-time conditions due to system disturbances (e.g. sudden line outages or changes in demand). However, in our initial experiments with the AMES framework we are not considering system disturbances that would cause such differences to arise. Consequently, all load obligations are fully met through Day-Ahead Market transactions and the Real-Time Market is inactive.

#### 4.4.6 Learning Configuration for the AMES Generators

In general, multiple Generators at multiple nodes could be under the control of a single generation company (“GenCo”). This control aspect is critically important to recognize for the study of real-world strategic trading. This situation can be handled in the AMES framework by permitting coordinated learning across Generators controlled by a single GenCo.

For initial simplicity, however, the AMES Generators are currently modeled as autonomous energy traders with strategic learning capabilities; see Figure 4.8. Each AMES Generator adaptively selects its supply offers on the basis of its own past profit outcomes using a version of a stochastic reinforcement learning algorithm developed by Roth-Erev (1995) based on human-subject experiments, hereafter referred to as the *VRE learning algorithm*. This section briefly outlines the implementation of the VRE learning algorithm for an arbitrary Generator

*i*.

<p><b>Public Access:</b></p> <p>// <b>Public Methods</b>  getMarketProtocols(posting, trade, settlement);  getMarketProtocols(ISO market power mitigation);  Methods for receiving data;  Methods for retrieving stored Generator data.</p>
<p><b>Private Access:</b></p> <p>// <b>Private Methods</b>  Method for calculating my expected profits;  Method for calculating my actual profit outcomes;  Method for updating my supply offers (<b>LEARNING</b>).</p> <p>// <b>Private Data</b>  My capacity, grid location, cost fct., current wealth... ;  Data recorded about external world (dispatch schedule...);  Address book (communication links).</p>

Figure 4.8 A Computational Generator (Seller)

Suppose it is the beginning of the initial day  $D=1$ , and Generator  $i$  must choose a supply offer from its *action domain* ( $AD_i$ ) to report to the AMES ISO for the Day-Ahead Market in day  $D+1$ . As will be seen below, for learning purposes the only relevant attribute of  $AD_i$  is that it has finite cardinality  $M_i \geq 1$ .<sup>17</sup>

The *initial propensity* of Generator  $i$  to choose supply offer  $m \in AD_i$  is given by a non-negative number  $q_{im}(0)$ . In general, these initial propensities can be any real numbers as specified by the AMES user. However, the default setting used in this study is that these initial propensities are equal. That is, we specify a fixed value  $q_i(0)$  such that

$$q_{im}(0) = q_i(0) \text{ for all supply offers } m \in AD_i \quad (4.20)$$

Now consider the beginning of any day  $D \geq 1$ , and suppose the current propensity of

<sup>17</sup>Technical details concerning the construction of each Generator  $i$ 's action domain  $AD_i$  are taken up in the appendix. The key issue is how to construct the sets  $AD_i$  to give each Generator an economically meaningful and realistically flexible selection of supply offers without introducing hidden structural biases favoring some Generators over others.

Generator  $i$  to choose supply offer  $m \in AD_i$  is given by  $q_{im}(D)$ . The *choice probabilities* that Generator  $i$  uses to select a supply offer for day  $D$  are then constructed from these propensities as follows:<sup>18</sup>

$$p_{im}(D) = \frac{\exp(q_{im}(D)/C_i)}{\sum_{j=1}^{M_i} \exp(q_{ij}(D)/C_i)}, \quad m \in AD_i \quad (4.21)$$

In (4.21),  $C_i$  is a *cooling parameter* that affects the degree to which Generator  $i$  makes use of propensity values in determining its choice probabilities. As  $C_i \rightarrow \infty$ , then  $p_{im}(D) \rightarrow 1/M_i$ , so that in the limit Generator  $i$  pays no attention to propensity values in forming its choice probabilities. On the other hand, as  $C_i \rightarrow 0$ , the choice probabilities (4.21) become increasingly peaked over the particular supply offers  $m$  having the highest propensity values  $q_{im}(D)$ , thereby increasing the probability that these supply offers will be chosen.

At the end of day  $D$ , the current propensity  $q_{im}(D)$  that Generator  $i$  associates with each supply offer  $m \in AD_i$  is updated in accordance with the following rule. Let  $m'$  denote the supply offer that was *actually* selected and reported into the Day-Ahead Market by Generator  $i$  in day  $D$ , and let  $\text{Profit}_{im'}(D)$  denote the profits (positive or negative) attained by Generator  $i$  in the settlement of the Day-Ahead Market at the end of day  $D$  in response to its choice of supply offer  $m'$ . Then, for each supply offer  $m \in AD_i$ ,<sup>19</sup>

$$q_{im}(D+1) = [1 - r_i]q_{im}(D) + \text{Response}_{im}(D), \quad (4.22)$$

where

$$\text{Response}_{im}(D) = \begin{cases} [1 - e_i] \cdot \text{Profit}_{im'}(D) & \text{if } m = m' \\ e_i \cdot q_{im}(D)/[M_i - 1] & \text{if } m \neq m', \end{cases} \quad (4.23)$$

<sup>18</sup>In the original algorithm developed by Erev and Roth (1998) and Roth and Erev (1995), the choice probabilities are defined in terms of relative propensity levels. Here, instead, use is made of a “simulated annealing” formulation in terms of exponentials. As will be seen below in (4.22), in the current context the propensity values can take on negative values if sufficiently large negative profit outcomes are experienced, and the use of exponentials ensures that the choice probabilities remain well defined even in this event.

<sup>19</sup>The response function appearing in (4.22) modifies the response function appearing in the original algorithm developed by Erev and Roth (1998) and Roth and Erev (1995). The modification is introduced to ensure that learning (updating of choice probabilities) occurs even in response to zero-profit outcomes, which are particularly likely to arise in initial periods when Generator  $i$  is just beginning to experiment with different supply offers and the risk of overbidding to the point of non-dispatch is relatively high. See Koesrindartoto (2002) for a detailed discussion and experimental exploration of this zero-profit updating problem with the original Roth-Erev learning algorithm. See Nicolaisen et al. (2001) for a detailed motivation, presentation, and experimental application of the modified response function.



where  $m \neq m'$  implies  $M_i \geq 2$ . The introduction of the *recency parameter*  $r_i$  in (4.22) acts as a damper on the growth of the propensities over time. The *experimentation parameter*  $e_i$  in (4.23) permits reinforcement to spill over to some extent from a chosen supply offer to other supply offers to encourage continued experimentation with various supply offers in the early stages of the learning process.

Generator  $i$  faces a trade-off in each day  $D$  between information exploitation and information exploration. The VRE learning algorithm outlined above resolves this trade-off by ensuring continual exploration but at a typically declining rate. More precisely, under the VRE learning algorithm, note that Generator  $i$  in day  $D$  does *not* necessarily choose a supply offer with the highest accumulated profits to date. Given a suitably small value for  $e_i$ , selected supply offers generating the highest accumulated profits tend to have a relatively higher *probability* of being chosen, but there is always a chance that other supply offers will be chosen instead. This ensures that Generator  $i$  continues to experiment with new supply offers to some degree, even if its choice probability distribution becomes peaked at a particular selected supply offer because of relatively good profit outcomes. This helps to reduce the risk of premature fixation on suboptimal supply offers in the early stages of the decision process when relatively few supply offers have been tried.

In summary, the complete VRE learning algorithm applied to Generator  $i$  is fully characterized once user-specified values are provided for the number  $M_i$  of possible supply offer selections and the following four learning parameters: the initial propensity value  $q_i(0)$  in (4.20); the cooling parameter  $C_i$  in (4.21); the recency parameter  $r_i$  in (4.22); and the experimentation parameter  $e_i$  in (4.23). It is interesting to note, in particular, that the VRE learning algorithm is well-defined for any action domain  $AD$  consisting of finitely many elements, regardless of the precise nature of these elements.

## 4.5 Dynamic Five-Node Test Case

### 4.5.1 Overview

Consider a situation in which five Generators and three LSEs are distributed across a 5-node transmission grid as depicted in Figure 5.2. An interesting aspect of this transmission grid is that not all nodes are directly connected; for example, node 5 is not directly connected to either node 2 or node 3.

Originally due to John Lally (2002), this five-node transmission grid configuration is now used extensively in ISO-NE/PJM training manuals to solve for DC-OPF solutions at a given point in time conditional on variously specified marginal costs and production limits for the Generators and variously specified price-insensitive loads for the LSEs. The implicit assumption in all of these static training exercises is that the true cost and true production limits of the Generators are known. Nowhere is any mention made of the possibility that Generators in real-world ISO-managed wholesale power markets might learn to exercise market power over time through strategic reporting of their cost and production attributes.

In this section we illustrate how the AMES wholesale power market framework can be used to transform these static training exercises into a more realistic dynamic form with strategically learning Generators. Detailed grid, production, and load input data for a specific dynamic five-node test case are provided in Table 5.8.<sup>20</sup> As seen in this table, and depicted graphically in Figure 5.4, the daily load profile for each LSE is price insensitive and peaks at hour 17. Note, also, that Generator 4 is a “peaker” unit with relatively high hourly marginal costs  $MC(p) = 30 + 0.012p$  for each  $p$ , where  $p$  denotes hourly real-power production in megawatts (MWs). Also, each Generator has a finite upper limit  $Cap^U$  on its hourly real power production.

We first run this dynamic five-node test case under a “no learning” assumption for Generators, i.e. Generators are assumed to report to the ISO their true marginal cost functions and true production limits. Our findings for this no-learning case, detailed in Section 4.5.2, reveal the complicated effects of daily load profiles, transmission congestion, and production limits

<sup>20</sup>The transmission grid configuration, reactances, locations of the Generators and LSEs, and initial hour-0 load levels in Table 5.8 are taken from Lally (2002). The general shape of the LSE load profiles is adopted from a 3-node example presented in Shahidehpour et al. (2002, pp. 296-297).

on LMP determination over time, even in the absence of strategic reporting by Generators.

We next run this dynamic five-node test case under the assumption that the profit-seeking Generators can report strategic supply offers to the ISO. More precisely, the Generators still must report their true production limits to the ISO; but they can now learn over time what marginal cost attributes to report to the ISO in an attempt to increase their profit earnings.<sup>21</sup>

As clarified in the Appendix, we construct each Generator  $i$ 's action domain  $AD_i$  using five action-domain parameter values  $\{M1, M2, RIMax^L, RIMax^U, SS\}$  set identically across the Generators to ensure identical cardinalities and similar densities. In addition, for simplicity, each Generator  $i$  selects supply offers from its action domain using VRE reinforcement learning with commonly specified values for the four learning parameters  $\{q(0), C, r, e\}$ ; cf. Section 4.4.6. These parameter values for action domain construction and learning are given in Table 4.4.

The existence of price-insensitive loads provides a potentially golden opportunity for the two largest Generators 3 and 5 to exercise market power. Note from Table 5.8 that the peak load in hour 17 is 1153.59, and that the combined capacity of the smallest three Generators 1, 2, and 4 is only 410MWs. It follows that this peak load cannot be met unless Generator 3 (520MWs) and Generator 5 (600MWs) are both dispatched to some extent. Consequently, if these profit-seeking Generators had full structural information, their reported marginal costs should be as high as permitted by their action domains. The question is whether the simple VRE reinforcement learning algorithm permits these Generators to learn to exercise this potential market power.

As detailed below in Section 4.5.3, the answer is a resounding “yes.” All five Generators learn to implicitly collude on higher-than-true reported marginal costs. Moreover, the marginal costs reported by Generators 3 and 5 typically are near or at the highest possible levels permitted by their action domains. Production and LMP solutions differ dramatically from the production and LMP solutions obtained for the no-learning case reported in Section 4.5.2. The result is a substantial increase in the total variable cost of operation at the ISO-determined

<sup>21</sup>The Generators thus behave as if they were in a leader-follower game with the ISO. Since the Generators as currently implemented do not explicitly recognize the presence of rival Generators in their choice environments, there is no strategic interaction among the Generators per se.

“optimal” Day-Ahead Market DC OPF solution for each hour of each day.

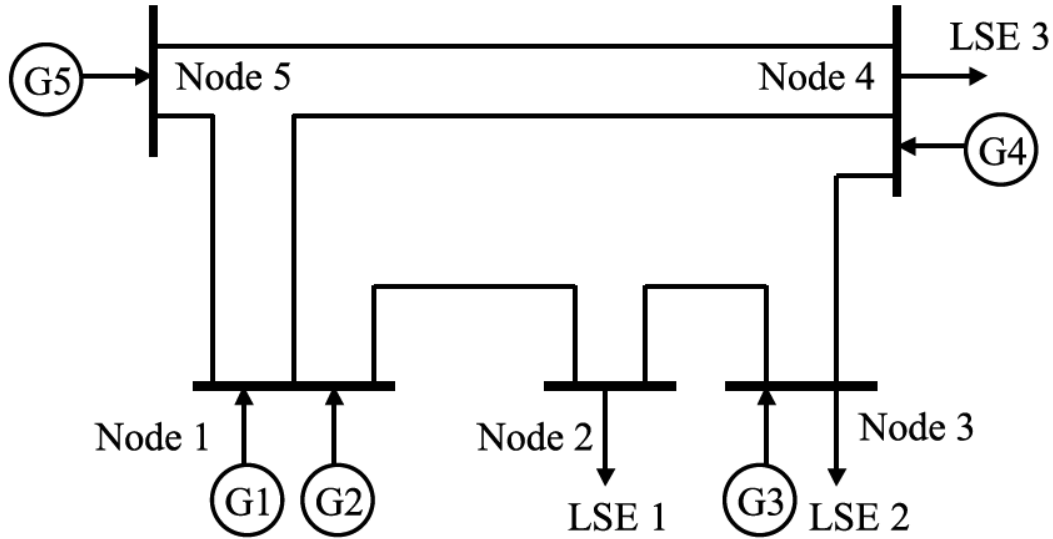


Figure 4.9 A Five-Node Transmission Grid Configuration

#### 4.5.2 Case 1: Generators Report True Supply Data

Suppose each Generator submits its true marginal cost function and true production limits into the Day-Ahead Market. That is, suppose Generators do not report strategic supply offers. In this case, the augmented DC OPF problem solved by the ISO for each hour  $H$  involves the minimization of true Generator total variable cost (subject to a small voltage angle difference penalty) conditional on LSE loads, nodal balance constraints, true Generator upper and lower production limits, and upper and lower thermal limits on each branch of the transmission grid; compare Section 4.4.5.

Tables 4.5 and 4.6 report outcomes in standard (SI) units obtained for this dynamic 5-node test case by means of QuadProgJ invoked through DCOPFJ. These outcomes include optimized solution values for real power branch flows, production levels, LMPs (nodal balance constraint

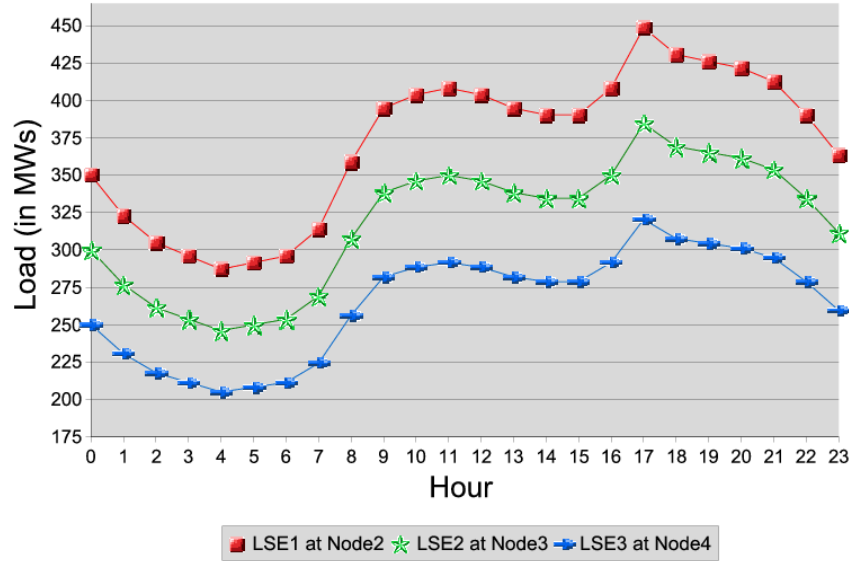


Figure 4.10 24 Hour Load Distribution for the Dynamic 5-Node Test Case

multipliers), and minimum total variable cost for 24 successive hours in the Day-Ahead Market.

These outcomes reveal that branch congestion occurs between node 1 and node 2 (and only these nodes) in each of the 24 hours. This can be verified by examining column  $P_{12}$  in Table 4.5, which shows that the real power flow  $P_{12}$  on branch  $km = 12$  is at its upper thermal limit (250 MWs) for each hour. The direct consequence of this branch congestion is the occurrence of widespread LMP separation, i.e. the LMP values differ across all nodes for each hour. This can be verified by examining output columns  $LMP_1$ - $LMP_5$  in Table 4.6.

Examining this LMP data more closely, it is seen that  $LMP_2$  and  $LMP_3$  (the LMPs for nodes 2 and 3) exhibit a sharp change in hour 17, increasing between hour 16 and hour 17 by about 100% and then dropping back to more normal levels in hour 18 and beyond. Interestingly, this type of sudden spiking in LMP values is also observed empirically in MISO's Dynamic LMP Contour Map for real-time market prices, which is updated every five minutes; see, for example, Figure 4.11.

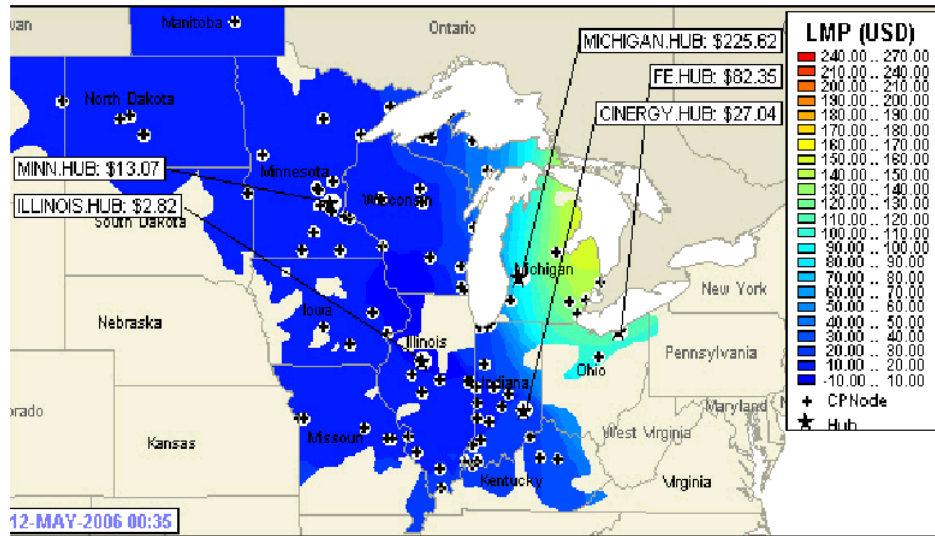


Figure 4.11 LMP Separation and Spiking in the MISO Energy Region

The rather dramatic LMP spiking in hour 17 can be traced to several factors. First, as seen in Figure 5.4, the load profile for each LSE peaks at hour 17. Second, when solving the DC OPF problem to meet the high load in hour 17, the ISO has to take into consideration the thermal limit constraining the flow of power on branch  $km = 12$  as well as the upper limit  $Cap^U$  constraining the production of Generator 3. Both of these constraints turn out to be binding in hour 17. As seen in Table 4.5, the real power flow in branch  $km = 12$  is at its upper limit (250 MWs) for all 24 hours. As seen in Table 4.6, Generator 3 is dispatched in hour 17 at its upper production limit (520 MWs).

Given the configuration of the transmission grid, to meet the hour 17 peak load the ISO is forced to back down (relative to hour 16) the less expensive production of Generators 1 and 2 and to use instead the more expensive production of the “peaker” Generator 4. After the peak hour 17, the load returns to lower levels. The ISO is then able to schedule Generator 1 and Generator 2 at their more normal levels, with Generator 1 at its upper production limit, and

to avoid scheduling any production from Generation 4; note from Table 5.8 that Generator 4's minimum production level ( $\text{Cap}^L$ ) is 0. Furthermore, the LMPs drop back to their more normal levels after hour 17.

These illustrative 5-node test case outcomes for 24 successive hours in the Day-Ahead Market raise intriguing economic issues concerning the operation of ISO-managed wholesale power markets in the presence of inequality constraints on branch flows and production levels. The strong sensitivity of the optimized LMP and real power production values to changes in the set of binding (active) constraints is of particular interest.

Equally intriguing, however, is whether the Generators might learn to make use of the outcomes for any particular operating day D to change their reported supply offers for day D+1 and beyond. The next section considers this issue.

#### 4.5.3 Case 2: Generators Report Strategic Supply Offers

Now suppose, in contrast to Case 1, that the Generators do not necessarily report their true marginal costs to the ISO for the Day-Ahead Market. Rather, using the VRE stochastic reinforcement learning algorithm detailed in Section 4.4.6, with parameter values as specified in Table 4.4, each profit-seeking Generator learns over time which marginal cost function to report to the ISO based on the profits it has earned from previously reported functions.

To control for random effects, outcomes for the learning case are reported below in the form of mean and standard deviation values obtained for twenty runs using the twenty different seed values reported in Table 4.4.<sup>22</sup> Moreover, in these twenty runs, all five Generators appear to “converge” by day 422 to a sharply peaked choice probability distribution in which a probability of 0.999 is assigned to a single supply offer.<sup>23</sup> Consequently, all learning outcomes reported below are for day 422.

Table 4.7 provides detailed numerical solution values (means and standard deviations) for branch flows on day 422. Recalling that the thermal limit on branch  $km = 12$  is 250MWs,

<sup>22</sup>Each Generator implements VRE learning by means of its own JReLM learning module, which must be initialized with a seed value for its pseudo-random number generator. Each initial seed value reported in Table 4.4 is used to generate five pseudo-random numbers, one for each Generator. Each of these numbers is then used in turn as the initial seed value for the corresponding Generator's JReLM learning module.

<sup>23</sup>The *mean* convergence time across the five Generators was actually only 62 days.

note that congestion occurs on branch  $km = 12$  in the peak hour 17 (and for several hours thereafter) in all 20 runs. Moreover, although the *mean* flow on branch  $km = 12$  is slightly below the thermal limit in other hours, in fact this branch is congested during all 24 hours of day 422 in all but three of the twenty runs. Moreover, no other branch is ever congested. These findings are similar to the no-learning case, in which branch  $km = 12$  (and only this branch) was found to be persistently congested.

Tables 4.8 and 4.9 provide detailed numerical solution values (means and standard deviations) for real power production levels and LMPs, respectively, on day 422. Table 4.10 gives the ordinate value  $a^R$  and slope value  $b^R$  for the (linear) marginal cost function reported to the ISO on Day 422 by each of the five Generators in each of the twenty runs. In the following discussion we highlight various aspects of these outcomes that differ significantly from the corresponding outcomes presented for the no-learning case in Section 4.5.2.

Figure 4.12 displays the (mean) solution values obtained for production for each of the 24 hours on day 422, along with the corresponding solution values obtained for day 422 in the absence of Generator learning.<sup>24</sup> In the no-learning case, note that the “peaker” (high cost) Generator 4 is only dispatched to produce energy at the peak load hour 17. In the learning case, however, Generator 4 is able to use strategic supply offers to ensure it is dispatched at approximately its upper production limit (200MWs) throughout each hour of the day. Also, in the no-learning case the “cheap” Generator 5 is regularly dispatched at a high production level during each hour of the day, but in the learning case it is backed way down because its strategic supply offers make it appear to be a relatively more expensive Generator.

This heavier reliance on costlier generation in the learning case substantially increases the total variable cost of operation. Indeed, as seen in Figure 4.13, the minimum total variable cost of operation under the learning case is roughly three times higher than under the no-learning case.

Figure 4.14 graphically depicts the 24-hour (mean) LMP solution values for the learn-

<sup>24</sup>Given the stationarity of the daily load profiles and the Generators’ cost functions and production limits, and the absence of system disturbances, in the no-learning case the 24-hour outcomes obtained for any one day are the same as for any other day.



ing case along with the 24-hour LMP solution values for the no-learning case. Interestingly, although the LMPs for the learning case are considerably higher than the LMPs for the no-learning case, they are also less volatile around the peak load hour 17. Consequently, the ISO is not able to use the appearance of price spikes in peak load hours to detect the considerable exercise of market power by the learning Generators. Rather, some form of direct auditing of the Generators' cost attributes would seem to be required.

Figure 4.15 displays the (mean) marginal cost functions that the five Generators report to the ISO on day 422, along with their true marginal cost functions. Despite the absence of any explicit collusion, all five Generators have learned to report higher-than-true marginal cost functions with respect to both ordinate and slope. In the case of Generators 3 and 5, the two largest generating units, the increase is substantial; these two Generators quickly learn to report a marginal cost function that is near or at the highest level permitted in their action domains.<sup>25</sup> Clearly the core aspects of the WPMP market design currently captured in the AMES framework do not provide sufficient mechanisms to prevent Generators from exercising substantial market power through strategic reporting of supply offers.

These findings can be compared with the findings of Wolfram (1999), who determined empirically that the (pre-NETA) uniform-price double auction design in effect for the UK wholesale power market at the time of her study provided incentives for generators to raise prices above costs. The Day-Ahead Market under the WPMP design collapses to a uniform-price double auction only in the absence of transmission grid congestion; LMP separation occurs if any branch is congested. Nevertheless, the AMES Generators are able to exercise substantial market power whether or not LMP separation occurs.

## 4.6 Concluding Remarks

The North American power transmission grid has been called “the largest and most complex machine in the world” (Amin, 2004, p. 31). An extraordinary experiment is under way to

<sup>25</sup>More precisely, the lower and upper range-index values implied by these Generators' reported marginal cost curves typically converge with rapidity to values that are near or at their highest permitted range-index levels  $RIMax^L = 0.75$  and  $RIMax^U = 0.75$ ; cf. Table 4.4.

see whether the physical operation of this complex machine can be successfully married with a restructured commercial architecture encouraging increased reliance on demand and supply forces. Smart electrical devices permitting more distributed physical control of the grid are being introduced along with market designs permitting more decentralized pricing and allocation mechanisms, a trend one commentator has called “electricity’s third great revolution” (Mazza, 2003).

Stakeholders, policy makers, and researchers all clearly recognize the critical need for this experiment to succeed (FERC, 2006). Nevertheless, the issues raised by this experiment are extremely challenging. How to analyze the potential dynamic performance of a system comprising multiple distributed entities, some physical and some human, all with finite information and computational capabilities? How to properly take into account the stability limits of physical components as well as the strategic behaviors of human participants responding to the incentives deliberately or inadvertently presented by system design features?

Agent-based modeling tools have been specifically developed to handle these types of complexities, hence it is not surprising to find agent-based researchers actively involved in this electricity restructuring movement. As detailed by Davidson and McArthur (2005) and Widergren et al. (2006), multi-agent systems are attracting significant research interest for power system applications. Indeed, the *IEEE Task Force on Multi-Agent Systems in Power Engineering* is charged with exploring the benefits, applications, and advanced functionality that can be provided for power systems through agent technology. The members of this MAS Task Force include economists as well as engineers, and academics as well as industry stakeholders.

In this study we explore the potential usefulness of agent-based tools for investigating the efficiency and reliability of the Wholesale Power Market Platform (WPMP), a market design proposed by the U.S. Federal Energy Regulatory Commission for common adoption by all U.S. wholesale power markets (FERC, 2003). We first describe a newly developed agent-based computational laboratory – the AMES framework – that models a wholesale power market operating in accordance with core WPMP features over a realistically rendered transmission grid. Using a dynamic 5-node test case for concrete illustration, we then explore the extent to

which these core WPMP features permit and even encourage the exercise of market power by Generators through strategic supply offer reporting.

More precisely, in the dynamic 5-node test case the AMES ISO does not know the AMES Generators' true cost attributes. Rather, in each operating day  $D$ , the AMES ISO must formulate its DC OPF problem for each hour of the Day-Ahead Market for day  $D+1$  based on the cost attributes reported to it by the Generators. The profit-seeking Generators learn over time what cost attributes to report to the ISO using a simple reinforcement learning algorithm based on past profit outcomes. As seen in Section 4.5, despite the absence of any explicit collusion the typical Generator converges within 62 days to a supply offer selection in which its reported marginal cost function is uniformly higher than its true marginal cost function, in some cases substantially higher. The resulting "optimal" DC OPF solutions determined by the AMES ISO appear to have desirable properties, e.g. low LMP volatility during peak load hours and congestion on only one branch. In fact, however, total variable costs of operation are roughly three times higher than they would have been had the Generators reported their true cost attributes. As captured in the current AMES framework, the core WPMP design features do not prevent the considerable exercise of market power by Generators.

As detailed in Section 4.3, the AMES framework needs to be further extended to incorporate additional key aspects of the WPMP design that could significantly impact the efficiency and reliability of market operations. Moreover, initial conditions and parameter specifications need to be more carefully calibrated to match real-world conditions. Nevertheless, we believe the preliminary findings reported in this study suggest the great potential of agent-based computational models to help ensure a successful restructuring of the electric power industry through intensive sensitivity experiments.

## 4.7 References

Amin, Massoud (2004). Balancing market priorities with security issues, *IEEE Power and Energy Magazine*, July/August, pp. 30-38.

Axelrod, Robert, and Tesfatsion, Leigh (2006). A guide for newcomers to agent-based model-

ing in the social sciences. In Leigh Tesfatsion and Kenneth L. Judd, *op. cit.*. Available: <http://www.econ.iastate.edu/tesfatsi/abmread.htm>

Barreteau, Olivier (2003). Our companion modeling approach, *Journal of Artificial Societies and Social Simulation* 6(1) (electronic), <http://jasss.soc.surrey.ac.uk/6/2/1.html>

Borenstein, Soren (2002). The trouble with electricity markets: Understanding California's restructuring disaster, *J. Econ. Perspectives* 16(1), 191-211.

Bower, John, and Bunn, Derek (2001). Experimental analysis of the efficiency of uniform-price versus discriminatory auctions in the England and Wales electricity market, *Journal of Economic Dynamics and Control* 25(3-4), 561-592.

Conzelmann, Guenter, North, Michael J., Boyd, Gale A., Cirillo, Richard R., Koritarov, Vladimir, Macal, Charles M., Thimmapuram, Prakash R., and Veselka, Thomas D. (2004). Simulating Strategic Market Behavior Using an Agent-Based Modeling Approach, *Proceedings, 6th IAEE European Conference, Zurich, Switzerland*.

Davidson, Euan M., and McArthur, Steven D. J. (2005). Concepts and approaches in multi-agent systems for power applications," *Proceedings, Intelligent System Applications in Power (ISAP) Conference, Washington D.C., November, pp. 391-395*.

Erev, Ido, and Roth, Alvin E. (1998). Predicting how people play games with unique mixed-strategy equilibria, *American Economic Review* 88, 848-881.

Fagiolo, Giorgio, Windrum, Paul, and Moneta, Alessio (2006). Empirical validation of agent-based models: A critical survey, LEM Working Paper 2006/14, Laboratory of Economics and Management, Sant'Anna School of Advanced Studies.

FERC (2003). *Notice of White Paper*, U.S. Federal Energy Regulatory Commission, 4/28.

FERC (2006). Report to Congress on competition in the wholesale and retail markets for electric energy, Docket No. AD05-17-000, U.S. Federal Energy Regulatory Commission, June. <http://www.ferc.gov/legal/staff-reports/competition-rpt.pdf>

- Gieseler, Charles J. (2005). A Java reinforcement learning module for the Repast toolkit: Facilitating study and experimentation with reinforcement learning in social science multi-agent simulations, M.S. Thesis, Computer Science, Iowa State University, November.
- ISO-NE (2006). Home Page, ISO New England, Inc. Available: <http://www.iso-ne.com/smd/>
- Joskow, Paul (2006). Markets for power in the United States: An interim assessment, *Energy Journal*, Vol. 27(1), 1-36.
- Kirschen, Daniel, and Strbac, Goran (2004). *Fundamentals of Power System Economics*, John Wiley & Sons, Inc., New York, NY.
- Koesrindartoto, Deddy (2002). A discrete double auction with artificial adaptive agents: A case study of an electricity market using a double-auction simulator,” Economics Working Paper No. 02005, Department of Economics, Iowa State University, Ames, IA. Available: <http://deddy.agenbased.net/res.html>
- Koesrindartoto, Deddy, Sun, Junjie, and Tesfatsion, Leigh (2005). An agent-based computational laboratory for testing the economic reliability of wholesale power market designs, *Proceedings*, Vol. 1, IEEE Power Engineering Society General Meeting, San Francisco, CA, June, 931-936.
- Lally, John (2002). Financial transmission rights: Auction example, Section 6, M-06 Financial Transmission Right Draft 01-10-02, ISO New England, Inc., January.
- Mazza, Patrick (2003). The smart energy network: Electricity’s third great revolution, Report prepared for Climate Solutions, Olympia, WA, June. Accessible: <http://www.climatesolutions.org/pubs/pdfs/SmartEnergy.pdf>
- McCalley, James, Ryan, Sarah, Sapp, Stephen, and Tesfatsion, Leigh (2005). Decision models for bulk energy transportation networks, Division of Electrical and Communication Systems, National Science Foundation Grant No. 0527460, 3/15/05 - 3/14/08.
- MISO (2006), Home Page, Midwest ISO, Inc.. Available: <http://www.midwestiso.org/>

- Nicolaisen, James, Petrov, Valentin, and Tesfatsion, Leigh (2001). Market power and efficiency in a computational electricity market with discriminatory double-auction pricing, *IEEE Transactions on Evolutionary Computation* 5(5), 504-523.
- Roth, Alvin E., and Erev, Ido (1995). Learning in extensive form games: Experimental data and simple dynamic models in the intermediate term, *Games and Econ. Behavior* 8, 164-212.
- Shahidehpour, Mohammad, Yamin, Hatim, and Li, Zuyi (2002). *Market Operations in Electric Power Systems*, IEEE/Wiley-Interscience, John Wiley & Sons, Inc., NY.
- Sun, Junjie (2005). U.S. financial transmission rights: Theory and practice, Economics Working Paper No. 05008, Economics Department, Iowa State University, March.
- Sun, Junjie, and Tesfatsion, Leigh (2006). DC optimal power flow formulation and solution using QuadProgJ,” Economics Working Paper No. 06014, Economics Department, Iowa State University, Revised: May.  
Available: <http://www.econ.iastate.edu/tesfatsi/DC-OPF.JSLT.pdf>
- Tesfatsion, Leigh (2006a). *ACE Research Area: Restructured Electricity Markets*, Website available at <http://www.econ.iastate.edu/tesfatsi/aelect.htm>, hosted by the Economics Department, Iowa State University.
- Tesfatsion, Leigh (2006b). *Website on Agent-based Computational Economics (ACE)*, Available: <http://www.econ.iastate.edu/tesfatsi/ace.htm>, hosted by the Economics Department, Iowa State University.
- Tesfatsion, Leigh (2006c). *Website on Empirical Validation of Agent-Based Computational Models*, Website available at <http://www.econ.iastate.edu/tesfatsi/EmpValid.htm>, hosted by the Economics Department, Iowa State University.
- Tesfatsion, Leigh (2006d). *RepastJ: A Software Toolkit for Agent-Based Social Science Modeling*, Website available at <http://www.econ.iastate.edu/tesfatsi/repastsg.htm>, hosted by the Economics Department, Iowa State University.

Tesfatsion, Leigh (2006e). *General Software and Toolkits: Agent-Based Computational Economics*, Website available at <http://www.econ.iastate.edu/tesfatsi/acecode.htm>, hosted by the Economics Department, Iowa State University.

Tesfatsion, Leigh, and Judd, Kenneth L., eds. (2006). *Handbook of Computational Economics, Vol. 2: Agent-Based Computational Economics*, Handbooks in Economics Series, North-Holland, Elsevier, Amsterdam, the Netherlands.

Weisfeld, Matt (2003). *The Object-Oriented Thought Process*, Second Edition, SAMS, MacMillan USA, Indiana.

Widergren, Steven, Roop, Joseph M., Guttromson, R. T., and Huang, Z. (2004). Simulating the dynamic coupling of market and physical system operations, *Proceedings*, 2004 IEEE PES General Meeting, Denver, Colorado.

Available: <http://gridwise.pnl.gov/docs/pnnl40415.pdf>

Widergren, Steven, Sun, Junjie, and Tesfatsion, Leigh (2006). Market design test environments, *Proceedings*, IEEE Power Engineering Society General Meeting, Montreal, June.

Wolfram, Catherine D. (1999). Electricity markets: Should the rest of the world adopt the United Kingdom's reforms?" *Regulation* 22(4), 48-53.

Veit, Daniel, Weidlich, Anke, Yao, Jian, and Oren, Shmuel (2006). Simulating the dynamics in two-settlement electricity markets via an agent-based approach, Working Paper.

Available: <http://www.ieor.berkeley.edu/~jyao/pubs/yao-MS06.pdf>

## 4.8 Appendix: Construction of Generator Action Domains

### 4.8.1 A.1 Overview

As detailed in Section 4.4.6, at the beginning of each day  $D$  each AMES Generator  $i$  uses a variant of a well known Roth-Erev reinforcement learning algorithm to choose a supply offer

$s_i^R$  to report to the AMES ISO for each hour  $H$  of the day  $D+1$  Day-Ahead Market. Each supply offer  $s_i^R$  takes the form of a reported marginal cost function

$$MC_i^R(p) = a_i^R + 2b_i^R p \quad (4.24)$$

defined over a reported feasible production interval

$$\text{Cap}_i^{RL} \leq p \leq \text{Cap}_i^{RU} \quad (4.25)$$

Here  $a_i^R$  and  $b_i^R$  are Generator  $i$ 's reported cost coefficients,  $p$  denotes Generator  $i$ 's hourly real-power production level, and  $\text{Cap}_i^{RL}$  and  $\text{Cap}_i^{RU}$  are Generator  $i$ 's reported lower and upper real-power production limits.

Each AMES Generator  $i$  chooses its supply offers  $s_i^R$  from an action domain  $AD_i$  with finite positive cardinality  $M_i$ . A key issue is how to construct this action domain in a manner that is both empirically sensible and computationally practical. Empirical sensibility suggests that, unless the modeler has information to the contrary, the action domain  $AD_i$  should provide Generator  $i$  with the flexibility to choose from among a wide range of possible supply offers, and that this degree of flexibility should be roughly similar across the Generators. Computational practicality suggests that the number of supply offers included in  $AD_i$  should not be unduly large.

In keeping with these modeling goals, the action domain  $AD_i$  for each AMES Generator  $i$  is constructed under five simplifying assumptions. First, we assume that Generator  $i$  always reports a non-trivial feasible production interval, i.e.,  $\text{Cap}_i^{RL} < \text{Cap}_i^{RU}$ . Second, we assume that Generator  $i$  only reports upward-sloping marginal cost functions (4.24), that is,  $b_i^R > 0$ .<sup>26</sup> Third, we assume that Generator  $i$ 's reported marginal cost curves always lie on or above Generator  $i$ 's true marginal cost curve over the respective reported feasible production intervals. Fourth, we assume that Generator  $i$  always reports its true lower production limit.<sup>27</sup> Fifth, we

<sup>26</sup>In the MISO and ISO-NE, reported supply functions are required to be non-decreasing.

<sup>27</sup>As explained in footnote 14, the Generators' reported lower production limits are treated as firm by the AMES ISO. Since the current version of AMES lacks market power mitigation rules, the AMES Generators could ensure themselves arbitrarily high profits if they were permitted to *report* arbitrarily high lower production limits into the Day-Ahead Market. For this reason, it is assumed in the current study that the AMES Generators are closely monitored by the AMES ISO with regard to these lower production limits, ensuring that they always



assume that Generator  $i$  always reports an upper production limit that is less than or equal to its true upper production limit.

We show below that, given any positive value for a *slope-start* parameter  $SS_i$ , we can construct an  $M_i \times 3$  matrix whose rows constitute  $M_i$  “admissible supply offers in (reduced) percentage form” that map uniquely into  $M_i$  reported supply offers  $s_i^R$  satisfying the five simplifying assumptions. This matrix is parameterized by two density-control parameters  $M1_i$  and  $M2_i$  (with  $M1_i \times M2_i = M_i$ ) and two range-index parameters  $RIMax_i^L$  and  $RIMax_i^U$  lying in  $[0, 1]$ .<sup>28</sup> If the five action-domain parameters ( $M1_i, M2_i, RIMax_i^L, RIMax_i^U, SS_i$ ) are set identically for each Generator  $i$ , and the above matrix construction is applied for each Generator  $i$ , then the result is a collection of Generator-specific action domains that have equal cardinalities and whose supply offer elements  $s^R$  provide similar densities of coverage of the regions lying above the Generators’ true marginal cost curves.

#### 4.8.2 A.2 Percentage Representation of Supply Offers

Let a reported supply offer  $s_i^R$  for Generator  $i$  be called *admissible* if it satisfies the five simplifying assumptions in Section A.1. Admissibility of  $s_i^R$  implies that  $s_i^R$  consists of a reported marginal cost function of form (4.24) defined over a reported production interval of form (4.25) such that  $0 < b_i^R$ ,  $0 \leq \text{Cap}_i^L = \text{Cap}_i^{RL} < \text{Cap}_i^{RU} \leq \text{Cap}_i^U$ ,  $0 < \text{MC}_i(\text{Cap}_i^L) = \text{MC}_i(\text{Cap}_i^{RL}) \leq \text{MC}_i^R(\text{Cap}_i^{RL})$ , and  $\text{MC}_i(p) \leq \text{MC}_i^R(p)$  for all  $p \in [\text{Cap}_i^L, \text{Cap}_i^{RU}]$ . Henceforth any admissible reported supply offer  $s_i^R$  will be compactly represented in the form

$$s_i^R = (a_i^R, b_i^R, \text{Cap}_i^{RL}, \text{Cap}_i^{RU}) \quad (4.26)$$

Also, let any vector

$$s_i^A = (RI_i^L, RI_i^U, \text{RCap}_i^L, \text{RCap}_i^U) \quad (4.27)$$

report their true lower limits. In the actual MISO and ISO-NE energy markets, generators are requested to report their true lower and upper production limits, but it is not clear from the MISO and ISO-NE business practices manuals just how closely generators are actually monitored to ensure compliance.

<sup>28</sup>As clarified below in Sections A.2 through A.4, these range-index parameters can be related to the “Lerner Index” used in industrial organization studies as an indicator of market power.

satisfying  $RI_i^L \in [0, 1)$ ,  $RI_i^U \in [0, 1)$ ,  $0 \leq RCap_i^L < RCap_i^U \leq 1$ , and  $RCap_i^L Cap_i^U = Cap_i^L$  be called an *admissible percentage supply offer*.

**CLAIM:** Let  $SS_i > 0$  be given. Then there exists a correspondence  $Q_{SS_i}$  conditional on  $SS_i$  that maps each admissible percentage supply offer  $s_i^A$  into a unique admissible reported supply offer  $s_i^R$ .

**Proof:** Let  $s_i^A = (RI_i^L, RI_i^U, RCap_i^L, RCap_i^U)$  denote any admissible percentage supply offer (4.27). It will now be shown how the elements of  $s_i^A$ , together with the structural attributes of Generator  $i$  as reported in Table 5.1, can be used to construct a unique admissible reported supply offer  $s_i^R$  for Generator  $i$ . This construction will be carried out in successive steps, some of which involve the determination of auxiliary variables. A schematic depiction of this construction process can be viewed in Figure 4.16.

*Step 0: Construction of  $Cap_i^{RL}$  and  $Cap_i^{RU}$  satisfying  $0 \leq Cap_i^L = Cap_i^{RL} < Cap_i^{RU} \leq Cap_i^U$*

Let  $l_i$  and  $u_i$  denote Generator  $i$ 's true marginal costs for producing at its true lower and upper production limits, respectively, i.e.,

$$l_i = MC_i(Cap_i^L) = a_i + 2b_i Cap_i^L > 0 \quad (4.28)$$

$$u_i = MC_i(Cap_i^U) = a_i + 2b_i Cap_i^U > l_i \quad (4.29)$$

Define  $Cap_i^{RL} = RCap_i^L \cdot Cap_i^U$  and  $Cap_i^{RU} = RCap_i^U \cdot Cap_i^U$ . Then, using the admissibility of  $s_i^A$ , it follows that  $Cap_i^U \geq Cap_i^{RU} = RCap_i^U \cdot Cap_i^U > RCap_i^L \cdot Cap_i^U = Cap_i^{RL} = Cap_i^L \geq 0$ .

*Step 1: To get  $l_i^R \geq l_i > 0$*

By admissibility of  $s_i^A$ ,  $RI_i^L \in [0, 1)$ , and  $l_i > 0$  from (4.28). Now define  $l_i^R$  as

$$l_i^R = \frac{l_i}{1 - RI_i^L} \geq l_i > 0 \quad (4.30)$$

Given (4.28), (4.30), and  $\text{Cap}_i^{RL} = \text{Cap}_i^L$  from Step 0, note that  $\text{RI}_i^L$  reduces to a standard Lerner Index<sup>29</sup> evaluation at the reported lower production limit  $\text{Cap}_i^{RL}$  if  $l_i^R = \text{MC}_i^R(\text{Cap}_i^{RL})$ . The latter equality is established in Step 6 below.

*Step 2: To get  $u_i^{\text{Start}} > l_i^R$*

By assumption,  $SS_i > 0$ , and we have  $u_i$  from (4.29) and  $l_i^R$  from (4.30). Now define  $u_i^{\text{Start}}$  as

$$u_i^{\text{Start}} = \begin{cases} u_i & \text{if } u_i > l_i^R \\ l_i^R + SS_i & \text{if } u_i \leq l_i^R \end{cases} \quad (4.31)$$

Clearly  $u_i^{\text{Start}} > l_i^R$  by construction.

As clarified in subsequent steps below, there are two reasons for introducing the auxiliary variable  $u_i^{\text{Start}}$  in such a way that  $u_i^{\text{Start}} > l_i^R$ : (a) to ensure that the reported marginal cost function associated with  $s_i^R$  is upward sloping; and (b) to ensure that the reported marginal cost function associated with  $s_i^R$  never dips below Generator  $i$ 's true marginal cost curve over Generator  $i$ 's reported feasible production interval.

*Step 3: To get  $u_i^R > l_i^R$*

We know  $u_i^{\text{Start}} > l_i^R$  from Step 2 and we know  $\text{RI}_i^U \in [0, 1)$  from the admissibility of  $s_i^A$ . Thus, we can define  $u_i^R$  to be

$$u_i^R = \frac{u_i^{\text{Start}}}{1 - \text{RI}_i^U} > l_i^R \quad (4.32)$$

Given (4.29) and (4.32), note that  $\text{RI}_i^U$  reduces to a standard Lerner Index evaluation at the reported upper production limit  $\text{Cap}_i^{RU}$  whenever  $u_i^{\text{Start}}$  equals  $u_i$  in (4.31), assuming  $u_i^R = \text{MC}^R(\text{Cap}_i^{RU})$ . The latter equality follows from Steps 4 and 5 below.

*Step 4: To get  $b_i^R > 0$*

<sup>29</sup>Given any quantity-price production point  $(Q, Pr)$ , the *Lerner Index*  $LI$  evaluated at this point is defined as follows:  $LI(Q, Pr) = [Pr - \text{MC}(Q)]/Pr$ .

Recall that  $\text{Cap}_i^L$  is an exogenously given structural attribute of Generator  $i$ . Also,  $\text{Cap}_i^{RU} > \text{Cap}_i^{RL} = \text{Cap}_i^L$  by Step 0, and  $u_i^R > l_i^R$  by Step 3. Referring to Figure 4.16 for a schematic depiction, one can then define  $2b_i^R$  (the slope of the reported marginal cost function) to be

$$2b_i^R = \frac{u_i^R - l_i^R}{\text{Cap}_i^{RU} - \text{Cap}_i^L} > 0. \quad (4.33)$$

*Step 5: To get  $a_i^R$*

Since we know  $\text{Cap}_i^{RL}$  from step 0,  $l_i^R$  from Step 1, and  $b_i^R$  from Step 4, we can define  $a_i^R$  by

$$a_i^R = l_i^R - 2b_i^R \text{Cap}_i^L \quad (4.34)$$

*Step 6: To get  $MC_i^R(\text{Cap}_i^{RL}) = l_i^R \geq MC_i(\text{Cap}_i^L) > 0$*

By assumption (see Table 5.1),  $MC_i(\text{Cap}_i^L) > 0$ . It then follows from Step 0, Step 1, the definition of  $a_i^R$  in Step 5, and the general definition of  $MC_i^R(p)$  that  $MC_i^R(\text{Cap}_i^{RL}) = l_i^R \geq l_i = MC_i(\text{Cap}_i^L) > 0$ .

*Step 7: To get  $MC_i^R(p) \geq MC_i(p)$  for all  $p \in [\text{Cap}_i^{RL}, \text{Cap}_i^{RU}]$*

From Step 0 one has  $\text{Cap}_i^{RL} = \text{Cap}_i^L$ , and from Step 6 one has  $MC_i^R(\text{Cap}_i^{RL}) \geq MC_i(\text{Cap}_i^L)$ . On the other hand, Steps 2 and 3 imply that  $u_i^R \geq u_i^{\text{Start}} \geq u_i = MC_i(\text{Cap}_i^{RU})$ , and Steps 4 and 5 imply that  $MC_i^R(\text{Cap}_i^{RU}) = a_i^R + 2b_i^R \text{Cap}_i^{RU} = u_i^R$ . Consequently,  $MC^R(p)$  lies on or above  $MC(p)$  at the interval endpoints  $\text{Cap}_i^{RL}$  and  $\text{Cap}_i^{RU}$ . By linearity, it follows that  $MC^R(p)$  lies on or above  $MC(p)$  at all points  $p$  between these two points.

In summary, Steps 0-7 constructively determine a correspondence (conditional on  $SS_i$ ) that uniquely maps any admissible percentage supply offer  $s_i^A = (RI_i^L, RI_i^U, \text{RCap}_i^L, \text{RCap}_i^U)$  into a reported supply offer  $s_i^R = (a_i^R, b_i^R, \text{Cap}_i^{RL}, \text{Cap}_i^{RU})$ . Step 0 establishes that  $s_i^R$  satisfies simplifying assumptions 1, 4, and 5, and Steps 4 and 7 establish that  $s_i^R$  satisfies simplifying assumptions 2 and 3. Consequently,  $s_i^R$  is admissible. This completes the proof of the Claim.

QED.

### 4.8.3 A.3 Action Domain Construction

Under the five simplifying assumptions described in Section A.1, AMES Generator learning only occurs with respect to the reported cost coefficients  $\{a^R, b^R\}$  and the reported upper production limit  $\text{Cap}^{RU}$ . The reported lower production limit  $\text{Cap}^{RL}$  always equals the true lower production limit  $\text{Cap}^L$ , and the entry  $\text{RCap}_i^L$  in any admissible percentage supply offer  $s_i^A = (\text{RI}_i^L, \text{RI}_i^U, \text{RCap}_i^L, \text{RCap}_i^U)$  is always equal to

$$\text{RCap}_i^L = \frac{\text{Cap}_i^L}{\text{Cap}_i^U} \quad (4.35)$$

Consequently, to construct the action domain for any Generator  $i$ , it suffices to focus attention on reduced-form versions of the admissible percentage supply offers  $s_i^A$  given by

$$\alpha_i = (\text{RI}_i^L, \text{RI}_i^U, \text{RCap}_i^U) \quad (4.36)$$

We will now take up the construction of the action domains for the AMES Generators as implemented for the current study. Recall from Table 5.1 that the exogenously specified attributes for each AMES Generator  $i$  include five action-domain attributes, as follows: the cardinality  $M_i \geq 1$  of its action domain  $AD_i$ ; a slope-start parameter  $SS_i > 0$ ; two density-control parameters  $M1_i \geq 1$  and  $M2_i \geq 1$  satisfying  $M1_i \times M2_i = M_i$ ; and two range-index parameters  $\text{RIMax}_i^L$  and  $\text{RIMax}_i^U \in [0, 1)$ .

Given these action-domain attributes for Generator  $i$ , it will next be shown how we construct an  $M_i \times 3$  action-domain matrix  $\text{ADMAT}_i = AD(M1_i, M2_i, \text{RIMax}_i^L, \text{RIMax}_i^U)$  having the following form:

$$\text{ADMAT}_i = \begin{bmatrix} \alpha_{i1} \\ \alpha_{i2} \\ \vdots \\ \alpha_{iM_i} \end{bmatrix} = \begin{bmatrix} \text{RI}_{i1}^L & \text{RI}_{i1}^U & \text{RCap}_{i1}^U \\ \text{RI}_{i2}^L & \text{RI}_{i2}^U & \text{RCap}_{i2}^U \\ \vdots & \vdots & \vdots \\ \text{RI}_{iM_i}^L & \text{RI}_{iM_i}^U & \text{RCap}_{iM_i}^U \end{bmatrix}_{M_i \times 3} \quad (4.37)$$

where each of the  $M_i$  rows  $\alpha_{im}$  of this matrix represents a (reduced-form) admissible percentage supply offer for Generator  $i$ ; cf. (4.36). As established by the Claim in Section A.2, given Generator  $i$ 's slope-start parameter value  $SS_i$  together with relation (4.35), each row  $\alpha_{im}$  can thus be used to generate an admissible reported supply offer  $s_{im}^R = (a_{im}^R, b_{im}^R, \text{Cap}_{im}^{RL}, \text{Cap}_{im}^{RU})$  for Generator  $i$ . The collection of all  $M_i$  of these generated supply offers  $s_{im}^R$  then constitutes Generator  $i$ 's action domain  $AD_i$ .

By construction, the marginal cost curves associated with the supply offers  $s_{im}^R$  in  $AD_i$  all lie in the region on or above the true marginal cost curve of Generator  $i$ . As clarified below, the larger the specifications of  $M1_i$  and  $M2_i$  for any given  $\text{RIMax}_i^L$  and  $\text{RIMax}_i^U$ , the greater the number of supply offer choices in  $AD_i$ . Also, the smaller the specifications of  $\text{RIMax}_i^L$  and  $\text{RIMax}_i^U$  for any given  $M1_i$  and  $M2_i$ , the denser is the marginal cost curve coverage provided by  $AD_i$  in the immediate upper neighborhood of the true marginal cost curve.

A more concrete understanding of the supply offer construction process can be gleaned from Figure 4.16. The parameter  $M1_i$  controls the number of lower marginal cost curve start-points  $l_i^R$  lying on the vertical line at  $\text{Cap}_i^{RL} = \text{Cap}_i^L$ , i.e. at Generator  $i$ 's reported (equal true) lower production limit. These start-points must all lie on or above Generator  $i$ 's true marginal cost at this production point, given by  $l_i = \text{MC}_i(\text{Cap}_i^L)$ . The parameter  $\text{RIMax}_i^L$  controls how far up along this line these start-points extend. The parameter  $M2_i$  controls how many marginal cost curves “flare out” from each of the start-points  $l_i^R$ , and the parameter  $\text{RIMax}_i^U$  controls the range of these flares by controlling the range of their end-points  $u_i^R$ . The slope-start parameter  $SS_i$  is used to guarantee that each of these flared marginal cost curves is upward sloping with an end-point  $u_i^R$  that lies on or above Generator  $i$ 's true marginal cost curve.<sup>30</sup>

For the illustrative experiments reported in Section 4.5, two additional simplifying assumptions are maintained. First, we assume the AMES Generators heed the regulations of the

<sup>30</sup>This flare approach to the construction of supply-offer action domains, here applied to linear marginal cost functions, can readily be extended to handle various other types of parameterized functional forms for the marginal cost functions. An even denser coverage would be obtained by extending to a double-flare approach in which flared marginal cost curves branch down and back from each end-point  $u_i^R$  as well as up and forward from each start-point  $l_i^R$ .

AMES ISO and always report their true upper production limits as well as their true lower production limits.<sup>31</sup> This assumption implies that all of the elements  $\text{RCap}_{im}^U$  in the third column of  $\text{ADMat}_i$  are equal to 1.00. Second, we assume that the AMES Generators always have the option of reporting their true marginal cost functions, which corresponds to settings of 0.00 for the lower and upper range-index entries  $\text{RI}^L$  and  $\text{RI}^U$ . This assumption implies that at least one row  $m$  of  $\text{ADMat}_i$  takes the form (0.00, 0.00, 1.00), which we always choose to be row  $m = 1$ .

Our construction process for the  $M_i \times 3$  matrix  $\text{ADMat}_i$  then proceeds as follows:

*CASE 1:*

If  $M1_i = M2_i = 1$ , the  $1 \times 3$  matrix  $\text{ADMat}_i$  is constructed as (0.00, 0.00, 1.00).

*CASE 2:*

Suppose  $M1_i = 1$  and  $M2_i = 2$ . In this case the first row of the  $2 \times 3$  matrix  $\text{ADMat}_i$  is filled in as (0.00, 0.00, 1.00) and the second row is filled in as (0.00,  $\text{RIMax}_i^U$ , 1.00).

*CASE 3:*

Suppose  $M1_i = 2$  and  $M2_i = 1$ . In this case the first row of the  $2 \times 3$  matrix  $\text{ADMat}_i$  is filled in as (0.00, 0.00, 1.00) and the second row is filled in as ( $\text{RIMax}_i^L$ , 0.00, 1.00).

*CASE 4:*

Suppose  $M1_i \geq 2$  and  $M2_i \geq 2$ . In this case we define step increments as follows:

$$\text{Inc}_1 = \frac{\text{RIMax}_i^L}{M1_i - 1} ; \quad (4.38)$$

$$\text{Inc}_2 = \frac{\text{RIMax}_i^U}{M2_i - 1} \quad (4.39)$$

We then specify  $M1_i$  equally spaced lower range-index values  $\{v_1, \dots, v_{M1_i}\}$  starting at  $v_1 = 0.00$  and ending at  $v_{M1_i} = \text{RIMax}_i^L$  and spaced at distance  $\text{Inc}_1$  from each other. Similarly, we specify  $M2_i$  equally spaced upper range-index values  $\{w_1, \dots, w_{M2_i}\}$  starting at  $w_1 = 0.00$  and ending at  $w_{M2_i} = \text{RIMax}_i^U$  and spaced at distance  $\text{Inc}_2$  from each other.

<sup>31</sup>As previously noted in Section A.1, footnote 27, generators in the MISO and ISO-NE are required to report their true lower and upper production limits as part of their supply offers.

The first column of  $\text{ADMat}_i$  is then filled in as follows: the first  $M2_i$  places are filled in with  $M2_i$  copies of  $v_1$ ; the second  $M2_i$  places are then filled in with  $M2_i$  copies of  $v_2$ , and so on through  $v_{M1_i}$ . (Recall that  $M1_i \times M2_i = M_i$ .) The second column of  $\text{ADMat}_i$  is then filled in as follows: the first  $M2_i$  places are successively filled in with the successive elements of  $w = (w_1, \dots, w_{M2_i})$ ; the second batch of  $M2_i$  places is then also successively filled in with the successive elements of  $w$ ; and so on through  $M1_i$  iterations. This completes the construction of  $\text{ADMat}_i$ .

Finally, note that the matrix  $\text{ADMat}_i$  does not depend on any specific structural or technological aspects of Generator  $i$ ; all entries are in unit-free percentage form. Consequently, if desired, a single parameter specification  $(M1, M2, \text{RIMax}^L, \text{RIMax}^U, SS)$  can be used to derive a single action domain matrix  $\text{ADMat}$ , from which all of the the individual action domains  $AD_i$  for Generators  $i = 1, \dots, I$  are then derived. In this case the Generators' action domains will all have the same cardinality  $M = M1 \times M2$ , thus guaranteeing that no Generator is advantaged by having more supply offer choices. Moreover, the supply offers in the individual action domains  $AD_i$  will provide roughly similar densities of coverage of the regions on or above the Generators' true marginal cost curves.

All of the experimental findings presented in Section 4.5 for the 5-node test case were generated using a single parameter specification  $(M1, M2, \text{RIMax}^L, \text{RIMax}^U, SS)$  for the construction of the Generators' action domains. This parameter specification is given in Table 4.4.

#### 4.8.4 A.4 A Numerical Example

In this section a simple numerical example is given to illustrate the process outlined in Section A.3 for constructing an action domain matrix  $\text{ADMat}_i$  for an arbitrary Generator  $i$ . The example is also used to show concretely how each row  $m$  of  $\text{ADMat}_i$  effectively constitutes an admissible percentage supply offer  $s_{im}^A$  that can be mapped into an admissible reported supply offer  $s_{im}^R$  suitable for submission into the Day-Ahead Market.

Suppose  $M1_i = 5$  and  $M2_i = 3$ , implying that  $M_i = 15$ . Suppose  $\text{RIMax}_i^L = \text{RIMax}_i^U = 0.40$ . Define  $\text{Inc}_1 = \text{RIMax}_i^L / [M1_i - 1] = 0.40/4 = 0.10$  and  $\text{Inc}_2 = \text{RIMax}_i^U / [M2_i - 1] =$



$0.40/2 = 0.20$ . Specify a vector  $v$  consisting of  $M1_i = 5$  lower range-index values and a vector  $w$  consisting of  $M2_i = 3$  upper range-index values, as follows:

$$v = (0.00, 0.10, 0.20, 0.30, 0.40)$$

$$w = (0.00, 0.20, 0.40)$$

Next, use the elements of the vectors  $v$  and  $w$  to fill out the  $15 \times 3$  matrix  $ADMat_i$  in the manner described in Section A.3, as follows:

$$ADMat_i = \begin{bmatrix} 0.00 & 0.00 & 1.00 \\ 0.00 & 0.20 & 1.00 \\ 0.00 & 0.40 & 1.00 \\ 0.10 & 0.00 & 1.00 \\ 0.10 & 0.20 & 1.00 \\ 0.10 & 0.40 & 1.00 \\ 0.20 & 0.00 & 1.00 \\ 0.20 & 0.20 & 1.00 \\ 0.20 & 0.40 & 1.00 \\ 0.30 & 0.00 & 1.00 \\ 0.30 & 0.20 & 1.00 \\ 0.30 & 0.40 & 1.00 \\ 0.40 & 0.00 & 1.00 \\ 0.40 & 0.20 & 1.00 \\ 0.40 & 0.40 & 1.00 \end{bmatrix}_{15 \times 3}$$

The rows of  $ADMat_i$  represent, in percentage form, the 15 possible action (supply offer) choices for Generator  $i$  for the Day-Ahead-Market in each day  $D$ . Consequently, they represent Generator  $i$ 's action domain  $AD_i$ .

To see this more concretely, suppose Generator  $i$ 's true marginal cost coefficients are given by  $a_i = 10.00$  and  $b_i = 0.025$ , its true lower production limit is  $\text{Cap}_i^L = 0.00$ , and its true upper production limit is  $\text{Cap}_i^U = 100.00$ . Suppose it is the morning of day D, and Generator  $i$  must report a supply offer to the AMES ISO for the day D+1 Day-Ahead Market.

To accomplish this, Generator  $i$  queries JReLM, its learning module, regarding which supply offer to choose from among the supply offers  $m = 1, \dots, 15$  in its action domain  $AD_i$ . Suppose JReLM returns an action choice  $m = 5$ . What does this mean?<sup>32</sup>

The selection  $m = 5$  in fact corresponds to the fifth row vector in Generator  $i$ 's action domain matrix  $\text{ADMat}_i$ : namely,  $\alpha_{i5} = (\text{RI}_{i5}^L, \text{RI}_{i5}^U, \text{RCap}_{i5}^U) = (0.10, 0.20, 1.00)$ . Given the maintained assumption that  $\text{Cap}_{i5}^{RL} = \text{Cap}_i^L$ , this row vector determines an admissible percentage supply offer  $s_{i5}^A$  of form (4.27) with  $\text{RCap}_{i5}^L = \text{Cap}_i^L / \text{Cap}_i^U$ . As established by the Claim in Section A.2,  $s_{i5}^A$  in turn corresponds to an admissible reported supply offer  $s_{i5}^R = (a_{i5}^R, b_{i5}^R, \text{Cap}_{i5}^L, \text{Cap}_{i5}^{RU})$ , which is the supply offer form Generator  $i$  actually reports to the AMES ISO.

To see the precise form  $s_{i5}^R$  takes, we first need to compute the start-point  $l_i$  and end-point  $u_i$  for Generator  $i$ ' true marginal cost curve; cf. Figure 4.16. By (4.28) and (4.29),

$$l_i = a_i + 2b_i \text{Cap}_i^L = 10.00 + 2 \cdot 0.025 \cdot 0.00 = 10.00$$

$$u_i = a_i + 2b_i \text{Cap}_i^U = 10.00 + 2 \cdot 0.025 \cdot 100.00 = 15.00$$

Using (4.30), the start-point  $l_{i5}^R$  of Generator  $i$ 's reported marginal cost curve can then be recovered from  $\text{RI}_{i5}^L$  as follows:

$$l_{i5}^R = \frac{l_{i5}}{1 - \text{RI}_{i5}^L} = \frac{10.00}{1 - 0.10} = 11.11$$

<sup>32</sup>Recall from Section 4.4.6 that, for implementation of Roth-Erev reinforcement learning, JReLM has no need to know anything about the action domain  $AD_i$  other than its cardinality  $M_i$ . In effect, JReLM operates on the index set for  $AD_i$  rather than on the elements themselves.

The next step is to recover the end-point  $u_{i5}^R$  of Generator  $i$ 's reported marginal cost curve from  $RI_{i5}^U$ . Since  $l_{i5}^R = 11.11 < u_i = 15.00$ , relation (4.31) gives  $u_{i5}^{Start} = u_i = 15.00$ . It then follows from (4.32) that

$$u_{i5}^R = \frac{u_{i5}^{Start}}{1 - RI_{i5}^U} = \frac{15.00}{1 - 0.20} = 18.75$$

Using (4.33) and (4.34), Generator  $i$ 's reported cost coefficients thus take the form

$$b_{i5}^R = \frac{u_{i5}^R - l_{i5}^R}{Cap_i^U - Cap_i^L} = \frac{18.75 - 11.11}{100.00 - 0.00} = 0.08 > 0$$

$$a_{i5}^R = l_{i5}^R - 2b_{i5}^R Cap_i^L = 11.11 - 2 * 0.08 * 0.00 = 11.11$$

Finally, it follows from  $RCap_{i5}^U = 1.00$  that  $Cap_{i5}^{RU} = Cap_i^U = 100.00$ .

In summary, given the action choice  $m = 5$  received from JReLM, the above calculations establish that Generator  $i$ 's reported supply offer to the AMES ISO in the morning of day D takes the form

$$s_{i5}^R = (a_{i5}^R, b_{i5}^R, Cap_{i5}^{RL}, Cap_{i5}^{RU}) = (11.11, 0.08, 0.00, 100.00) \quad (4.40)$$

After collecting a reported supply offer from each Generator in the morning of day D, the AMES ISO submits these supply offers along with grid and load input data into its DCOPFJ module to solve for optimal power commitments and LMPs for the day D+1 Day-Ahead Market. The AMES ISO posts and settles these solution values by the end of day D. Generator  $i$  then reports its profit outcome from this settlement to its learning module, JReLM, which uses this profit outcome to update Generator  $i$ 's action choice probabilities, i.e. the probabilities attached to the indices  $m = 1, \dots, 15$  corresponding to the 15 rows of  $ADMat_i$ . When Generator  $i$  calls upon JReLM the next day for an action (supply offer) choice for the day D+2 Day-Ahead Market, JReLM chooses from among these indices in accordance with the updated action choice probabilities.

This daily process is schematically depicted in Figure 4.17 for an AMES wholesale power market consisting of just two generators.

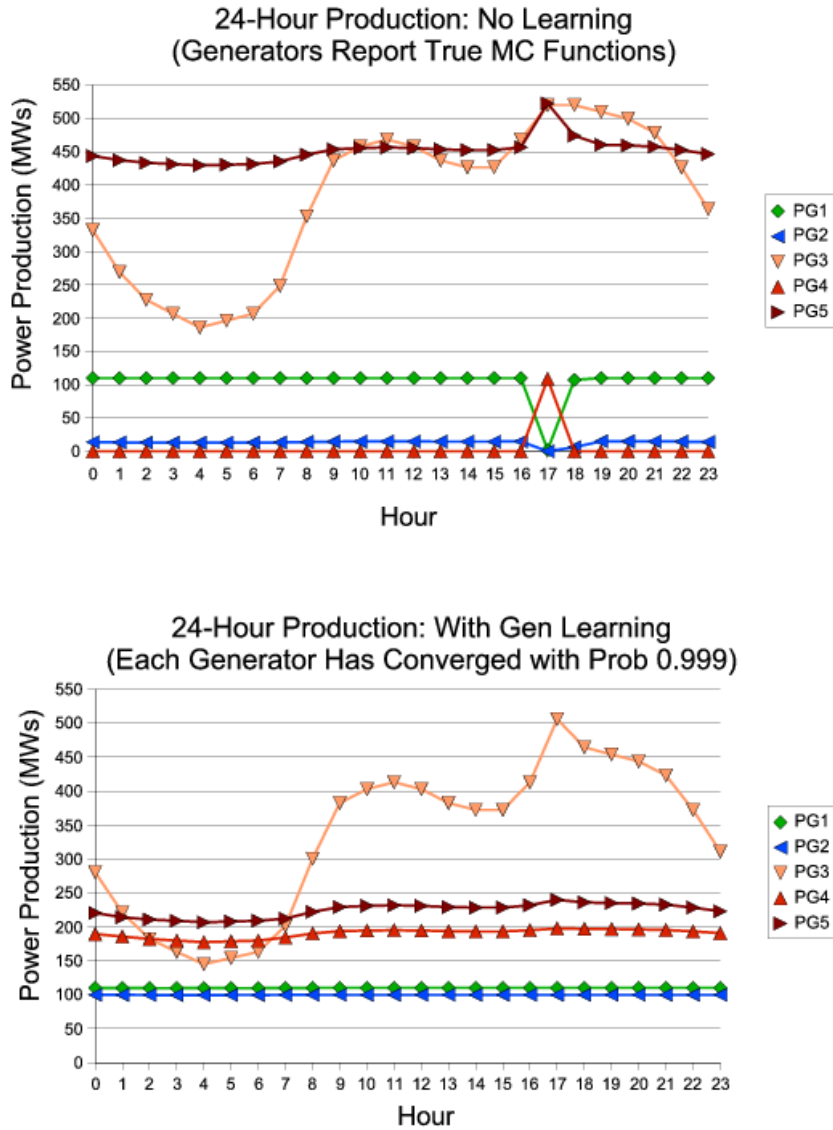


Figure 4.12 Dynamic 5-Node Test Case Solution Values for 24-Hour Real Power Production Levels (Day 422) – Generator Learning Compared with No Learning

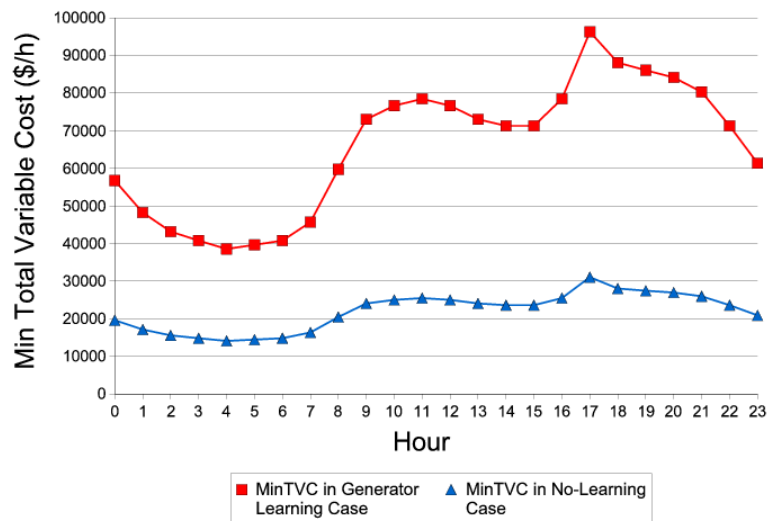


Figure 4.13 Dynamic 5-Node Test Case Solution Values for 24-Hour Minimum Total Variable Cost (Day 422) – Generator Learning Compared with No Learning

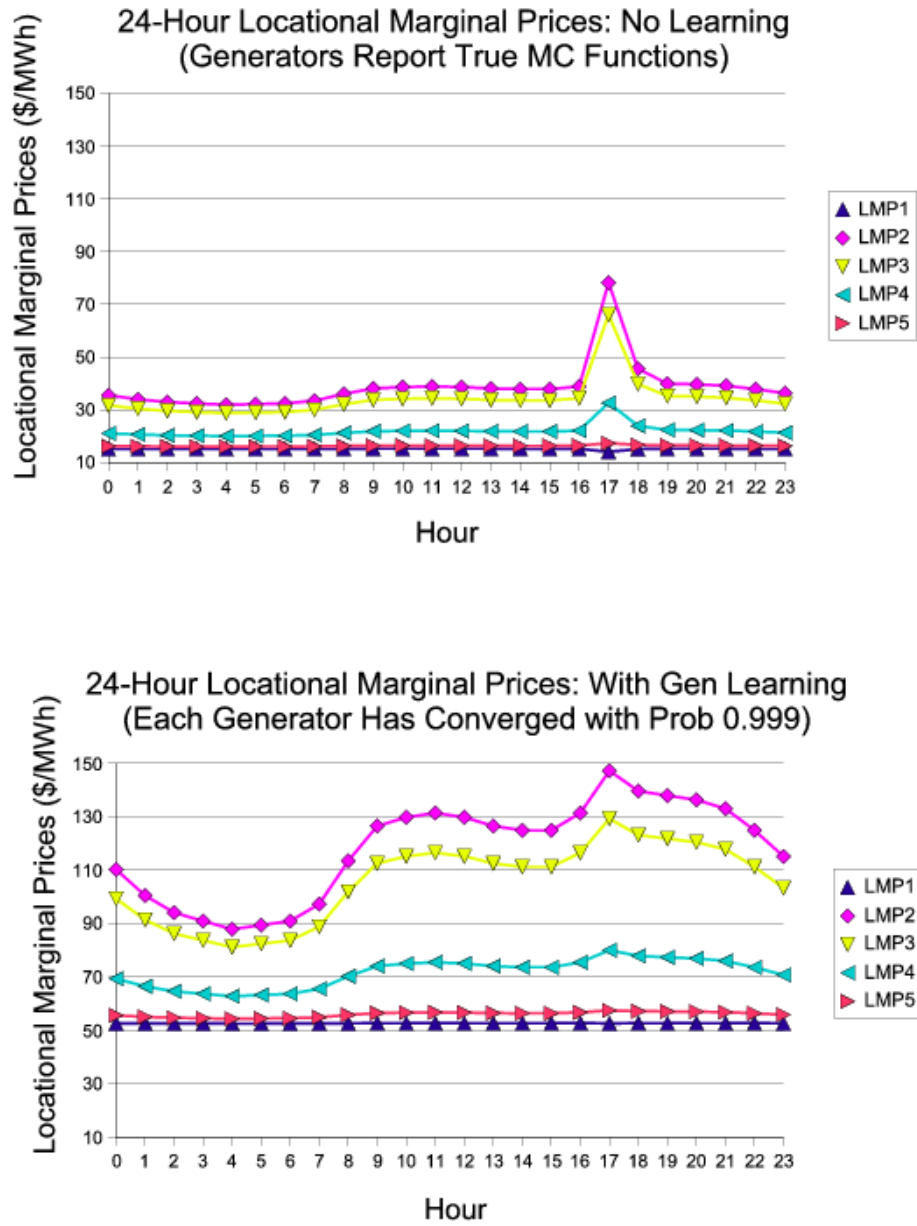


Figure 4.14 Dynamic 5-Node Test Case Solution Values for 24-Hour LMPs (Day 422) – Generator Learning Compared with No Learning

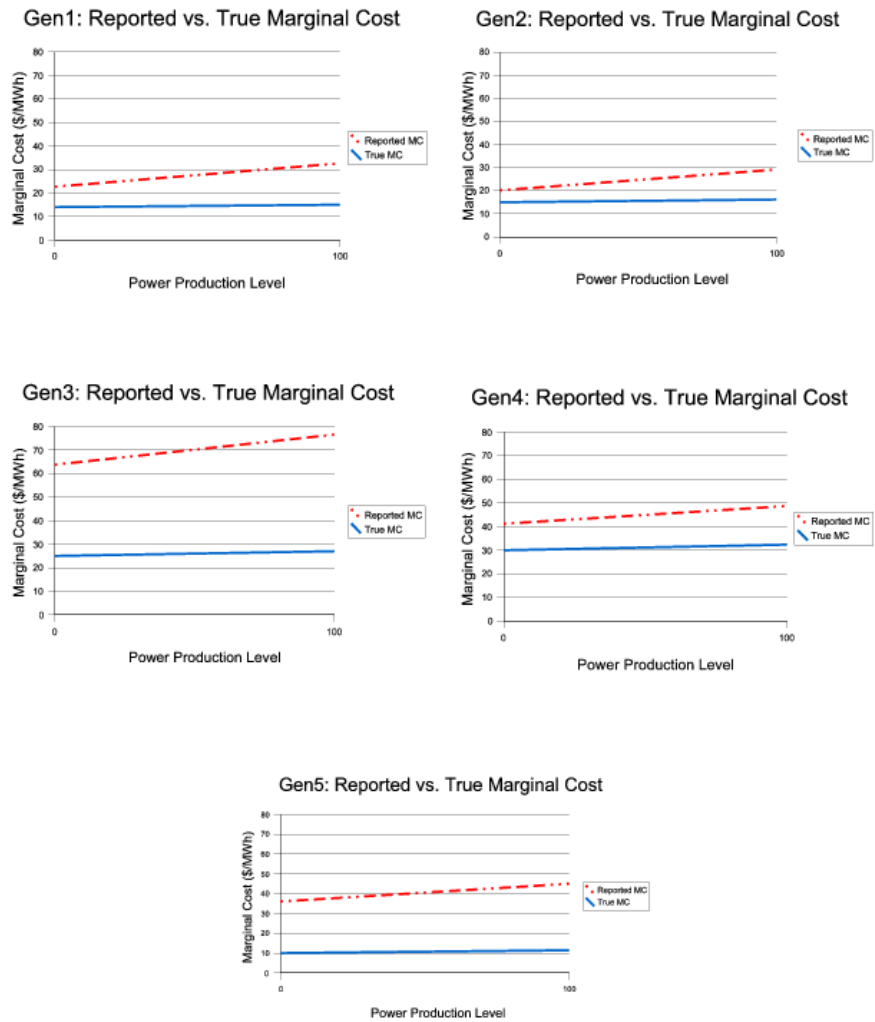


Figure 4.15 Dynamic 5-Node Test Case – Mean Reported Marginal Cost Function Versus True Marginal Cost Function for Each Generator (Day 422)

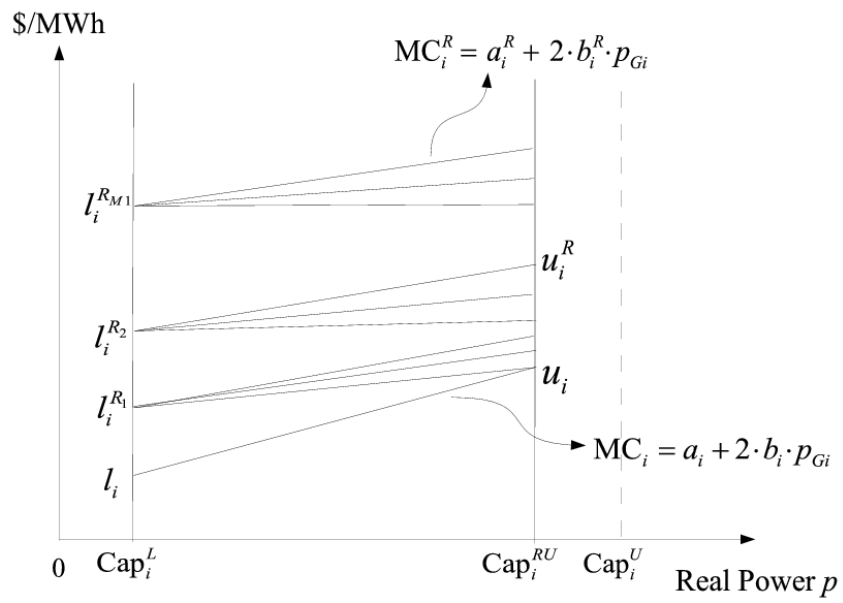


Figure 4.16 Generator  $i$ 's Feasible Supply Offers and True Marginal Cost Function



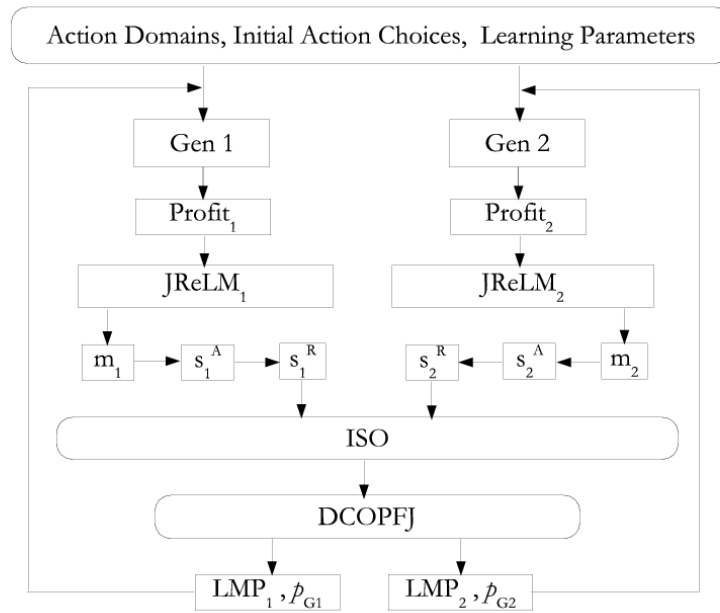


Figure 4.17 AMES Dynamic Flow with Learning Implementations for Generators 1 and 2

Table 4.1 Admissible Exogenous Variables for the AMES Framework

Variable	Description	Admissibility Restrictions
$K$	Total number of transmission grid nodes	$K > 0$
$N$	Total number of distinct network branches	$N > 0$
$I$	Total number of Generators	$I > 0$
$J$	Total number of LSEs	$J > 0$
$I_k$	Set of Generators located at node $k$	$\text{Card}(\cup_{k=1}^K I_k) = I$
$J_k$	Set of LSEs located at node $k$	$\text{Card}(\cup_{k=1}^K J_k) = J$
$S_o$	Base apparent power (three-phase MVAs)	$S_o \geq 1$
$V_o$	Base voltage (line-to-line kVs)	$V_o > 0$
$V_k$	Voltage magnitude (kVs) at node $k$	$V_k = V_o, k = 1, \dots, K$
$p_{Lj}$	Real power load (MWs) withdrawn by LSE $j$	$p_{Lj} \geq 0, j = 1, \dots, J$
$km$	Branch connecting nodes $k$ and $m$ (if one exists)	$k \neq m$
$BR$	Set of all distinct branches $km, k < m$	$BR \neq \emptyset$
$X_{km}$	Reactance (ohms) for branch $km$	$X_{km} = X_{mk} > 0, km \in BR$
$B_{km}$	$[1/X_{km}]$ for branch $km$	$B_{km} = B_{mk} > 0, km \in BR$
$P_{km}^U$	Thermal limit (MWs) for real power flow on $km$	$P_{km}^U > 0, km \in BR$
$\delta_1$	Reference node 1 voltage angle (radians)	$\delta_1 = 0$
$\pi$	Soft penalty weight for voltage angle differences	$\pi > 0$
$\text{Money}_i^o$	Initial money holdings (\$) for Gen $i$	$\text{Money}_i^o > 0, i = 1, \dots, I$
$\text{Cap}_i^L$	True lower production limit (MWs) for Gen $i$	$\text{Cap}_i^L \geq 0, i = 1, \dots, I$
$\text{Cap}_i^U$	True upper production limit (MWs) for Gen $i$	$\text{Cap}_i^U > \text{Cap}_i^L, i = 1, \dots, I$
$a_i, b_i$	True cost coefficients for Gen $i$	$b_i > 0, i = 1, \dots, I$
$\text{MC}_i(p)$	$\text{MC}_i(p) = a_i + 2b_i p =$ Gen $i$ 's true MC function	$\text{MC}_i(\text{Cap}_i^L) > 0, i = 1, \dots, I$
$\text{FCost}_i$	Fixed costs (hourly prorated) for Gen $i$	$\text{FCost}_i \geq 0, i = 1, \dots, I$
$M_i$	Cardinality of the action domain $AD_i$ for Gen $i$	$M_i \geq 1, i = 1, \dots, I$
$M1_i, M2_i$	Density-control parameters for $AD_i$ construction	$M1_i \times M2_i = M_i, i = 1, \dots, I$
$\text{RIMax}_i^L$	Range-index parameter for $AD_i$ construction	$\text{RIMax}_i^L \in [0, 1), i = 1, \dots, I$
$\text{RIMax}_i^U$	Range-index parameter for $AD_i$ construction	$\text{RIMax}_i^U \in [0, 1), i = 1, \dots, I$
$SS_i$	Slope-start parameter for $AD_i$ construction	$SS_i > 0, i = 1, \dots, I$
$q_i(0)$	Initial propensity (learning)	any real value, $i = 1, \dots, I$
$C_i$	Cooling parameter (learning)	$C_i > 0, i = 1, \dots, I$
$r_i$	Recency parameter (learning)	$0 \leq r_i \leq 1, i = 1, \dots, I$
$e_i$	Experimentation parameter (learning)	$0 \leq e_i < 1, i = 1, \dots, I$

Table 4.2 Endogenous Variables for the AMES Framework

Variable	Description
$p_{Gi}$	Real power injection (MWs) by Gen $i = 1, \dots, I$
$\delta_k$	Voltage angle (radians) at node $k = 2, \dots, K$
$LMP_k$	Locational marginal price (\$/MWh) at node $k = 1, \dots, K$
$P_{km}$	Real power (MWs) flowing in branch $km \in BR$
$P_{Gen_k}$	Total real power injection (MWs) at node $k = 1, \dots, K$
$P_{Load_k}$	Total real power withdrawal (MWs) at node $k = 1, \dots, K$
$P_{NetInject_k}$	Total net real power injection (MWs) at node $k = 1, \dots, K$
$Profit_i$	Realized profit (\$/h) for Gen $i = 1, \dots, I$
$Money_i$	Cumulative money holdings (\$) for Gen $i = 1, \dots, I$
$Cap_i^{RL}$	Reported lower production limit (MWs) for Gen $i = 1, \dots, I$
$Cap_i^{RU}$	Reported upper production limit (MWs) for Gen $i = 1, \dots, I$
$a_i^R, b_i^R$	Reported cost coefficients for Gen $i = 1, \dots, I$

Table 4.3 Dynamic 5-Node Test Case – DC OPF Structural Input Data (SI)

$S_o$	$V_o$								
100	10								
$K^a$	$\pi^b$								
5	0.05								
Branch									
From	To	lineCap <sup>c</sup>	$X^d$						
1	2	250.0	0.0281						
1	4	150.0	0.0304						
1	5	400.0	0.0064						
2	3	350.0	0.0108						
3	4	240.0	0.0297						
4	5	240.0	0.0297						
Gen ID	atNode	FCost	$a$	$b$	Cap <sup>L</sup>	Cap <sup>U</sup>	Init\$		
1	1	1600.0	14.0	0.005	0.0	110.0	\$1M		
2	1	1200.0	15.0	0.006	0.0	100.0	\$1M		
3	3	8500.0	25.0	0.010	0.0	520.0	\$1M		
4	4	1000.0	30.0	0.012	0.0	200.0	\$1M		
5	5	5400.0	10.0	0.007	0.0	600.0	\$1M		
LSE									
ID	atNode	L-00 <sup>e</sup>	L-01	L-02	L-03	L-04	L-05	L-06	L-07
1	2	350.00	322.93	305.04	296.02	287.16	291.59	296.02	314.07
2	3	300.00	276.80	261.47	253.73	246.13	249.93	253.73	269.20
3	4	250.00	230.66	217.89	211.44	205.11	208.28	211.44	224.33
ID	atNode	L-08	L-09	L-10	L-11	L-12	L-13	L-14	L-15
1	2	358.86	394.80	403.82	408.25	403.82	394.80	390.37	390.37
2	3	307.60	338.40	346.13	349.93	346.13	338.40	334.60	334.60
3	4	256.33	282.00	288.44	291.61	288.44	282.00	278.83	278.83
ID	atNode	L-16	L-17	L-18	L-19	L-20	L-21	L-22	L-23
1	2	408.25	448.62	430.73	426.14	421.71	412.69	390.37	363.46
2	3	349.93	384.53	369.20	365.26	361.47	353.73	334.60	311.53
3	4	291.61	320.44	307.67	304.39	301.22	294.78	278.83	259.61

<sup>a</sup>Total number of nodes

<sup>b</sup>Soft penalty weight  $\pi$  for voltage angle differences

<sup>c</sup>Upper limit  $P_{km}^U$  (in MWs) on the magnitude of real power flow in branch  $km$

<sup>d</sup>Reactance  $X_{km}$  (in ohms) for branch  $km$

<sup>e</sup>L-H: Load (in MWs) for hour H, where H=00,01,...,23

Table 4.4 Dynamic 5-Node Test Case – Action Domain and Learning Input Data

Action Domain and Learning Parameters										
Gen ID	$M$	$M1$	$M2$	$RIMax^L$	$RIMax^U$	$SS$	$q(0)$	$C$	$r$	$e$
1	100	10	10	0.75	0.75	0.001	6000	1000	0.04	0.97
2	100	10	10	0.75	0.75	0.001	6000	1000	0.04	0.97
3	100	10	10	0.75	0.75	0.001	6000	1000	0.04	0.97
4	100	10	10	0.75	0.75	0.001	6000	1000	0.04	0.97
5	100	10	10	0.75	0.75	0.001	6000	1000	0.04	0.97

Initial Seed Values for All 20 Runs					
RunID	InitialSeed	RunID	InitialSeed	RunID	InitialSeed
01	695672061	08	324702357	15	-734837588
02	857398845	09	903534301	16	-219860821
03	507304343	10	205753353	17	-845925752
04	748974391	11	-597305450	18	-367413463
05	494375928	12	-494232424	19	-629523701
06	289658396	13	-158932839	20	-257802760
07	158324732	14	-934341230		

Table 4.5 No-Learning Dynamic 5-Node Test Case – Solution Values (SI) for Real Power Branch Flow  $P_{km}$ , with Associated Thermal Limit  $P_{km}^U$ , for Each Distinct Branch  $km$

Hour	$P_{12}^a$	$P_{14}$	$P_{15}$	$P_{23}$	$P_{34}$	$P_{45}$
00	250.00	129.65	-255.77	-100.00	-67.47	-187.82
01	250.00	126.71	-253.27	-72.93	-80.32	-184.27
02	250.00	124.77	-251.61	-55.04	-88.81	-181.93
03	250.00	123.79	-250.77	-46.02	-93.09	-180.74
04	250.00	122.83	-249.95	-37.16	-97.30	-179.58
05	250.00	123.31	-250.36	-41.59	-95.19	-180.16
06	250.00	123.79	-250.77	-46.02	-93.09	-180.74
07	250.00	125.75	-252.45	-64.07	-84.52	-183.11
08	250.00	130.61	-256.60	-108.86	-63.26	-188.98
09	250.00	134.51	-259.92	-144.80	-46.20	-193.69
10	250.00	135.49	-260.76	-153.82	-41.92	-194.87
11	250.00	135.97	-261.17	-158.25	-39.81	-195.45
12	250.00	135.49	-260.76	-153.82	-41.92	-194.87
13	250.00	134.51	-259.92	-144.80	-46.20	-193.69
14	250.00	134.03	-259.51	-140.37	-48.30	-193.11
15	250.00	134.03	-259.51	-140.37	-48.30	-193.11
16	250.00	135.97	-261.17	-158.25	-39.81	-195.45
17	250.00	98.83	-346.76	-198.62	-63.15	-175.88
18	250.00	137.64	-274.17	-180.73	-29.93	-199.96
19	250.00	137.91	-262.83	-176.14	-31.32	-197.80
20	250.00	137.43	-262.42	-171.71	-33.42	-197.22
21	250.00	136.45	-261.58	-162.69	-37.71	-196.03
22	250.00	134.03	-259.51	-140.37	-48.30	-193.11
23	250.00	131.11	-257.02	-113.46	-61.08	-189.58
	$P_{12}^U$	$P_{14}^U$	$P_{15}^U$	$P_{23}^U$	$P_{34}^U$	$P_{45}^U$
	250.00	150.00	400.00	350.00	240.00	240.00

<sup>a</sup>In accordance with the usual convention, the real power  $P_{km}$  flowing along a branch  $km$  is positively valued if and only if real power is flowing from node  $k$  to node  $m$ .

Table 4.6 No-Learning Dynamic 5-Node Test Case – Solution Values (SI) for Real Power Production Levels (in MWs) and Associated Upper Production Limits, together with LMPs (Nodal Balance Constraint Multipliers, \$/MWh) and Minimum Total Variable Cost (\$/h)

Hour	$p_{G1}^*$	$p_{G2}^*$	$p_{G3}^*$	$p_{G4}^*$	$p_{G5}^*$	LMP <sub>1</sub>	LMP <sub>2</sub>	LMP <sub>3</sub>	LMP <sub>4</sub>	LMP <sub>5</sub>	minTVC
0	110.0	13.9	332.5	0.0	443.6	15.17	35.50	31.65	21.05	16.21	19587.1
1	110.0	13.4	269.4	0.0	437.5	15.16	33.95	30.39	20.60	16.13	17107.3
2	110.0	13.2	227.7	0.0	433.5	15.16	32.92	29.55	20.30	16.07	15556.8
3	110.0	13.0	206.7	0.0	431.5	15.16	32.40	29.13	20.15	16.04	14800.9
4	110.0	12.9	186.0	0.0	429.5	15.15	31.89	28.72	20.00	16.01	14076.1
5	110.0	13.0	196.3	0.0	430.5	15.16	32.15	28.93	20.07	16.03	14436.5
6	110.0	13.0	206.7	0.0	431.5	15.16	32.40	29.13	20.15	16.04	14800.9
7	110.0	13.3	248.8	0.0	435.6	15.16	33.44	29.97	20.45	16.10	16330.2
8	110.0	14.0	353.2	0.0	445.6	15.17	36.01	32.06	21.20	16.24	20433.9
9	110.0	14.6	437.0	0.0	453.6	15.18	38.08	33.74	21.81	16.35	24043.6
10	110.0	14.7	458.0	0.0	455.6	15.18	38.60	34.16	21.96	16.38	24993.9
11	110.0	14.8	468.4	0.0	456.6	15.18	38.85	34.37	22.03	16.39	25467.5
12	110.0	14.7	458.0	0.0	455.6	15.18	38.60	34.16	21.96	16.38	24993.9
13	110.0	14.6	437.0	0.0	453.6	15.18	38.08	33.74	21.81	16.35	24043.6
14	110.0	14.5	426.7	0.0	452.6	15.17	37.82	33.53	21.73	16.34	23583.1
15	110.0	14.5	426.7	0.0	452.6	15.17	37.82	33.53	21.73	16.34	23583.1
16	110.0	14.8	468.4	0.0	456.6	15.18	38.85	34.37	22.03	16.39	25467.5
17	2.1	0.0	520.0	108.9	522.6	14.02	78.24	66.07	32.61	17.32	31038.5
18	107.4	6.1	520.0	0.0	474.1	15.07	45.55	39.78	23.90	16.64	28006.9
19	110.0	15.1	510.1	0.0	460.6	15.18	39.88	35.20	22.33	16.45	27422.4
20	110.0	15.0	499.8	0.0	459.6	15.18	39.63	35.00	22.26	16.43	26931.9
21	110.0	14.9	478.7	0.0	457.6	15.18	39.11	34.57	22.11	16.41	25945.9
22	110.0	14.5	426.7	0.0	452.6	15.17	37.82	33.53	21.73	16.34	23583.1
23	110.0	14.1	363.9	0.0	446.6	15.17	36.28	32.28	21.28	16.25	20879.5

Table 4.7 Learning Dynamic 5-Node Test Case – Means and Standard Deviations for Solution Values (SI) on Day 422 for Real Power Branch Flow  $P_{km}$ , with Associated Thermal Limit  $P_{km}^U$ , for Each Distinct Branch  $km$

Hour	$\overline{P}_{12}$	$P_{12}^{SD}$	$\overline{P}_{14}$	$P_{14}^{SD}$	$\overline{P}_{15}$	$P_{15}^{SD}$	$\overline{P}_{23}$	$P_{23}^{SD}$	$\overline{P}_{34}$	$P_{34}^{SD}$	$\overline{P}_{45}$	$P_{45}^{SD}$
00	249.3	3.3	77.0	9.2	-116.5	10.4	-100.7	3.3	-120.3	9.6	-103.9	11.6
01	248.0	6.4	74.8	11.7	-113.2	13.9	-74.9	6.4	-130.8	13.1	-100.9	14.7
02	247.1	9.1	73.7	13.3	-111.3	16.7	-58.0	9.1	-137.3	16.2	-99.4	16.9
03	246.4	10.5	73.2	14.2	-110.3	18.3	-49.6	10.5	-140.1	17.8	-98.7	18.1
04	245.5	12.0	72.6	15.2	-108.9	20.1	-41.6	12.0	-142.8	19.5	-97.8	19.4
05	246.0	11.2	72.9	14.7	-109.6	19.2	-45.6	11.2	-141.5	18.6	-98.2	18.7
06	246.4	10.5	73.2	14.2	-110.3	18.3	-49.6	10.5	-140.1	17.8	-98.7	18.1
07	247.5	7.8	74.1	12.5	-112.1	15.3	-66.5	7.8	-134.1	14.7	-100.0	15.8
08	249.4	2.9	77.8	8.5	-117.3	9.5	-109.5	2.9	-116.5	8.7	-104.8	10.6
09	249.8	1.1	80.7	5.6	-120.6	5.9	-145.0	1.1	-101.0	5.7	-108.6	7.0
10	249.9	0.6	81.4	5.1	-121.4	5.2	-154.0	0.6	-97.1	5.1	-109.5	6.3
11	249.9	0.4	81.8	4.8	-121.9	4.9	-158.3	0.4	-95.1	4.9	-110.0	6.0
12	249.9	0.6	81.4	5.1	-121.4	5.2	-154.0	0.6	-97.1	5.1	-109.5	6.3
13	249.8	1.1	80.7	5.6	-120.6	5.9	-145.0	1.1	-101.0	5.7	-108.6	7.0
14	249.7	1.3	80.3	5.9	-120.2	6.3	-140.7	1.3	-102.9	6.1	-108.1	7.4
15	249.7	1.3	80.3	5.9	-120.2	6.3	-140.7	1.3	-102.9	6.1	-108.1	7.4
16	249.9	0.4	81.8	4.8	-121.9	4.9	-158.3	0.4	-95.1	4.9	-110.0	6.0
17	250.0	0.0	85.3	3.2	-125.5	3.2	-198.6	0.0	-77.0	3.3	-114.4	3.9
18	250.0	0.0	83.6	4.1	-123.8	4.1	-180.7	0.0	-85.2	4.2	-112.3	5.1
19	250.0	0.0	83.2	4.2	-123.4	4.2	-176.1	0.0	-87.3	4.3	-111.7	5.1
20	250.0	0.0	82.9	4.3	-123.0	4.3	-171.7	0.0	-89.3	4.4	-111.3	5.3
21	250.0	0.2	82.1	4.6	-122.3	4.6	-162.7	0.2	-93.2	4.7	-110.4	5.7
22	249.7	1.3	80.3	5.9	-120.2	6.3	-140.7	1.3	-102.9	6.1	-108.1	7.4
23	249.4	2.7	78.1	8.1	-117.7	9.0	-114.0	2.7	-114.5	8.3	-105.3	10.1



Table 4.8 Learning Dynamic 5-Node Test Case – Means and Standard Deviations for Solution Values (SI) on Day 422 for Real Power Production Levels (in MWs)

Hour	$\overline{p_{G1}^{*SD}}$	$\overline{p_{G2}^{*SD}}$	$\overline{p_{G3}^{*SD}}$	$\overline{p_{G4}^{*SD}}$	$\overline{p_{G5}^{*SD}}$				
00	110.00	99.80	0.88	280.40	10.92	189.37	29.60	220.42	21.84
01	109.92	99.64	1.59	220.92	17.07	185.74	37.25	214.17	28.21
02	109.85	99.53	2.10	182.18	22.66	182.11	42.50	210.73	32.93
03	109.81	99.47	2.35	163.20	25.51	179.72	45.31	208.98	35.57
04	109.78	99.42	2.60	144.96	28.69	177.50	48.31	206.74	38.51
05	109.80	99.45	2.48	154.08	27.03	178.61	46.79	207.86	37.00
06	109.81	99.47	2.35	163.20	25.51	179.72	45.31	208.98	35.57
07	109.88	99.59	1.84	201.60	19.83	184.36	39.92	212.17	30.52
08	110.00	99.81	0.86	300.60	9.85	190.23	27.16	222.16	19.91
09	110.00	99.82	0.80	382.48	5.95	193.70	18.22	229.20	12.83
10	110.00	99.82	0.79	403.03	5.22	194.57	16.43	230.97	11.41
11	110.00	99.83	0.78	413.12	4.92	195.00	15.65	231.84	10.81
12	110.00	99.82	0.79	403.03	5.22	194.57	16.43	230.97	11.41
13	110.00	99.82	0.80	382.48	5.95	193.70	18.22	229.20	12.83
14	110.00	99.82	0.81	372.38	6.36	193.27	19.19	228.33	13.60
15	110.00	99.82	0.81	372.38	6.36	193.27	19.19	228.33	13.60
16	110.00	99.83	0.78	413.12	4.92	195.00	15.65	231.84	10.81
17	110.00	99.84	0.71	506.19	3.25	197.68	10.36	239.88	7.11
18	110.00	99.83	0.74	464.70	4.18	197.02	13.32	236.04	9.13
19	110.00	99.83	0.75	454.09	4.26	196.73	13.57	235.14	9.30
20	110.00	99.83	0.76	443.90	4.37	196.30	13.91	234.36	9.53
21	110.00	99.83	0.77	423.24	4.69	195.43	14.97	232.71	10.29
22	110.00	99.82	0.81	372.38	6.36	193.27	19.19	228.33	13.60
23	110.00	99.81	0.86	311.06	9.30	190.67	25.92	223.06	18.93

Table 4.9 Learning Dynamic 5-Node Test Case – Means and Standard Deviations for Solution Values (SI) on Day 422 for LMPs (Nodal Balance Constraint Multipliers, in \$/MWh)

Hour	$\overline{\text{LMP}}_1$	$\text{LMP}_1^{SD}$	$\overline{\text{LMP}}_2$	$\text{LMP}_2^{SD}$	$\overline{\text{LMP}}_3$	$\text{LMP}_3^{SD}$	$\overline{\text{LMP}}_4$	$\text{LMP}_4^{SD}$	$\overline{\text{LMP}}_5$	$\text{LMP}_5^{SD}$
00	52.74	12.33	110.30	58.16	99.39	48.02	69.40	21.56	55.70	13.06
01	52.70	12.26	100.56	49.61	91.49	41.16	66.56	19.44	55.16	12.82
02	52.68	12.23	94.18	44.34	86.32	36.92	64.69	18.12	54.81	12.67
03	52.66	12.22	91.02	41.79	83.75	34.86	63.77	17.46	54.63	12.60
04	52.63	12.23	87.96	39.38	81.27	32.90	62.86	16.84	54.45	12.54
05	52.65	12.23	89.49	40.57	82.51	33.86	63.32	17.15	54.54	12.57
06	52.66	12.22	91.02	41.79	83.75	34.86	63.77	17.46	54.63	12.60
07	52.69	12.24	97.38	46.96	88.91	39.03	65.63	18.78	54.98	12.75
08	52.75	12.37	113.52	61.04	102.01	50.33	70.35	22.28	55.87	13.15
09	52.79	12.56	126.59	73.16	112.61	60.05	74.15	25.31	56.58	13.52
10	52.80	12.62	129.87	76.28	115.27	62.55	75.11	26.09	56.75	13.61
11	52.80	12.65	131.48	77.83	116.57	63.79	75.58	26.48	56.84	13.66
12	52.80	12.62	129.87	76.28	115.27	62.55	75.11	26.09	56.75	13.61
13	52.79	12.56	126.59	73.16	112.61	60.05	74.15	25.31	56.58	13.52
14	52.78	12.53	124.98	71.64	111.30	58.83	73.68	24.93	56.49	13.47
15	52.78	12.53	124.98	71.64	111.30	58.83	73.68	24.93	56.49	13.47
16	52.80	12.65	131.48	77.83	116.57	63.79	75.58	26.48	56.84	13.66
17	52.73	12.81	147.26	92.89	129.34	75.90	80.10	30.38	57.58	14.07
18	52.80	12.81	139.68	85.72	123.22	70.13	77.95	28.50	57.26	13.93
19	52.80	12.78	138.00	84.10	121.86	68.83	77.46	28.08	57.17	13.87
20	52.80	12.75	136.38	82.54	120.55	67.58	77.00	27.68	57.09	13.82
21	52.81	12.68	133.09	79.38	117.88	65.04	76.05	26.87	56.93	13.71
22	52.78	12.53	124.98	71.64	111.30	58.83	73.68	24.93	56.49	13.47
23	52.76	12.39	115.19	62.56	103.36	51.54	70.83	22.66	55.96	13.19

Table 4.10 Learning Dynamic 5-Node Test Case – Ordinate Values ( $a^R$ ) and Slope Values ( $b^R$ ) for the Linear Marginal Cost Functions Reported to the ISO by the Five Generators on Day 422 in Each of the Twenty Runs, with Summary Statistics

Run	$a_1^R$	$b_1^R$	$a_2^R$	$b_2^R$	$a_3^R$	$b_3^R$	$a_4^R$	$b_4^R$	$a_5^R$	$b_5^R$
1	21.0	0.031824	18.0	0.000005	75.0	0.036059	36.0	0.090005	40.0	0.033335
2	24.0	0.036370	25.7	0.011694	100.0	0.288465	32.7	0.067325	40.0	0.100003
3	24.0	0.036370	18.0	0.126012	75.0	0.100964	30.0	0.273000	40.0	0.066669
4	42.0	0.017360	15.0	0.063857	100.0	0.019232	72.0	0.000003	40.0	0.023811
5	18.7	0.060614	16.4	0.027279	37.5	0.072118	45.0	0.000002	30.0	0.025002
6	33.6	0.013889	25.7	0.011694	75.0	0.036059	32.7	0.048682	40.0	0.006668
7	15.3	0.013890	45.0	0.020460	25.0	0.112115	36.0	0.030003	40.0	0.033335
8	24.0	0.054552	16.4	0.027279	42.9	0.082420	60.0	0.000002	30.0	0.075003
9	14.0	0.054026	22.5	0.010233	100.0	0.096156	32.7	0.048682	30.0	0.050002
10	15.3	0.069431	16.4	0.081828	75.0	0.024040	40.0	0.020003	40.0	0.100003
11	16.8	0.054553	22.5	0.056257	37.5	0.072118	36.0	0.030003	40.0	0.000001
12	42.0	0.095461	30.0	0.000005	60.0	0.028848	51.4	0.025717	40.0	0.066669
13	16.8	0.038189	16.4	0.114557	75.0	0.024040	32.7	0.005182	30.0	0.035002
14	14.0	0.054026	20.0	0.000005	75.0	0.144234	60.0	0.000002	30.0	0.075003
15	24.0	0.009922	16.4	0.016370	30.0	0.039231	36.0	0.018003	40.0	0.006668
16	28.0	0.090917	16.4	0.114557	42.9	0.041211	36.0	0.000002	30.0	0.050002
17	21.0	0.095464	15.0	0.168000	37.5	0.018030	40.0	0.009094	40.0	0.016668
18	21.0	0.047734	16.4	0.016370	37.5	0.018030	40.0	0.020003	30.0	0.050002
19	14.0	0.011240	16.4	0.027279	75.0	0.024040	30.0	0.029400	40.0	0.033335
20	24.0	0.109100	15.0	0.006000	100.0	0.000001	45.0	0.037503	30.0	0.050002
Mean	22.7	0.049747	20.2	0.044987	63.8	0.063871	41.2	0.037631	36.0	0.044859
SD	8.4	0.030342	7.2	0.049954	25.6	0.065315	11.4	0.060501	5.0	0.029031
Min	14.0	0.009922	15.0	0.000005	25.0	0.000001	30.0	0.000002	30.0	0.000001
Max	42.0	0.109100	45.0	0.168000	100.0	0.288465	72.0	0.273000	40.0	0.100003

## CHAPTER 5. DC OPTIMAL POWER FLOW FORMULATION AND SOLUTION USING QUADPROGJ

### 5.1 Abstract

Nonlinear AC Optimal Power Flow (OPF) problems are commonly approximated by linearized DC OPF problems to obtain real power solutions for restructured wholesale power markets. We first present a standard DC OPF problem, which has the numerically desirable form of a strictly convex quadratic programming (SCQP) problem when voltage angles are eliminated by substitution. We next augment this standard DC OPF problem in a physically meaningful way, still retaining an SCQP form, so that solution values for voltage angles and locational marginal prices are directly obtained along with real power injections and branch flows. We then show how this augmented DC OPF problem can be solved using *QuadProgJ*, an open-source Java SCQP solver newly developed by the authors that implements the well-known dual active-set SCQP algorithm by Goldfarb and Idnani (1983). To demonstrate the accuracy of QuadProgJ, comparative results are reported for a well-known suite of numerical QP test cases with up to 1500 decision variables plus constraints. Detailed QuadProgJ results are also reported for 3-node and 5-node DC OPF test cases taken from power systems texts and ISO-NE/MISO/PJM training manuals.

**Keywords:** AC optimal power flow, DC OPF approximation, Strictly convex quadratic programming, Dual active-set method; Lagrangian augmentation, Java implementation, QuadProgJ, AMES Market Package

**JEL Codes:** C61, C63, C88

## 5.2 Introduction

The standard AC Optimal Power Flow (OPF) problem involves the minimization of total variable generation costs subject to nonlinear balance, branch flow, and production constraints for real and reactive power; see Wood and Wollenberg (1996, Chpt. 13). In practice, AC OPF problems are typically approximated by a more tractable “DC OPF” problem that focuses exclusively on real power constraints in linearized form.

We first present a standard DC OPF problem in per unit form. This standard problem can be represented as a *strictly convex quadratic programming (SCQP)* problem, that is, as the minimization of a positive definite quadratic form subject to linear constraints. An SCQP problem can be expressed in matrix form as follows:

**Minimize**

$$\mathbf{f}(\mathbf{x}) = \frac{1}{2}\mathbf{x}^T\mathbf{G}\mathbf{x} + \mathbf{a}^T\mathbf{x} \quad (5.1)$$

**with respect to**

$$\mathbf{x} = (\mathbf{x}_1, \mathbf{x}_2, \dots, \mathbf{x}_M)^T \quad (5.2)$$

**subject to**

$$\mathbf{C}_{\text{eq}}^T\mathbf{x} = \mathbf{b}_{\text{eq}} \quad (5.3)$$

$$\mathbf{C}_{\text{iq}}^T\mathbf{x} \geq \mathbf{b}_{\text{iq}} \quad (5.4)$$

where  $\mathbf{G}$  is an  $M \times M$  symmetric<sup>1</sup> positive definite matrix.

As will be clarified below, the solution of this standard DC OPF problem as an SCQP problem directly provides solution values for real power injections. However, solution values for locational marginal prices (LMPs), voltage angles, and real power branch flows have to be recovered indirectly by additional manipulations of these solution values.

<sup>1</sup>Symmetry is assumed here without loss of generality. Since  $x^T G x = x^T G^T x$ , the matrix  $G$  in (5.1) can always be replaced by the symmetric matrix  $\bar{G} = [G + G^T]/2$ .

We next show how this standard DC OPF problem can be augmented in a physically meaningful way, still retaining an SCQP form, so that solution values for LMPs, voltage angles, and voltage angle differences are directly recovered along with solution values for real power injections and branch flows. We then carefully explain how this augmented SCQP problem can be solved using *QuadProgJ*, an SCQP solver newly developed by the authors. QuadProgJ implements the well-known dual active-set SCQP algorithm by Goldfarb and Idnani (1983) and appears to be the first open-source SCQP solver developed completely in Java. It is designed for the fast and efficient desktop solution of small to medium-scale SCQP problems for research and training purposes.

More precisely, we show how the augmented DC OPF problem in SCQP form can be solved using QuadProgJ optionally coupled with an outer Java shell (DCOPFJ). This outer shell automatically converts input data from standard SI units to per unit (pu), puts this pu data into the matrix form required by QuadProgJ, and then converts the pu output back into SI units. To demonstrate the accuracy of QuadProgJ, we report comparative findings for a well-known suite of numerical QP test cases with up to 1500 decision variables plus constraints. As a test of DCOPFJ coupled with QuadProgJ, we also present detailed numerical findings for illustrative three-node and five-node DC OPF test cases taken from power systems texts and ISO-NE/MISO/PJM training manuals.

Section 5.3 presents the basic configuration of a restructured wholesale power market operating over an AC transmission grid, making use of a computational framework developed by the authors in previous studies. Section 5.4 carefully derives a standard DC OPF problem in per unit form for this wholesale power market and discusses how this standard formulation can be usefully augmented to enable the direct generation of solution values for LMPs, voltage angles, voltage angle differences, real power injections, and branch flows. Section 5.5 explicitly derives and presents a complete matrix SCQP representation for this augmented DC OPF problem. Section 5.6 illustrates this representation for three-node and five-node DC OPF test cases.

Section 5.7 then explains how the augmented DC OPF problem in SCQP form can be solved

using QuadProgJ optionally coupled with the DCOPFJ shell. Section 5.8 reports comparative QP test case results, and Section 5.9 presents detailed numerical findings for the three-node and five-node DC OPF test cases. Concluding remarks are given in Section 5.10. Technical notes on the derivation of AC power flow equations from Ohm's Law and on the SCQP representation of the standard DC OPF problem are provided in appendices.

### 5.3 Configuration of the Wholesale Power Market

Formulation of DC OPF problems for restructured wholesale power markets requires detailed structural information about the transmission grid as well as supply offer and demand bid information for market participants. This section briefly but carefully describes a computational framework ("AMES") previously developed by the authors for the dynamic study of restructured wholesale power markets. The following Section 5.4 then sets out a standard DC OPF problem based on this wholesale power market framework.

#### 5.3.1 Overview of the AMES Framework

In April 2003 the U.S. Federal Energy Regulatory Commission proposed a *Wholesale Power Market Platform (WPMP)* for common adoption by all U.S. wholesale power markets (FERC, 2003). In a series of previous studies<sup>2</sup> we have developed a Java framework modeling a restructured wholesale power market operating over an AC transmission grid in accordance with core features of the WPMP as implemented by the ISO New England in its Standard Market Design (ISO-NE, 2003).

This framework – referred to as *AMES*<sup>3</sup> – includes an Independent System Operator (ISO) and a collection of bulk energy traders consisting of Load-Serving Entities (LSEs) and Generators distributed across the nodes of the transmission grid.<sup>4</sup> In general, multiple Generators

<sup>2</sup>See Koesrindartoto and Tesfatsion (2004), Koesrindartoto et al. (2005), and Sun and Tesfatsion (2006).

<sup>3</sup>AMES is an acronym for Agent-based Modeling of Electricity Systems.

<sup>4</sup>An *Independent System Operator (ISO)* is an organization charged with the primary responsibility of maintaining the security of a power system and often with system operation responsibilities as well. The ISO is "independent" to the extent that it does not have a conflict of interest in carrying out these responsibilities, such as an ownership stake in generation or transmission facilities within the power system. A *Load-Serving Entity (LSE)* is an electric utility, transmitting utility, or Federal power marketing agency that has an obligation under Federal, State, or local law, or under long-term contracts, to provide electrical power to end-use

at multiple nodes could be under the control of a single generation company (“GenCo”), and similarly for LSEs. This control aspect is critically important to recognize for the study of strategic trading, but it plays no role in the current study.

The AMES ISO undertakes the daily operation of the transmission grid within a two-settlement system using *Locational Marginal Pricing*.<sup>5</sup> More precisely, at the beginning of each operating day  $D$  the AMES ISO determines hourly power commitments and *Locational Marginal Prices (LMPs)*<sup>6</sup> for the day-ahead market for day  $D + 1$  based on Generator supply offers and LSE demand bids (forward financial contracting). Any differences that arise during day  $D + 1$  between real-time conditions and the contracts cleared and settled in day  $D$  for the day-ahead market for  $D + 1$  are settled by the AMES ISO in the real-time market for  $D + 1$  at real-time LMPs. Transmission grid congestion is managed by the inclusion of congestion components in LMPs.

As discussed more carefully in Sections 5.3.3 and 5.3.4 below, the current study makes the usual empirically-based assumption that the daily demand bids of the AMES LSEs exhibit negligible price sensitivity and hence reduce to daily load profiles. In addition, it is assumed for notational simplicity that the AMES Generators submit supply offers consisting of their true marginal cost functions and true production limits (i.e., they do not make strategic offers). In this case the optimization problem faced by the ISO for each hour of the day-ahead market reduces to a standard AC OPF problem requiring the minimization of (true) total variable generation costs subject to balance constraints, branch flow constraints, (true) production constraints, and given loads. As is commonly done in practice, the AMES ISO approximates this nonlinear AC OPF problem by means of a DC OPF problem with linearized constraints. The AMES ISO invokes QuadProgJ through the DCOPFJ shell in order to solve this DC OPF problem in per unit form.

---

(residential or commercial) consumers or to other LSEs with end-use consumers. An LSE aggregates individual end-use consumer demand into “load blocks” for bulk buying at the wholesale level. A *Generator* is a unit that produces and sells electrical power in bulk at the wholesale level. A *node* is a point on the transmission grid where power is injected or withdrawn.

<sup>5</sup>*Locational Marginal Pricing* is the pricing of electrical power according to the location of its withdrawal from, or injection into, a transmission grid.

<sup>6</sup>A *Locational Marginal Price (LMP)* at any particular node of a transmission grid is the least cost of meeting demand for one additional unit (MW) of power at that node.



The remainder of this section explains the configuration of the AMES transmission grid and market participants.

### 5.3.2 Configuration of the AMES Transmission Grid

The AMES transmission grid is an alternating current (AC) grid modeled as a balanced three-phase network with  $N \geq 1$  branches and  $K \geq 2$  nodes. Reactances on branches are assumed to be total reactances (rather than per mile reactances), meaning that branch length is already taken into account. All transformer phase angle shifts are assumed to be zero, all transformer tap ratios are assumed to be 1, all line-charging capacitances are assumed to be 0, and the temperature is assumed to remain constant over time.

The AMES transmission grid is assumed to be *connected* in the sense that it has no isolated components; each pair of nodes  $k$  and  $m$  is connected by a linked branch path consisting of one or more branches. If two nodes are in direct connection with each other, it is assumed to be through at most one branch, i.e., branch groups are not explicitly considered. However, complete connectivity is *not* assumed, that is, node pairs are *not* necessarily in direct connection with each other through a single branch.

For per unit normalization in DC OPF implementations, it is conventional to specify base value settings for apparent power (voltampere) and voltage.<sup>7</sup> For the AMES transmission grid, the base apparent power, denoted by  $S_o$ , is assumed to be measured in three-phase megavoltamperes (MVAs), and the base voltage, denoted by  $V_o$ , is assumed to be measured in line-to-line kilovolts (kVs).

It is also assumed that *Kirchoff's Current Law (KCL)* governing current flows in electrical networks holds for the AMES transmission grid for each hour of operation. As detailed in Kirschen and Strbac (2004, Section 6.2.2.1), KCL implies that real and reactive power must each be in balance at each node. Thus, real power must also be in balance across the entire grid, in the sense that aggregate real power withdrawal plus aggregate transmission losses must equal aggregate real power injection.

<sup>7</sup>For a detailed and careful discussion of base value determinations and per unit calculations for power system applications, see Anderson (1995, Chpt. 1) and Gönen (1988, Chpt. 2).

In wholesale power markets restructured in accordance with FERC's proposed WPMP market design (FERC, 2003), the transmission grid is overlaid with a commercial network consisting of "pricing locations" for the purchase and sale of electric power. A *pricing location* is a location at which market transactions are settled using publicly available LMPs. For simplicity, it is assumed that the set of pricing locations for AMES coincides with the set of transmission grid nodes.

### 5.3.3 Configuration of the AMES LSEs

The AMES LSEs purchase bulk power in the AMES wholesale power market in order to service customer demand (load) in a downstream retail market. The user specifies the number  $J$  of LSEs as well as the location of these LSEs at various nodes of the transmission grid. LSEs do not engage in production or sale activities in the wholesale power market. Hence, LSEs purchase power only from Generators, not from each other.

At the beginning of each operating day  $D$ , each AMES LSE  $j$  submits a *daily load profile* into the day-ahead market for day  $D + 1$ . This daily load profile indicates the real power demand  $p_{Lj}(H)$  that must be serviced by LSE  $j$  in its downstream retail market for each of 24 successive hours  $H$ . In the current AMES modeling, the standard assumption is made that these demands are not price sensitive. One possible interpretation of this price-insensitivity assumption is that the AMES LSEs are required by retail regulations to service their load profiles as "native"<sup>8</sup> load obligations, and that the profit (revenues net of costs) received by LSEs for servicing these load obligations is regulated to be a simple dollar mark-up over cost that is independent of the cost level. Under these conditions, LSEs have no incentive to submit price-sensitive demand bids into the day-ahead market.

### 5.3.4 Configuration of the AMES Generators

The Ames Generators are electric power generating units. The user specifies the number  $I$  of Generators as well as the location of these Generators at various nodes of the transmission

<sup>8</sup>Native load customers for an LSE are customers whose power needs the LSE is obliged to meet by statute, franchise, regulatory requirement, or contract.

grid. Generators sell power only to LSEs, not to each other.

Each AMES Generator is user-configured with technology, endowment, and learning attributes. Only the technology attributes are relevant for the current study. With regard to the latter, it is assumed that each Generator has variable and fixed costs of production. However, Generators do not incur no-load, startup, or shutdown costs, and they do not face ramping constraints.<sup>9</sup>

More precisely, the technology attributes assumed for each Generator  $i$  take the following form. Generator  $i$  has minimum and maximum capacities for its hourly real power production level  $p_{Gi}$  (in MWs), denoted by  $p_{Gi}^L$  and  $p_{Gi}^U$ , respectively.<sup>10</sup> That is, for each  $i$ ,

$$p_{Gi}^L \leq p_{Gi} \leq p_{Gi}^U \quad (5.5)$$

In addition, Generator  $i$  has a *total cost function* giving its total costs of production per hour for each hourly production level  $p$ . This total cost function takes the form

$$TC_i(p) = a_i \cdot p + b_i \cdot p^2 + \text{FCost}_i \quad (5.6)$$

where  $a_i$  (\$/MWh),  $b_i$  (\$/MW<sup>2</sup>h), and  $\text{FCost}_i$  (\$/h) are exogenously given constants. Note that  $TC_i(p)$  is measured in dollars per hour (\$/h). Generator  $i$ 's *total variable cost function* and (*prorated*) *fixed costs* for any feasible hourly production level  $p$  are then given by

$$\text{TVC}_i(p) = TC_i(p) - TC_i(0) = a_i \cdot p + b_i \cdot p^2 \quad (5.7)$$

and

$$\text{FCost}_i = TC_i(0) \quad (5.8)$$

<sup>9</sup>As is standard in economics, *variable costs* are costs that vary with the level of production, and *fixed costs* are costs such as debt and equity obligations associated with plant investments that are not dependent on the level of production and that are incurred even if production ceases. As detailed by Kirschen and Strbac (2004, Section 4.3), the concept of *no-load costs* in power engineering refers to *quasi-fixed costs* that would be incurred by Generators if they could be kept running at zero output but that would vanish once shut-down occurs. *Startup costs* are costs specifically incurred when a Generator starts up, and *shutdown costs* are costs specifically incurred when a Generator shuts down. Finally, *ramping constraints* refer to physical restrictions on the rates at which Generators can increase or decrease their outputs.

<sup>10</sup>In the current AMES modeling, the lower production limit  $p_{Gi}^L$  for each Generator  $i$  is interpreted as a firm “must run” minimum power production level. That is, if  $p_{Gi}^L$  is positive, then shutting down Generator  $i$  is not an option for the AMES ISO. Consequently, for most applications of AMES, these lower production limits should be set to zero.

respectively. Finally, the *marginal cost function* for Generator  $i$  takes the form

$$MC_i(p) = a_i + 2 \cdot b_i \cdot p \quad (5.9)$$

At the beginning of each operating day  $D$ , each Generator  $i$  submits a *supply offer* into the day-ahead market for use in each hour  $H$  of day  $D+1$ . This supply offer consists of a reported marginal cost function defined over a reported feasible production interval. In general, this supply offer could be strategic in the sense that the reported marginal cost function deviates from Generator  $i$ 's true marginal cost function  $MC_i(p)$  and the reported feasible production interval differs from Generator  $i$ 's true feasible production interval  $[p_{Gi}^L, p_{Gi}^U]$ . For the purposes of this paper, however, it can be assumed without loss of generality that each Generator  $i$  reports its true marginal cost function and its true feasible production interval.<sup>11</sup>

#### 5.4 DC OPF Problem Formulation

A DC OPF problem is an approximation for an underlying AC OPF problem under several simplifying restrictions regarding voltage magnitudes, voltage angles, admittances, and reactive power. To lessen the chances of numerical instability, the variables appearing in the resulting DC OPF problem are commonly expressed in normalized *per unit (pu)* values so that the magnitudes of these variables are more nearly equal to each other.<sup>12</sup> In Section 5.4.1 we briefly but carefully outline the manner in which a standard DC OPF problem *expressed in pu values* is derived from an underlying AC OPF problem expressed in standard SI (International System of Units).

Using the results of Section 5.4.1, we then derive in Section 5.4.2 a standard DC OPF problem in full structural pu form for the AMES wholesale power market set out in Section 5.3. In particular, we show that this problem can be expressed as a strictly convex quadratic

<sup>11</sup>Thus, the Generators' supply offers take the form of linear upward-sloping supply curves. As detailed in Sun and Tesfatsion (2006), this representation for supply offers greatly facilitates the modeling of Generator learning. In the actual ISO-NE wholesale power market, Generators submit their supply offers in the form of step functions defined over their feasible production intervals, but they can check a "UseOfferSlope" box permitting the ISO to approximate these step functions by smooth curves.

<sup>12</sup>As will be clarified in subsequent sections, QuadProgJ can directly accept DC OPF variable inputs expressed in pu form so that all internal calculations are carried out in pu terms. Alternatively, as explained in Section 5.7, QuadProgJ can be coupled with an outer DCOPFJ shell that automatically converts wholesale power market variables from standard SI to per unit form prior to invoking QuadProgJ.

programming (SCQP) problem once voltage angles are eliminated by substitution from the problem constraints. An SCQP formulation is highly desirable from the standpoint of stable numerical solution. Unfortunately, this voltage angle substitution eliminates the nodal balance constraints and hence the ability to directly generate solution values for LMPs, which by definition are the shadow prices for the nodal balance constraints.

Consequently, in Sections 5.4.3 and 5.4.4 we develop an alternative version of this standard DC OPF problem in pu form making use of a physically meaningful Lagrangian augmentation. This augmented DC OPF problem directly generates solution values for LMPs, voltage angles, and voltage angle differences as well as real power injections and branch flows while still retaining a numerically desirable SCQP form.

#### 5.4.1 From AC OPF to DC OPF Per Unit

Conversion of an AC OPF problem to a DC OPF approximation in per unit form requires careful attention to variable conversions in both the problem constraints and the problem objective function. Here we first consider constraint conversions and then take up the needed conversions for the objective function.

The key constraints in an AC OPF problem that are simplified in a DC OPF approximation are the representations for real and reactive power branch flows. Let  $km$  denote a branch that connects nodes  $k$  and  $m$  with  $k \neq m$ . Let  $P_{km}$  (in MWs) denote the real power branch flow for  $km$ , and let  $Q_{km}$  (in MVARs) denote the reactive power branch flow for  $km$ . Let  $V_k$  and  $V_m$  denote the voltage magnitudes (in kVs) at nodes  $k$  and  $m$ , and let  $\delta_k$  and  $\delta_m$  denote the voltage angles (in radians) at nodes  $k$  and  $m$ . Finally, let  $g_{km}$  and  $b_{km}$  denote the conductance and the susceptance (in mhos) for branch  $km$ .<sup>13</sup>

Given these notational conventions,  $P_{km}$  and  $Q_{km}$  ( $k \neq m$ ) can be expressed as follows:<sup>14</sup>

$$P_{km} = V_k^2 g_{km} - V_k V_m [g_{km} \cos(\delta_k - \delta_m) + b_{km} \sin(\delta_k - \delta_m)] \quad (5.10)$$

<sup>13</sup>Impedance takes the complex form  $z = r + \sqrt{-1}x$ , where  $r$  (in ohms) denotes resistance and  $x$  (in ohms) denotes reactance. Admittance (the inverse of impedance) then takes the complex form  $y = g + \sqrt{-1}b$ , where the conductance is given by  $g = r/[r^2 + x^2]$  (in mhos) and the susceptance is given by  $b = -x/[r^2 + x^2]$  (in mhos).

<sup>14</sup>See Appendix A for a rigorous derivation of these power flow equations from Ohm's Law.

$$Q_{km} = -V_k^2 b_{km} - V_k V_m [g_{km} \sin(\delta_k - \delta_m) - b_{km} \cos(\delta_k - \delta_m)] \quad (5.11)$$

The three basic assumptions used to derive a DC OPF approximation from an underlying AC OPF problem are as follows (c.f. Kirschen and Strabac, 2004, p. 186, and McCalley, 2006):

[A1] The resistance  $r_{km}$  for each branch  $km$  is negligible compared to the reactance  $x_{km}$  and can therefore be set to 0.

[A2] The voltage magnitude at each node is equal to the base voltage  $V_o$ .

[A3] The voltage angle difference  $\delta_k - \delta_m$  across any branch  $km$  is sufficiently small in magnitude so that  $\cos(\delta_k - \delta_m) \approx 1$  and  $\sin(\delta_k - \delta_m) \approx [\delta_k - \delta_m]$ .

Given assumption [A1], it follows that  $g_{km} = 0$  and  $b_{km} = [-1/x_{km}]$ , where  $x_{km}$  denotes the reactance (in ohms) for branch  $km$ . Thus,  $P_{km} = V_k V_m [1/x_{km}] \sin(\delta_k - \delta_m)$  and  $Q_{km} = V_k^2 [1/x_{km}] - V_k V_m [1/x_{km}] \cos(\delta_k - \delta_m)$ . Adding assumption [A2],  $P_{km} = V_o^2 [1/x_{km}] \sin(\delta_k - \delta_m)$  and  $Q_{km} = V_o^2 [1/x_{km}] - V_o^2 [1/x_{km}] \cos(\delta_k - \delta_m)$ . Finally, adding assumption [A3],

$$P_{km} = V_o^2 \cdot [1/x_{km}] \cdot [\delta_k - \delta_m] \quad (5.12)$$

and the reactive power branch flow  $Q_{km}$  in equation (5.11) reduces to  $Q_{km} = V_o^2 [1/x_{km}] - V_o^2 [1/x_{km}] \cdot 1 = 0$ .

As detailed in Anderson (1995, Chpt. 1) and Gönen (1988, Chpt. 2), any quantity in an electrical network can be converted to a dimensionless pu quantity by dividing its numerical value by a base value of the same dimension. In power system calculations, only two base values are needed; and these are usually taken to be base voltage and base apparent power (voltampere). Assuming a balanced three-phase network with a base voltage  $V_o$  measured in line-to-line kVs and a base apparent power  $S_o$  measured in three-phase MVAs, the *base impedance*  $Z_o$  (in ohms) is specified to be

$$Z_o = V_o^2 / S_o \quad (5.13)$$

Given  $Z_o$ , the *pu reactance*  $x_{km}$  for branch  $km$  is defined to be

$$x_{km} \text{ pu} = x_{km}/Z_o \quad (5.14)$$

Note that  $x_{km} \text{ pu}$  is a dimensionless quantity. Using assumption [A3], the *pu susceptance*  $b_{km}$  for branch  $km$  is given by

$$b_{km} \text{ pu} = -1/[x_{km} \text{ pu}] \quad (5.15)$$

Also, the *pu real power branch flow*  $F_{km}$  for branch  $km$  is given by

$$F_{km} = P_{km}/S_o \quad (5.16)$$

Now divide each side of the real power branch flow equation (5.12) by the base apparent power  $S_o$ . Also, let  $B_{km}$  denote the negative of the susceptance pu on branch  $km$ . That is, define

$$B_{km} = -b_{km} \text{ pu} = [1/x_{km} \text{ pu}] \quad (5.17)$$

It then follows from equations (5.13) through (5.17) that the real power branch flow equation (5.12) can be expressed in the following simple linear pu form commonly seen in power systems textbooks:

$$F_{km} = B_{km}[\delta_k - \delta_m] \quad (5.18)$$

As will be clarified below, an additional change of variables needed to express the DC OPF problem in pu terms is to everywhere divide real power quantities by base apparent power  $S_o$ . Thus, for example, the real power  $p_{Gi}$  injected by each Generator  $i$  is expressed in pu terms as

$$P_{Gi} = p_{Gi}/S_o \quad (5.19)$$

and the real power load  $p_{Lj}$  withdrawn by each LSE  $j$  is expressed in pu terms as

$$P_{Lj} = p_{Lj}/S_o \quad (5.20)$$

The objective function for the DC OPF problem must be expressed in pu terms as well as the constraints. Thus, the total cost function and variable cost function defined in Section 5.3.4 for each Generator  $i$  are expressed as a function of pu real power  $P_{Gi}$  as follows:

$$TC_i(P_{Gi}) = A_i \cdot P_{Gi} + B_i \cdot P_{Gi}^2 + \text{FCost}_i \quad (5.21)$$

$$\text{TVC}_i(P_{Gi}) = A_i \cdot P_{Gi} + B_i \cdot P_{Gi}^2 \quad (5.22)$$

where  $A_i$  (\$/h) and  $B_i$  (\$/h) are pu-adjusted cost coefficients defined by

$$A_i = a_i S_o \quad (5.23)$$

$$B_i = b_i S_o^2 \quad (5.24)$$

Note that the pu-adjusted cost functions  $TC_i(P_{Gi})$  and  $\text{TVC}_i(P_{Gi})$  are still measured in dollars per hour (\$/h).

Finally, as usual, one node needs to be selected as the reference node with a specified voltage angle. For concreteness, we make the following assumption:

[A4] Node 1 is the reference node with voltage angle normalized to 0.

#### 5.4.2 Standard DC OPF in Structural PU Form

This subsection sets out a standard DC OPF problem for the AMES wholesale power market in full structural pu form, making use of the developments in Section 5.4.1. It is then seen that this standard problem can be expressed in numerically desirable SCQP form if the voltage angles are eliminated by substitution from the problem constraints.

For easy reference, the admissible exogenous variables and endogenous variables used in the standard DC OPF formulation are gathered together in Tables 5.1 and 5.2, respectively. These variable definitions will be used throughout the remainder of this study.

Given the variable definitions in Tables 5.1 and 5.2, the standard DC OPF problem for the AMES wholesale power market formulated in pu terms is as follows:

**Minimize**

$$\sum_{i=1}^I [A_i P_{Gi} + B_i P_{Gi}^2] \quad (5.25)$$



Table 5.1 DC OPF Admissible Exogenous Variables Per Unit

Variable	Description	Admissibility Restrictions
$K$	Total number of transmission grid nodes	$K > 0$
$N$	Total number of distinct network branches	$N > 0$
$I$	Total number of Generators	$I > 0$
$J$	Total number of LSEs	$J > 0$
$I_k$	Set of Generators located at node $k$	$\text{Card}(\cup_{k=1}^K I_k) = I$
$J_k$	Set of LSEs located at node $k$	$\text{Card}(\cup_{k=1}^K J_k) = J$
$S_o$	Base apparent power (in three-phase MVAs)	$S_o \geq 1$
$V_o$	Base voltage (in line-to-line kVs)	$V_o > 0$
$V_k$	Voltage magnitude (in kVs) at node $k$	$V_k = V_o, k = 1, \dots, K$
$P_{Lj}$	Real power load (pu) withdrawn by LSE $j$	$P_{Lj} \geq 0, j = 1, \dots, J$
$km$	Branch connecting nodes $k$ and $m$ (if one exists)	$k \neq m$
$BR$	Set of all distinct branches $km, k < m$	$BR \neq \emptyset$
$x_{km}$	Reactance (pu) for branch $km$	$x_{km} = x_{mk} > 0, km \in BR$
$B_{km}$	$[1/x_{km}]$ for branch $km$	$B_{km} = B_{mk} > 0, km \in BR$
$F_{km}^U$	Thermal limit (pu) for real power flow on $km$	$F_{km}^U > 0, km \in BR$
$\delta_1$	Reference node 1 voltage angle (in radians)	$\delta_1 = 0$
$P_{Gi}^L$	Lower real power limit (pu) for Generator $i$	$P_{Gi}^L \geq 0, i = 1, \dots, I$
$P_{Gi}^U$	Upper real power limit (pu) for Generator $i$	$P_{Gi}^U > 0, i = 1, \dots, I$
$A_i, B_i$	Cost coefficients (pu adjusted) for Generator $i$	$B_i > 0, i = 1, \dots, I$
$\text{FCost}_i$	Fixed costs (hourly prorated) for Generator $i$	$\text{FCost}_i \geq 0, i = 1, \dots, I$
$\text{MC}_i(P)$	$\text{MC}_i(P) = A_i + 2B_iP =$ Generator $i$ 's MC function	$\text{MC}_i(P_{Gi}^L) \geq 0, i = 1, \dots, I$

with respect to

$$P_{Gi}, i = 1, \dots, I; \quad \delta_k, k = 1, \dots, K$$

subject to:

**Real power balance constraint for each node  $k = 1, \dots, K$ :**

$$0 = \text{PLoad}_k - \text{PGen}_k + \text{PNetInject}_k \quad (5.26)$$

where

Table 5.2 DC OPF Endogenous Variables Per Unit

Variable	Description
$P_{Gi}$	Real power injection (pu) by Generator $i = 1, \dots, I$
$\delta_k$	Voltage angle (in radians) at node $k = 2, \dots, K$
$F_{km}$	Real power (pu) flowing in branch $km \in \text{BR}$
$\text{PGen}_k$	Total real power injection (pu) at node $k = 1, \dots, K$
$\text{PLoad}_k$	Total real power withdrawal (pu) at node $k = 1, \dots, K$
$\text{PNetInject}_k$	Total net real power injection (pu) at node $k = 1, \dots, K$

$$\text{PLoad}_k = \sum_{j \in J_k} P_{Lj} \quad (5.27)$$

$$\text{PGen}_k = \sum_{i \in I_k} P_{Gi} \quad (5.28)$$

$$\text{PNetInject}_k = \sum_{km \text{ or } mk \in \text{BR}} F_{km} \quad (5.29)$$

$$F_{km} = B_{km} [\delta_k - \delta_m] \quad (5.30)$$

**Real power thermal constraint for each branch  $km \in \text{BR}$ :**

$$|F_{km}| \leq F_{km}^U \quad (5.31)$$

**Real power production constraint for each Generator  $i = 1, \dots, I$ :**

$$P_{Gi}^L \leq P_{Gi} \leq P_{Gi}^U \quad (5.32)$$

**Voltage angle setting at reference node 1:**

$$\delta_1 = 0 \quad (5.33)$$

As it stands, this standard DC OPF problem in pu form is a positive *semi-definite* quadratic programming problem. To see this, recall the general matrix form of a quadratic programming problem depicted in Section 5.2. The objective function (5.25) expressed in the quadratic form (5.1) with  $x = (P_{G1}, \dots, P_{GI}, \delta_1, \dots, \delta_K)^T$  entails a diagonal matrix  $G$  with positive entries in its first  $I$  diagonal elements corresponding to the real power injections  $P_{Gi}$  but zeroes in its remaining  $K$  diagonal elements corresponding to the voltage angles  $\delta_k$ , implying that  $G$  is a positive semi-definite matrix.

As shown in Appendix B, it is possible to use the nodal balance constraints (5.26) for  $k = 2, \dots, K$  together with the normalization constraint (5.33) to express the voltage angle vector  $(\delta_2, \dots, \delta_K)$  as a linear affine function of the real power injection vector  $(P_{G1}, \dots, P_{GI})$ . Using this relation to everywhere eliminate the voltage angles does result in a numerically more desirable SCQP problem. Unfortunately, this voltage angle elimination also prevents the direct determination of solution values for LMPs since, by definition, the LMPs are the shadow prices for the nodal balance constraints.

The following subsection develops a simple physically meaningful augmentation of the standard DC OPF objective function that permits direct generation of optimal LMPs and voltage angle solutions while retaining a numerically desirable SCQP form.

### 5.4.3 Augmentation of the Standard DC OPF Problem

Consider the following augmentation of the standard DC OPF objective function (5.25) with a soft penalty function on the sum of the squared voltage angle differences:

$$\sum_{i=1}^I [A_i P_{Gi} + B_i P_{Gi}^2] + \pi \left[ \sum_{km \in BR} [\delta_k - \delta_m]^2 \right] \quad (5.34)$$

As demonstrated carefully in Section 5.5 below, this augmentation transforms the standard DC OPF problem into an SCQP problem that can be used to directly generate solution values for LMPs and voltage angles as well as real power injections and branch flows, a clear benefit. However, this augmentation also has two additional potential benefits based on physical and mathematical considerations:

- *Physical Considerations:* The augmentation provides a way to conduct sensitivity experiments on the size of the voltage angle differences that could be informative for estimating the size and pattern of AC-DC approximation errors.
- *Mathematical Considerations:* The augmentation could help to improve the numerical stability and convergence properties of any applied solution method.

On the other hand, the augmentation would also seem to come with a potential cost. Specifically, could it cause significant distortions in the standard DC OPF solution values?

This subsection takes up each consideration in turn. The bottom line, supported by experimental evidence, is that solution distortions appear to be practically controllable to arbitrarily small levels through appropriately small settings of the soft penalty weight  $\pi$ . Consequently, the benefits of augmentation would seem to strongly outweigh the costs.

#### 5.4.3.1 Potential Benefits Based on Physical Considerations

The standard DC OPF problem in pu form set out in Section 5.4.2 requires the minimization of total variable costs subject to a set of linearized constraints. As detailed in Section 5.4.1, this pu form relies on the four simplifying assumptions [A1] through [A4]. In particular, the linear form of the branch flow constraints relies on assumption [A3] asserting that voltage angle differences across branches remain small.

Consequently, small voltage angle differences is the basis upon which a DC approximation to a true underlying AC OPF problem is formulated. Nevertheless, the standard DC OPF problem does not constrain voltage angle differences apart from the constraints imposed through branch flow limits, a conceptually distinct type of constraint motivated in terms of the physical attributes of transmission lines. If the presumption of small voltage angle differences is violated, the errors induced by reliance on a DC approximation could become unacceptably large.

Much remains to be done regarding how small is small enough for voltage angle differences in order to achieve satisfactory DC OPF approximations not only for AC OPF quantity solutions (real power injections and branch flows) but also for AC OPF price solutions (the LMP at each

node). We have only been able to find one study of this issue (Overbye et al., 2004) that takes both quantity and price solutions into account. The conclusions reached by the authors on the basis of two case studies are cautiously optimistic with regard to quantity solutions. However, as the authors note, the LMPs are determined by the binding branch flow constraints, hence small branch flow changes causing changes in the binding branch flow constraints can have discrete and potentially large impacts on LMP solutions. For example, in the authors' second case study, the DC approximation missed almost 50% of the binding constraints for the AC problem. Although many of these were "near misses," the effects of these near-misses on the LMP approximations were in some cases significant.

For these reasons, it would seem prudent to pay close attention to the sizes of the voltage angle differences when undertaking DC OPF approximations to AC OPF problems. DC solutions obtained with large voltage angle differences could diverge significantly from AC solutions, thus giving misleading signals - particularly price signals - for the operation of restructured wholesale power markets.

Introducing a soft penalty function on voltage angle differences permits sensitivity checks to be conducted to determine the sensitivity of DC OPF solutions to impositions of this precondition for AC-DC approximation. Ideally, the DC OPF solutions obtained with sufficiently small soft penalty weights  $\pi$  should reproduce the DC OPF solutions obtained in the absence of any soft penalty imposition, as a baseline for comparison. This is indeed seen to be the case in the numerical  $\pi$  sensitivity results reported in Section 5.9.4.

#### 5.4.3.2 Potential Benefits Based on Mathematical Considerations

As is well known, numerical stability and convergence properties of nonlinear programming problems with minimization (maximization) objectives can often be enhanced by increasing the convexity (concavity) of their objective functions through suitable augmentations.

For example, the Fortran package ZQPCVX developed by Powell (1983) for convex QP minimization problems includes a simple artificial augmentation to induce strict convexity. Specifically, the matrix diagonal of the positive semi-definite quadratic form representing the

nonlinear part of the objective function is augmented with positively-valued constants to induce positive definiteness. More generally, Shahidehpour et al. (2002, Appendix B.2) discuss an entire class of artificial augmentations suitable for nonlinear programming problems with inequality constraints. The authors use versions of these augmentations on pages 288-289 and elsewhere in their text to improve the convexity (hence the convergence properties) of various types of optimization problems arising for electric power systems.

Although artificial augmentations can work well to ensure stability and convergence, they do not provide meaningful sensitivity information for the physical problem at hand. Happily, as explained above, a physically meaningful augmentation is available for the standard DC OPF problem that accomplishes strict convexification of the objective function with several important side benefits.

#### 5.4.3.3 Potential Costs in Terms of Solution Distortions

In Section 5.9.4 we report findings for extensive tests conducted with 3-node and 5-node DC OPF problems to check the extent to which the soft penalty function augmentation affects standard DC OPF solution values. To briefly summarize, these findings indicate that the effects of this augmentation on the resulting solution values are negligible for a sufficiently small setting of the soft penalty weight  $\pi$ . Moreover, no numerical instability or convergence problems were detected for any of the tested  $\pi$  values.

#### 5.4.4 Augmented DC OPF in Reduced PU Form

The augmented DC OPF problem in structural pu form obtained by replacing the standard DC OPF objective function (5.25) by the augmented objective function (5.34) can be compactly represented in the following reduced form:

**Minimize**

$$\sum_{i=1}^I [A_i P_{Gi} + B_i P_{Gi}^2] + \pi \left[ \sum_{1m \in BR} \delta_m^2 + \sum_{km \in BR, k \geq 2} [\delta_k - \delta_m]^2 \right] \quad (5.35)$$

with respect to

$$P_{Gi}, i = 1, \dots, I; \quad \delta_k, k = 2, \dots, K$$

subject to:

**Real power balance constraint for each node  $k = 1, \dots, K$  (with  $\delta_1 \equiv 0$ ):**

$$\sum_{i \in I_k} P_{Gi} - \sum_{km \text{ or } mk \in BR} B_{km}[\delta_k - \delta_m] = \sum_{j \in J_k} P_{Lj} \quad (5.36)$$

**Real power thermal constraints for each branch  $km \in BR$  (with  $\delta_1 \equiv 0$ ):**

$$-B_{km}[\delta_k - \delta_m] \geq -F_{km}^U \quad (5.37)$$

$$B_{km}[\delta_k - \delta_m] \geq -F_{km}^U \quad (5.38)$$

**Real power production constraints for each Generator  $i = 1, \dots, I$ :**

$$P_{Gi} \geq P_{Gi}^L \quad (5.39)$$

$$-P_{Gi} \geq -P_{Gi}^U \quad (5.40)$$

## 5.5 Augmented DC OPF in SCQP Form

As a preliminary step towards a SCQP depiction for the augmented DC OPF problem in reduced pu form presented in Section 5.4.4, it is useful to introduce some notational conventions to simplify the exposition. The next two subsections develop matrix representations for the objective function and constraints. The final subsection then presents the complete SCQP depiction in a matrix form suitable for QuadProgJ solution.

### 5.5.1 Objective Function Depiction

Consider, first, the development of a quadratic form representation for the soft penalty function applied to voltage angle differences in the augmented DC OPF objective function (5.35). As detailed in Section 5.3.2, care must be taken in this representation to account for the possible lack of direct branch connections between nodes.

To this end, define the *branch connection matrix*  $\mathbb{E}$  as follows:

$$\mathbb{E} = \begin{bmatrix} 0 & \mathbb{I}(1 \leftrightarrow 2) & \mathbb{I}(1 \leftrightarrow 3) & \cdots & \mathbb{I}(1 \leftrightarrow K) \\ \mathbb{I}(2 \leftrightarrow 1) & 0 & \mathbb{I}(2 \leftrightarrow 3) & \cdots & \mathbb{I}(2 \leftrightarrow K) \\ \mathbb{I}(3 \leftrightarrow 1) & \mathbb{I}(3 \leftrightarrow 2) & 0 & \cdots & \mathbb{I}(3 \leftrightarrow K) \\ \vdots & \vdots & \vdots & \ddots & \vdots \\ \mathbb{I}(K \leftrightarrow 1) & \mathbb{I}(K \leftrightarrow 2) & \mathbb{I}(K \leftrightarrow 3) & \cdots & 0 \end{bmatrix}_{K \times K} \quad (5.41)$$

where  $\mathbb{I}(\cdot)$  is an indicator function defined as:

$$\mathbb{I}(k \leftrightarrow m) = \begin{cases} 1 & \text{if either } km \text{ or } mk \in BR \\ 0 & \text{otherwise} \end{cases}$$

Since  $\mathbb{I}(k \leftrightarrow m) = \mathbb{I}(m \leftrightarrow k)$  for all  $k$  and  $m$ , it follows that  $\mathbb{E}_{km} = \mathbb{E}_{mk}$  for all  $k$  and  $m$ . Thus,  $\mathbb{E}$  is a symmetric matrix.

Using this indicator function construct, the number  $N$  of distinct transmission grid branches can be determined as follows:

$$N = \left[ \sum_{k,m=1}^K \mathbb{I}(k \leftrightarrow m) \right] / 2 \quad (5.42)$$

If the transmission grid is completely connected, then  $N = K[K - 1]/2$ .

Next, define the (*voltage angle difference*) *weight matrix*  $\mathbf{W}(\mathbf{K})$  as



$$\mathbf{W}(\mathbf{K}) = 2\pi \begin{bmatrix} \sum_{k \neq 1} \mathbb{E}_{k1} & -\mathbb{E}_{12} & -\mathbb{E}_{13} & \cdots & -\mathbb{E}_{1K} \\ -\mathbb{E}_{21} & \sum_{k \neq 2} \mathbb{E}_{k2} & -\mathbb{E}_{23} & \cdots & -\mathbb{E}_{2K} \\ -\mathbb{E}_{31} & -\mathbb{E}_{32} & \sum_{k \neq 3} \mathbb{E}_{k3} & \cdots & -\mathbb{E}_{3K} \\ \vdots & \vdots & \vdots & \ddots & \vdots \\ -\mathbb{E}_{K1} & -\mathbb{E}_{K2} & -\mathbb{E}_{K3} & \cdots & \sum_{k \neq K} \mathbb{E}_{kK} \end{bmatrix}_{K \times K} \quad (5.43)$$

For example, in the special case of a completely connected grid, the weight matrix  $\mathbf{W}(\mathbf{K})$  takes the form

$$\mathbf{W}(\mathbf{K}) = 2\pi \begin{bmatrix} K-1 & -1 & -1 & \cdots & -1 \\ -1 & K-1 & -1 & \cdots & -1 \\ -1 & -1 & K-1 & \cdots & -1 \\ \vdots & \vdots & \vdots & \ddots & \vdots \\ -1 & -1 & -1 & \cdots & K-1 \end{bmatrix}_{K \times K} \quad (5.44)$$

Let  $\delta(\mathbf{K})^T = [\delta_1 \dots \delta_K]$  denote an arbitrary  $K$ -dimensional voltage angle vector with at least one non-zero element. For  $K = 2$  it is easily verified that

$$\frac{1}{2} \delta(\mathbf{2})^T \mathbf{W}(\mathbf{2}) \delta(\mathbf{2}) = \pi [\delta_1 - \delta_2]^2 = \pi \left[ \sum_{km \in BR} [\delta_k - \delta_m]^2 \right] > 0 \quad (5.45)$$

Consequently,  $\mathbf{W}(\mathbf{2})$  is a symmetric positive definite matrix. A simple induction argument on  $K$  then establishes that  $\mathbf{W}(\mathbf{K})$  is a symmetric positive definite matrix for arbitrary  $K \geq 2$ .

Now suppose  $\delta_1 \equiv 0$  and  $\delta_k \neq 0$  for some  $k = 2, \dots, K$ , and let  $\delta_{-1}^T(K) = [\delta_2 \dots \delta_K]$ . Also, let  $\mathbf{W}_{\text{rr}}(\mathbf{K})$  denote the *reduced weight matrix* constructed from  $\mathbf{W}(\mathbf{K})$  by deleting its first row and its first column as follows:

$$\mathbf{W}_{\text{rr}}(\mathbf{K}) = 2\pi \begin{bmatrix} \sum_{k \neq 2} \mathbb{E}_{k2} & -\mathbb{E}_{23} & \cdots & -\mathbb{E}_{2K} \\ -\mathbb{E}_{32} & \sum_{k \neq 3} \mathbb{E}_{k3} & \cdots & -\mathbb{E}_{3K} \\ \vdots & \vdots & \ddots & \vdots \\ -\mathbb{E}_{K2} & -\mathbb{E}_{K3} & \cdots & \sum_{k \neq K} \mathbb{E}_{kK} \end{bmatrix}_{(K-1) \times (K-1)} \quad (5.46)$$

It is then easily shown by a simple induction argument that

$$\begin{aligned} \frac{1}{2}\delta(\mathbf{K})^T \mathbf{W}(\mathbf{K})\delta(\mathbf{K}) &= \frac{1}{2}\delta_{-1}(\mathbf{K})^T \mathbf{W}_{\mathbf{rr}}(\mathbf{K})\delta_{-1}(\mathbf{K}) \\ &= \pi \left[ \sum_{1m \in BR} \delta_m^2 + \sum_{km \in BR, k \geq 2} [\delta_k - \delta_m]^2 \right] > 0 \end{aligned} \quad (5.47)$$

Consequently,  $\mathbf{W}_{\mathbf{rr}}(\mathbf{K})$  is a symmetric positive definite matrix whose quadratic form expresses the soft penalty term in the augmented DC OPF objective function (5.35). For expositional simplicity, the dimension argument  $K$  for this matrix will hereafter be suppressed.

Let the Generators' *cost attribute matrix*  $\mathbf{U}$  be defined as

$$\mathbf{U} = \text{diag}[2B_1, 2B_2, \dots, 2B_I] = \begin{bmatrix} 2B_1 & 0 & \cdots & 0 \\ 0 & 2B_2 & \cdots & 0 \\ \vdots & \vdots & \ddots & \vdots \\ 0 & 0 & \cdots & 2B_I \end{bmatrix}_{I \times I} \quad (5.48)$$

Recalling from Table 5.1 that the Generator cost coefficients  $B_i$  are assumed to be strictly positive, it is easily seen that  $\mathbf{U}$  is a symmetric positive definite matrix.

Finally, let the matrix  $\mathbf{G}$  be defined by

$$\mathbf{G} = \text{blockDiag} \begin{bmatrix} \mathbf{U} & \mathbf{0} \\ \mathbf{0} & \mathbf{W}_{\mathbf{rr}} \end{bmatrix}_{(I+K-1) \times (I+K-1)} \quad (5.49)$$

The matrix  $\mathbf{G}$  is clearly symmetric. Moreover,  $\mathbf{G}$  is positive definite since its associated quadratic form maps any vector  $\mathbf{x}^T = [P_{G1}, \dots, P_{GI}, \delta_2, \dots, \delta_K]$  with at least one non-zero component into a strictly positive scalar. That is,

$$\frac{1}{2}\mathbf{x}^T \mathbf{G} \mathbf{x} = \sum_{i=1}^I [B_i P_{Gi}^2] + \pi \left[ \sum_{1m \in BR} \delta_m^2 + \sum_{km \in BR, k \geq 2} [\delta_k - \delta_m]^2 \right] > 0 \quad (5.50)$$

In particular, comparing (5.50) with (5.35), it is seen that (5.50) provides a positive definite quadratic form representation for the nonlinear terms in the augmented DC OPF objective function.

### 5.5.2 Constraint Depiction

The main factor complicating the matrix representation of the constraints for the augmented DC OPF problem is, once again, the need to allow for the possible absence of direct branch connections between nodes. This subsection derives special matrices to facilitate this constraint representation.

Let the definition (5.17) for  $B_{km}$  be extended for all  $k \neq m$  as follows:

$$B_{km} = \begin{cases} \frac{1}{x_{km} \text{ pu}} > 0 & \text{if } km \text{ or } mk \in BR \\ 0 & \text{otherwise} \end{cases}$$

Since  $x_{km} \text{ pu} = x_{mk} \text{ pu}$  for all  $km \in BR$ , it follows that  $B_{km} = B_{mk}$  for all  $k \neq m$ . Using this definition for  $B_{km}$ , construct the *bus admittance matrix*  $\mathbf{B}'$  as follows:

$$\mathbf{B}' = \begin{bmatrix} \sum_{k \neq 1} B_{k1} & -B_{12} & -B_{13} & \cdots & -B_{1K} \\ -B_{21} & \sum_{k \neq 2} B_{k2} & -B_{23} & \cdots & -B_{2K} \\ -B_{31} & -B_{32} & \sum_{k \neq 3} B_{k3} & \cdots & -B_{3K} \\ \vdots & \vdots & \vdots & \ddots & \vdots \\ -B_{K1} & -B_{K2} & -B_{K3} & \cdots & \sum_{k \neq K} B_{kK} \end{bmatrix}_{K \times K} \quad (5.51)$$

The *reduced bus admittance matrix*  $\mathbf{B}'_r$ , consisting of  $\mathbf{B}'$  with its first row omitted then takes the following form:

$$\mathbf{B}'_r = \begin{bmatrix} -B_{21} & \sum_{k \neq 2} B_{k2} & -B_{23} & \cdots & -B_{2K} \\ -B_{31} & -B_{32} & \sum_{k \neq 3} B_{k3} & \cdots & -B_{3K} \\ \vdots & \vdots & \vdots & \ddots & \vdots \\ -B_{K1} & -B_{K2} & -B_{K3} & \cdots & \sum_{k \neq K} B_{kK} \end{bmatrix}_{(K-1) \times K} \quad (5.52)$$

Let  $\mathbf{BI}$  denote the listing of the  $N$  distinct branches  $km \in BR$  constituting the transmission grid, lexicographically sorted as in a dictionary from lower to higher numbered nodes. Let  $\mathbf{BI}_n$  denote the  $n$ th branch listed in  $\mathbf{BI}$ . Then the *adjacency matrix*  $\mathbf{A}$  with entries of 1 for the “from” node and  $-1$  for the “to” node can be expressed as follows:

$$\mathbb{A} = \begin{bmatrix} \mathbb{J}(1, \mathbf{BI}_1) & \mathbb{J}(2, \mathbf{BI}_1) & \cdots & \mathbb{J}(K, \mathbf{BI}_1) \\ \mathbb{J}(1, \mathbf{BI}_2) & \mathbb{J}(2, \mathbf{BI}_2) & \cdots & \mathbb{J}(K, \mathbf{BI}_2) \\ \vdots & \vdots & \ddots & \vdots \\ \mathbb{J}(1, \mathbf{BI}_N) & \mathbb{J}(2, \mathbf{BI}_N) & \cdots & \mathbb{J}(K, \mathbf{BI}_N) \end{bmatrix}_{N \times K} \quad (5.53)$$

where  $\mathbb{J}(\cdot)$  is an indicator function defined as:

$$\mathbb{J}(i, \mathbf{BI}_n) = \begin{cases} +1 & \text{if } \mathbf{BI}_n \text{ takes the form } ij \in BR \text{ for some node } j > i \\ -1 & \text{if } \mathbf{BI}_n \text{ takes the form } ji \in BR \text{ for some node } j < i \\ 0 & \text{otherwise} \end{cases}$$

for all nodes  $i = 1, \dots, K$  and for all branches  $n = 1, \dots, N$

Let the *reduced adjacency matrix*  $\mathbb{A}_r$  be defined as  $\mathbb{A}$  with its first column deleted. Thus,  $\mathbb{A}_r$  is expressed as

$$\mathbb{A}_r = \begin{bmatrix} \mathbb{J}(2, \mathbf{BI}_1) & \cdots & \mathbb{J}(K, \mathbf{BI}_1) \\ \mathbb{J}(2, \mathbf{BI}_2) & \cdots & \mathbb{J}(K, \mathbf{BI}_2) \\ \vdots & \ddots & \vdots \\ \mathbb{J}(2, \mathbf{BI}_N) & \cdots & \mathbb{J}(K, \mathbf{BI}_N) \end{bmatrix}_{N \times (K-1)} \quad (5.54)$$

Also, define the matrix  $\mathbb{II}$  by

$$\mathbb{II} = \begin{bmatrix} \mathbb{I}(1 \in I_1) & \mathbb{I}(2 \in I_1) & \cdots & \mathbb{I}(I \in I_1) \\ \mathbb{I}(1 \in I_2) & \mathbb{I}(2 \in I_2) & \cdots & \mathbb{I}(I \in I_2) \\ \vdots & \vdots & \ddots & \vdots \\ \mathbb{I}(1 \in I_K) & \mathbb{I}(2 \in I_K) & \cdots & \mathbb{I}(I \in I_K) \end{bmatrix}_{K \times I} \quad (5.55)$$

where

$$\mathbb{I}(i \in I_k) = \begin{cases} 1 & \text{if } i \in I_k \\ 0 & \text{if } i \notin I_k \end{cases}$$

for each  $i = 1, \dots, I$  and  $k = 1, \dots, K$ . Finally, define the matrix  $\mathbf{D}$  to be the diagonal matrix whose diagonal entries give the  $B_{km}$  values for all distinct connected branches  $km \in BR$  ordered as in  $BI$ . That is, with some slight abuse of notation:

$$\mathbf{D} = \text{diag} \left[ \begin{array}{cccc} D_1 & D_2 & \cdots & D_N \end{array} \right]_{N \times N} \quad (5.56)$$

where  $D_n = B_{km}$  if  $BI_n$  (the  $n$ th element of  $BI$ ) corresponds to branch  $km \in BR$ .<sup>15</sup>

### 5.5.3 The Complete SCQP Depiction

Using the notation from Sections 5.5.1 and 5.5.2, the complete SCQP depiction for the augmented DC OPF problem in reduced pu form set out in Section 5.4.4 can be expressed as follows:

**Minimize**

$$\mathbf{f}(\mathbf{x}) = \frac{1}{2} \mathbf{x}^T \mathbf{G} \mathbf{x} + \mathbf{a}^T \mathbf{x} \quad (5.57)$$

**with respect to**

$$\mathbf{x} = \left[ \begin{array}{cccccc} P_{G1} & \cdots & P_{GI} & \delta_2 & \cdots & \delta_K \end{array} \right]_{(I+K-1) \times 1}^T$$

**subject to**

$$\mathbf{C}_{\text{eq}}^T \mathbf{x} = \mathbf{b}_{\text{eq}} \quad (5.58)$$

$$\mathbf{C}_{\text{iq}}^T \mathbf{x} \geq \mathbf{b}_{\text{iq}} \quad (5.59)$$

In this SCQP depiction, the symmetric positive definite matrix  $\mathbf{G}$  is defined as in (5.49), and the vector  $\mathbf{a}^T$  is given by

$$\mathbf{a}^T = \left[ \begin{array}{cccccc} A_1 & \cdots & A_I & 0 & \cdots & 0 \end{array} \right]_{1 \times (I+K-1)}$$

The equality constraint matrix  $\mathbf{C}_{\text{eq}}^T$  takes the form:

<sup>15</sup>Note that the matrix  $\mathbf{H} \equiv \mathbf{D} \mathbf{A}_r$  maps the vector  $\delta = (\delta_2, \dots, \delta_K)^T$  of voltage angles into the  $N \times 1$  real power branch flow vector  $\mathbf{F} \equiv \mathbf{H} \delta$ . Also, as established in Appendix B,  $\mathbf{P} \mathbf{Inject} = \mathbf{B}'_{rr} \delta$ , where  $\mathbf{P} \mathbf{Inject}$  denotes the  $(K-1) \times 1$  vector of net nodal real power injections  $\text{PNetInject}_k$ ,  $k = 2, \dots, K$ , and  $\mathbf{B}'_{rr}$  denotes the matrix  $\mathbf{B}'$  in (5.51) with its first row and first column eliminated (corresponding to the reference node 1). Defining the *shift matrix*  $\mathbf{S} \equiv \mathbf{H} [\mathbf{B}'_{rr}]^{-1}$ , it follows that  $\mathbf{F} = \mathbf{S} \mathbf{P} \mathbf{Inject}$ . Compare CAISO (2003, pp. 24-25).

$$\mathbf{C}_{\text{eq}}^{\text{T}} = \left[ \mathbf{II} \quad -\mathbf{B}'_{\text{r}}{}^{\text{T}} \right]_{K \times (I+K-1)}$$

where  $\mathbf{B}'_{\text{r}}$  is defined as in (5.52) and  $\mathbf{II}$  is defined as in (5.55). The associated equality constraint vector  $\mathbf{b}_{\text{eq}}$  takes the form:

$$\mathbf{b}_{\text{eq}} = \left[ \sum_{j \in J_1} P_{Lj} \quad \sum_{j \in J_2} P_{Lj} \quad \cdots \quad \sum_{j \in J_K} P_{Lj} \right]_{K \times 1}^{\text{T}}$$

Finally, consider the inequality constraint matrix  $\mathbf{C}_{\text{iq}}$ . This matrix can be decomposed into several column-wise submatrices corresponding to the thermal constraints (5.37) (call it  $\mathbf{C}_{\text{t1}}$ ), the thermal constraints (5.38) (call it  $\mathbf{C}_{\text{t2}}$ ), the lower production constraints (5.39) (call it  $\mathbf{C}_{\text{pL}}$ ), and the upper production constraints (5.40) (call it  $\mathbf{C}_{\text{pU}}$ ). Note, further, that  $\mathbf{C}_{\text{t1}} = -\mathbf{C}_{\text{t2}}$  and  $\mathbf{C}_{\text{pL}} = -\mathbf{C}_{\text{pU}}$ . For easier notation, let  $\mathbf{C}_{\text{t}} \equiv \mathbf{C}_{\text{t1}}$  and  $\mathbf{C}_{\text{p}} \equiv \mathbf{C}_{\text{pL}}$ . The inequality constraint matrix  $\mathbf{C}_{\text{iq}}$  can then be expressed as follows:

$$\mathbf{C}_{\text{iq}} = \left[ \mathbf{C}_{\text{t}} \quad -\mathbf{C}_{\text{t}} \quad \mathbf{C}_{\text{p}} \quad -\mathbf{C}_{\text{p}} \right]_{(I+K-1) \times (2N+2I)}$$

or

$$\mathbf{C}_{\text{iq}}^{\text{T}} = \left[ \mathbf{C}_{\text{t}}^{\text{T}} \quad -\mathbf{C}_{\text{t}}^{\text{T}} \quad \mathbf{C}_{\text{p}}^{\text{T}} \quad -\mathbf{C}_{\text{p}}^{\text{T}} \right]_{(2N+2I) \times (I+K-1)}^{\text{T}}$$

In this expression,

$$\mathbf{C}_{\text{t}}^{\text{T}} = \left[ \mathbf{O}_{\text{t}} \quad -\mathbf{D}\mathbb{A}_{\text{r}} \right]_{N \times (I+K-1)}$$

where  $\mathbf{O}_{\text{t}}$  is an  $N \times I$  zero matrix,  $\mathbb{A}_{\text{r}}$  is defined as in (5.54), and  $\mathbf{D}$  is defined as in (5.56).

Also,

$$\mathbf{C}_{\text{p}}^{\text{T}} = \left[ \mathbf{I}_{\text{p}} \quad \mathbf{O}_{\text{p}} \right]_{I \times (I+K-1)}$$

where  $\mathbf{I}_{\text{p}}$  is an  $I \times I$  identity matrix and  $\mathbf{O}_{\text{p}}$  is an  $I \times (K-1)$  zero matrix. Putting all these terms together, one has:

$$\mathbf{C}_{\mathbf{iq}}^{\mathbf{T}} = \begin{bmatrix} \mathbf{O}_t & -\mathbf{D}\mathbf{A}_r \\ -\mathbf{O}_t & \mathbf{D}\mathbf{A}_r \\ \mathbf{I}_p & \mathbf{O}_p \\ -\mathbf{I}_p & -\mathbf{O}_p \end{bmatrix}_{(2N+2I) \times (I+K-1)}$$

Finally, the associated inequality constraint vector  $\mathbf{b}_{\mathbf{iq}}$  can be similarly decomposed as follows:

$$\mathbf{b}_{\mathbf{iq}} = \begin{bmatrix} \mathbf{b}_t & \mathbf{b}_t & \mathbf{b}_{pL} & \mathbf{b}_{pU} \end{bmatrix}_{(2N+2I) \times 1}^{\mathbf{T}}$$

where

$$\mathbf{b}_t = \begin{bmatrix} -F_{\mathbf{BI}_1}^U & -F_{\mathbf{BI}_2}^U & \cdots & -F_{\mathbf{BI}_N}^U \end{bmatrix}_{N \times 1}^{\mathbf{T}}$$

$$\mathbf{b}_{pL} = \begin{bmatrix} P_{G1}^L & P_{G2}^L & \cdots & P_{GI}^L \end{bmatrix}_{I \times 1}^{\mathbf{T}}$$

$$\mathbf{b}_{pU} = \begin{bmatrix} -P_{G1}^U & -P_{G2}^U & \cdots & -P_{GI}^U \end{bmatrix}_{I \times 1}^{\mathbf{T}}$$

## 5.6 Illustrative Examples

### 5.6.1 A Three-Node Illustration

Consider the special case of a completely connected transmission grid consisting of three nodes  $\{1, 2, 3\}$ , three Generators, and three LSEs, with Generator  $k$  and LSE  $k$  located at node  $k$  for  $k = 1, 2, 3$ . This three-node case is depicted in Figure 5.1.

For this three-node case, the augmented DC OPF problem set out in Section 5.4.4 reduces to the following form:

**Minimize**

$$\sum_{i=1}^3 [A_i P_{Gi} + B_i P_{Gi}^2] + \pi \delta_2^2 + \pi \delta_3^2 + \pi [\delta_2 - \delta_3]^2 \quad (5.60)$$

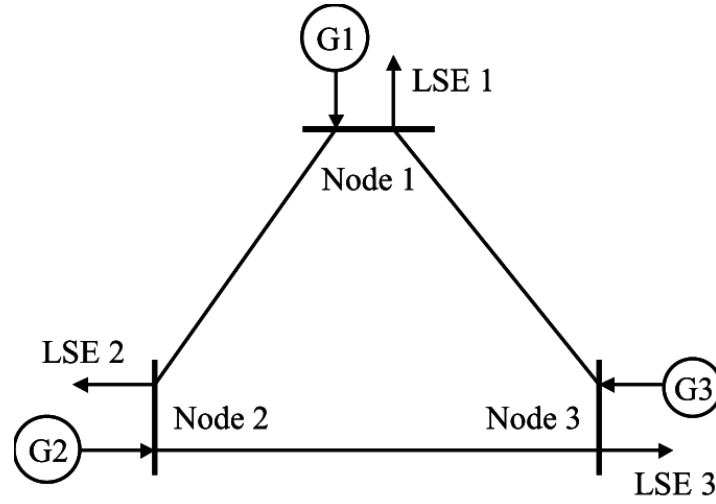


Figure 5.1 A Three-Node Transmission Grid

with respect to

$$P_{G1}, P_{G2}, P_{G3}, \delta_2, \delta_3$$

subject to:

Real power balance constraint for each node  $k = 1, \dots, 3$ :

$$P_{G1} + B_{12}\delta_2 + B_{13}\delta_3 = P_{L1} \quad (5.61)$$

$$P_{G2} - [B_{12} + B_{23}]\delta_2 + B_{23}\delta_3 = P_{L2} \quad (5.62)$$

$$P_{G3} + B_{23}\delta_2 - [B_{13} + B_{23}]\delta_3 = P_{L3} \quad (5.63)$$

Real power thermal constraints for each branch  $km \in \text{BR}$ :

$$B_{12}\delta_2 \geq -F_{12}^U \quad (5.64)$$



$$B_{13}\delta_3 \geq -F_{13}^U \quad (5.65)$$

$$-B_{23}\delta_2 + B_{23}\delta_3 \geq -F_{23}^U \quad (5.66)$$

$$-B_{12}\delta_2 \geq -F_{12}^U \quad (5.67)$$

$$-B_{13}\delta_3 \geq -F_{13}^U \quad (5.68)$$

$$B_{23}\delta_2 - B_{23}\delta_3 \geq -F_{23}^U \quad (5.69)$$

**Real power production constraints for each Generator  $i = 1, \dots, 3$ :**

$$P_{G1} \geq P_{G1}^L \quad (5.70)$$

$$P_{G2} \geq P_{G2}^L \quad (5.71)$$

$$P_{G3} \geq P_{G3}^L \quad (5.72)$$

$$-P_{G1} \geq -P_{G1}^U \quad (5.73)$$

$$-P_{G2} \geq -P_{G2}^U \quad (5.74)$$

$$-P_{G3} \geq -P_{G3}^U \quad (5.75)$$

Using the notation introduced in Section 5.5, the SCQP depiction for this three-node case is as follows:

Minimize

$$f(\mathbf{x}) = \frac{1}{2}\mathbf{x}^T\mathbf{G}\mathbf{x} + \mathbf{a}^T\mathbf{x} \quad (5.76)$$

with respect to

$$\mathbf{x} = [P_{G1}, P_{G2}, P_{G3}, \delta_2, \delta_3]_{(5 \times 1)}^T \quad (5.77)$$

subject to

$$\mathbf{C}_{\text{eq}}^T\mathbf{x} = \mathbf{b}_{\text{eq}} \quad (5.78)$$

$$\mathbf{C}_{\text{iq}}^T\mathbf{x} \geq \mathbf{b}_{\text{iq}} \quad (5.79)$$

where

$$\mathbf{G} = \begin{bmatrix} 2B_1 & 0 & 0 & 0 & 0 \\ 0 & 2B_2 & 0 & 0 & 0 \\ 0 & 0 & 2B_3 & 0 & 0 \\ 0 & 0 & 0 & 4\pi & -2\pi \\ 0 & 0 & 0 & -2\pi & 4\pi \end{bmatrix}_{(5 \times 5)}$$

$$\mathbf{a}^T = \begin{bmatrix} A_1 & A_2 & A_3 & 0 & 0 \end{bmatrix}_{(1 \times 5)}$$

$$\mathbf{C}_{\text{eq}}^T = \begin{bmatrix} 1 & 0 & 0 & B_{12} & B_{13} \\ 0 & 1 & 0 & -[B_{12} + B_{23}] & B_{23} \\ 0 & 0 & 1 & B_{23} & -[B_{13} + B_{23}] \end{bmatrix}_{(3 \times 5)}$$

$$\mathbf{b}_{\text{eq}} = \begin{bmatrix} P_{L1} & P_{L2} & P_{L3} \end{bmatrix}_{(3 \times 1)}^T$$

$$\mathbf{C}_{\text{iq}}^{\text{T}} = \begin{bmatrix} 0 & 0 & 0 & B_{12} & 0 \\ 0 & 0 & 0 & 0 & B_{13} \\ 0 & 0 & 0 & -B_{23} & B_{23} \\ 0 & 0 & 0 & -B_{12} & 0 \\ 0 & 0 & 0 & 0 & -B_{13} \\ 0 & 0 & 0 & B_{23} & -B_{23} \\ 1 & 0 & 0 & 0 & 0 \\ 0 & 1 & 0 & 0 & 0 \\ 0 & 0 & 1 & 0 & 0 \\ -1 & 0 & 0 & 0 & 0 \\ 0 & -1 & 0 & 0 & 0 \\ 0 & 0 & -1 & 0 & 0 \end{bmatrix}_{(12 \times 5)}$$

$$\mathbf{b}_{\text{iq}} = \begin{bmatrix} -F_{12}^U & -F_{13}^U & -F_{23}^U & -F_{12}^U & -F_{13}^U & -F_{23}^U & P_{G1}^L & P_{G2}^L & P_{G3}^L & -P_{G1}^U & -P_{G2}^U & -P_{G3}^U \end{bmatrix}_{(12 \times 1)}^{\text{T}}$$

Note that the first six rows in matrix  $\mathbf{C}_{\text{iq}}^{\text{T}}$  correspond to thermal inequality constraints and the next six rows correspond to power production inequality constraints.

### 5.6.2 A Five-Node Illustration

Now consider a five-node case for which the transmission grid is not completely connected. As depicted in Figure 5.2, let five Generators and three LSEs be distributed across the grid as follows: Generators 1 and 2 are located at node 1; LSE 1 is located at node 2; Generator 3 and LSE 2 are located at node 3; Generator 4 and LSE 3 are located at node 4; and Generator 5 is located node 5.

This information implies the following structural configuration for the transmission grid:

$$K = 5; I = 5; J = 3;$$

$$I_1 = \{G1, G2\}, I_2 = \{\emptyset\}, I_3 = \{G3\}, I_4 = \{G4\}, I_5 = \{G5\};$$



$$\mathbf{W} = 2\pi \begin{bmatrix} 3 & -1 & 0 & -1 & -1 \\ -1 & 2 & -1 & 0 & 0 \\ 0 & -1 & 2 & -1 & 0 \\ -1 & 0 & -1 & 3 & -1 \\ -1 & 0 & 0 & -1 & 2 \end{bmatrix}_{5 \times 5} \quad (5.81)$$

$$\mathbf{W}_{rr} = 2\pi \begin{bmatrix} 2 & -1 & 0 & 0 \\ 1 & 2 & -1 & 0 \\ 0 & -1 & 3 & -1 \\ 0 & 0 & -1 & 2 \end{bmatrix}_{4 \times 4} \quad (5.82)$$

The Generators' cost attribute matrix  $\mathbf{U}$  is:

$$\mathbf{U} = \text{diag} \left[ 2B_1 \quad 2B_2 \quad 2B_3 \quad 2B_4 \quad 2B_5 \right]_{5 \times 5} \quad (5.83)$$

The matrix  $\mathbf{B}'$  and its reduced form  $\mathbf{B}'_r$  are as follows:

$$\mathbf{B}' = \begin{bmatrix} B_{12} + B_{14} + B_{15} & -B_{12} & 0 & -B_{14} & -B_{15} \\ -B_{21} & B_{21} + B_{23} & -B_{23} & 0 & 0 \\ 0 & -B_{32} & B_{32} + B_{34} & -B_{34} & 0 \\ -B_{41} & 0 & -B_{43} & B_{41} + B_{43} + B_{45} & -B_{45} \\ -B_{51} & 0 & 0 & -B_{54} & B_{51} + B_{54} \end{bmatrix}_{5 \times 5} \quad (5.84)$$

$$\mathbf{B}'_r = \begin{bmatrix} -B_{21} & B_{21} + B_{23} & -B_{23} & 0 & 0 \\ 0 & -B_{32} & B_{32} + B_{34} & -B_{34} & 0 \\ -B_{41} & 0 & -B_{43} & B_{41} + B_{43} + B_{45} & -B_{45} \\ -B_{51} & 0 & 0 & -B_{54} & B_{51} + B_{54} \end{bmatrix}_{4 \times 5} \quad (5.85)$$

With a slight abuse of notation, the ordered list  $\mathbf{BI}$  of distinct transmission grid branches can be denoted as follows:

$$\mathbf{BI} = [(1, 2), (1, 4), (1, 5), (2, 3), (3, 4), (4, 5)]_{6 \times 1}^T \quad (5.86)$$

The adjacency matrix  $\mathbf{A}$  with entries of 1 for the “from” node and  $-1$  for the “to” node can be expressed as

$$\mathbf{A} = \begin{bmatrix} 1 & -1 & 0 & 0 & 0 \\ 1 & 0 & 0 & -1 & 0 \\ 1 & 0 & 0 & 0 & -1 \\ 0 & 1 & -1 & 0 & 0 \\ 0 & 0 & 1 & -1 & 0 \\ 0 & 0 & 0 & 1 & -1 \end{bmatrix}_{6 \times 5} \quad (5.87)$$

and its reduced form  $\mathbf{A}_r$  can be expressed as

$$\mathbf{A}_r = \begin{bmatrix} -1 & 0 & 0 & 0 \\ 0 & 0 & -1 & 0 \\ 0 & 0 & 0 & -1 \\ 1 & -1 & 0 & 0 \\ 0 & 1 & -1 & 0 \\ 0 & 0 & 1 & -1 \end{bmatrix}_{6 \times 4} \quad (5.88)$$

The matrix  $\mathbf{II}$  takes the form

$$\mathbf{II} = \begin{bmatrix} 1 & 1 & 0 & 0 & 0 \\ 0 & 0 & 0 & 0 & 0 \\ 0 & 0 & 1 & 0 & 0 \\ 0 & 0 & 0 & 1 & 0 \\ 0 & 0 & 0 & 0 & 1 \end{bmatrix}_{5 \times 5} \quad (5.89)$$

Finally, the matrix  $\mathbf{D}$  takes the form

$$\mathbf{D} = \text{diag} \left[ B_{12} \quad B_{14} \quad B_{15} \quad B_{23} \quad B_{34} \quad B_{45} \right]_{6 \times 6} \quad (5.90)$$

Using the above developments, the SCQP depiction for the augmented DC-OPF problem for this five-node case can be expressed as follows:

**Minimize**

$$f(\mathbf{x}) = \frac{1}{2} \mathbf{x}^T \mathbf{G} \mathbf{x} + \mathbf{a}^T \mathbf{x}$$

**with respect to**

$$\mathbf{x} = \begin{bmatrix} P_{G1} & P_{G2} & P_{G3} & P_{G4} & P_{G5} & \delta_2 & \delta_3 & \delta_4 & \delta_5 \end{bmatrix}_{9 \times 1}^T$$

**subject to**

$$\mathbf{C}_{\text{eq}}^T \mathbf{x} = \mathbf{b}_{\text{eq}}$$

$$\mathbf{C}_{\text{iq}}^T \mathbf{x} \geq \mathbf{b}_{\text{iq}}$$

where the input matrices and vectors  $\mathbf{G}$ ,  $\mathbf{a}^T$ ,  $\mathbf{C}_{\text{eq}}^T$ ,  $\mathbf{b}_{\text{eq}}$ ,  $\mathbf{C}_{\text{iq}}^T$ , and  $\mathbf{b}_{\text{iq}}$  take the following explicit forms:

$$\mathbf{G} = \text{blockDiag} \begin{bmatrix} \mathbf{U} & \mathbf{W}_{\text{rr}} \end{bmatrix}_{9 \times 9}$$

$$\mathbf{a}^T = \begin{bmatrix} A_1 & A_2 & A_3 & A_4 & A_5 & 0 & 0 & 0 & 0 \end{bmatrix}_{1 \times 9}$$

$$\mathbf{C}_{\text{eq}}^T = \begin{bmatrix} \mathbf{II} & -\mathbf{B}'^T \end{bmatrix}_{5 \times 9}$$

where

$\mathbf{B}'$  is defined as in (5.85)

$\mathbf{II}$  is defined as in (5.89)

$$\mathbf{b}_{\text{eq}} = \begin{bmatrix} 0 & P_{L1} & P_{L2} & P_{L3} & 0 \end{bmatrix}_{5 \times 1}^{\mathbf{T}}$$

$$\mathbf{C}_{\text{iq}}^{\mathbf{T}} = \begin{bmatrix} \mathbf{C}_{\text{t}}^{\mathbf{T}} & -\mathbf{C}_{\text{t}}^{\mathbf{T}} & \mathbf{C}_{\text{p}}^{\mathbf{T}} & -\mathbf{C}_{\text{p}}^{\mathbf{T}} \end{bmatrix}_{22 \times 9}^{\mathbf{T}}$$

where

$$\mathbf{C}_{\text{t}}^{\mathbf{T}} = \begin{bmatrix} \mathbf{O}_{\text{t}} & -\mathbf{D}\mathbb{A}_{\text{r}} \end{bmatrix}_{6 \times 9}$$

$\mathbf{O}_{\text{t}} = 6 \times 5$  zero matrix

$\mathbb{A}_{\text{r}}$  is defined as in (5.88)

$\mathbf{D}$  is defined as in (5.90)

$$\mathbf{C}_{\text{p}}^{\mathbf{T}} = \begin{bmatrix} \mathbf{I}_{\text{p}} & \mathbf{O}_{\text{p}} \end{bmatrix}_{5 \times 9}$$

$\mathbf{I}_{\text{p}} = 5 \times 5$  identity matrix

$\mathbf{O}_{\text{p}} = 5 \times 4$  zero matrix

$$\mathbf{b}_{\text{iq}} = \begin{bmatrix} \mathbf{b}_{\text{t}} & \mathbf{b}_{\text{t}} & \mathbf{b}_{\text{pL}} & \mathbf{b}_{\text{pU}} \end{bmatrix}_{22 \times 1}^{\mathbf{T}}$$

where

$$\mathbf{b}_{\text{t}} = \begin{bmatrix} -F_{12}^U & -F_{14}^U & -F_{15}^U & -F_{23}^U & -F_{34}^U & -F_{45}^U \end{bmatrix}_{6 \times 1}^{\mathbf{T}}$$

$$\mathbf{b}_{\text{pL}} = \begin{bmatrix} P_{G1}^L & P_{G2}^L & P_{G3}^L & P_{G4}^L & P_{G5}^L \end{bmatrix}_{5 \times 1}^{\mathbf{T}}$$



$$\mathbf{b}_{pU} = \left[ \begin{array}{ccccc} -P_{G1}^U & -P_{G2}^U & -P_{G3}^U & -P_{G4}^U & -P_{G5}^U \end{array} \right]_{5 \times 1}^T$$

## 5.7 QuadProgJ Input/Output and Logical Progression

The matrix form of a general SCQP problem is presented in Section 5.2. QuadProgJ accepts input in this matrix form. In particular, QuadProgJ can be directly used to solve any DC OPF problem expressed in this matrix form whether the DC OPF variables are expressed in standard SI units (e.g. ohms, megawatts,...) or in normalized per unit (pu) terms.

On the other hand, to help ensure numerical stability, it is customary when solving DC OPF problems to carry out all internal calculations in pu terms so that variables have roughly the same order of magnitude. The pu solution output is then often converted back into SI units for easier readability.

Consequently, to facilitate the application of QuadProgJ to DC OPF problems, we have developed an optional outer Java shell for QuadProgJ, referred to as *DCOPFJ*, that carries out the following data manipulations: (a) accepts DC OPF input data in SI units and converts it to pu; (b) uses this pu input data to form the SCQP matrix and vector expressions required by QuadProgJ; (c) invokes QuadProgJ to solve this SCQP problem; (d) converts the resulting pu solution output back into SI units.

Consider the augmented DC OPF problem set out in Section 5.4.4. The required input data for this problem, expressed in SI units, can be schematically depicted as follows:

(SI gridData, SI genData, SI lseData)

where

$$\begin{aligned}
\text{SI gridData} &= (\text{SI nodeData}, \text{SI branchData}) \\
\text{SI nodeData} &= (K, \pi) \\
\text{SI branchData} &= (\mathbf{BI}, p_{\mathbf{BI}_1}^U \dots p_{\mathbf{BI}_N}^U, X \text{ ohms}) \\
\text{SI genData} &= (I, I_1 \dots I_K, a_1 \dots a_I, b_1 \dots b_I, p_{G1}^L \dots p_{GI}^L, p_{G1}^U \dots p_{GI}^U) \\
\text{SI lseData} &= (J, J_1 \dots J_K, \sum_{j \in J_1} P_{Lj} \dots \sum_{j \in J_K} P_{Lj})
\end{aligned}$$

This SI input data is fed into DCOPFJ along with a base apparent power value  $S_o$  and a base voltage value  $V_o$ . The DCOPFJ shell first uses the base values to transform the SI input data into pu terms. Using the pu notation introduced in Section 5.4.1, this pu input data can be schematically depicted as follows:

$$(\text{pu gridData}, \text{pu genData}, \text{pu lseData})$$

where

$$\begin{aligned}
\text{pu gridData} &= (\text{pu nodeData}, \text{pu branchData}) \\
\text{pu nodeData} &= (K, \pi) \\
\text{pu branchData} &= (\mathbf{BI}, F_{\mathbf{BI}_1}^U \dots F_{\mathbf{BI}_N}^U, X \text{ pu}) \\
\text{pu genData} &= (I, I_1 \dots I_K, A_1 \dots A_I, B_1 \dots B_I, P_{G1}^L \dots P_{GI}^L, P_{G1}^U \dots P_{GI}^U) \\
\text{pu lseData} &= (J, J_1 \dots J_K, \sum_{j \in J_1} P_{Lj} \dots \sum_{j \in J_K} P_{Lj})
\end{aligned}$$

DCOPFJ next uses this pu input data to form the matrices and vectors  $(\mathbf{G}, \mathbf{a}, \mathbf{C}_{\text{eq}}, \mathbf{b}_{\text{eq}}, \mathbf{C}_{\text{iq}}, \mathbf{b}_{\text{iq}})$  as detailed in Section 5.5.3. It then feeds these matrix and vector components into the Quad-ProgJ solver to obtain a solution in pu terms. This pu solution can be expressed in the following vector form:

$$(P_{G1}^* \dots P_{GI}^*, \delta_2^* \dots \delta_K^*, \lambda_{\text{eq}}^*, \lambda_{\text{iq}}^*) \quad (5.91)$$

In this output vector,  $(P_{G1}^* \dots P_{GI}^*)$  denotes the vector of optimal pu real power production commitments in the day-ahead market for Generators  $i = 1, \dots, I$ , and  $(\delta_2^* \dots \delta_K^*)$  denotes the vector of optimal voltage angles (in radians) at nodes  $k = 2, \dots, K$  (omitting the reference node 1 where  $\delta_1$  is normalized to 0). The solution vector for the Lagrange multipliers corresponding to the equality constraints is contained in the  $K \times 1$  vector  $\lambda_{eq}^*$ . Since each of these multipliers is a shadow price corresponding to a nodal balance constraint in pu form,  $\lambda_{eq}^*$  provides the vector of Locational Marginal Prices (LMPs) in pu form.

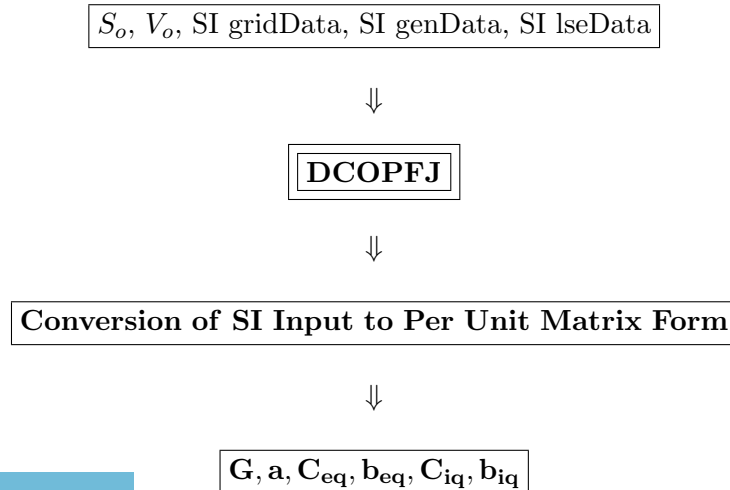
The solution vector for the Lagrange multipliers corresponding to the inequality constraints is contained in the  $(2N + 2I) \times 1$  vector  $\lambda_{iq}^*$ . These multipliers provide valuable additional sensitivity information, including “flow gate” prices (in pu) measuring the optimal cost reductions that would result from relaxations in the branch flow constraints.

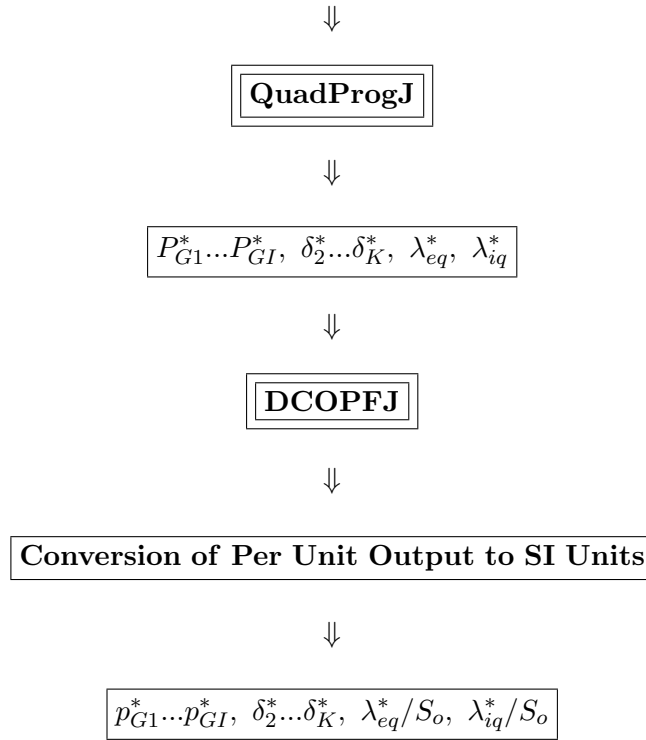
Finally, the pu solution (5.91) is fed back into DCOPFJ for conversion into SI units for reporting purposes. Recalling from Section 5.4.1 that pu real power terms are obtained from SI real power terms (in MWs) by dividing through by the base apparent power  $S_o$ , this SI output data can be schematically depicted as follows:

$$(p_{G1}^* \dots p_{GI}^*, \delta_2^* \dots \delta_K^*, \lambda_{eq}^*/S_o, \lambda_{iq}^*/S_o), \quad (5.92)$$

where the voltage angles  $\delta_k^*$  are still reported in radians.

In summary, the overall logical flow of the QuadProgJ program can be depicted as follows:





## 5.8 QP Test Results for QuadProgJ

### 5.8.1 Overview

QuadProgJ is an open-source plug-and-play Java SCQP solver newly developed by the authors. QuadProgJ implements the well-known dual active-set SCQP method developed by Goldfarb and Idnani (1983) in a numerically stable way by utilizing Cholesky decomposition and QR factorization. For ease of use, QuadProgJ modifies the original Goldfarb and Idnani method to permit the direct explicit imposition of equality as well as inequality constraints.

As with any dual active-set SCQP method (Fletcher, 1987, pp. 243-245), QuadProgJ proceeds as follows. In the first iteration all problem constraints are ignored and the tentative optimal solution is taken to be the unconstrained minimum (which exists by strict convexity of the objective function). A test is then made to see if any of the original problem constraints are violated. If so, one of these violated constraints is selected and added to the “active set,” i.e., the set of constraints to be imposed as equalities. A new optimal solution is then generated, subject to the active set of constraints, and again a test is made to see if any of the

original problem constraints are violated. If so, one is selected to be added to the active set (and a test is made to see if any of the previously active constraints should now be relaxed). A new constrained optimal solution is then generated. This process continues until no violated original problem constraints are found.

Compared to other QP methods, such as interior point and primal active-set QP methods, a dual active-set SCQP method such as QuadProgJ has two major advantages. First, it has a well-defined starting point: namely, the unconstrained minimum of the objective function. In contrast, other types of methods typically have to guess or search for a “good” starting point, which can be very costly in terms of actual computing time. Second, since there are only finitely many distinct permutations of the inequality constraints to determine which if any are active (binding), and each activated constraint leads to an increase in the current objective function value, a dual active-set SCQP method is guaranteed to terminate in a finite number of steps. Infinite looping can arise with other types of methods for reasons such as a flat starting point.

On the downside, however, QuadProgJ has two main limitations. First, QuadProgJ requires the QP objective function to be a strictly convex function.<sup>16</sup> Second, QuadProgJ does not incorporate sparse matrix techniques. Consequently, it is not designed to handle large-scale problems for which speed and efficiency of computations become critical limiting factors.

In this section a well-known repository of QP test cases is used to demonstrate the accuracy of QuadProgJ for small to medium-scale QP problems.

### 5.8.2 QP Test Case Results

The accuracy of QuadProgJ has been tested on a collection of small to medium-sized SCQP minimization problems included in the QP test case repository prepared by Maros and Mészáros (1997).<sup>17</sup> For each of these problems, the solution value for the minimized objective

<sup>16</sup>See Section 5.4.3.2 for brief notes on Lagrangian augmentation methods that can be used to induce strict convexity for convex QP objective functions. Solution algorithms designed to handle non-strictly convex QP problems have been developed by Boland (1997), Fletcher (1987), Powell (1983), and Stoer (1992).

<sup>17</sup>Detailed input and output data for the SCQP test cases are available online at: <http://www.sztaki.hu/~meszaros/public ftp/qpdata/>. Most of the test cases are in standard QPS format. The QPS format is an extension of the MPS format, which is the industrial standard format for linear

function obtained by QuadProgJ is compared against the corresponding solution value reported for BPMPD, a well-known QP solver implementing an interior-point algorithm.<sup>18</sup>

The general structure of these SCQP test cases is given in Table 5.3, along with the reported BPMPD solution values. Corresponding test case results for QuadProgJ are then reported in Table 5.4.<sup>19</sup> Specifically, Table 5.4 reports the relative difference (RD) between the minimum objective function value  $f^* = f(x^*)$  obtained by QuadProgJ and the minimum objective function value  $f_{BPMPD}$  attained by BPMPD, where

$$RD \equiv \frac{f^* - f_{BPMPD}}{|f_{BPMPD}|} \quad (5.93)$$

To help ensure a fair comparison,  $f^*$  has been rounded off to the same number of decimal places as  $f_{BPMPD}$ .

In addition, Table 5.4 reports tests conducted to check whether all equality and inequality constraints are satisfied at the minimizing solution  $x^*$  obtained by QuadProgJ. More precisely, for any given SCQP test case, the equality constraints take the form

$$\mathbf{C}_{eq}^T \mathbf{x} = \mathbf{b}_{eq} \quad (5.94)$$

and the inequality constraints take the form

$$\mathbf{C}_{iq}^T \mathbf{x} \geq \mathbf{b}_{iq} \quad (5.95)$$

Let TNEC denote the total number of equality constraints for this test case (i.e. the row dimension of  $\mathbf{C}_{eq}^T$ ), and let TNIC denote the total number of inequality constraints for this test case (i.e. the row dimension of  $\mathbf{C}_{iq}^T$ ). Also, let  $x^*$  denote the solution obtained by QuadProgJ for this test case.

The equality constraints for each SCQP test case are checked by computing the *Equality Constraint Error (ECE)* for this test case, defined to be the  $TNEC \times 1$  residual vector

$$ECE \equiv \mathbf{C}_{eq} \mathbf{x}^* - \mathbf{b}_{eq} \quad (5.96)$$

programming test cases.

<sup>18</sup>See the BPMPD web site for detailed information. URL: <http://www.sztaki.hu/~meszaros/bpmpd/>

<sup>19</sup>All of the results reported in Table 5.4 for QuadProgJ were obtained from runs on a laptop PC: namely, a Compaq Presario 2100 running under Windows XP SP2 (mobile AMD Athlon XP 2800+ 2.12 GHz, 496 MB of RAM). The reported results for the BPMPD solver are taken from Maros and Mészáros (1997), who do not identify the hardware platform on which the BPMPD solver runs were made.

Table 5.4 reports the mean and maximum of the absolute values of the components of this ECE vector for each SCQP test case, denoted by  $\text{Mean|ECE|}$  and  $\text{Max|ECE|}$  respectively.

Similarly, the inequality constraints for each SCQP test case are checked by computing the *Inequality Constraint Error (ICE)*, defined to be the  $\text{TNIC} \times 1$  residual vector

$$\text{ICE} \equiv \mathbf{C}_{\text{iq}}\mathbf{x}^* - \mathbf{b}_{\text{iq}} \quad (5.97)$$

Table 5.4 reports the *Number of Violated Inequality Constraints (NVIC)* for each SCQP test case, meaning the number of negative components in this ICE vector.

Table 5.3 SCQP Test Cases: Structural Attributes and BPMPD Solution Values

NAME <sup>a</sup>	TND <sup>b</sup>	TNEC <sup>c</sup>	TNIC <sup>d</sup>	TNC <sup>e</sup>	TN <sup>f</sup>	fBPMPD <sup>g</sup>
DUAL1	85	1	170	171	256	3.50129662E-02
DUAL2	96	1	192	193	289	3.37336761E-02
DUAL3	111	1	222	223	234	1.35755839E-01
DUAL4	75	1	150	151	226	7.46090842E-01
DUALC1	9	1	232	233	242	6.15525083E+03
DUALC5	8	1	293	294	302	4.27232327E+02
HS118	15	0	59	59	74	6.64820452E+02
HS21	2	0	5	5	7	-9.99599999E+01
HS268	5	0	5	5	10	5.73107049E-07
HS35	3	0	4	4	7	1.11111111E-01
HS35MOD	3	0	5	5	8	2.50000001E-01
HS76	4	0	7	7	11	-4.68181818E+00
KSIP	20	0	1001	1001	1021	5.757979412E-01
QPCBLEND	83	43	114	157	240	-7.84254092E-03
QPCBOEI1	384	9	971	980	1364	1.15039140E+07
QPCBOEI2	143	4	378	382	525	8.17196225E+06
QPCSTAIR	467	209	696	905	1372	6.20438748E+06
S268	5	0	5	5	10	5.73107049E-07
MOSARQP2	900	0	600	600	1500	-0.159748211E+04

<sup>a</sup>Case name (in QPS format), see Maros and Mészáros (1997) for a detailed description of the QPS format

<sup>b</sup>Total number of decision variables

<sup>c</sup>Total number of equality constraints

<sup>d</sup>Total number of inequality constraints

<sup>e</sup>Total number of constraints (equality and inequality).  $\text{TNC}=\text{TNEC}+\text{TNIC}$

<sup>f</sup>Total number of decision variables and constraints (problem size).  $\text{TN}=\text{TND}+\text{TNC}$

<sup>g</sup>Minimizing solution value obtained by the BPMPD solver on an unknown hardware platform

Based on the results presented in Table 5.4, it appears that the QuadProgJ solver has

Table 5.4 QuadProgJ Test Case Results

NAME	Mean ECE  <sup>a</sup>	Max ECE  <sup>b</sup>	NVIC <sup>c</sup>	f* <sup>d</sup>	RD <sup>e</sup>
DUAL1	0.0	0.0	0	3.50129657E-2	-1.42804239E-8
DUAL2	0.0	0.0	0	3.37336761E-2	0.0
DUAL3	6.66E-16	6.66E-16	0	1.35755837E-1	-1.47323313E-8
DUAL4	2.11E-15	2.11E-15	0	7.46090842E-1	0.0
DUALC1	2.40E-12	2.40E-12	0	6.15525083E+3	0.0
DUALC5	5.33E-15	5.33E-15	0	4.27232327E+2	0.0
HS118	NA <sup>f</sup>	NA	0	6.64820450E+2	-3.00833103E-9
HS21	NA	NA	0	-99.96	-1.00040010E-9
HS268	NA	NA	0	-5.47370291E-8	-1.09550926
HS35	NA	NA	0	1.11111111E-1	0.0
HS35MOD	NA	NA	0	2.50000000E-1	-4.00000009E-9
HS76	NA	NA	0	-4.68181818	0.0
KSIP	NA	NA	0	5.75797941E-1	0.0
QPCBLEND	5.66E-16	8.94E-15	0	-7.84254307E-3	-2.74145844E-7
QPCBOEI1	2.05E-6	9.58E-6	0	1.15039140E+7	0.0
QPCBOEI2	3.42E-6	1.37E-5	0	8.17196224E+6	-1.22369628E-9
QPCSTAIR	4.34E-7	6.01E-6	0	6.20438745E+6	-4.83528799E-9
S268	NA	NA	0	-5.47370291E-8	-1.09550926
MOSARQP2	NA	NA	—	OOME <sup>g</sup>	—

<sup>a</sup>Mean of the absolute values of the components of ECE (Equality Constraint Error)

<sup>b</sup>Maximum of the absolute values of the components of ECE

<sup>c</sup>Total number of violated inequality constraints

<sup>d</sup>Minimum objective function value as computed by QuadProgJ

<sup>e</sup>Relative difference  $[(f^* - f_{BPMPD}) / |f_{BPMPD}|]$  between the QuadProgJ and BPMPD solution values for the minimized objective function. A negative value indicates QuadProgJ improves on BPMPD.

<sup>f</sup>NA indicates “Not Applicable,” meaning there are no constraints of the indicated type.

<sup>g</sup>Out-of-Memory Error indicated by a run-time Java Exception: java.lang.OutOfMemoryError

an accuracy level slightly better than the BPMPD solver for small to medium-sized SCQP problems, that is, for SCQP problems for which the total number (TN) of decision variables plus constraints is less than 1500. This conclusion is supported by the observation that, for each of these test cases, the minimized objective function value  $f^* = f(x^*)$  obtained by QuadProgJ either equals or is strictly smaller than the corresponding minimized objective function value  $f_{BPMPD}$  obtained by BPMPD, with no indication that the QuadProgJ solution  $x^*$  violates any equality or inequality constraints.<sup>20</sup>

<sup>20</sup>Maros and Mészáros (1997) do not provide constraint checks for the BPMPD solutions reported in their repository.



Even in cases in which QuadProgJ improves on the BPMPD solution, however, the relative difference between the two solutions tends to be extremely small, generally on the order of  $10^{-7}$ . The only exceptions are the two cases HS268 and S268 where QuadProgJ appears to improve significantly on the BPMPD solver. HS268 and S268 are relatively simple SCQP minimization problems subject only to inequality constraints, none of which turns out to be binding at the optimal solution. Why the interior-point BPMPD solver appears to degrade in accuracy on such problems is unclear.

All in all, QuadProgJ either matches or improves on the BPMPD solutions for all of the small and medium-sized SCQP test cases reported in Table 5.4, i.e. for all of the test cases for which TN (the total number of constraints plus decision variables) is less than 1500. Since the BPMPD solver has been in use since 1998, and is considered to have a proven high quality for solving QP problems, this finding suggests that QuadProgJ is at least as accurate a solver as BPMPD for SCQP problems of this size.

As noted previously, however, QuadProgJ is not designed for large-scale problems. The test results presented in Table 5.4 show that an out-of-memory error was triggered when an attempt was made to use QuadProgJ to solve test case MOSARQP2 with size  $TN = 1500$ . Whether this finding reflects an intrinsic limitation of QuadProgJ or is simply a desktop limitation that could be ameliorated by installing additional memory or by using a different hardware platform is an issue requiring further study.

## 5.9 DC OPF Test Case Results

### 5.9.1 Overview

In this section, QuadProgJ is used to solve illustrative three-node and five-node DC OPF test cases taken from power systems texts and ISO-NE/MISO/PJM training manuals.

Each of these DC OPF test cases is solved by invoking QuadProgJ through the outer Java shell DCOPFJ. Specifically, given SI input data and base apparent power and base voltage values as detailed in Section 5.7, DCOPFJ invokes QuadProgJ to solve for optimal real power injections, real power branch flows, voltage angles, LMPs, total variable costs, and various

other output values. In particular, DCOPFJ automates the conversion of SI data to pu form for internal calculations and forms all needed matrix/vector representations.

These illustrative DC OPF test cases raise intriguing economic issues concerning the ISO operation of wholesale power markets in the presence of constraints on branch flows and production levels. The information content of LMPs in relation to these constraints is of particular interest. For the study at hand, however, these test cases are simply used to illustrate concretely the capability of QuadProgJ to generate detailed DC OPF solution values. The systematic study and interpretation of DC OPF solutions generated via QuadProgJ in the context of carefully constructed experimental designs is left for future studies.

The section concludes with a separate reporting of sensitivity results for the soft penalty weight  $\pi > 0$  for both the three-node and five-node DC OPF test cases. These results demonstrate that the DC OPF solution values depend on the value of  $\pi$  in the expected way. The magnitude of the summed voltage angle differences is inversely related to the magnitude of  $\pi$ . However, for sufficiently small  $\pi$  the sensitivity of the DC OPF solution values to further decreases in  $\pi$  becomes negligible. Moreover, no numerical instability or convergence problems were detected at any of these tested  $\pi$  values.

### 5.9.2 Three-Node Test Results

Table 5.5 provides SI input as well as base apparent power and base voltage levels  $S_o$  and  $V_o$  for a day-ahead wholesale power market operating over a three-node transmission grid as depicted in Figure 5.1. The daily (24 hour) load distribution for the day-ahead market is depicted in Figure 5.3. Note that LSE 2 and LSE 3 have identical load profiles. In addition, Generator 1 has the least expensive cost (as measured by the cost attributes  $a$  and  $b$ ), and Generator 2's cost is between the cost of Generator 1 and Generator 3. This input data is adopted from Tables 8.2-8.4 (p. 297) in Shahidehpour et al. (2002).<sup>21</sup>

Tables 5.6-5.7 present DC OPF solution results in SI units for this day-ahead market for

<sup>21</sup>Unfortunately, Shahidehpour et al. (2002) do not provide corresponding DC OPF solution values that could be used to compare against QuadProgJ solution values. Their focus is on the derivation of unit commitment schedules subject to additional security constraints that help to ensure reliability in the event of line outages.

24 successive hours. Specifically, Table 5.6 reports solution values for the real power injection  $p_{G_i}^*$  for each Generator  $i$ , the optimal voltage angle  $\delta_k^*$  for each non-reference node  $k$ , and the LMP ( $\lambda_{e_{qk}}^*/S_o$ ) for each node  $k$ . Table 5.7 reports solution values for the twelve inequality constraint multipliers, the first six corresponding to thermal limits on branch flows and the final six corresponding to lower and upper bounds on production levels. Also reported in this table are the solution values for real power branch flows.

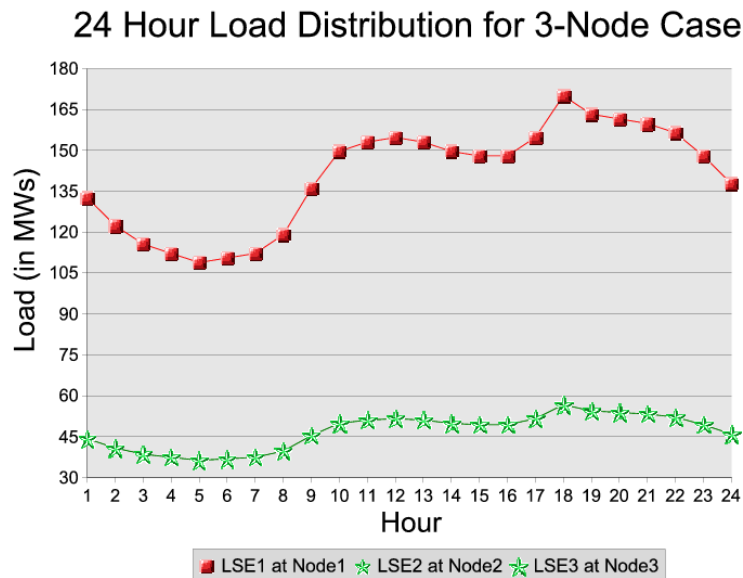


Figure 5.3 24 Hour Load Distribution for a 3-Node Case

As seen in Table 5.7, the branch flow multipliers are all zero. This means there are no binding branch flow constraints, hence no branch congestion that would force higher-cost Generators to be dispatched prior to lower-cost Generators. Consequently, one would expect to see Generator 1 used to meet load demand as much as possible. Generator 2 should only produce more than its minimum production level when the load demand is so high that it exceeds the maximum production level of Generator 1, and Generator 3 should only produce more

than its minimum production level when load demand is so high that it exceeds the maximum production level of Generator 2.

The solution results reported in Table 5.6 are consistent with these theoretical predictions. Examining the output columns for  $p_{G1}^*$ ,  $p_{G2}^*$ , and  $p_{G3}^*$ , one sees the following pattern. For the low-demand off-peak hours (i.e. hours 02-08), Generator 1 is supplying as much of the load as possible; Generator 2 and Generator 3 are producing at their minimum production levels (10 MWs and 5 MWs, respectively). In contrast, for the high-demand peak hours (i.e. hours 01 and 09-24), Generator 1 is producing at its maximum production level (200 MWs) and Generator 2's production exceeds its minimum production level (10Mws). This clearly shows that dispatch priority is being based on cost attributes.

The column "minTVC" in Table 5.6 reports minimized total variable cost for each hour summed across all Generators. For the three-node example at hand, which has three Generators,

$$\text{minTVC} = \sum_{i=1}^3 [a_i \cdot p_{G_i}^* + b_i \cdot p_{G_i}^{*2}] \quad (5.98)$$

As expected, minTVC changes hour by hour to reflect changes in the corresponding load; compare the daily load profile depicted in Figure 5.3.

Another important consistency check follows from the observation, made above, that all of the branch flow multipliers in Table 5.7 are zero, indicating the absence of any branch congestion. The absence of branch congestion implies that the LMPs should be the same across all nodes for each hour. This is verified by output columns  $LMP_1$ ,  $LMP_2$ , and  $LMP_3$  in Table 5.6.

Finally, Table 5.7 reports six multiplier values corresponding to six real power production constraints, two (lower and upper) for each of the three Generators. These multiplier values are entirely consistent with the results in Table 5.6. For example, the multiplier value associated with the minimum (lower) production level for Generator 3 is strictly positive for each hour, which is consistent with the result in Table 5.6 that Generator 3 is scheduled to produce at its minimum production level (5 MWs) for each hour.

### 5.9.3 Five-Node Test Results

Table 5.8 presents SI input data for a day-ahead wholesale power market operating over a five-node transmission grid as depicted in Figure 5.2.<sup>22</sup> The daily (24 hour) load distribution in SI units for the day-ahead market is depicted in Figure 5.4. Tables 5.9-5.13 report the optimal solution values in SI units for real power production levels, voltage angles, LMP values, minimum total variable cost, inequality constraint multipliers, and branch flows for 24 successive hours in the day-ahead market.

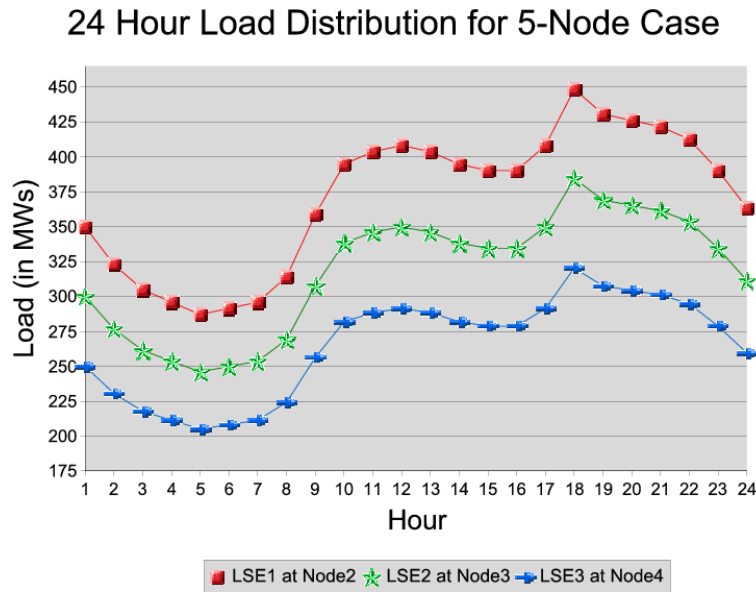


Figure 5.4 24 Hour Load Distribution for a 5-Node Case

In contrast to the three-node case, this five-node case exhibits branch congestion. Specifically, branch congestion occurs between node 1 and node 2 (and only these nodes) in each of the 24 hours. This can be verified directly by column  $P_{12}$  in Table 5.13, which shows that the real power flow  $P_{12}$  on branch  $km = 12$  is at its upper thermal limit (250 MWs) for each hour.

<sup>22</sup>The transmission grid, reactances, and locations of Generators and LSEs for this 5-node example are adopted from an example developed by John Lally (2002) for the ISO-NE that is now included in training manuals prepared by the ISO-NE (2006), the MISO (2006), and PJM (2006). The general shape of the LSE load profiles is adopted from a 3-node example presented in Shahidehpour et al. (2002, pp. 296-297).

It can also be verified indirectly by column “12” in Table 5.11, which shows that the thermal inequality constraint multiplier for branch  $km = 12$  is positively valued for each hour, indicating a binding constraint. The direct consequence of this branch congestion is the occurrence of widespread LMP separation, i.e. the LMP values differ across all nodes for each hour. This can be verified by examining output columns LMP<sub>1</sub>-LMP<sub>5</sub> in Table 5.10.

Examining this LMP data more closely, it is seen that LMP<sub>2</sub> and LMP<sub>3</sub> (the LMPs for nodes 2 and 3) exhibit a sharp change in hour 18, increasing between hour 17 and hour 18 by about 100% and then dropping back to “normal” levels in hour 19 and beyond. Interesting, this type of sudden spiking in LMP values is also observed empirically in MISO’s Dynamic LMP Contour Map<sup>23</sup> for real-time market prices, which is updated every five minutes.

This rather dramatic LMP peaking in hour 18 can be traced to several factors. First, as seen in Figure 5.4, the load profile for each LSE peaks at hour 18. Second, when solving the DC OPF problem to meet the high load in hour 18, the ISO has to take into consideration the maximum production limit for Generator 3 as well as the thermal inequality constraint between node 1 and node 2. Both of these constraints turn out to be binding. Specifically, as seen in Table 5.9, Generator 3 is dispatched in hour 18 at its maximum production limit (520 MWs); and, as seen in Table 5.13, the real power flow in branch  $km = 12$  is at its upper limit (250 MWs) for all 24 hours. Given the configuration of the transmission grid, to meet the hour 18 peak load the ISO is forced to back down (relative to hour 17) the less expensive production of Generators 1 and 2 and to use instead the more expensive production of the “peaker” Generator 4.

After the peak hour 18, the load returns to lower levels. The ISO is then able to dispatch Generator 1 and Generator 2 at their more “normal” levels, with Generator 1 at its upper production limit, and to avoid dispatching any production from generation 4; note from Table 5.8 that the minimum production level of Generator 4 is 0. Furthermore, the LMPs drop back to their more normal levels after hour 18.

<sup>23</sup><http://www.midwestmarket.org/page/LMP%20Contour%20Map%20&%20Data>

#### 5.9.4 II Sensitivity Test Results

Sensitivity tests were conducted to check the extent to which the solution values reported in Sections 5.9.2 and 5.9.3 for the three-node and five-node DC OPF test cases depend on the specific choice of the soft penalty weight  $\pi$ .

For the three-node case, a separate solution set was generated for each of the following five  $\pi$  values: 100, 10, 1, 0.1 and 0.01. These five solution sets are reported in Tables 5.14-5.18. These solution results show that decreasing the value of  $\pi$  over the tested range from 100 to 0.01 had little impact on the resulting solution values. The only perceptible changes at the reported precision level (four decimal places) were in the LMP values in their second and higher decimal places. Moreover, the LMP values stabilized through two decimal places (i.e. to values rounded off to pennies) once  $\pi$  decreased to the level 1.0.

Tables 5.19 and 5.20 report the sum of squared voltage angle differences for the three-node and five-node DC OPF test cases as the soft penalty weight  $\pi$  is decreased in value from 100 to 0.01. As can be seen, these sums are extremely small: namely, about  $10^{-15}$  in magnitude for the three-node case and about  $10^{-7}$  in magnitude for the five-node case. In the three-node case, any change in these sums in response to the changes in the value of  $\pi$  are below visibility in the reported data. In the five-node case, however, the sums are seen to increase slightly as the value of  $\pi$  decreases, which is the expected result of decreasing the penalty attached to the sum.

Also as expected, the sum of squared voltage angle differences increases with an increase in nodes from three to five for each tested value of  $\pi$ . This suggests that a researcher might need to tailor the value of  $\pi$  to the problem at hand in order to achieve a desired degree of smallness for voltage angle differences. In addition, in some situations it might be desirable to introduce individual weights on the voltage angle differences instead of using a common weight  $\pi$ , e.g. in order to represent transmission grid losses. This could easily be accomplished by a simple respecification of the weight matrix  $\mathbf{W}$  in (5.43).

## 5.10 Concluding Remarks

Restructured electricity markets are extraordinarily complex. For example, restructured wholesale power markets in the U.S. typically involve spot and forward energy markets operated by ISO/RTOs over AC transmission grids subject to congestion effects. As reported by Joskow (2006, Table 1), over 50% of the generation capacity in the U.S. is now operating under this market design, and other regions of the U.S. are moving towards this form of organization.

The complexity of restructured electricity markets essentially forces electricity researchers to resort to computational methods of analysis. Unfortunately, much of the software currently available for computational electricity modeling is commercial and hence proprietary. This restricts the ability of electricity researchers to publish self-sufficient studies permitting full access to implementation.

A key stumbling block to developing open-source software for general academic research into restructured electricity markets is the need to model the AC/DC optimal power flow (OPF) problems that must repeatedly be solved by ISO/RTO operators in order to generate daily unit commitment and dispatch schedules, as well as locational marginal prices (LMPs), for both spot and forward energy markets. Developing algorithms for the successful solution of optimization problems involving mixed collections of equality and inequality constraints, even when specialized to quadratic objective functions (as in DC OPF approximations to AC OPF problems), is a daunting task full of pitfalls for the unwary.

This study reports the development of QuadProgJ, an open-source plug-and-play Java solver for strictly convex quadratic programming (SCQP) problems that can be applied to standard DC OPF problems for research and training purposes. QuadProgJ implements the well-known dual active-set SCQP algorithm developed by Goldfarb and Idnani (1983). The accuracy of QuadProgJ is demonstrated by means of comparative results for a well-known suite of QP test problems with up to 1500 decision variables plus constraints.

In addition, this study proposes a physically meaningful augmentation of the standard DC OPF problem that permits the direct generation of solution values for LMPs, voltage angles, and voltage angle differences together with real power injections and branch flows. Three-node



and five-node test cases are used to demonstrate how QuadProgJ, coupled with a Java outer shell DCOPFJ, can be used to directly generate complete solution values for this augmented DC OPF problem. In particular, DCOPFJ automates the SI/pu conversion and matrix/vector representation of all needed input data for this augmented DC OPF problem.

### 5.11 References

- Anderson, Paul (1995), *Analysis of Faulted Power Systems*, Wiley-IEEE Press, New York.
- Boland, Natasha L. (1997), "A Dual-Active-Set Algorithm for Positive Semi-Definite Quadratic Programming," *Mathematical Programming* 78, 1-27.
- CAISO (2003), "Locational Marginal Pricing (LMP) Study: Analysis of Cost-Based Differentials," *Market Design 2002*, CAISO Market Operations, California ISO, February 4 release.
- FERC (2003), *Notice of White Paper*, U.S. Federal Energy Regulatory Commission, April.
- Fletcher, Roger (1987), *Practical Methods of Optimization*, Second Edition, John Wiley & Sons, New York.
- Goldfarb, Donald, and Ashok Udhawdas Idnani (1983), "A Numerically Stable Dual Method for Solving Strictly Convex Quadratic Programs," *Mathematical Programming* 27, 1-33.
- Gönen, Turan (1988), *Modern Power System Analysis*, Wiley-Interscience, John Wiley & Sons, Inc., New York.
- Hogan, William W. (2002), "Financial Transmission Rights Formulations," Report, Center for Business and Government, John F. Kennedy School of Government, Harvard University, Cambridge, MA.
- ISO-NE (2006), Home Page, ISO New England, Inc., accessible at <http://www.iso-ne.com/>
- ISO-NE (2003), Standard Market Design Reference Guide, ISO New England, Inc., 45pp. Available at <http://www.iso-ne.com/smd/>

Joskow, Paul (2006), "Markets for Power in the United States: An Interim Assessment," *The Energy Journal*, Vol. 27(1), 1-36.

Kirschen, Daniel S., and Goran Strbac (2004), *Fundamentals of Power System Economics*, John Wiley & Sons, Ltd.

Koesrindartoto, Deddy, and Leigh Tesfatsion (2004), "Testing the Economic Reliability of FERC's Wholesale Power Market Platform: An Agent-Based Computational Approach," *Energy, Environment, and Economics in a New Era*, Proceedings of the 24th USAEE/IAEE North American Conference, Washington, D.C., July 8-10.

Koesrindartoto, Deddy, Junjie Sun, and Leigh Tesfatsion (2005), "An Agent-Based Computational Laboratory for Testing the Economic Reliability of Wholesale Power Market Designs," *Proceedings*, Vol. 1, IEEE Power Engineering Society General Meeting, San Francisco, CA, June 2005, pp. 931-936.

Lally, John (2002), "Financial Transmission Rights: Auction Example," Section 6, M-06 Financial Transmission Rights Draft 01-10-02, ISO New England, Inc., January.

Maros, Istvan, and Csaba Meszaros (1997), "A Repository of Convex Quadratic Programming Problems," Department Technical Report DOC 97/6, Department of Computing, Imperial College, London, U.K.

McCalley, James D. (2006), "The Power Flow Equations," Lecture Notes, Department of Electrical Engineering, Iowa State University.

MISO (2006), Home Page, Midwest ISO, Inc., accessible at <http://www.midwestiso.org/>

Overbye, Thomas J., Xu Cheng, and Yan Sun (2004), "A Comparison of the AC and DC Power Flow Models for LMP Calculations," *Proceedings*, 37th Hawaii International Conference on System Sciences. <http://csdl.computer.org/comp/proceedings/hicss/>

PJM (2006), PJM Home Page, accessible at [www.pjm.com](http://www.pjm.com) .

Powell, Michael J. D. (1983), “ZQPCVX: A Fortran Subroutine for Convex Quadratic Programming,” Technical Report DAMTP/1983/NA17, Department of Applied Mathematics and Theoretical Physics, University of Cambridge, England.

Shahidehpour, Mohammad, Hatim Yamin, and Zuyi Li (2002), *Market Operations in Electric Power Systems*, IEEE/Wiley-Interscience, John Wiley & Sons, Inc., New York.

Stoer, Josef (1992), “A Dual Algorithm for Solving Degenerate Linearly Constrained Linear Least Squares Problems,” *J. of Numerical Linear Algebra with Applications* 1, 103-131.

Sun, Junjie and Leigh Tesfatsion (2006), “Dynamic Testing of Wholesale Power Market Designs: An Agent-Based Computational Approach”, presented at the International Industrial Organization Conference, Northeastern University, Boston, MA, April 8.

Wood, Allen J., and Bruce F. Wollenberg (1996), *Power Generation, Operation, and Control*, Second Edition, John Wiley & Sons, Inc., New York.

## 5.12 Appendix

### 5.12.1 Appendix A: Derivation of Power Flow Branch Equations

Recall from Section 5.4.1 that equations for the flow of real and reactive power in any transmission grid branch  $km$  ( $k \neq m$ ) are depicted as follows:

$$P_{km} = V_k^2 g_{km} - V_k V_m [g_{km} \cos(\delta_k - \delta_m) + b_{km} \sin(\delta_k - \delta_m)] \quad (5.99)$$

$$Q_{km} = -V_k^2 b_{km} - V_k V_m [g_{km} \sin(\delta_k - \delta_m) - b_{km} \cos(\delta_k - \delta_m)] \quad (5.100)$$

This appendix provides a rigorous derivation of these equations from Ohm’s Law.

#### A.1 Preliminary: The Relationship Between Impedance and Admittance

Using standard notational conventions, the impedance  $z$  on a transmission grid branch is expressed as

$$z = r + jx \quad (\text{impedance} = \text{resistance} + \sqrt{-1} \text{ reactance}) \quad (5.101)$$

and the admittance  $y$  on a transmission grid branch is expressed as

$$y = g + jb \quad (\text{admittance} = \text{conductance} + \sqrt{-1} \text{ susceptance}) \quad (5.102)$$

Since  $y = 1/z$ , it follows that

$$y = \frac{1}{z} = \frac{1}{r + jx} = \frac{r}{r^2 + x^2} + j \frac{-x}{r^2 + x^2} \quad (5.103)$$

Thus,

$$g = \frac{r}{r^2 + x^2}$$

$$b = \frac{-x}{r^2 + x^2}$$

## A.2 Derivation of Equations (5.99) and (5.100)

The following derivation<sup>24</sup> is based on Gönen (1988, (2.4)). Boldface letters denote complex variables while letters in normal font denote real variables. Also, the following trigonometric identities will be used in this derivation:

$$\cos(\alpha - \beta) = \cos \alpha \cos \beta + \sin \alpha \sin \beta$$

$$\sin(\alpha - \beta) = \sin \alpha \cos \beta - \cos \alpha \sin \beta$$

Let  $km$  denote any transmission grid branch, and let  $\mathbf{S}_{km}$  (in MVA) denote the complex power flowing in this branch. This complex power can be represented as

$$\mathbf{S}_{km} = P_{km} + jQ_{km} = \mathbf{V}_k \mathbf{I}_{km}^* \quad (5.104)$$

where

$$j = \sqrt{-1}$$

$$\mathbf{V}_k = V_k \cos \delta_k + jV_k \sin \delta_k$$

$$\mathbf{I}_{km} = \text{Current (in Amperes) on branch } km$$

$$\mathbf{I}_{km}^* = \text{Complex conjugate of } \mathbf{I}_{km}$$

<sup>24</sup>Recall from Section 5.3.2 that all transformer tap ratios are assumed to be 1, and all transformer phase angle shifts and line-charging capacitances are assumed to be 0. For an alternative derivation of the power flow equations that permits general settings for these variables, see Hogan (2002, Appendix).

By Ohm's Law in AC settings,

$$\mathbf{I}_{km} = \frac{\mathbf{V}_k - \mathbf{V}_m}{\mathbf{z}_{km}} \quad (5.105)$$

where the impedance  $\mathbf{z}_{km}$  on branch  $km$  can be expressed as

$$\mathbf{z}_{km} = r_{km} + jx_{km}$$

The complex conjugate of the impedance  $\mathbf{z}_{km}^*$  is then written as

$$\mathbf{z}_{km}^* = r_{km} - jx_{km}$$

Consequently,  $\mathbf{S}_{km}$  can be written as:

$$\begin{aligned} \mathbf{S}_{km} &= \mathbf{V}_k \frac{\mathbf{V}_k^* - \mathbf{V}_m^*}{\mathbf{z}_{km}^*} \\ &= [V_k \cos \delta_k + jV_k \sin \delta_k] \frac{[V_k \cos \delta_k - jV_k \sin \delta_k] - [V_m \cos \delta_m - jV_m \sin \delta_m]}{r_{km} - jx_{km}} \\ &= \frac{[V_k^2 \cos^2 \delta_k + V_k^2 \sin^2 \delta_k] - V_k [\cos \delta_k + j \sin \delta_k] V_m [\cos \delta_m - j \sin \delta_m]}{r_{km} - jx_{km}} \\ &= \frac{V_k^2 - V_k V_m [(\cos \delta_k \cos \delta_m + \sin \delta_k \sin \delta_m) + j(\sin \delta_k \cos \delta_m - \cos \delta_k \sin \delta_m)]}{r_{km} - jx_{km}} \\ &= \frac{V_k^2 - V_k V_m [\cos(\delta_k - \delta_m) + j \sin(\delta_k - \delta_m)]}{r_{km} - jx_{km}} \quad (\text{Let } \theta = \delta_k - \delta_m) \\ &= \frac{[r_{km} + jx_{km}]V_k^2 - [r_{km} + jx_{km}]V_k V_m [\cos \theta + j \sin \theta]}{[r_{km} + jx_{km}][r_{km} - jx_{km}]} \\ &= \frac{r_{km}V_k^2 - V_k V_m [r_{km} \cos \theta - x_{km} \sin \theta]}{r_{km}^2 + x_{km}^2} + j \frac{x_{km}V_k^2 - V_k V_m [r_{km} \sin \theta + x_{km} \cos \theta]}{r_{km}^2 + x_{km}^2} \\ &= (V_k^2 g_{km} - V_k V_m [g_{km} \cos \theta + b_{km} \sin \theta]) + j (-V_k^2 b_{km} - V_k V_m [g_{km} \sin \theta - b_{km} \cos \theta]) \\ &= P_{km} + jQ_{km} \end{aligned}$$

Hence, we can infer that (5.99) and (5.100) hold.

### 5.12.2 Appendix B: Expressing DC OPF Voltage Angles as a Linear Affine Function of Real Power Injections

This section establishes that the vector of non-reference voltage angles in the standard DC OPF problem in pu form presented in Section 5.4.2 can be expressed as a linear affine function of the vector of real power injections.

The basic equations to consider are the real power nodal balance constraints (5.26) for  $k = 2, \dots, K$  together with the normalization  $\delta_1 = 0$  imposed on the reference node voltage angle  $\delta_1$  by constraint (5.33). When the nodal balance constraint for any node  $k \geq 2$  is expressed solely in terms of voltage angles, real power injections, and real power loads, it takes the following form:

$$\sum_{i \in I_k} P_{Gi} - \sum_{km \text{ or } mk \in BR} B_{km} [\delta_k - \delta_m] = \sum_{j \in J_k} P_{Lj} \quad (5.106)$$

This collection of nodal balance constraints for  $k = 2, \dots, K$  can equivalently be expressed in matrix form as follows:

$$\mathbf{PNetInject} = \mathbf{B}'_{rr} \delta \quad (5.107)$$

where  $\mathbf{PNetInject}$  denotes the  $(K-1) \times 1$  vector of net nodal real power injections  $\mathbf{PNetInject}_k$  for nodes  $k = 2, \dots, K$ , and  $\mathbf{B}'_{rr}$  denotes the bus admittance matrix  $\mathbf{B}'$  in (5.51) with its first row and first column eliminated (corresponding to the reference node 1). For concrete illustration, equation (5.107) for the 5-node test case presented in Section 5.6.2 takes the following specific form:

$$\begin{bmatrix} 0 - P_{L1} \\ P_{G3} - P_{L2} \\ P_{G4} - P_{L3} \\ P_{G5} - 0 \end{bmatrix} = \begin{bmatrix} B_{21} + B_{23} & -B_{23} & 0 & 0 \\ -B_{32} & B_{32} + B_{34} & -B_{34} & 0 \\ 0 & -B_{43} & B_{41} + B_{43} + y_{45} & -B_{45} \\ 0 & 0 & -B_{54} & B_{51} + B_{54} \end{bmatrix}_{4 \times 4} \begin{bmatrix} \delta_2 \\ \delta_3 \\ \delta_4 \\ \delta_5 \end{bmatrix} \quad (5.108)$$

Since the matrix  $\mathbf{B}'_{rr}$  is invertible by construction, we have the following relationship between the voltage angles and the net nodal power injections:

$$\delta = [\mathbf{B}'_{rr}]^{-1} \mathbf{PNetInject} \quad (5.109)$$

In terms of the 5-node test case, equation (5.109) takes the following form:

$$\begin{bmatrix} \delta_2 \\ \delta_3 \\ \delta_4 \\ \delta_5 \end{bmatrix} = \begin{bmatrix} B_{21} + B_{23} & -B_{23} & 0 & 0 \\ -B_{32} & B_{32} + B_{34} & -B_{34} & 0 \\ 0 & -B_{43} & B_{41} + B_{43} + y_{45} & -B_{45} \\ 0 & 0 & -B_{54} & B_{51} + B_{54} \end{bmatrix}_{4 \times 4}^{-1} \begin{bmatrix} 0 - P_{L1} \\ P_{G3} - P_{L2} \\ P_{G4} - P_{L3} \\ P_{G5} - 0 \end{bmatrix} \quad (5.110)$$

The net nodal power injection vector  $\mathbf{PNetInject}$  can be further decomposed into a linear affine function of the real power injection vector  $\mathbf{P}_G = (P_{G1}, \dots, P_{GI})^T$  as follows:

$$\mathbf{PNetInject} = \mathbf{R}\mathbf{P}_G + \beta \quad (5.111)$$

where  $\mathbf{R}$  is a  $(K - 1) \times I$  matrix and  $\beta$  is a  $(K - 1) \times 1$  vector defined as follows

$$\mathbf{R} = \begin{bmatrix} \mathbb{I}(1 \in I_2) & \mathbb{I}(2 \in I_2) & \cdots & \mathbb{I}(I \in I_2) \\ \mathbb{I}(1 \in I_3) & \mathbb{I}(2 \in I_3) & \cdots & \mathbb{I}(I \in I_3) \\ \vdots & \vdots & \ddots & \vdots \\ \mathbb{I}(1 \in I_K) & \mathbb{I}(2 \in I_K) & \cdots & \mathbb{I}(I \in I_K) \end{bmatrix}_{(K-1) \times I} \quad (5.112)$$

where

$$\mathbb{I}(i \in I_k) = \begin{cases} 1 & \text{if } i \in I_k \\ 0 & \text{if } i \notin I_k \end{cases}$$

$$\beta = \left[ -\sum_{j \in J_2} P_{Lj} \quad -\sum_{j \in J_3} P_{Lj} \quad \cdots \quad -\sum_{j \in J_K} P_{Lj} \right]_{(K-1) \times 1}^T \quad (5.113)$$

Again using the 5-node test case for concrete illustration, we can write out equation (5.111) as

$$\begin{bmatrix} 0 - P_{L1} \\ P_{G3} - P_{L2} \\ P_{G4} - P_{L3} \\ P_{G5} - 0 \end{bmatrix} = \begin{bmatrix} 0 & 0 & 0 & 0 & 0 \\ 0 & 0 & 1 & 0 & 0 \\ 0 & 0 & 0 & 1 & 0 \\ 0 & 0 & 0 & 0 & 1 \end{bmatrix} \begin{bmatrix} P_{G1} \\ P_{G2} \\ P_{G3} \\ P_{G4} \\ P_{G5} \end{bmatrix} + \begin{bmatrix} -P_{L1} \\ -P_{L2} \\ -P_{L3} \\ 0 \end{bmatrix} \quad (5.114)$$

Finally, combining (5.109) and (5.111), we see that it is possible to solve explicitly for the voltage angle vector  $\delta$  as a linear affine function of the real power injection vector  $\mathbf{P}_G$ : namely,

$$\delta = \mathbf{R}^* \mathbf{P}_G + \nu \quad (5.115)$$

where  $\mathbf{R}^* = [\mathbf{B}'_{\mathbf{r}\mathbf{r}}]^{-1} \mathbf{R}$  and  $\nu = [\mathbf{B}'_{\mathbf{r}\mathbf{r}}]^{-1} \beta$ .



Table 5.5 DC OPF Input Data in SI Units for Three-Node Case

$S_o$	$V_o$								
100	10								
$K^a$	$\pi^b$								
3	0.05								
Branch									
From	To	lineCap <sup>c</sup>	$x^d$						
1	2	55	0.20						
1	3	55	0.40						
2	3	55	0.25						
Gen									
ID	atNode	FCost	a	b	pMin <sup>e</sup>	pMax <sup>f</sup>			
1	1	14	10.6940	0.00463	20	200			
2	2	21	18.1000	0.00612	10	150			
3	3	11	37.8896	0.01433	5	20			
LSE									
ID	atNode	L-01 <sup>g</sup>	L-02	L-03	L-04	L-05	L-06	L-07	L-08
1	1	132.66	122.4	115.62	112.2	108.84	110.52	112.2	119.04
2	2	44.22	40.8	38.54	37.4	36.28	36.84	37.4	39.68
3	3	44.22	40.8	38.54	37.4	36.28	36.84	37.4	39.68
ID	atNode	L-09	L-10	L-11	L-12	L-13	L-14	L-15	L-16
1	1	136.02	149.64	153.06	154.74	153.06	149.64	147.96	147.96
2	2	45.34	49.88	51.02	51.58	51.02	49.88	49.32	49.32
3	3	45.34	49.88	51.02	51.58	51.02	49.88	49.32	49.32
ID	atNode	L-17	L-18	L-19	L-20	L-21	L-22	L-23	L-24
1	1	154.74	170.04	163.26	161.52	159.84	156.42	147.96	137.76
2	2	51.58	56.68	54.42	53.84	53.28	52.14	49.32	45.92
3	3	51.58	56.68	54.42	53.84	53.28	52.14	49.32	45.92

<sup>a</sup>Total number  $K$  of nodes

<sup>b</sup>Soft penalty weight  $\pi$  for voltage angle differences

<sup>c</sup>Upper limit  $P_{km}^U$  (in MWs) on magnitude of real power flow in branch  $km$

<sup>d</sup>Reactance  $x_{km}$  (in ohms) for branch  $km$

<sup>e</sup>Lower limit  $p_{Gi}^L$  (in MWs) on real power production for Generator  $i$

<sup>f</sup>Upper limit  $p_{Gi}^U$  (in MWs) on real power production for Generator  $i$

<sup>g</sup>L-H: Load (in MWs) for hour H, where H=01,02,...,24

Table 5.6 DC OPF Solution Results in SI Units for Three-Node Case

Hour	$p_{G1}^*$	$p_{G2}^*$	$p_{G3}^*$	$\delta_2^{*a}$	$\delta_3^*$	$LMP_1^b$	$LMP_2$	$LMP_3$	minTVC <sup>c</sup>
01	200.0	16.1	5.0	-0.0799	-0.1095	18.30	18.30	18.30	2993.95
02	189.0	10.0	5.0	-0.0808	-0.1048	12.44	12.44	12.44	2724.33
03	177.7	10.0	5.0	-0.0752	-0.0979	12.34	12.34	12.34	2565.12
04	172.0	10.0	5.0	-0.0724	-0.0944	12.29	12.29	12.29	2485.70
05	166.4	10.0	5.0	-0.0696	-0.0910	12.23	12.23	12.23	2408.27
06	169.2	10.0	5.0	-0.0710	-0.0927	12.26	12.26	12.26	2446.91
07	172.0	10.0	5.0	-0.0724	-0.0944	12.29	12.29	12.29	2485.70
08	183.4	10.0	5.0	-0.0780	-0.1014	12.39	12.39	12.39	2645.13
09	200.0	21.7	5.0	-0.0741	-0.1077	18.37	18.37	18.37	3097.90
10	200.0	44.4	5.0	-0.0506	-0.1002	18.64	18.64	18.64	3527.13
11	200.0	50.1	5.0	-0.0447	-0.0983	18.71	18.71	18.71	3636.90
12	200.0	52.9	5.0	-0.0418	-0.0974	18.75	18.75	18.75	3691.11
13	200.0	50.1	5.0	-0.0447	-0.0983	18.71	18.71	18.71	3636.90
14	200.0	44.4	5.0	-0.0506	-0.1002	18.64	18.64	18.64	3527.13
15	200.0	41.6	5.0	-0.0535	-0.1011	18.61	18.61	18.61	3473.51
16	200.0	41.6	5.0	-0.0535	-0.1011	18.61	18.61	18.61	3473.51
17	200.0	52.9	5.0	-0.0418	-0.0974	18.75	18.75	18.75	3691.11
18	200.0	78.4	5.0	-0.0154	-0.0890	19.06	19.06	19.06	4193.64
19	200.0	67.1	5.0	-0.0271	-0.0927	18.92	18.92	18.92	3968.98
20	200.0	64.2	5.0	-0.0301	-0.0937	18.89	18.89	18.89	3911.83
21	200.0	61.4	5.0	-0.0330	-0.0946	18.85	18.85	18.85	3856.85
22	200.0	55.7	5.0	-0.0389	-0.0965	18.78	18.78	18.78	3745.51
23	200.0	41.6	5.0	-0.0535	-0.1011	18.61	18.61	18.61	3473.51
24	200.0	24.6	5.0	-0.0711	-0.1067	18.40	18.40	18.40	3152.03

<sup>a</sup>Voltage angle solutions  $\delta_k^*$  are reported in radians

<sup>b</sup>Locational marginal price,  $LMP_k = \lambda_{eqk}^*/S_o$  for each node  $k$

<sup>c</sup>Minimized total variable cost

Table 5.7 DC OPF Solution Results in SI Units for Three-Node Case -  
Inequality Constraint Multipliers and Real Power Branch Flows

Hour	Branch $km$ multipliers						Production constraint multipliers						Branch Flow		
	12	13	23	21	31	32	$P_{G1}^L$	$P_{G2}^L$	$P_{G3}^L$	$P_{G1}^U$	$P_{G2}^U$	$P_{G3}^U$	$P_{12}$	$P_{13}$	$P_{23}$
01	0	0	0	0	0	0	0	0	19.74	5.75	0	0	39.96	27.38	11.84
02	0	0	0	0	0	0	0	5.78	25.59	0	0	0	40.40	26.20	9.60
03	0	0	0	0	0	0	0	5.88	25.69	0	0	0	37.61	24.47	9.07
04	0	0	0	0	0	0	0	5.94	25.75	0	0	0	36.20	23.60	8.80
05	0	0	0	0	0	0	0	5.99	25.80	0	0	0	34.82	22.74	8.54
06	0	0	0	0	0	0	0	5.96	25.77	0	0	0	35.51	23.17	8.67
07	0	0	0	0	0	0	0	5.94	25.75	0	0	0	36.20	23.60	8.80
08	0	0	0	0	0	0	0	5.83	25.64	0	0	0	39.02	25.34	9.34
09	0	0	0	0	0	0	0	0	19.67	5.82	0	0	37.06	26.92	13.42
10	0	0	0	0	0	0	0	0	19.39	6.10	0	0	25.31	25.05	19.83
11	0	0	0	0	0	0	0	0	19.32	6.17	0	0	22.36	24.58	21.44
12	0	0	0	0	0	0	0	0	19.29	6.20	0	0	20.91	24.35	22.23
13	0	0	0	0	0	0	0	0	19.32	6.17	0	0	22.36	24.58	21.44
14	0	0	0	0	0	0	0	0	19.39	6.10	0	0	25.31	25.05	19.83
15	0	0	0	0	0	0	0	0	19.42	6.06	0	0	26.76	25.28	19.04
16	0	0	0	0	0	0	0	0	19.42	6.06	0	0	26.76	25.28	19.04
17	0	0	0	0	0	0	0	0	19.29	6.20	0	0	20.91	24.35	22.23
18	0	0	0	0	0	0	0	0	18.97	6.51	0	0	7.71	22.25	29.43
19	0	0	0	0	0	0	0	0	19.11	6.38	0	0	13.56	23.18	26.24
20	0	0	0	0	0	0	0	0	19.15	6.34	0	0	15.06	23.42	25.42
21	0	0	0	0	0	0	0	0	19.18	6.31	0	0	16.51	23.65	24.63
22	0	0	0	0	0	0	0	0	19.25	6.24	0	0	19.46	24.12	23.02
23	0	0	0	0	0	0	0	0	19.42	6.06	0	0	26.76	25.28	19.04
24	0	0	0	0	0	0	0	0	19.63	5.86	0	0	35.56	26.68	14.24
													$P_{12}^U$	$P_{13}^U$	$P_{23}^U$
													55	55	55

Table 5.8 DC OPF Input Data in SI Units for Five-Node Case

$S_o$	$V_o$								
100	10								
K	$\pi$								
5	0.05								
Branch									
From	To	lineCap	x						
1	2	250	0.0281						
1	4	150	0.0304						
1	5	400	0.0064						
2	3	350	0.0108						
3	4	240	0.0297						
4	5	240	0.0297						
Gen									
ID	atNode	FCost	a	b	pMin	pMax			
1	1	16	14	0.005	0	110			
2	1	19	15	0.006	0	100			
3	3	28	25	0.010	0	520			
4	4	10	30	0.012	0	200			
5	5	24	10	0.007	0	600			
LSE									
ID	atNode	L-01	L-02	L-03	L-04	L-05	L-06	L-07	L-08
1	2	350.00	322.93	305.04	296.02	287.16	291.59	296.02	314.07
2	3	300.00	276.80	261.47	253.73	246.13	249.93	253.73	269.20
3	4	250.00	230.66	217.89	211.44	205.11	208.28	211.44	224.33
ID	atNode	L-09	L-10	L-11	L-12	L-13	L-14	L-15	L-16
1	2	358.86	394.80	403.82	408.25	403.82	394.80	390.37	390.37
2	3	307.60	338.40	346.13	349.93	346.13	338.40	334.60	334.60
3	4	256.33	282.00	288.44	291.61	288.44	282.00	278.83	278.83
ID	atNode	L-17	L-18	L-19	L-20	L-21	L-22	L-23	L-24
1	2	408.25	448.62	430.73	426.14	421.71	412.69	390.37	363.46
2	3	349.93	384.53	369.20	365.26	361.47	353.73	334.60	311.53
3	4	291.61	320.44	307.67	304.39	301.22	294.78	278.83	259.61

Table 5.9 DC OPF Solution Results in SI Units for Five-Node Case - Optimal Real Power Production Levels and Optimal Voltage Angles (in Radians)

Hour	$p_{G1}^*$	$p_{G2}^*$	$p_{G3}^*$	$p_{G4}^*$	$p_{G5}^*$	$\delta_2^*$	$\delta_3^*$	$\delta_4^*$	$\delta_5^*$
01	110.00	13.87	332.53	0.00	443.59	-0.0702	-0.0595	-0.0394	0.0164
02	110.00	13.44	269.41	0.00	437.54	-0.0702	-0.0624	-0.0385	0.0162
03	110.00	13.16	227.70	0.00	433.54	-0.0702	-0.0643	-0.0379	0.0161
04	110.00	13.01	206.66	0.00	431.52	-0.0703	-0.0653	-0.0376	0.0160
05	110.00	12.87	185.99	0.00	429.53	-0.0703	-0.0662	-0.0373	0.0160
06	110.00	12.95	196.33	0.00	430.53	-0.0702	-0.0658	-0.0375	0.0160
07	110.00	13.01	206.66	0.00	431.52	-0.0703	-0.0653	-0.0376	0.0160
08	110.00	13.30	248.75	0.00	435.55	-0.0703	-0.0633	-0.0382	0.0162
09	110.00	14.01	353.20	0.00	445.58	-0.0703	-0.0585	-0.0397	0.0164
10	110.00	14.58	437.00	0.00	453.61	-0.0702	-0.0546	-0.0409	0.0166
11	110.00	14.73	458.03	0.00	455.63	-0.0702	-0.0536	-0.0412	0.0167
12	110.00	14.80	468.37	0.00	456.62	-0.0702	-0.0532	-0.0413	0.0167
13	110.00	14.73	458.03	0.00	455.63	-0.0702	-0.0536	-0.0412	0.0167
14	110.00	14.58	437.00	0.00	453.61	-0.0702	-0.0546	-0.0409	0.0166
15	110.00	14.51	426.67	0.00	452.62	-0.0702	-0.0551	-0.0407	0.0166
16	110.00	14.51	426.67	0.00	452.62	-0.0702	-0.0551	-0.0407	0.0166
17	110.00	14.80	468.37	0.00	456.62	-0.0702	-0.0532	-0.0413	0.0167
18	2.07	0.00	520.00	108.88	522.63	-0.0702	-0.0488	-0.0300	0.0222
19	107.35	6.12	520.00	0.00	474.13	-0.0702	-0.0507	-0.0418	0.0175
20	110.00	15.08	510.08	0.00	460.63	-0.0702	-0.0512	-0.0419	0.0168
21	110.00	15.01	499.76	0.00	459.63	-0.0702	-0.0517	-0.0418	0.0168
22	110.00	14.87	478.71	0.00	457.62	-0.0702	-0.0527	-0.0415	0.0167
23	110.00	14.51	426.67	0.00	452.62	-0.0702	-0.0551	-0.0407	0.0166
24	110.00	14.09	363.91	0.00	446.60	-0.0702	-0.0580	-0.0399	0.0164

Table 5.10 DC OPF Solution Results in SI Units for Five-Node Case - LMP Values (Equality Constraint Multipliers) and Minimized Total Variable Cost

Hour	LMP <sub>1</sub>	LMP <sub>2</sub>	LMP <sub>3</sub>	LMP <sub>4</sub>	LMP <sub>5</sub>	minTVC
01	15.17	35.50	31.65	21.05	16.21	19587.11
02	15.16	33.95	30.39	20.60	16.13	17107.25
03	15.16	32.92	29.55	20.30	16.07	15556.75
04	15.16	32.40	29.13	20.15	16.04	14800.93
05	15.15	31.89	28.72	20.00	16.01	14076.09
06	15.16	32.15	28.93	20.07	16.03	14436.48
07	15.16	32.40	29.13	20.15	16.04	14800.93
08	15.16	33.44	29.97	20.45	16.10	16330.20
09	15.17	36.01	32.06	21.20	16.24	20433.88
10	15.18	38.08	33.74	21.81	16.35	24043.63
11	15.18	38.60	34.16	21.96	16.38	24993.90
12	15.18	38.85	34.37	22.03	16.39	25467.47
13	15.18	38.60	34.16	21.96	16.38	24993.90
14	15.18	38.08	33.74	21.81	16.35	24043.63
15	15.17	37.82	33.53	21.73	16.34	23583.10
16	15.17	37.82	33.53	21.73	16.34	23583.10
17	15.18	38.85	34.37	22.03	16.39	25467.47
18	14.02	78.24	66.07	32.61	17.32	31038.51
19	15.07	45.55	39.78	23.90	16.64	28006.88
20	15.18	39.88	35.20	22.33	16.45	27422.37
21	15.18	39.63	35.00	22.26	16.43	26931.89
22	15.18	39.11	34.57	22.11	16.41	25945.85
23	15.17	37.82	33.53	21.73	16.34	23583.10
24	15.17	36.28	32.28	21.28	16.25	20879.49

Table 5.11 DC OPF Solution Results in SI Units for Five-Node Case  
- Thermal Limit Inequality Constraint Multipliers for Each  
Branch in Each Direction ( $km$  and  $mk$ )

Hour	Branch $km$ multipliers											
	12	14	15	23	34	45	21	41	51	32	43	54
01	30.36	0	0	0	0	0	0	0	0	0	0	0
02	28.05	0	0	0	0	0	0	0	0	0	0	0
03	26.52	0	0	0	0	0	0	0	0	0	0	0
04	25.74	0	0	0	0	0	0	0	0	0	0	0
05	24.99	0	0	0	0	0	0	0	0	0	0	0
06	25.37	0	0	0	0	0	0	0	0	0	0	0
07	25.74	0	0	0	0	0	0	0	0	0	0	0
08	27.29	0	0	0	0	0	0	0	0	0	0	0
09	31.12	0	0	0	0	0	0	0	0	0	0	0
10	34.20	0	0	0	0	0	0	0	0	0	0	0
11	34.97	0	0	0	0	0	0	0	0	0	0	0
12	35.35	0	0	0	0	0	0	0	0	0	0	0
13	34.97	0	0	0	0	0	0	0	0	0	0	0
14	34.20	0	0	0	0	0	0	0	0	0	0	0
15	33.82	0	0	0	0	0	0	0	0	0	0	0
16	33.82	0	0	0	0	0	0	0	0	0	0	0
17	35.35	0	0	0	0	0	0	0	0	0	0	0
18	95.88	0	0	0	0	0	0	0	0	0	0	0
19	45.50	0	0	0	0	0	0	0	0	0	0	0
20	36.88	0	0	0	0	0	0	0	0	0	0	0
21	36.50	0	0	0	0	0	0	0	0	0	0	0
22	35.73	0	0	0	0	0	0	0	0	0	0	0
23	33.82	0	0	0	0	0	0	0	0	0	0	0
24	31.51	0	0	0	0	0	0	0	0	0	0	0

Table 5.12 DC OPF Solution Results in SI Units for Five-Node Case - Lower and Upper Production Inequality Constraint Multipliers for Each Generator

Hour	$P_{G1}^L$	$P_{G2}^L$	$P_{G3}^L$	$P_{G4}^L$	$P_{G5}^L$	$P_{G1}^U$	$P_{G2}^U$	$P_{G3}^U$	$P_{G4}^U$	$P_{G5}^U$
01	0	0	0	8.95	0	0.07	0	0	0	0
02	0	0	0	9.40	0	0.06	0	0	0	0
03	0	0	0	9.70	0	0.06	0	0	0	0
04	0	0	0	9.85	0	0.06	0	0	0	0
05	0	0	0	10.00	0	0.05	0	0	0	0
06	0	0	0	9.93	0	0.06	0	0	0	0
07	0	0	0	9.85	0	0.06	0	0	0	0
08	0	0	0	9.55	0	0.06	0	0	0	0
09	0	0	0	8.80	0	0.07	0	0	0	0
10	0	0	0	8.19	0	0.08	0	0	0	0
11	0	0	0	8.04	0	0.08	0	0	0	0
12	0	0	0	7.97	0	0.08	0	0	0	0
13	0	0	0	8.04	0	0.08	0	0	0	0
14	0	0	0	8.19	0	0.08	0	0	0	0
15	0	0	0	8.27	0	0.07	0	0	0	0
16	0	0	0	8.27	0	0.07	0	0	0	0
17	0	0	0	7.97	0	0.08	0	0	0	0
18	0	0.98	0	0	0	0	0	30.67	0	0
19	0	0	0	6.10	0	0	0	4.38	0	0
20	0	0	0	7.67	0	0.08	0	0	0	0
21	0	0	0	7.74	0	0.08	0	0	0	0
22	0	0	0	7.89	0	0.08	0	0	0	0
23	0	0	0	8.27	0	0.07	0	0	0	0
24	0	0	0	8.72	0	0.07	0	0	0	0



Table 5.13 DC OPF Solution Results in SI Units for Five-Node Case - Optimal Real Power Branch Flow  $P_{km}$  and Its Associated Thermal Limit  $P_{km}^U$  for Each  $km \in \mathbf{BI}$

Hour	$P_{12}^a$	$P_{14}$	$P_{15}$	$P_{23}$	$P_{34}$	$P_{45}$
01	250.00	129.65	-255.77	-100.00	-67.47	-187.82
02	250.00	126.71	-253.27	-72.93	-80.32	-184.27
03	250.00	124.77	-251.61	-55.04	-88.81	-181.93
04	250.00	123.79	-250.77	-46.02	-93.09	-180.74
05	250.00	122.83	-249.95	-37.16	-97.30	-179.58
06	250.00	123.31	-250.36	-41.59	-95.19	-180.16
07	250.00	123.79	-250.77	-46.02	-93.09	-180.74
08	250.00	125.75	-252.45	-64.07	-84.52	-183.11
09	250.00	130.61	-256.60	-108.86	-63.26	-188.98
10	250.00	134.51	-259.92	-144.80	-46.20	-193.69
11	250.00	135.49	-260.76	-153.82	-41.92	-194.87
12	250.00	135.97	-261.17	-158.25	-39.81	-195.45
13	250.00	135.49	-260.76	-153.82	-41.92	-194.87
14	250.00	134.51	-259.92	-144.80	-46.20	-193.69
15	250.00	134.03	-259.51	-140.37	-48.30	-193.11
16	250.00	134.03	-259.51	-140.37	-48.30	-193.11
17	250.00	135.97	-261.17	-158.25	-39.81	-195.45
18	250.00	98.83	-346.76	-198.62	-63.15	-175.88
19	250.00	137.64	-274.17	-180.73	-29.93	-199.96
20	250.00	137.91	-262.83	-176.14	-31.32	-197.80
21	250.00	137.43	-262.42	-171.71	-33.42	-197.22
22	250.00	136.45	-261.58	-162.69	-37.71	-196.03
23	250.00	134.03	-259.51	-140.37	-48.30	-193.11
24	250.00	131.11	-257.02	-113.46	-61.08	-189.58
	$P_{12}^U$	$P_{14}^U$	$P_{15}^U$	$P_{23}^U$	$P_{34}^U$	$P_{45}^U$
	250.00	150.00	400.00	350.00	240.00	240.00

<sup>a</sup>In accordance with the usual convention, the real power  $P_{km}$  flowing along a branch  $km$  is positively valued if and only if real power is flowing from node  $k$  to node  $m$ .

Table 5.14 Sensitivity Test Results for Three-Node Case ( $\pi = 100$ , Angles in Radians)

Hour	$p_{G1}^*$	$p_{G2}^*$	$p_{G3}^*$	$\delta_2^*$	$\delta_3^*$	LMP <sub>1</sub>	LMP <sub>2</sub>	LMP <sub>3</sub>	minTVC
01	200.0	16.1	5.0	-0.079920	-0.109520	18.2555	18.2971	18.3239	2993.95
02	189.0	10.0	5.0	-0.080800	-0.104800	12.4441	12.4858	12.5094	2724.33
03	177.7	10.0	5.0	-0.075216	-0.097887	12.3395	12.3783	12.4005	2565.12
04	172.0	10.0	5.0	-0.072400	-0.094400	12.2867	12.3240	12.3455	2485.70
05	166.4	10.0	5.0	-0.069633	-0.090974	12.2349	12.2708	12.2915	2408.27
06	169.2	10.0	5.0	-0.071016	-0.092687	12.2608	12.2974	12.3185	2446.91
07	172.0	10.0	5.0	-0.072400	-0.094400	12.2867	12.3240	12.3455	2485.70
08	183.4	10.0	5.0	-0.078033	-0.101374	12.3923	12.4325	12.4554	2645.13
09	200.0	21.7	5.0	-0.074122	-0.107675	18.3266	18.3656	18.3941	3097.90
10	200.0	44.4	5.0	-0.050621	-0.100198	18.6149	18.6435	18.6786	3527.13
11	200.0	50.1	5.0	-0.044720	-0.098320	18.6873	18.7132	18.7500	3636.90
12	200.0	52.9	5.0	-0.041821	-0.097398	18.7229	18.7475	18.7851	3691.11
13	200.0	50.1	5.0	-0.044720	-0.098320	18.6873	18.7132	18.7500	3636.90
14	200.0	44.4	5.0	-0.050621	-0.100198	18.6149	18.6435	18.6786	3527.13
15	200.0	41.6	5.0	-0.053520	-0.101120	18.5794	18.6092	18.6435	3473.51
16	200.0	41.6	5.0	-0.053520	-0.101120	18.5794	18.6092	18.6435	3473.51
17	200.0	52.9	5.0	-0.041821	-0.097398	18.7229	18.7475	18.7851	3691.11
18	200.0	78.4	5.0	-0.015421	-0.088998	19.0468	19.0596	19.1047	4193.64
19	200.0	67.1	5.0	-0.027120	-0.092720	18.9033	18.9213	18.9631	3968.98
20	200.0	64.2	5.0	-0.030122	-0.093675	18.8664	18.8858	18.9267	3911.83
21	200.0	61.4	5.0	-0.033021	-0.094598	18.8309	18.8515	18.8916	3856.85
22	200.0	55.7	5.0	-0.038922	-0.096475	18.7585	18.7818	18.8202	3745.51
23	200.0	41.6	5.0	-0.053520	-0.101120	18.5794	18.6092	18.6435	3473.51
24	200.0	24.6	5.0	-0.071120	-0.106720	18.3634	18.4011	18.4304	3152.03

Table 5.15 Sensitivity Test Results for Three-Node Case ( $\pi = 10$ , Angles in Radians)

Hour	$p_{G1}^*$	$p_{G2}^*$	$p_{G3}^*$	$\delta_2^*$	$\delta_3^*$	LMP <sub>1</sub>	LMP <sub>2</sub>	LMP <sub>3</sub>	minTVC
01	200.0	16.1	5.0	-0.079920	-0.109520	18.2929	18.2971	18.2997	2993.95
02	189.0	10.0	5.0	-0.080800	-0.104800	12.4441	12.4483	12.4507	2724.33
03	177.7	10.0	5.0	-0.075216	-0.097887	12.3395	12.3434	12.3456	2565.12
04	172.0	10.0	5.0	-0.072400	-0.094400	12.2867	12.2905	12.2926	2485.70
05	166.4	10.0	5.0	-0.069633	-0.090974	12.2349	12.2385	12.2405	2408.27
06	169.2	10.0	5.0	-0.071016	-0.092687	12.2608	12.2645	12.2666	2446.91
07	172.0	10.0	5.0	-0.072400	-0.094400	12.2867	12.2905	12.2926	2485.70
08	183.4	10.0	5.0	-0.078033	-0.101374	12.3923	12.3963	12.3986	2645.13
09	200.0	21.7	5.0	-0.074122	-0.107675	18.3617	18.3656	18.3685	3097.90
10	200.0	44.4	5.0	-0.050621	-0.100198	18.6406	18.6435	18.6470	3527.13
11	200.0	50.1	5.0	-0.044720	-0.098320	18.7106	18.7132	18.7169	3636.90
12	200.0	52.9	5.0	-0.041821	-0.097398	18.7450	18.7475	18.7513	3691.11
13	200.0	50.1	5.0	-0.044720	-0.098320	18.7106	18.7132	18.7169	3636.90
14	200.0	44.4	5.0	-0.050621	-0.100198	18.6406	18.6435	18.6470	3527.13
15	200.0	41.6	5.0	-0.053520	-0.101120	18.6062	18.6092	18.6126	3473.51
16	200.0	41.6	5.0	-0.053520	-0.101120	18.6062	18.6092	18.6126	3473.51
17	200.0	52.9	5.0	-0.041821	-0.097398	18.7450	18.7475	18.7513	3691.11
18	200.0	78.4	5.0	-0.015421	-0.088998	19.0583	19.0596	19.0641	4193.64
19	200.0	67.1	5.0	-0.027120	-0.092720	18.9195	18.9213	18.9255	3968.98
20	200.0	64.2	5.0	-0.030122	-0.093675	18.8839	18.8858	18.8899	3911.83
21	200.0	61.4	5.0	-0.033021	-0.094598	18.8495	18.8515	18.8555	3856.85
22	200.0	55.7	5.0	-0.038922	-0.096475	18.7794	18.7818	18.7856	3745.51
23	200.0	41.6	5.0	-0.053520	-0.101120	18.6062	18.6092	18.6126	3473.51
24	200.0	24.6	5.0	-0.071120	-0.106720	18.3973	18.4011	18.4040	3152.03

Table 5.16 Sensitivity Test Results for Three-Node Case ( $\pi = 1$ , Angles in Radians)

Hour	$p_{G1}^*$	$p_{G2}^*$	$p_{G3}^*$	$\delta_2^*$	$\delta_3^*$	LMP <sub>1</sub>	LMP <sub>2</sub>	LMP <sub>3</sub>	minTVC
01	200.0	16.1	5.0	-0.079920	-0.109520	18.2966	18.2971	18.2973	2993.95
02	189.0	10.0	5.0	-0.080800	-0.104800	12.4441	12.4446	12.4448	2724.33
03	177.7	10.0	5.0	-0.075216	-0.097887	12.3395	12.3399	12.3401	2565.12
04	172.0	10.0	5.0	-0.072400	-0.094400	12.2867	12.2871	12.2873	2485.70
05	166.4	10.0	5.0	-0.069633	-0.090974	12.2349	12.2352	12.2354	2408.27
06	169.2	10.0	5.0	-0.071016	-0.092687	12.2608	12.2612	12.2614	2446.91
07	172.0	10.0	5.0	-0.072400	-0.094400	12.2867	12.2871	12.2873	2485.70
08	183.4	10.0	5.0	-0.078033	-0.101374	12.3923	12.3927	12.3929	2645.13
09	200.0	21.7	5.0	-0.074122	-0.107675	18.3652	18.3656	18.3659	3097.90
10	200.0	44.4	5.0	-0.050621	-0.100198	18.6432	18.6435	18.6438	3527.13
11	200.0	50.1	5.0	-0.044720	-0.098320	18.7130	18.7132	18.7136	3636.90
12	200.0	52.9	5.0	-0.041821	-0.097398	18.7473	18.7475	18.7479	3691.11
13	200.0	50.1	5.0	-0.044720	-0.098320	18.7130	18.7132	18.7136	3636.90
14	200.0	44.4	5.0	-0.050621	-0.100198	18.6432	18.6435	18.6438	3527.13
15	200.0	41.6	5.0	-0.053520	-0.101120	18.6089	18.6092	18.6095	3473.51
16	200.0	41.6	5.0	-0.053520	-0.101120	18.6089	18.6092	18.6095	3473.51
17	200.0	52.9	5.0	-0.041821	-0.097398	18.7473	18.7475	18.7479	3691.11
18	200.0	78.4	5.0	-0.015421	-0.088998	19.0595	19.0596	19.0601	4193.64
19	200.0	67.1	5.0	-0.027120	-0.092720	18.9211	18.9213	18.9217	3968.98
20	200.0	64.2	5.0	-0.030122	-0.093675	18.8856	18.8858	18.8862	3911.83
21	200.0	61.4	5.0	-0.033021	-0.094598	18.8513	18.8515	18.8519	3856.85
22	200.0	55.7	5.0	-0.038922	-0.096475	18.7815	18.7818	18.7822	3745.51
23	200.0	41.6	5.0	-0.053520	-0.101120	18.6089	18.6092	18.6095	3473.51
24	200.0	24.6	5.0	-0.071120	-0.106720	18.4007	18.4011	18.4014	3152.03

Table 5.17 Sensitivity Test Results for Three-Node Case ( $\pi = 0.1$ , Angles in Radians)

Hour	$p_{G1}^*$	$p_{G2}^*$	$p_{G3}^*$	$\delta_2^*$	$\delta_3^*$	LMP <sub>1</sub>	LMP <sub>2</sub>	LMP <sub>3</sub>	minTVC
01	200.0	16.1	5.0	-0.079920	-0.109520	18.2970	18.2971	18.2971	2993.95
02	189.0	10.0	5.0	-0.080800	-0.104800	12.4441	12.4442	12.4442	2724.33
03	177.7	10.0	5.0	-0.075216	-0.097887	12.3395	12.3395	12.3396	2565.12
04	172.0	10.0	5.0	-0.072400	-0.094400	12.2867	12.2868	12.2868	2485.70
05	166.4	10.0	5.0	-0.069633	-0.090974	12.2349	12.2349	12.2349	2408.27
06	169.2	10.0	5.0	-0.071016	-0.092687	12.2608	12.2608	12.2608	2446.91
07	172.0	10.0	5.0	-0.072400	-0.094400	12.2867	12.2868	12.2868	2485.70
08	183.4	10.0	5.0	-0.078033	-0.101374	12.3923	12.3923	12.3923	2645.13
09	200.0	21.7	5.0	-0.074122	-0.107675	18.3656	18.3656	18.3656	3097.90
10	200.0	44.4	5.0	-0.050621	-0.100198	18.6434	18.6435	18.6435	3527.13
11	200.0	50.1	5.0	-0.044720	-0.098320	18.7132	18.7132	18.7133	3636.90
12	200.0	52.9	5.0	-0.041821	-0.097398	18.7475	18.7475	18.7475	3691.11
13	200.0	50.1	5.0	-0.044720	-0.098320	18.7132	18.7132	18.7133	3636.90
14	200.0	44.4	5.0	-0.050621	-0.100198	18.6434	18.6435	18.6435	3527.13
15	200.0	41.6	5.0	-0.053520	-0.101120	18.6092	18.6092	18.6092	3473.51
16	200.0	41.6	5.0	-0.053520	-0.101120	18.6092	18.6092	18.6092	3473.51
17	200.0	52.9	5.0	-0.041821	-0.097398	18.7475	18.7475	18.7475	3691.11
18	200.0	78.4	5.0	-0.015421	-0.088998	19.0596	19.0596	19.0597	4193.64
19	200.0	67.1	5.0	-0.027120	-0.092720	18.9213	18.9213	18.9213	3968.98
20	200.0	64.2	5.0	-0.030122	-0.093675	18.8858	18.8858	18.8858	3911.83
21	200.0	61.4	5.0	-0.033021	-0.094598	18.8515	18.8515	18.8516	3856.85
22	200.0	55.7	5.0	-0.038922	-0.096475	18.7817	18.7818	18.7818	3745.51
23	200.0	41.6	5.0	-0.053520	-0.101120	18.6092	18.6092	18.6092	3473.51
24	200.0	24.6	5.0	-0.071120	-0.106720	18.4011	18.4011	18.4011	3152.03

Table 5.18 Sensitivity Test Results for Three-Node Case ( $\pi = 0.01$ , Angles in Radians)

Hour	$p_{G1}^*$	$p_{G2}^*$	$p_{G3}^*$	$\delta_2^*$	$\delta_3^*$	LMP <sub>1</sub>	LMP <sub>2</sub>	LMP <sub>3</sub>	minTVC
01	200.0	16.1	5.0	-0.079920	-0.109520	18.2971	18.2971	18.2971	2993.95
02	189.0	10.0	5.0	-0.080800	-0.104800	12.4441	12.4441	12.4441	2724.33
03	177.7	10.0	5.0	-0.075216	-0.097887	12.3395	12.3395	12.3395	2565.12
04	172.0	10.0	5.0	-0.072400	-0.094400	12.2867	12.2867	12.2867	2485.70
05	166.4	10.0	5.0	-0.069633	-0.090974	12.2349	12.2349	12.2349	2408.27
06	169.2	10.0	5.0	-0.071016	-0.092687	12.2608	12.2608	12.2608	2446.91
07	172.0	10.0	5.0	-0.072400	-0.094400	12.2867	12.2867	12.2867	2485.70
08	183.4	10.0	5.0	-0.078033	-0.101374	12.3923	12.3923	12.3923	2645.13
09	200.0	21.7	5.0	-0.074122	-0.107675	18.3656	18.3656	18.3656	3097.90
10	200.0	44.4	5.0	-0.050621	-0.100198	18.6435	18.6435	18.6435	3527.13
11	200.0	50.1	5.0	-0.044720	-0.098320	18.7132	18.7132	18.7132	3636.90
12	200.0	52.9	5.0	-0.041821	-0.097398	18.7475	18.7475	18.7475	3691.11
13	200.0	50.1	5.0	-0.044720	-0.098320	18.7132	18.7132	18.7132	3636.90
14	200.0	44.4	5.0	-0.050621	-0.100198	18.6435	18.6435	18.6435	3527.13
15	200.0	41.6	5.0	-0.053520	-0.101120	18.6092	18.6092	18.6092	3473.51
16	200.0	41.6	5.0	-0.053520	-0.101120	18.6092	18.6092	18.6092	3473.51
17	200.0	52.9	5.0	-0.041821	-0.097398	18.7475	18.7475	18.7475	3691.11
18	200.0	78.4	5.0	-0.015421	-0.088998	19.0596	19.0596	19.0596	4193.64
19	200.0	67.1	5.0	-0.027120	-0.092720	18.9213	18.9213	18.9213	3968.98
20	200.0	64.2	5.0	-0.030122	-0.093675	18.8858	18.8858	18.8858	3911.83
21	200.0	61.4	5.0	-0.033021	-0.094598	18.8515	18.8515	18.8515	3856.85
22	200.0	55.7	5.0	-0.038922	-0.096475	18.7818	18.7818	18.7818	3745.51
23	200.0	41.6	5.0	-0.053520	-0.101120	18.6092	18.6092	18.6092	3473.51
24	200.0	24.6	5.0	-0.071120	-0.106720	18.4011	18.4011	18.4011	3152.03

Table 5.19 Sensitivity Test Results for Three-Node Case - Cross Comparison for Sum of Squared Voltage Angle Differences for  $\pi = 100, 10, 1, 0.1, 0.01$ , Angles in Radians

Hour	SSVAD <sub>100</sub> <sup>a</sup>	SSVAD <sub>10</sub>	SSVAD <sub>1</sub>	SSVAD <sub>0.1</sub>	SSVAD <sub>0.01</sub>	MaxAD <sup>b</sup>
01	0.019257997	0.019257997	0.019257997	0.019257997	0.019257997	8.10E-15
02	0.018087680	0.018087680	0.018087680	0.018087680	0.018087680	4.16E-14
03	0.015753349	0.015753349	0.015753349	0.015753349	0.015753349	3.95E-14
04	0.014637120	0.014637120	0.014637120	0.014637120	0.014637120	3.83E-14
05	0.013580482	0.013580482	0.013580482	0.013580482	0.013580482	3.71E-14
06	0.014103844	0.014103844	0.014103844	0.014103844	0.014103844	3.77E-14
07	0.014637120	0.014637120	0.014637120	0.014637120	0.014637120	3.83E-14
08	0.016910662	0.016910662	0.016910662	0.016910662	0.016910662	4.05E-14
09	0.018213892	0.018213892	0.018213892	0.018213892	0.018213892	7.30E-15
10	0.015059898	0.015059898	0.015059898	0.015059898	0.015059898	4.50E-15
11	0.014539661	0.014539661	0.014539661	0.014539661	0.014539661	3.80E-15
12	0.014324057	0.014324057	0.014324057	0.014324057	0.014324057	3.80E-15
13	0.014539661	0.014539661	0.014539661	0.014539661	0.014539661	3.80E-15
14	0.015059898	0.015059898	0.015059898	0.015059898	0.015059898	4.50E-15
15	0.015355405	0.015355405	0.015355405	0.015355405	0.015355405	4.70E-15
16	0.015355405	0.015355405	0.015355405	0.015355405	0.015355405	4.70E-15
17	0.014324057	0.014324057	0.014324057	0.014324057	0.014324057	3.80E-15
18	0.013571891	0.013571891	0.013571891	0.013571891	0.013571891	1.19E-14
19	0.013635853	0.013635853	0.013635853	0.013635853	0.013635853	1.50E-14
20	0.013721393	0.013721393	0.013721393	0.013721393	0.013721393	1.63E-14
21	0.013830775	0.013830775	0.013830775	0.013830775	0.013830775	1.76E-14
22	0.014134773	0.014134773	0.014134773	0.014134773	0.014134773	1.99E-14
23	0.015355405	0.015355405	0.015355405	0.015355405	0.015355405	4.70E-15
24	0.017714573	0.017714573	0.017714573	0.017714573	0.017714573	7.00E-15

<sup>a</sup>Sum of squared voltage angle differences for a specific choice of  $\pi$ , where  $\pi$  is specified to be 100, 10, 1, 0.1 or 0.01. More precisely,  $SSVAD = \sum_{km \in BI} [\delta_k^* - \delta_m^*]^2$

<sup>b</sup>Maximum absolute difference between any two SSVAD values

Table 5.20 Sensitivity Test Results for Five-Node Case - Cross Comparison for Sum of Squared Voltage Angle Differences for  $\pi = 100, 10, 1, 0.1, 0.01$ , Angles in Radians

Hour	SSVAD <sub>100</sub>	SSVAD <sub>10</sub>	SSVAD <sub>1</sub>	SSVAD <sub>0.1</sub>	SSVAD <sub>0.01</sub>	MaxAD
01	0.010386061	0.010386162	0.010386172	0.010386173	0.010386173	1.12E-07
02	0.010307655	0.010307759	0.010307769	0.010307770	0.010307771	1.16E-07
03	0.010283485	0.010283591	0.010283602	0.010283603	0.010283603	1.18E-07
04	0.010279443	0.010279550	0.010279561	0.010279562	0.010279562	1.19E-07
05	0.010280962	0.010281070	0.010281081	0.010281082	0.010281082	1.20E-07
06	0.010279593	0.010279701	0.010279712	0.010279713	0.010279713	1.20E-07
07	0.010279443	0.010279550	0.010279561	0.010279562	0.010279562	1.19E-07
08	0.010292874	0.010292979	0.010292989	0.010292990	0.010292991	1.17E-07
09	0.010422608	0.010422708	0.010422718	0.010422719	0.010422719	1.11E-07
10	0.010625778	0.010625874	0.010625884	0.010625885	0.010625885	1.07E-07
11	0.010690587	0.010690682	0.010690691	0.010690692	0.010690692	1.05E-07
12	0.010724577	0.010724671	0.010724680	0.010724681	0.010724681	1.05E-07
13	0.010690587	0.010690682	0.010690691	0.010690692	0.010690692	1.05E-07
14	0.010625778	0.010625874	0.010625884	0.010625885	0.010625885	1.07E-07
15	0.010595866	0.010595962	0.010595972	0.010595973	0.010595973	1.07E-07
16	0.010595866	0.010595962	0.010595972	0.010595973	0.010595973	1.07E-07
17	0.010724577	0.010724671	0.010724680	0.010724681	0.010724681	1.05E-07
18	0.009870395	0.009870652	0.009870678	0.009870680	0.009870681	2.86E-07
19	0.010980723	0.010980723	0.010980723	0.010980723	0.010980722	6.60E-10
20	0.010875114	0.010875206	0.010875215	0.010875216	0.010875216	1.03E-07
21	0.010835704	0.010835797	0.010835806	0.010835807	0.010835807	1.03E-07
22	0.010759863	0.010759957	0.010759967	0.010759968	0.010759968	1.04E-07
23	0.010595866	0.010595962	0.010595972	0.010595973	0.010595973	1.07E-07
24	0.010443596	0.010443696	0.010443705	0.010443707	0.010443707	1.10E-07



## CHAPTER 6. GENERAL CONCLUSIONS

The restructuring process in the U.S. wholesale electric power industry has been undergoing for more than a decade. There have been increasingly intensive debates among academic researchers, industrial stakeholders and government policy makers regarding the direction of current restructuring efforts. There are also tremendous amount of

In this dissertation research, I apply analytical, statistical and agent-based computational simulation tools to investigate and test financial and real market operations in the restructured U.S. wholesale power industry. The main findings are summarized in the following paragraphs.

In my first paper, I develop a theoretical model to assess the welfare enhance property of financial transmission rights (FTRs). Specifically, I am able to show that under network uncertainty the acquisition of optimal FTRs by the risk averse market traders will increase the social welfare compared with the case where there are no FTRs available. This result presents a counterexample to the somewhat negative views about FTRs held by some economists in the literature and provides some economic explanations to the fact that FTRs are widely adopted as a financial hedge instrument in the major U.S. wholesale power markets.

Different from the theoretical nature of the first study, my second paper investigates a specific FTR market, namely the the FTR auction market in the Midwest energy region (MISO), using a set of econometric estimation tools such as linear regression, nonparametric kernel regression and goodness-of-fit tests. As a first attempt to study this newly established market, we are interested in analyzing the performance of the MISO FTR auction market. The main results show that during the current sample periods the MISO FTR market is systematically losing money (revenue insufficiency), which on the other hand suggests that market participants on average exhibit some degree of risk loving behavior. More data are needed in

order to obtain meaningful economic analysis such as estimating the impact of an agent's risk preference on his willingness to pay for the premium of FTR in this complex market.

Distinct from the first two studies, my third paper goes a further micro level to examine the market design issues in the general wholesale power market context. Specifically, we want to test the FERC's WPMP design that has been implemented or adopted in major wholesale power markets in the U.S. This study reports on the agent-based modeling development and open-source implementation (in Java) of a computational wholesale power market organized in accordance with core WPMP features and operating over a realistically rendered transmission grid. Findings from a dynamic 5-node test case are presented for concrete illustration. With traders being able to submit their offers strategically, it found that traders (Generators) are able to acquire substantial market power without any explicitly collusions. This suggests that the core WPMP design features, as captured in our current computational framework, do not prevent the considerable exercise of market power by traders.

My last paper focuses on an critical optimization component of my third paper that the optimal hourly locational marginal prices (LMPs) and commitment/dispatch quantities have to be cleared by a means of DC Optimal Power Flow (OPF) procedure in the wholesale power market. The main contribution of this paper is to present an open-source strictly convex quadratic programming (SCQP) solver QuadProgJ and shows how to use QuadProgJ to solve DC OPF problems.